Supramolecular Polymerization

Tom F. A. De Greef, Maarten M. J. Smulders, Martin Wolffs, Albert P. H. J. Schenning, Rint P. Sijbesma, and E. W. Meijer*

Institute for Complex Molecular Systems and Laboratory of Macromolecular and Organic Chemistry, Eindhoven University of Technology, P.O. Box 513, 5600 MB Eindhoven, The Netherlands

Received May 7, 2009

Contents

* Corresponding author.

1. Definitions

1.1. Background

In his historic review titled "Polymerization" in *Chemical Reviews* of 1931, Wallace H. Carothers described his brilliant ideas about the rapidly developing field of synthetic polymers (Figure 1).[1] Only a few years after the general acceptance of the proposal of Hermann Staudinger that polymeric substances are long chains of short repeating molecular units linked by covalent bonds,[2] Carothers classified macromolecules by types of compounds that are capable of polymerizing and by the types of polymerization. Even today, this classification is a commonly used strategy and is extremely useful to clarify the difference between macromolecules made by step, chain, or ring-opening polymerizations. Many different polymers are made following these three mechanisms, whereas a large variety of modern polymerization techniques, such as metathesis, living ionic, and radical polymerizations, were added, but they all follow Carothers' classification. With the increasing number of different polymers prepared, the interactions between macromolecules became equally important to explain the materials properties at the molecular level. The importance of supramolecular interactions within polymer science actually dates back to the first synthesis of synthetic polymers; the materials properties of, for example, nylons are mainly the result of cooperative hydrogen bonding. More recently, many exciting examples of programmed structure formation of polymeric architectures based on the combination of a variety of secondary supramolecular interactions have been disclosed.[3−17]

It is then not surprising that at a certain point it was questioned whether it is a requirement to use macromolecules to obtain polymer materials. With the introduction of supramolecular polymers—polymers based on monomeric units held together by directional and reversible secondary interactions—the playground for polymer scientists broadened and is no longer limited to macromolecular species only. In addition, the self-assembly of molecules to form large clusters under equilibrium conditions is a general phenomenon widely found in chemistry, physics, and biology. Examples in each

10.1021/cr900181u CCC: $71.50
Published on Web 09/21/2009

Tom de Greef (third from left) received his Ph.D. in supramolecular chemistry at the Eindhoven University of Technology in 2008 with Professors E. W. Meijer and R. P. Sijbesma. His Ph.D. research was focused on mechanistic aspects of supramolecular polymerizations via quadruple hydrogen bonding, and a small part of the research was performed in the group of Prof. C. J. Hawker at the University of Santa Barbara. He did his undergraduate research in the research group of Prof. E. W. Meijer at the Eindhoven University of Technology and partially in the research group of Prof. G. N. Tew at the University of Amherst, Massachusetts, on the synthesis of novel foldamers. His main research interest is the physical chemistry of supramolecular polymers. Currently he is working as a postdoctoral fellow in the BioMedical Imaging and Modeling group of Prof. P. Hilbers at the Eindhoven University of Technology, where he is focusing on the kinetics of nucleated supramolecular polymerizations.

Maarten Smulders (second from right) received his M.Sc. degree (cum laude) in chemical engineering and chemistry in 2005 at the Eindhoven University of Technology. His undergraduate work was performed in the group of Prof. Dr. E. W. Meijer on the topic of self-assembled, bis-urea-based surfactants as templates for biomineralization. Currently he is completing his Ph.D. research in the group of Prof. Dr. E. W. Meijer. His main interest focuses on studying the mechanisms of supramolecular polymerizations, using chiral amplification as a tool for studying two-component systems.

Martin Wolffs (third from right) received his M.Sc. degree (cum laude) in chemical engineering and chemistry in 2005 at the Eindhoven University of Technology. His undergradauate work was performed in the group of Prof. Dr. E. W. Meijer, where he is currently completing his Ph.D. research. He is a laureate of the KIVI-Niria award and recipient of the Mignot award. His main research interest focuses on multicomponent supramolecular polymerization of π-conjugated molecules. A short stay in the group of Dr. I. Huc enabled him to study the synthesis and characterization of foldamers, which allowed him to use these structures to investigate the organization of chromophores.

Dr. A. P. H. J. Schenning (right) is associate professor at the Eindhoven University of Technology. His research interests center on self-assembled π-conjugated systems. Schenning received his Ph.D. degree at the University of Nijmegen in 1996 on supramolecular architectures based on porphyrin and receptor molecules with Dr. M. C. Feiters and Prof. Dr. R. J. M. Nolte. Between June and December 1996, he was a postdoctoral fellow in the group of Prof. Dr. E. W. Meijer at the Eindhoven, University of Technology working on dendrimers. In 1997, he joined the group of Prof. Dr. F. Diederich at the ETH in Zurich, where he investigated π-conjugated oligomers and polymers based on triacetylenes. From 1998 until 2002, he was a Royal Netherlands Academy of Science (KNAW) fellow at the Eindhoven University of Technology (Laboratory of Macromolecular and Organic Chemistry) active in the field of supramolecular organization of π-conjugated polymers. He received the European Young Investigators Award from the European Heads of Research Councils and the European Science Foundation in 2004, the Golden Medal of the Royal Dutch Chemical Society in 2005, and a Vici grant from The Netherlands Organisation for Scientific Research (NWO) in 2007.

Prof. Dr. Rint Sijbesma (second from left) is full professor in supramolecular polymer chemistry at the Eindhoven University of Technology. Between 1987 and 1992, Sijbesma worked on synthetic receptor molecules under the supervision of Prof. Dr. Roeland Nolte at the University of Nijmegen, where he obtained his Ph.D. degree in 1992. Subsequently, he moved to the University of California, Santa Barbara (UCSB), to work as a postdoctoral researcher in the group of Prof. Fred Wudl on the organic chemistry of C60 (buckminsterfullerene). In 1993, he joined the group of Prof. E. W. Meijer as a lecturer and started his work on supramolecular polymers. In 2002, he became senior lecturer, and in the same year he received a "Pionier" grant from the Dutch Science foundation (NWO) to set up a research line in the area of "Functional Self-Assembled Polymers". He was appointed full professor in 2006. His current research interests include supramolecular polymers based on multiple hydrogen bonding and metal coordination, responsive, "smart" materials, and the use of mechanical forces to perform chemical reactions.

E. W. "Bert" Meijer (left) is a distinguished university professor at the Eindhoven University of Eindhoven. He studied at the University of Groningen, where he received his Ph.D. in 1982 in the field of organic chemistry. From 1982 to 1989 he was as a research chemist at Philips Research Laboratories in Eindhoven. From 1989 to 1992 he headed a group in polymer chemistry at DSM Research in Geleen, The Netherlands. In 1991 he became a professor in organic chemistry at the Eindhoven University of Technology. He received the 1993 Golden Medal of the Royal Dutch Chemical Society and the 2000 Silver Medal of the MacroGroup U.K. In 2001, he was given the SPINOZA award of the Dutch National Science Foundation, and in 2006 he received the ACS Award in Polymer Chemistry. He is a member of the Royal Netherlands Academy of Art and Sciences and the Royal Holland Society of Sciences and Humanities. Bert's main research interests are the design, synthesis, characterization, and possible applications of supramolecular architectures, with special emphasis on chirality, dendrimers, π-conjugated oligomers and polymers, hydrogen-bonding architectures, and the noncovalent synthesis of complex molecular systems.

field are ubiquitous and include living ionic polymerizations,[18,19] the formation of molecular Bose−Einstein condensates,[20] and the self-assembly of clathrin proteins[21] during endocytosis. When the interaction between the monomers is generated by moderately strong, reversible noncovalent, but highly directional, forces that result in high molecular weight linear polymers under dilute conditions, the self-assembly is classified as a supramolecular polymerization.

Although the area of self-assembly of molecules into one-dimensional multicomponent structures has been known for decades, it is only of recent date that these supramolecular polymers enjoy a steadily increasing interest due to the fact that these polymers exhibit unprecedented and highly useful functional properties. For our research group, the breakthrough was established by showing that supramolecular polymers exhibit mechanical properties in the bulk that were thought to be reachable only with covalently linked monomers in macromolecules.[22] In Figure 2, a material is shown that is made of a supramolecular polymer built by the reversible linking of repeating molecular units by quadruple hydrogen-bonded end groups. The high association constant and self-complementarity of this unit is responsible for excellent mechanical properties, whereas the reversibility takes care of the ease in processing at elevated temperatures of these supramolecular polymers.

POLYMERIZATION[1]

WALLACE H. CAROTHERS

Experimental Station, E. I. du Pont de Nemours and Company, Wilmington, Delaware

Received March 21, 1931

TABLE OF CONTENTS

[1] Studies on polymerization and ring formation. IX. Communication No. 55 from the Experimental Station of the E. I. du Pont de Nemours and Company.

Figure 1. First page of Wallace H. Carothers' *Chemical Reviews* paper in 1931. (Reprinted from ref 1. Copyright 1931 American Chemical Society.)

Through the years, many excellent reviews and books have been published describing progress in the area of supramolecular polymers.[23−35] In 2001, our research group published a *Chemical Reviews* paper titled "Supramolecular Polymers"; at that time it was already almost impossible to describe all details known to the field.[36] In 2009, it is even more problematic to survey all compounds that form supramolecular polymers and discuss their functional properties. In this review, we will therefore restrict coverage to the most fundamental of supramolecular polymerizations, that of ditopic monomers in solution leading to linear polymers with high aspect ratio, the formation of which is driven by the reversible association of two end groups, A and B. Although the two end groups can be connected via a (polymeric) spacer, this is not necessarily the case. In self-assembling disc-like monomers such spacers are absent. With any ditopic monomer, the reversible interaction can occur either between two self-complementary end groups (A = B) or between two complementary end groups (A ≠ B). As a tribute to the seminal work of Carothers, we apply the same classification for supramolecular polymers as he used for macromolecules. Doing so proves to be extremely helpful to understand many aspects of supramolecular polymerizations.

In our earlier review, we proposed the following definition for supramolecular polymers:[36] "*Supramolecular polymers are defined as polymeric arrays of monomeric units that are brought together by reversible and highly directional secondary interactions, resulting in polymeric properties in dilute and concentrated solution as well as in the bulk. The directionality and strength of the supramolecular bonding are important features of systems that can be regarded as polymers and that behave according to well-established theories of polymer physics.*" In the past the term "living polymers", that is, polymers that reversibly assemble and disassemble, has been used for these types of polymers. However, to exclude confusion with the important field of living polymerizations, we use the term supramolecular polymers instead.

1.2. Classification

Supramolecular polymerizations can be classified on the basis of three different principles: (1) the physical nature of the noncovalent force that lies at the origin of the reversible interaction (physical origin classification), (2) the type of monomer(s) used (structural monomer classification), and (3) the evolution of the Gibbs free energy of the polymer as a function of conversion (thermodynamical classification). In principle, a fourth classification scheme based on the dimensionality of the aggregate is possible. However, the addition of a second and third dimension will result in additional interaction energies and hence will directly influence the free energy of the self-assembled polymer as the concentration or temperature is changed.

In an earlier review, we classified different supramolecular polymers on the basis of the physical nature of the various types of interactions that can act as driving forces for the formation of large supramolecular assemblies and we discussed their possible directional character.[36] Examples of types of polymers in this classification include supramolecular polymers formed by (1) hydrogen bonds, (2) $\pi-\pi$ interactions, (3) hydrophobic interactions, or (4) metal−ligand binding. With this scheme, it is possible to directly link the association constant of the intermolecular interaction to the virtual molecular weight and hence the degree of supramolecular polymerization (Figure 3). Although very useful at first glance, this scheme overlooks many mechanistic details that have become evident in recent times.

In the second classification scheme two groups are defined. The first group involves a *single* monomer containing either self-complementary or complementary end-group interac-

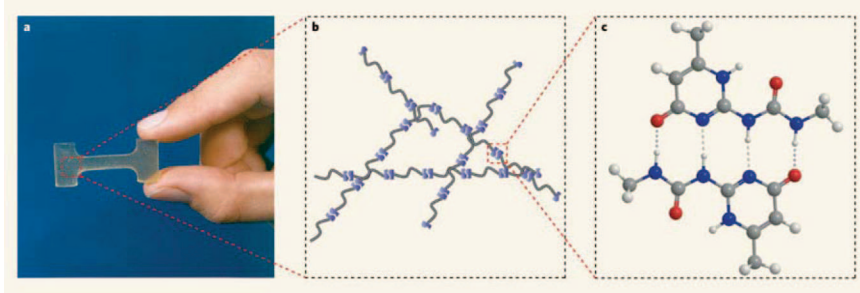

Figure 2. (a) Supramolecular polymeric material based on a low molecular weight compound equipped with two ureido-pyrimidinone (UPy) units. (b) Schematic picture of the underlying polymeric network. (c) Schematic picture of the self-complementary UPy dimer. (Reprinted with permission from ref 23. Copyright 2008 Nature Publishing Group.)

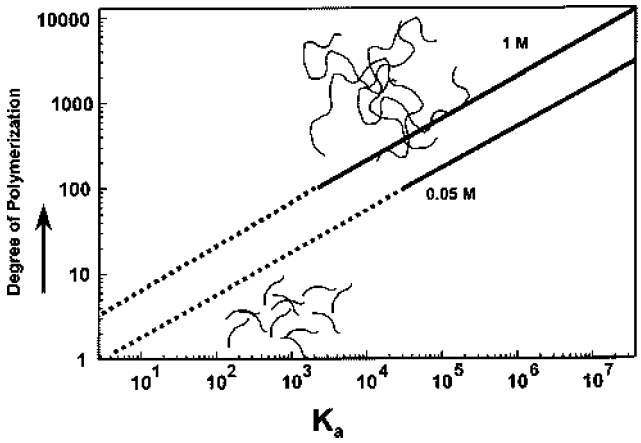

Figure 3. Theoretical plot of the degree of supramolecular polymerization versus association constant, K_a (M^{-1}), at two different concentrations according to an isodesmic self-assembly model. (Reprinted from ref 36. Copyright 2001 American Chemical Society).

tions. Examples of this group include the supramolecular polymerization of an A_2 monomer in solution in which the reversible A:A interaction is self-complementary. Another example in this group is the supramolecular polymerization of an A−B type monomer in which the reversible A:B interaction is complementary in nature. The second group involves *two* different bifunctional monomers containing only one type of interaction. Examples of the second group include the supramolecular polymerization of an A_2 monomer with a B_2 monomer driven by a complementary A:B interaction.

The third classification scheme is based on the evolution of the Gibbs free energy of the supramolecular polymer as the conversion, p, goes from zero to full conversion ($p = 1$). Hence, in this classification scheme the main concern is the mechanism by which the supramolecular polymers grow from their monomeric components into their polymeric structure as the concentration or temperature is changed. In this review we will use this approach to classify the different supramolecular polymerizations, a method that has been so successful for macromolecules. By introducing the concept of conversion, we can understand also the most fundamental difference between covalent polymer chemistry and supramolecular polymer chemistry.

1.3. Supramolecular Polymerization Mechanisms

Polymerization reactions involving covalent bond formation mostly occur under kinetic control because the potential barrier for the back reaction (depolymerization) is often much larger than for the forward reaction. As a result, dilution (or heating) of the macromolecule will not result in a decrease of the molecular weight and, hence, the degree of conversion. This situation is very much different in supramolecular polymerizations where, due to reversibility, the extent of reaction p is directly coupled to thermodynamic forces such as concentration, temperature, and pressure. Without loss of generality we will consider the thermodynamic aspects of supramolecular polymerization processes in which a *single* ditopic monomer is capable of forming a supramolecular polymer via noncovalent association of its end groups. It is important to realize that the same phenomena can occur for supramolecular polymerizations involving two structurally different monomers, although in such a case the Gibbs free energy as a function of conversion is also dependent on the stoichiometric ratio of the two monomers.

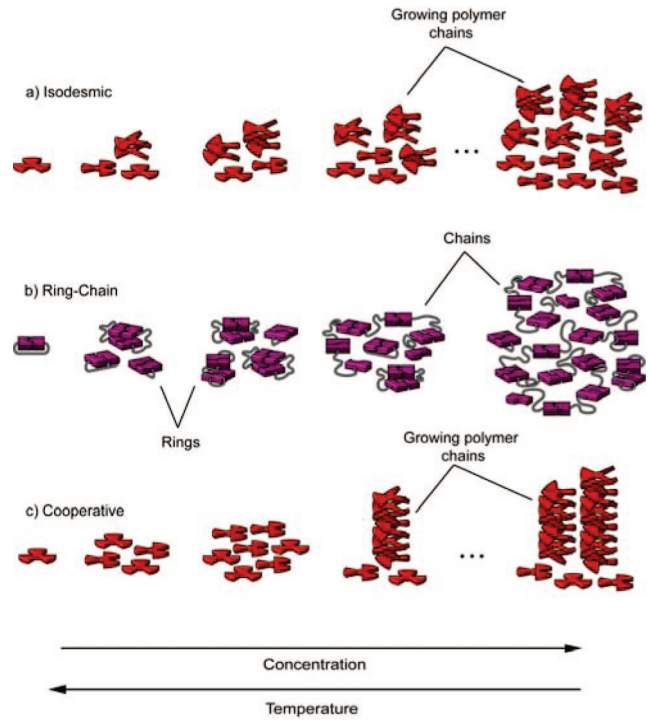

Figure 4. Graphical representation of the three growth mechanisms by which a monomer can polymerize into a supramolecular polymer: (a) isodesmic supramolecular polymerization; (b) ring−chain mediated supramolecular polymerization; (c) cooperative supramolecular polymerization.

As mentioned, only linear supramolecular polymerization processes that occur under (quasi-) dilute solutions will be treated in this review. By restricting our analysis to linear supramolecular polymerizations occurring under dilute conditions, a wide variety of structural transitions are not treated in this review. For example, the transition from a single supramolecular polymer to a supramolecular gel and the induction of a nematic phase due to formation of self-assembled columns will not be treated.

In this review we will discuss the three major growth mechanisms, namely, isodesmic, ring−chain, and cooperative growth (Figure 4), by which supramolecular polymerizations occur and discuss their physical characteristics as well as give selected examples from the literature. The isodesmic polymerization is similar to the step polymerization of polyesters and is characterized by a high polydispersity, and the degree of polymerization strongly depends on the association constant of the linking supramolecular units. The equilibrium between linear supramolecular polymers and their cyclic counterparts determines the second class of supramolecular polymerizations. Finally, the cooperative mechanism of supramolecular polymerization is characterized by nonlinear growth and is often nucleated. The current review classifies supramolecular polymers according to these three mechanisms by combining theoretical descriptions with a variety of examples from recent literature. An important physical aspect shared by some of these mechanisms is that they exhibit a critical point in their self-assembly pathway, which is characterized by a rapid change in the degree of polymerization. We draw attention to the intimate relationship between these mechanisms and phase transitions, which, by definition, are always critical phenomena. Although not the focus of the review, we will end this review with a collection of intriguing new properties of supramolecular polymers that lead to unprecedented functions.

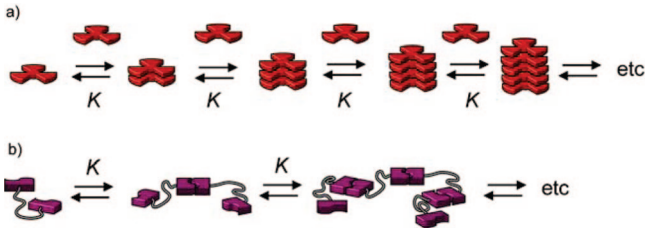

Figure 5. Schematic representation of isodesmic supramolecular polymerizations: (a) isodesmic supramolecular polymerization of a rigid discotic molecule into a linear supramolecular polymer; (b) isodesmic supramolecular polymerization of a bifunctional monomer in which the two binding groups are connected via a flexible spacer. In both cases, *K* represents the intermolecular equilibrium constant, which, for an isodesmic supramolecular polymerization, is independent of the chain length.

2. Isodesmic Supramolecular Polymerization

2.1. Definition and Covalent Counterpart

The first class of supramolecular polymerizations is represented by the reversible formation of a single noncovalent bond that is *identical* at all steps of the polymerization process. This implies that the reactivity of the end groups during the supramolecular polymerization process does not change due to neighboring group effects or additional interaction energies between nonadjacent sites. In addition, an isodesmic supramolecular polymerization is characterized by the absence of cyclic intermediates in the self-assembly pathway. The equivalent in covalent polymer chemistry is a step-by-step reversible polycondensation that obeys Flory's "principle of equal reactivity"[37] and in which intramolecular cyclization reactions do not occur (vide infra). An example of such a polymerization is the polycondensation of sebacoyl chloride (Cl−OC$(CH_2)_8$CO−Cl) with 1,10-decamethylene glycol (HO−$(CH_2)_{10}$−OH) in dioxane. Kinetic measurements on this polycondensation have shown that the reactivity of the functional groups is indeed independent of the degree of polymerization.[38] Furthermore, when this polycondensation is performed at very high concentrations or in the bulk, cyclization during the reaction is considered to be negligible as the smallest cycle that can be formed is a cyclic 20-mer.[39]

2.2. Thermodynamic Aspects of Isodesmic Supramolecular Polymerizations

An isodesmic (after isos, meaning equal, and desmos, meaning bond) supramolecular polymerization of a ditopic monomer in dilute solution is characterized by a single binding constant (*K*) for each reversible step in the assembly pathway (Figure 5). This supramolecular polymerization mechanism is also called the multistage open association model[40] or free association model.[41] In an isodesmic supramolecular polymerization, the successive addition of monomer to the growing chain leads to a constant decrease in the free energy, which in turn indicates that the affinity of a subunit for a polymer end is independent of the length of the polymer (Figure 6). Although all isodesmic polymerizations are characterized by this feature, the energy diagram can still be complicated by the presence of kinetic barriers during the self-assembly pathway from monomer to supramolecular polymer.

The general scheme of an isodesmic supramolecular polymerization can be written as in Scheme 1, in which M_1 represents the monomer and *K* the molar equilibrium constant

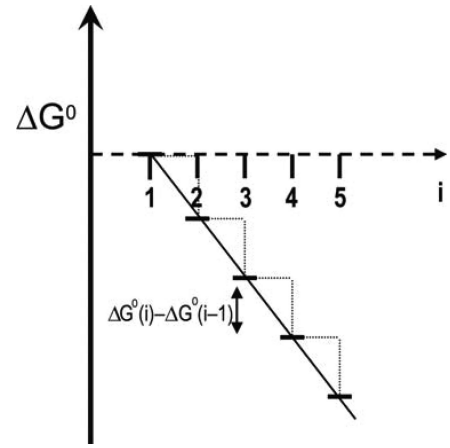

Figure 6. Schematic energy diagram of an isodesmic supramolecular polymerization. The abscissa in this plot represents the size of the oligomer (*i*), whereas the ordinate measures the free energy $\Delta G°$ in arbitrary units.

Scheme 1

$$M_1 + M_1 \overset{K}{\rightleftharpoons} M_2 \qquad [M_2]=K[M_1]^2$$

$$M_2 + M_1 \overset{K}{\rightleftharpoons} M_3 \qquad [M_3]=K^2[M_1]^3$$

$$\vdots \qquad\qquad \vdots$$

$$M_{i-1} + M_1 \overset{K}{\rightleftharpoons} M_i \qquad [M_i]= K^{-1}(K[M_1])^i \quad i = 1, 2,...,\infty$$

(M^{-1}). Due to the equivalence of each step during the polymerization, isodesmic supramolecular polymerizations are characterized by the absence of a critical concentration or critical temperature for self-assembly.[40−48]

To illustrate this important fact, several concentration-dependent properties of isodesmic supramolecular polymerizations have been calculated using the classical mean-field chemical equilibrium model as discussed, for example, by Zhao and Moore.[48] This model is very similar to Flory's mean-field theory of condensation polymerization, which makes use of statistical instead of equilibrium considerations.[37,49] Figure 7a displays the fraction of monomer that is converted to supramolecular polymer, ϕ, as a function of the dimensionless concentration KC_t (with C_t defined as the total concentration of monomer and the fraction of polymerized material, ϕ, defined as $(C_t - M_1)/C_t$). As can be observed, the fraction of monomer incorporated in polymeric species rises gradually as the concentration of ditopic monomer in dilute solution is increased. This gradual transition is also observed when the weight- and number-averaged degrees of polymerization (DP_W and DP_N, respectively) are plotted as a function of the dimensionless concentration (Figure 7b). Scaling theory,[50] renormalization group calculations,[51,52] and Monte Carlo simulations[53] all agree on a general growth law for isodesmic supramolecular polymers, which manifests itself as a power law: $DP_N \sim C_t^{\lambda}$. Mean-field theory shows that the exponent λ is equal to 0.5 both in dilute (nonoverlapping) and in semidilute (entangled) solutions.[53−55] However, as shown by Cates, deviations from this square root dependence can be expected when non-mean-field effects such as excluded volume interactions are taken into account and the exponent λ can take on different values in dilute and semidilute solutions.[53,56]

The graphs in Figure 7 immediately reveal a major drawback of supramolecular polymerizations occurring via an isodesmic, linear growth mechanism. Only at very high

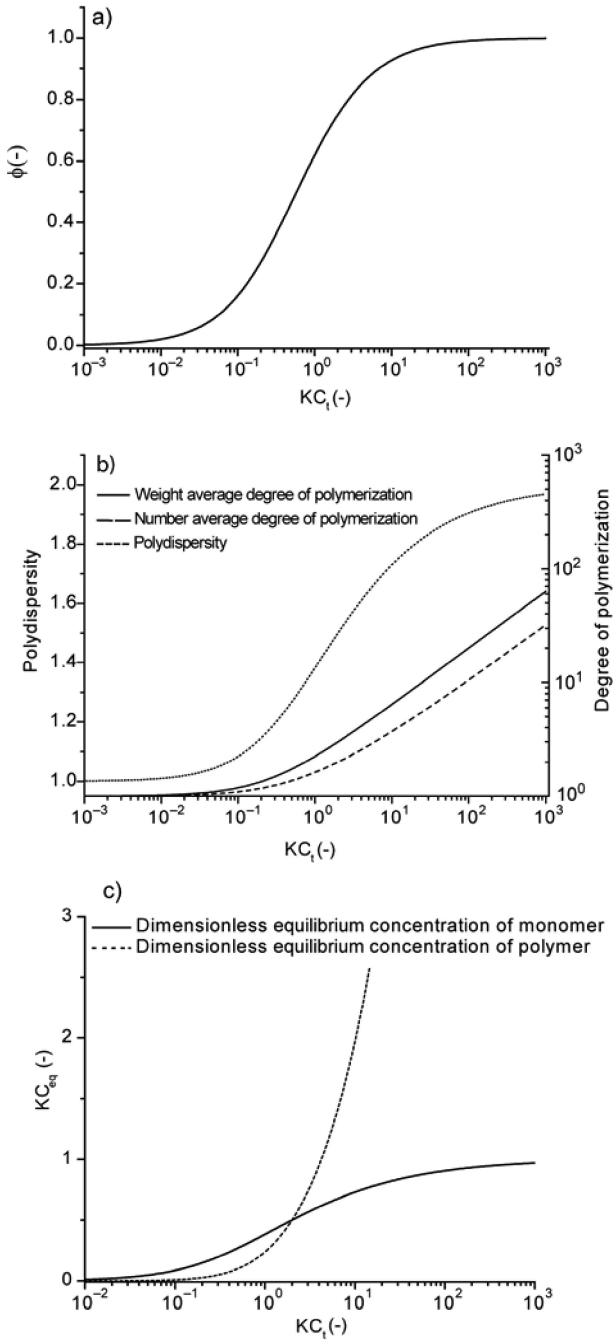

Figure 7. Concentration-dependent properties of isodesmic supramolecular polymers in ideal solutions based on the sequence of reactions as depicted in Scheme 1: (a) fraction of polymerized material, ϕ, as a function of the dimensionless concentration KC_t; (b) weight- and number-averaged degrees of polymerization and polydispersity as a function of the dimensionless concentration KC_t; (c) dimensionless equilibrium concentration of monomer and polymer (defined as the concentration of all oligomers $M_2 + M_3 + ... + M_\infty$, multiplied by K) as a function of the dimensionless total concentration KC_t.

values of KC_t are supramolecular polymers with a high degree of polymerization (DP) obtained (Figure 7b). Hence, to obtain supramolecular polymers with high DP in dilute solutions ($C_t < 1$ M), a high value of the equilibrium constant K is needed ($K > 10^6$ M^{-1}). Another characteristic feature of isodesmic supramolecular polymerizations is the gradual increase of the concentration of monomers and polymers (which includes all species except the monomer) as the total concentration is increased (Figure 7c). As a result of the simultaneous increase of monomer and polymer concentrations, the monomer coexists with polymers of various lengths. At high concentrations, the equilibrium concentration of monomer reaches a maximum value that is equal to K^{-1}. For isodesmic supramolecular polymerizations the monomer is always the most abundant species *in number* within the system, regardless of the values of the equilibrium constant and the total concentration.[48] Further analysis of isodesmic supramolecular polymerizations shows that the polydispersity index at equilibrium, characteristic of the width of the molecular weight distribution, grows steadily to a value of 2 as the dimensionless concentration is increased. Additionally, the size distribution of the polymers in the high molecular weight limit ($DP_N \gg 1$) corresponds to a broad exponential distribution.[43,44]

Similar to covalent polymers, the length and entanglement of the chains also give rise to the polymeric properties in supramolecular polymers. However, characterization of the length of supramolecular polymers is not a trivial task due to the fact that direct techniques such as size exclusion chromatography or mass spectroscopy are not suitable to probe this property because minute changes in temperature, solvent composition, and concentration, which occur in most analytical techniques, can result in changes in the degree of polymerization.[57] Therefore, obtaining equilibrium constants for supramolecular polymers at different temperatures is an important task as this allows the calculation of the chain length at any concentration or temperature. The value of the isodesmic equilibrium constant, K, is usually obtained by concentration-dependent spectroscopic (UV−vis,[58] infrared,[59] fluorescence,[60,61] NMR,[62] circular dichroism[63]) or calorimetric[64] measurements and subsequent nonlinear least-squares minimization of the data using an isodesmic binding isotherm. In most cases, the changes in the experimentally measured signal are assumed to be proportional with the concentration or fraction of aggregated material and only nearest-neighbor interactions are taken into account.[42] In such a case an additional difficulty arises because the equations describing the concentration of self-assembled material in the case of dimerization and isodesmic aggregation are algebraically identical apart from a factor of 2.[42] Therefore, the quality of the fits cannot be used to distinguish between dimerization and isodesmic association and additional measurements that probe the degree of polymerization as a function of concentration (for example, diffusion-ordered NMR spectroscopy,[65] ultracentrifugation,[66,67] vapor pressure osmometry,[62] or light scattering[68]) need to be used to distinguish between the two possibilities. Recently, it was shown that the measurements of the isodesmic equilibrium constant at different temperatures can also be used to distinguish between the two mechanisms.[69]

Whereas in the previous section the concentration-dependent properties of isodesmic supramolecular polymerization were discussed, the temperature-dependent properties of isodesmic supramolecular polymerizations will be discussed in the next section. In general, the supramolecular polymerization of bifunctional monomers resembles the polymerization of monomers by equilibrium covalent bond formation.[41,45,70−72] For equilibrium covalent polymerizations an important aspect is the appearance of an ideal polymerization temperature (T_p^0), as first noted by Dainton and Ivin for covalent ring-opening polymerizations and addition polymerizations.[73,74] The Dainton−Ivin equation links the enthalpy of propagation (ΔH_{pr}), the entropy of propagation (ΔS_{pr}), and

Scheme 2

$$M_i + M_j \rightleftharpoons M_{i+j} \qquad i,j = 1, 2,...,\infty$$

the initial mole fraction of monomer to the ideal polymerization temperature T_p^0. If ΔH_{pr} and ΔS_{pr} are both positive, then polymerization of the monomer occurs only at a temperature high enough for the entropy term to be larger than the enthalpy term. In such a case the system exhibits a floor temperature. When ΔH_{pr} and ΔS_{pr} are both negative, the polymerization of the monomer is enthalpically driven and occurs only below a certain temperature called the ceiling temperature. By constructing a plot of the initial monomer concentration versus an experimentally determined polymerization temperature, one can obtain a polymerization transition line, separating monomer-rich and polymer-rich phases. However, as discussed by Dudowicz, Freed, and Douglas,[41] the Dainton−Ivin equation is exact only for (supramolecular) polymerizing systems that exhibit a sharp transition from monomer to polymer such as ring-opening polymerizations, living polymerizations, or cooperative polymerizations (vide infra). For isodesmic supramolecular polymerizations, the transition between monomer and polymer is extremely broad and the polymer-rich and monomer-rich "phases" coexist. Hence, the interpretation of the polymerization line as a boundary between the monomer-rich and polymer-rich "phases" is less appropiate for isodesmic supramolecular polymerizations.[41]

In contrast to concentration-dependent isodesmic self-assembly models, which have been developed using chemical equilibrium considerations, temperature-dependent models have been mainly constructed using the framework of statistical mechanics. For a historical summary of this process and a discussion of the two different approaches, the reader is referred to an excellent review by Greer.[70]

To illustrate the temperature-dependent properties of isodesmic supramolecular polymerizations two mean-field models will be discussed, both based on the type of reaction shown in Scheme 2.

Both temperature-dependent mean-field models place no restriction on the mechanism of chain formation, and chain growth may either occur via addition of a single monomer or by linkage of two chains.

The first model under consideration has been analyzed by van der Schoot.[43] The two parameters in this model are the concentration-dependent melting temperature T_m, defined as the temperature at which the fraction of monomer present in supramolecular polymers equals 0.5, and a temperature-independent polymerization enthalpy, ΔH_p (in kJ mol^{-1}). Figure 8a shows the fraction of polymerized material, ϕ, as a function of the dimensionless temperature T/T_m for several realistic values of ΔH_p for a supramolecular polymer that polymerizes upon cooling. As can be observed, the shape of the curve is clearly sigmoidal, whereas the steepness of the transition depends on the value of the polymerization enthalpy ΔH_p and is not related to any degree of cooperativity. Figure 8b displays the number-averaged degree of polymerization (DP_N) as a function of the dimensionless temperature T/T_m according to the same model. This plot shows a gradual increase in DP_N when the temperature is lowered.

The second model under consideration is the "free association model" developed by Dudowicz, Douglas, and Freed (DDF).[41,45,75−79] The DDF lattice model is based on a mean-field Flory−Huggins incompressible lattice model[80,81]

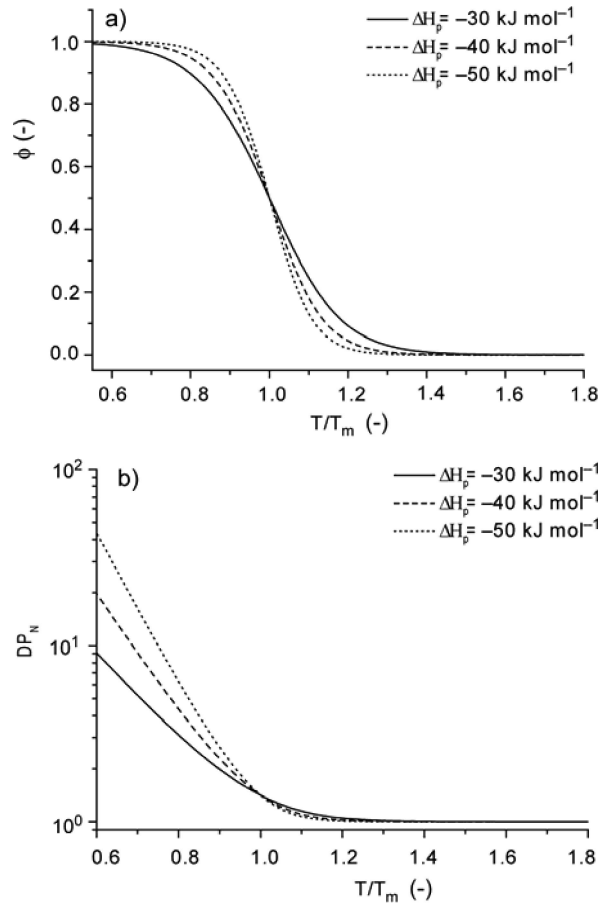

Figure 8. Characteristic properties of temperature-dependent isodesmic supramolecular polymerizations illustrated using the model analyzed by van der Schoot:[43] (a) fraction of polymerized material, ϕ, versus the dimensionless temperature T/T_m for various values of ΔH_p (−30, −40, and −50 kJ mol^{-1}, respectively); (b) number-averaged degree of polymerization DP_N versus the dimensionless temperature T/T_m for various values of ΔH_p (−30, −40, and −50 kJ mol^{-1}, respectively).

and has the advantage that it includes a parameter that describes the flexibility of the polymer and a monomer−solvent interaction parameter (χ) that describes weak van der Waals interactions between monomer and solvent. The DDF lattice model allows for the calculation of various temperature-dependent properties of isodesmic polymerizations such as the number-average degree of polymerization (DP_N), the constant volume specific heat C_V (exclusive of vibrational contributions), and the osmotic pressure. As shown by Dudowicz, Douglas, and Freed, the distribution of oligomers and the development of DP_N and C_V as a function of temperature are insensitive to the monomer−solvent interaction parameter.[41,82] However, other thermodynamic properties such as the osmotic pressure, theta temperature, and critical temperature for phase separation between monomer and solvent are strongly influenced by the value of χ. The DDF lattice model contains two free energy parameters that describe the reversible polymerization of the monomer, that is, a temperature-independent polymerization enthalpy ΔH_p and a temperature-independent polymerization entropy ΔS_p. Figure 9a displays the fraction of monomers incorporated into supramolecular polymers as a function of the dimensionless temperature T/T_m for an isodesmic supramolecular polymer that reversibly polymerizes upon cooling, as determined by using the DDF lattice model.[45]

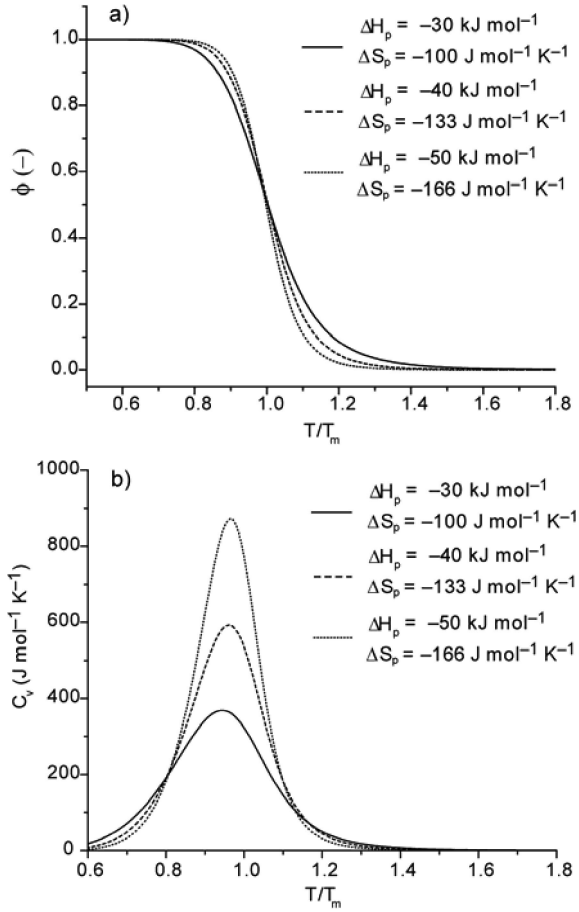

Figure 9. Characteristic properties of temperature-dependent isodesmic supramolecular polymerizations illustrated using the "free association" model analyzed by Dudowicz, Freed, and Douglas:[41,45] (a) fraction of polymerized material, ϕ, versus the dimensionless temperature T/T_m for various values of ΔH_p (−30, −40, and −50 kJ mol^{-1}, respectively) and ΔS_p (−100, −133, and −166 J mol^{-1} K^{-1}, respectively) for fully flexible chains and a cubic lattice; (b) constant volume heat capacity C_v versus the dimensionless temperature T/T_m for various values of ΔH_p (−30, −40, and −50 kJ mol^{-1}, respectively) and ΔS_p (−100, −133, and −166 J mol^{-1} K^{-1}, respectively) for fully flexible chains and a cubic lattice. The initial volume fraction of monomer in all calculations is 0.1.

Similar to the model developed by van der Schoot, the shape of the curve is clearly sigmoidal and the steepness of the curve increases as the values of ΔH_p and ΔS_p become increasingly more negative. The heat capacity at constant volume (C_v) as a function of temperature for a fixed monomer concentration shows a broad, rounded, and symmetric transition for all cases (Figure 9b). The broadness and symmetry of this transition is an indicative feature of isodesmic supramolecular polymerizations in which the addition of each monomer to the chain occurs with the same equilibrium constant. In contrast, the heat capacity as a function of temperature for cooperative supramolecular polymerizations and supramolecular polymerizations in which rings are in competition with chains is asymmetric and exhibits a much sharper transition (vide infra).

The formation of supramolecular copolymers in which at least two different noncovalent interactions of different thermodynamic strengths operate is much less understood, and properly analyzed examples of such systems remain scarce. In this respect, an equilibrium association model for linear supramolecular copolymers based on the isodesmic growth of the individual components has been recently described by Wärnmark and co-workers.[83] Furthermore, we have recently reported a variation on the isodesmic growth model for supramolecular polymers that takes the self-complementary dimerization of end-group A as well as the usual complementary association of end-group A with end-group B into account.[84] On the basis of the theoretical analysis of this model it was shown that the presence of the reversible AA interaction results in lowering of the limiting value of polydispersity index to a value of 1.5 compared to the limiting value of 2 as obtained using the previously described model for isodesmic growth. Furthermore, an analogy was drawn between such a supramolecular polymerization and a multichain polycondensation in which the addition of a small amount of bifunctional initiator results in lowering of the limiting value of the polydispersity index to a value of 1.5 as first described by Flory.[85]

2.3. Examples of Isodesmic Supramolecular Polymerization

In this section several examples will be discussed that have either been shown to polymerize via an isodesmic mechanism or show all of the characteristic properties of such a mechanism. According to Figure 5 the examples can be subdivided into supramolecular polymers that grow via the addition of a monomer in which the two end goups are either electronically coupled (Figure 5a) or connected via a linker and hence are electronically uncoupled (Figure 5b).

2.3.1. Systems with Electronically Coupled Polymerizable Functionalities

This group consists of π-conjugated molecules, and therefore $\pi-\pi$ interactions[86] are the main driving force for the supramolecular polymerization. The isodesmic model postulates that each addition of monomer occurs with the same equilibrium constant. This suggests that the strength of the $\pi-\pi$ interactions should remain constant during the supramolecular polymerization. Indeed, MP2 calculations by Ye and co-workers indicate that the average electronic interaction energy for five $\pi-\pi$ stacked benzenes (−7.09 kcal mol^{-1}) was somewhat larger (12%) than one might expect by thinking of the pentamer simply as four benzene dimers (−6.24 kcal mol^{-1}).[87] This implies that non-nearest-neighbor interactions are only marginally important in the stabilization of the pentamer. This is further supported by recent calculations by Sherrill and Tauer, who have shown that the electronic interaction energies in large $\pi-\pi$ stacked benzene clusters are fairly close to the sum of the interaction energies of isolated benzene dimers when diffuse functions are taken into account.[88] Hence, if the dominant contribution to the total Gibbs free energy of the supramolecular polymer arises only due to simple (i.e., benzene type) $\pi-\pi$ interactions, one would expect simple isodesmic growth of supramolecular polymers, especially in apolar solvents. However, this analysis neglects other contributions to the total Gibbs free energy such as solvophobic interactions, steric interactions between aliphatic side chains,[89] the presence of large quadrupole moments due to heteroaromatic rings and the loss of translational and rotational degrees of freedom upon aggregation,[90] all of which could result in deviation from the proposed isodesmic supramolecular polymerization mechanism of face-to-face $\pi-\pi$ stacked molecules.

Important contributions to the field of isodesmic supramolecular polymerization have been made by Moore and co-

Chart 1

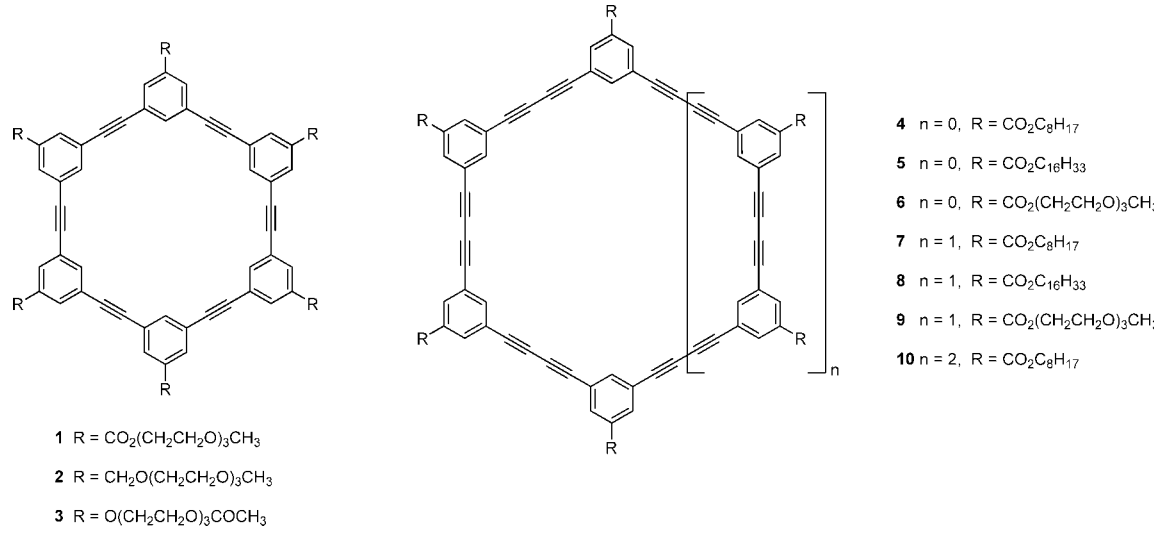

workers. They have studied the supramolecular polymerization of meta-linked phenyl acetylene macrocycles having a flat π-conjugated surface (**1**−**3**, Chart 1).[48,91] By carefully studying the dimerization of these macrocycles[92] and the application of the electrostatic theory of $\pi-\pi$ interactions developed by Hunter and Sanders,[93] they were able to evolve the system into supramolecular polymers by introducing electron-withdrawing substituents at the periphery of the macrocycles as shown for **1** with respect to **2** and **3**, for which only dimerization could be observed.[94] Concentration-dependent ^{1}H NMR measurements on **1** showed the characteristics of an isodesmic supramolecular polymerization process, and the formation of higher order oligomers was confirmed with vapor pressure osmometry (VPO) measurements.[91,94] Analysis of the ^{1}H NMR data using an isodesmic self-assembly model allowed the determination of the thermodynamic parameters and revealed an enthalpically driven polymerization of the macrocycles.[91] The magnitude of the equilibrium constant was increased in more polar solvents; however, the exact reason for this observation was not clear.[94] Replacing two acetylene bonds by an imine bond decreased the tendency to self-assemble as evidenced by the lower association constant.[95] The additional dipolar interactions generated by introduction of the imine functionality showed significant influences on the supramolecular polymerization process in solvents with high polarity, such as acetone (vide infra; section 4.7).[95] By studying the supramolecular polymerization of macrocycles with different sizes and increased number of acetylenes that connect the phenyl rings (**4**−**10**) Tobe and co-workers were able to confirm the observations made by Moore et al.[96] The increased electron-withdrawing effect of the butadiynes enlarged the association constant of **7**−**10** with respect to **1** as determined by concentration-dependent ^{1}H NMR and VPO measurements.[91,96] Tour et al. studied the influence of additional hydrogen bonding in these shape-persistent macrocycles; however, they mainly investigated the process of dimerization and gel formation and did not comment on the one-dimensional supramolecular polymerization mechanism.[97] More recently, the supramolecular polymerization of highly electron-rich tetrathiafulvalene macrocycles was investigated.[98] In this case no oligomers were detected in chloroform or tetrahydrofuran (THF) and only dimer formation was observed in toluene.[98] Addition of water to the THF solution enabled the supramolecular polymerization, which is most likely driven by hydrophobic interactions.[98] It would be interesting to study the effect of hydrogen bonding and the hydrophobic effect on the supramolecular polymerization mechanism of these materials.

Chart 2

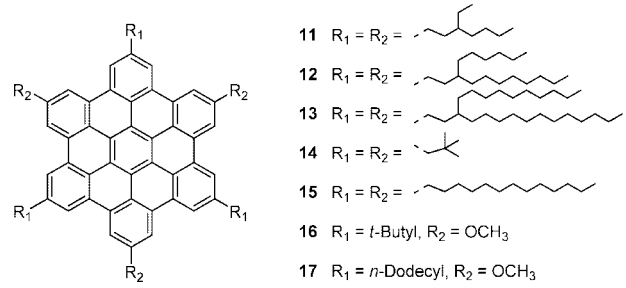

Gómez-Lor and García-Frutos investigated the supramolecular polymerization of hexakis(*p*-substituted-phenylethynyl)triindoles in various solvents of different polarities.[99] These molecules self-associate through aromatic π-stacking as is evident by a strong upfield shift of the NMR signal of the aromatic protons at higher concentrations. Analysis of the concentration-dependent chemical shifts using an isodesmic self-association model revealed that the stacking tendency of these molecules is increased upon attaching electron-donating groups at the periphery. This result is in clear contrast with previous studies on substituent effects (vide supra), which generally showed that substitution with electron-withdrawing groups results in increased stacking tendency. To explain this observation it was suggested that the strength of the $\pi-\pi$ interaction in this system is mainly determined by solvophobic effects and not by electrostatic effects.

Hexa-*peri*-hexabenzocoronenes (abbreviated as HBC) (**11**−**17**) are well-known discotic liquid crystals partly because of the high anisotropic charge carrier mobility.[100] HBC molecules are graphene derivatives and consist of a flat π-conjugated core that is solubilized by the addition of side tails (Chart 2). An impressive amount of research has been conducted concerning their organization in the liquid crystalline state (Figure 10).[100] In recent years details about the supramolecular polymerization in dilute solution have been reported by Müllen and co-workers.[101] Although the number of experimental data points is limited, concentration-

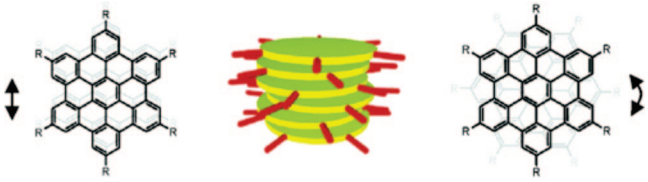

Figure 10. Proposed packing arrangement of HBC derivatives **11**−**17**. (Reprinted from ref 101. Copyright 2005 American Chemical Society.)

and temperature-dependent ^{1}H NMR experiments showed all of the characteristic properties of an isodesmic supramolecular polymerization for compounds **11**−**15** in several different solvents with different polarities, such as benzene, cyclohexane, tetrahydrofuran, and tetrachloroethane.[101]

The decrease in association constant for the HBC having longer and more branched alkyl tails revealed a decreased tendency to polymerize, which was attributed to the higher steric demand of the side chains. Van't Hoff analysis indicated that the supramolecular polymerization of HBC is enthapically favored, whereas it is entropically disfavored, implying that the molecules polymerize by lowering the temperature.[101] A similar association constant as was measured for compound **15** was found for C_3-symmetrical HBCs **16** and **17** having three electron-donating methoxy groups attached to the π-conjugated core.[102] In contrast to the results obtained for macrocyclic systems, an increased electron density in the HBCs does not significantly influence the association constant. Recently, the incorporation of additional hydrogen-bonding interaction[103] or phenyl rings[104] at the periphery was achieved. In light of observations made by others (see section 4.7.2) it will be intriguing to check whether the supramolecular polymerization mechanism will be different.

Fukazawa and co-workers reported on tris(phenylisoxazolyl)benzene (**18**−**21**, Chart 3) stacks in solution and in the gelled state. DFT calculation showed that the molecules were flat as a result of the large dipole moment that is present in the isoxazolyl group.[105] Concentration-dependent ^{1}H NMR in chloroform and UV−vis measurements in methylcyclohexane could be analyzed using the isodesmic self-assembly model.[105] Due to solvophobic effects, $\pi-\pi$ stacking, and dipole−dipole interactions, the association constant in chloroform ($K = 3.7\ M^{-1}$) is much lower than that in methylcyclohexane ($K = 1.8 \times 10^5\ M^{-1}$).[105]

In the late 1990s the research group of Kraft reported an example of the supramolecular polymerization of a disc-like acid−base complex between tetrazoles and 1,3,5-tris(4,5-dihydroimidazol-2-yl)benzene compounds.[106] A large number of complexes that differed in solubilizing tails and number of aromatic rings were shown to assemble into polymeric structures.[106] The concentration-dependent ^{1}H NMR data were analyzed using an isodesmic supramolecular polymerization model and showed low association constants in chloroform and significantly higher constants in less polar solvents such as benzene.[106] The presence of oligomers longer than dimers was shown by VPO measurements.[106] Similar to our research group, these authors used chirality as a probe to study the presence of helical architectures in solution.[106,107] Additionally, we used temperature-dependent chiroptical and optical techniques to study the supramolecular polymerization mechanism of chiral supramolecular polymers.[108]

The supramolecular polymerization of C_3-symmetrical acylated 3,3′-diamino-2,2′-bipyridine discs **22** and **23** into helical columnar stacks (Chart 4), both in the liquid crystalline state and in dilute alkane solvents, has been studied.[107−110] In dodecane, chiral **22** shows a very strong Cotton effect associated with the $\pi-\pi^*$ absorption band of the bipyridine moiety. Heating of dilute dodecane solutions of **22** results in a gradual decrease of the Cotton effect, reflecting a shift in the equilibrium from long helical columns to short, disordered stacks.[111] The monotonic decrease in Cotton effect upon increasing the temperature is indicative of an isodesmic growth mechanism, although care must be exercised in drawing a firm conclusion based on such a small number of data points. Recently these measurements were repeated with a larger number of data points and confirmed that the supramolecular polymerization proceeds via an isodesmic polymerization mechanism.[111] Replacing the solubilizing alkyl groups by oligo(ethylene glycol) tails as in **24**, drastically alters the supramolecular polymerization mechanism (vide infra).

By far the largest contribution to the supramolecular polymerization of perylene bisimide derivatives has been made by Würthner and co-workers, and this contribution was recently concisely reviewed by them.[112] Perylene bisimides are colored compounds that are used as dyes in, for example, the automotive industry or as n-type materials.[112] Their chemical robustness and inherently flat molecular structure make them ideal candidates to study self-assembly in solution. In the beginning of this decade, Würthner and coworkers reported on the supramolecular polymerization of compounds **27**−**30** (Chart 5).[113] By using concentration-dependent UV−vis spectroscopy in alkane solvents (for example, methylcyclohexane) they were able to determine the association constant for each of the compounds. The introduction of substituents at the bay position of the perylene changed the twist angle of the two naphthalene rings, and as a result the association constant decreased significantly

Chart 3. Molecular Structure of Tris(phenylisoxazolyl)benzene Derivatives 18−21 and Their Stacking Arrangement in Solution As Determined by Molecular Modeling (Reprinted with Permission from Reference 105; Copyright 2008 The Royal Society of Chemistry)

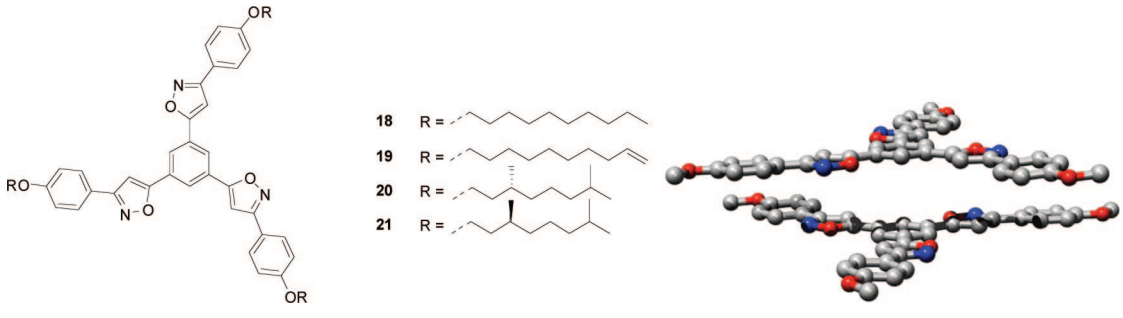

Chart 4. Molecular Structure of C_3-Symmetrical Bipyridine-Based Discotics and Schematic Representation of the Supramolecular Polymer

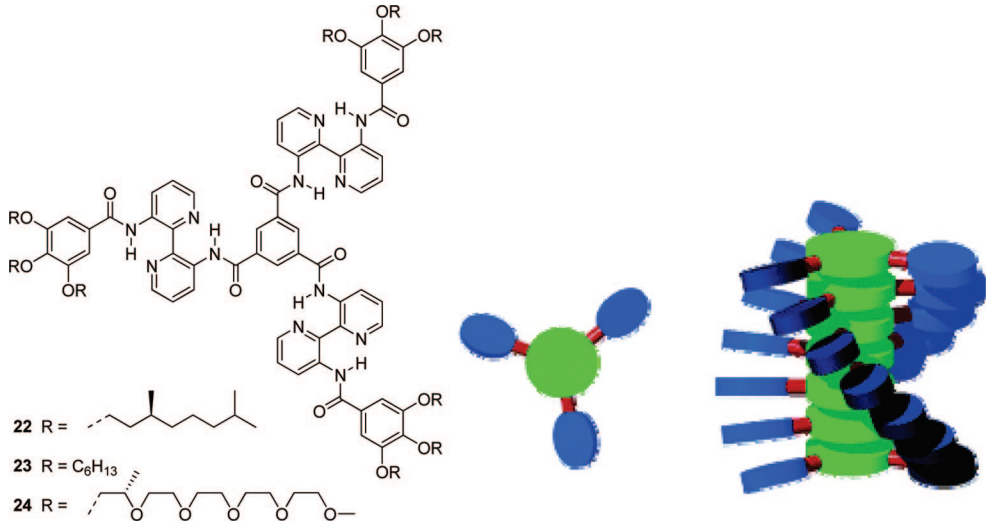

Chart 5

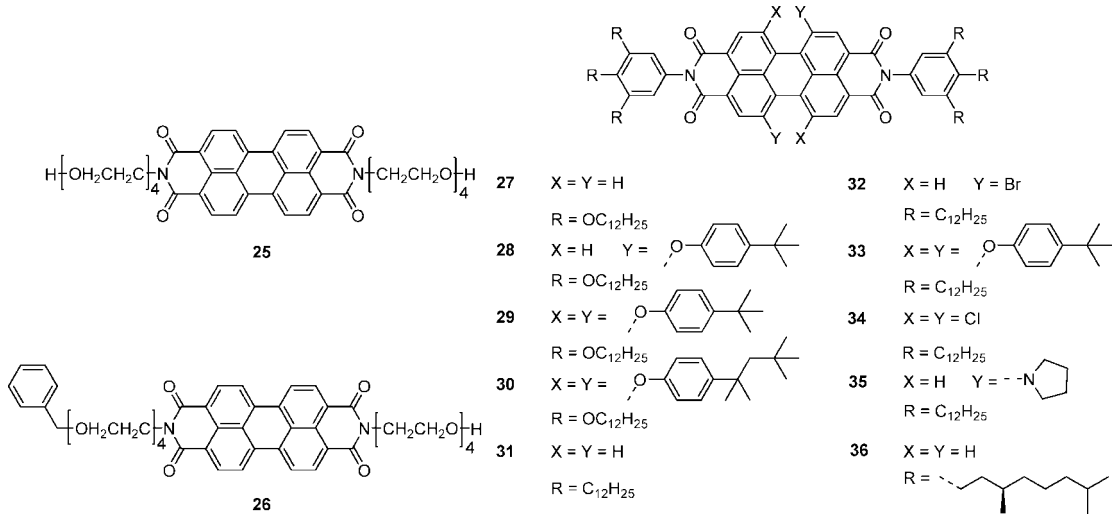

for **28**−**30**. Upon polymerization bathochromically shifted absorption maxima were observed, indicative of the formation of J-type aggregates.[114] By using electrostatic surface potential calculations they showed that the electron-poor π-cloud in the center of the perylene tends to stack on the electron-rich π-cloud of the phenoxy substituents, which is a highly favorable $\pi-\pi$ interaction according to Hunter and Sanders.[93,113] The electron-rich phenoxy groups in **27** were also shown to be electron donors for the perylene, and as a consequence the fluorescence was quenched.[113] In an attempt to restore the usually high fluorescence quantum yield of the perylene bisimides, the solubilizing dodecyl groups were directly attached to the phenyl group by Sonagashira coupling yielding compound **31**.[115] Although the fluorescence quantum yield was restored, concentration-dependent UV−vis spectroscopy showed a hypsochromic shift upon supramolecular polymerization of **31**, indicating H-type aggregation.[115] This gradual spectral change could be analyzed using an isodesmic supramolecular polymerization model.[115] The calculated association constant of **31** was decreased by 3 orders of magnitude with respect to that of **27**.[115] A tentative explanantion could be that the introduction of the more electron-deficient group lowers the attraction between the perylene and the aryl group at the periphery, inducing a change in the packing arrangement from J-type to H-type. This indicates that in aggregates of **31** it is more favorable for the perylene core to interact with the neighboring perylene cores.[112] Because in this case both π-clouds are electron deficient, this results in a decreased $\pi-\pi$ interaction[93] and hence in a lower association constant when compared to **27**. Temperature-dependent VPO and NMR measurements for **31** independently allowed the determination of the aggregate size. In combination with temperature-dependent UV−vis spectroscopy it was shown that the supramolecular polymerization of **31** is an enthalpically driven process.[116] As a result of the decreased $\pi-\pi$ interactions and increased steric interaction, the introduction of a twist in the perylene core by the bulky side groups in the case of **32**−**35** did not result in supramolecular polymers, and only dimerization was observed.[117] The introduction of chirality by synthesis of **36** did not change the mechanism for supramolecular polymerization when investigated by UV−vis spectroscopy, and clear isosbestic points were observed, which indicate a two-state equilibrium process.[118] However, monitoring the polymerization process with chiroptical techniques did not show isodichroic points, and hence the authors state that at least three species participate in the equilibrium.[118] By combining calculations of the average aggregation numbers with the circular dichroic spectra, they made the interesting observation that M-dimers are present at high temperatures, whereas

subsequent lowering of the temperature shifts the equilibrium to the formation of P-aggregates.[118] A recent report by the same group showed a temperature-dependent UV−vis measurement of zinc chlorin light harvesting dye aggregates that displayed all of the characteristics of an isodesmic supramolecular polymerization; however, the association constant has not yet been determined.[119]

Our research group reported on the isodesmic supramolecular polymerization of perylene bisimide derivatives equipped with solubilizing alkyl tails having an isodesmic equilibrium constant of $K = 1.3 \times 10^4$ M^{-1} as determined by UV−vis spectroscopy in methylcyclohexane.[120] X. Li and co-workers investigated the influence of the number of perylene bisimide chromophores on the association constant by comparing the isodesmic supramolecular polymerization of triazines equipped with three perylene bisimides and the corresponding monofunctional structure.[121] Concentration-dependent UV−vis spectroscopy in methanol/chloroform showed a characteristic sigmoidal polymerization profile, and determination of the equilibrium constant using an isodesmic polymerization model revealed that the trisubstituted compound had a significantly higher association constant with respect to the monofunctional compound. This increase was explained by the larger π-conjugated surface of the trisubstituted compound.[121] The research group of A. Li reported on the supramolecular polymerization of perylene bisimides **25** and **26** in chloroform (Chart 5).[122] Temperature- and concentration-dependent ^{1}H NMR measurements confirmed the isodesmic nature of the supramolecular polymerization of these compounds. The polymerization was enthalpically driven, and in this case the association constant increased with the solvent polarity as a direct result of the higher polarity of the solubilizing tails.[122] The formation of higher order oligomers was confirmed by light scattering experiments.[122]

2.3.2. Supramolecular Polymers Built by Monomers Containing Electronically Noncoupled End Groups

In this section isodesmic supramolecular polymerizations are discussed of ditopic monomers in which the binding groups are connected via a (flexible) spacer (Figure 5b). Different classes of intermolecular interactions can be distinguished that drive the supramolecular polymerization process: hydrogen bonding, host−guest interactions, Coulombic interactions, and metal coordination. These classes will be discussed below.

2.3.2.1. Hydrogen-Bonded Supramolecular Polymers. The group of Lehn is recognized to be first to have put forward the concept of (main-chain) supramolecular polymers in 1990.[123] They reported liquid crystalline supramolecular polymers based on tartaric acids having two diaminopyridines or two uracil derivatives at the telechelic position. Triple intermolecular hydrogen bonding allows for the formation of supramolecular polymers. Next to that, the group of Lehn reported on supramolecular liquid crystalline polymers with a rigid, anthracenic linker.[124,125] Griffith and co-workers soon after also reported on liquid crystalline supramolecular polymers formed via hydrogen bonding in the main chain.[126,127]

As a continuation on their research on hydrogen-bond-mediated supramolecular polymerizations, Lehn and co-workers also reported on supramolecular polymers that are formed in dilute solution instead of in the liquid crystalline state. To this end, homoditopic bis-receptor **37** and a homoditopic bis-wedge **38** (Chart 6) were synthesized. Upon polymerization, six hydrogen bonds between the diaminopyridine-substituted isophthalimide receptor and the cyanuric acid wedge are formed.[128]

An association constant of 4.0×10^4 M^{-1} in chloroform was determined by ^{1}H NMR titration studies using the monotopic cyanurate wedge **39**. Qualitative evidence for aggregate formation was obtained from variable-temperature NMR spectroscopy. Upon cooling of a solution of stoichiometric amounts of **37** and **38** in tetrachloroethane, a shift in the amide proton resonances was observed, indicative for the formation of supramolecular polymers due to hydrogen bonding. Also, at lower temperatures, the broadening of the signals supports the formation of (relatively) long polymeric structures. Replacing ditopic **37** for tritopic derivative **41** resulted in earlier (i.e., at higher temperature) and stronger broadening of signals, indicating that a polymeric and interconnected supramolecular network is formed. The addition of monotopic **40** restored the sharpness of the signals, as **40** acts as an end-capping agent that prevents formation of polymeric species. A theoretical model was developed to calculate the behavior of the homoditopic two-component **37**:**38** system, assuming a single equilibrium constant of 4.0×10^4 M^{-1} (i.e., isodesmic polymerization), no length effects, and the absence of cyclization. The results obtained from this model, in terms of degree of polymerization, were in good agreement with the trends observed in solution and were supported by electron microscopy studies.

By replacing the four propyl groups at the periphery of **37** by longer nonyl tails, it was possible to study the formation of supramolecular polymers in decane solution using small-angle neutron scattering (SANS) and viscometry as a function of both temperature and concentration.[129,130] In addition, by introduction of a reversible covalent (acylhydrazone) bond into the homoditopic bis-wedge substrate **42** (Chart 7), supramolecular polymers of **42**:**38** could be prepared that displayed dynamic character both at the molecular level and at the supramolecular level.[131]

The group of Zimmerman has used multiple hydrogen-bonding interactions to prepare supramolecular polymers from homoditopic (macro)monomers. They functionalized a poly(butyl methacrylate) (PBMA, 100 kDa) chain with 2,7-diamido-1,8-naphthyridine (**43**, Chart 8) and a poly(ethylene glycol) (PEG, 2 kDa) chain with a guanosine derivative (**44**, Chart 8).[132]

The association constant of the hydrogen-bonding complex between **43** and **44** was found to be as high as 5×10^7 M^{-1} in chloroform, as determined from fluorescence energy transfer studies.[133] In addition, the self-association constant for both functionalities was found to be negligible (**43**, $K_{dimer} < 10$ M^{-1}; **44**, $K_{dimer} = 200$ M^{-1}). The formation of supramolecular polymers was studied with solution viscometry as a function of the ratio **43**:**44**, which yielded a maximum in specific viscosity at a 1:1 ratio. Also at this ratio, the specific viscosity was considerably higher than for solutions of either **43** or **44** (Figure 11).

Because ^{1}H NMR confirmed heterocomplexation, the combined results strongly suggest an alternating chain growth. Although dynamic light scattering confirmed the formation of larger aggregates, a fraction of oligomeric material was also present. This was explained by the authors as being caused by a kinetic barrier in the self-assembly process that separates the small and large aggregates.

Chart 6

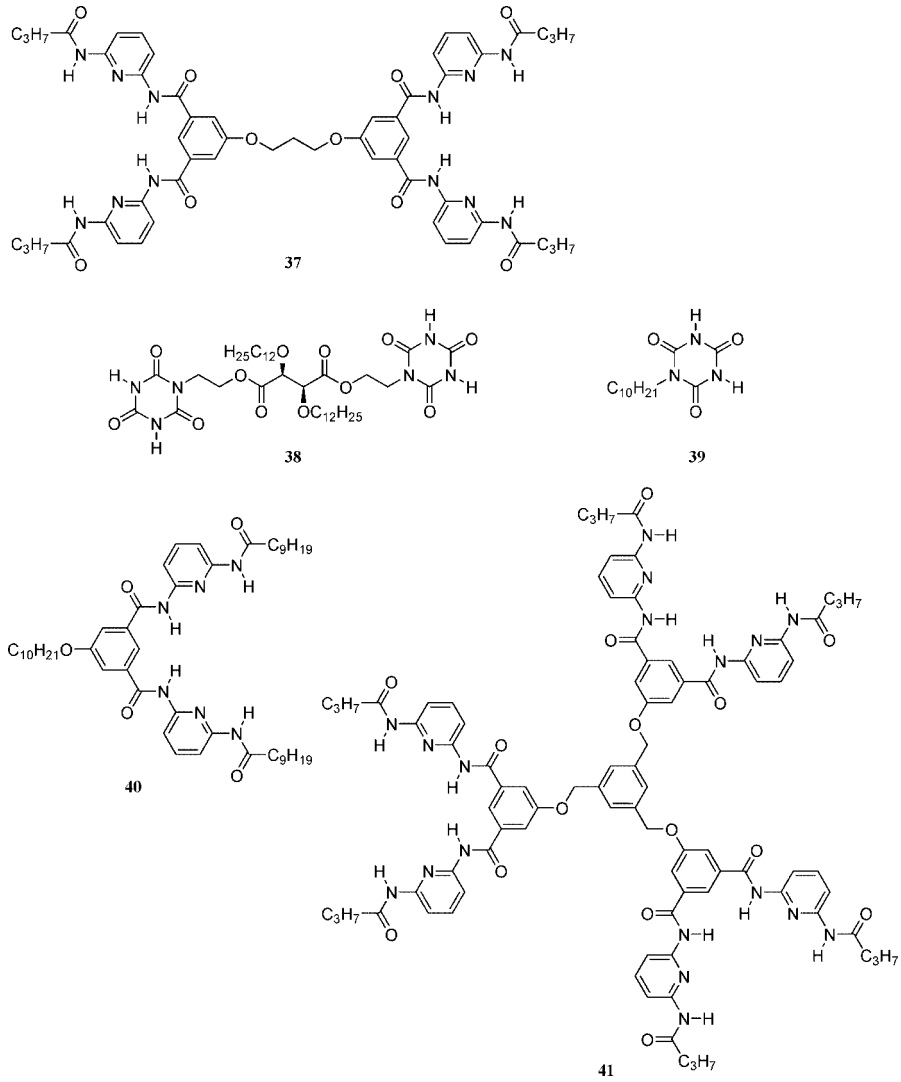

Chart 7

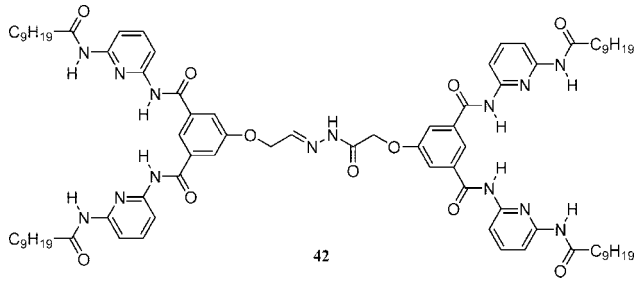

Using the same hydrogen-bonding complex, Zimmerman and co-workers also showed the possibility to append DAN or UG functionalities to a polymer backbone to have more control over the physical properties and to prepare polymer blends.[134−136]

Our research group has reported on the supramolecular polymerization of homoditopic 2-ureido-pyrimidinone (UPy) derivatives (**45**, Chart 9). The ureido-pyrimidinone unit displays a very strong self-complementary quadruple hydrogen-bonding array in which the donor (D) and acceptors (A) are arranged either in a DDAA array or in a DADA array (Scheme 3) depending on the nature of the substituent of the pyrimidinone ring.[137,138]

Chart 8

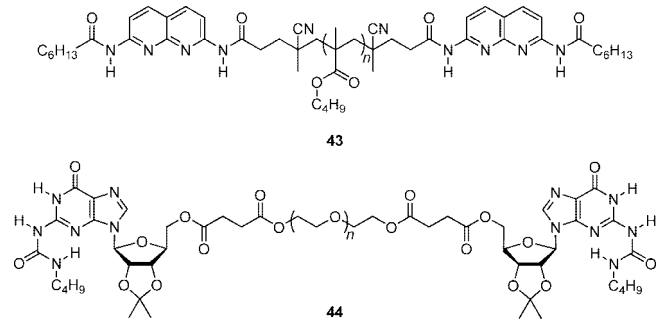

As a result of the high number of attractive secondary interactions, the DDAA array of the 2-ureido-4[1*H*]-pyrimidinone dimer displays a dimerization constant of 6×10^7 M^{-1} in chloroform[139] and is therefore ideally suited to create high molecular weight supramolecular polymers via an isodesmic growth mechanism.

Bifunctional derivative **45** (Chart 9), containing two ureido-pyrimidinone units tethered with an aliphatic hexyl spacer, yields viscous solutions in chloroform at concentrations as low as 40 mM. The observed viscous behavior is a direct result of the formation of long supramolecular chains in solutions by reversible hydrogen bonding. Titration of monofunctional stopper **46** (Chart 9) to solutions of su-

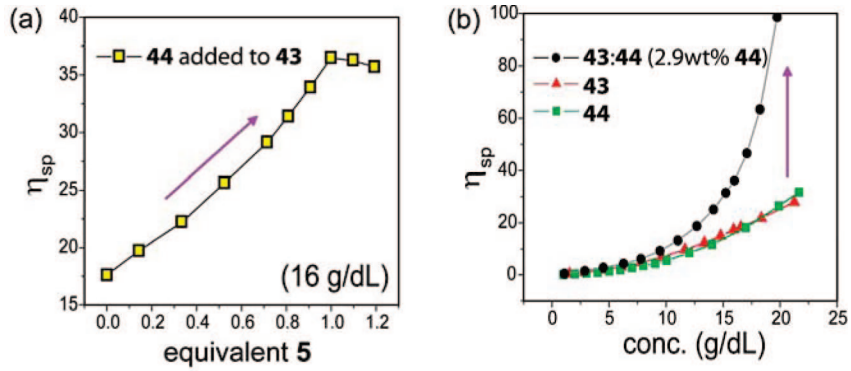

Figure 11. (a) Specific viscosity of a 16 g dL^{-1} solution of **43** in chloroform with **44** added; (b) specific viscosity of chloroform solutions of **43**, **44**, and a 1:1 mixture of **43**:**44** versus concentration. (Reprinted from ref 132. Copyright 2006 American Chemical Society.)

Chart 9

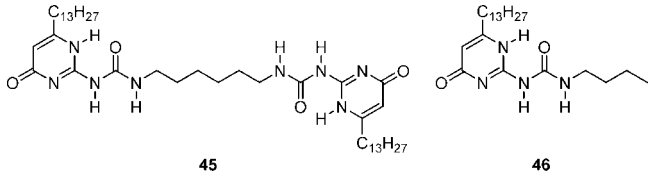

45 **46**

Scheme 3

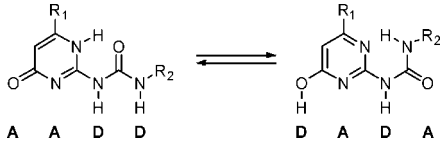

pramolecular polymer $[\mathbf{45}]_n$ in chloroform results in a monotonic decrease of the specific viscosity (Figure 12) as a result of a concomitant decrease in the average degree of polymerization.[22] Fitting of the specific viscosity as a function of **46** assuming an isodesmic polymerization of **45** (with an estimated K_{dim} of 2.2×10^6 M^{-1}) resulted in an estimated degree of polymerization of $DP_N = 700$ for pure **45** at 40 mM. Additionally, these experiments highlight the inherent reversibility in supramolecular polymers.

Further analysis of the supramolecular polymerization process of UPy derivatives with different aliphatic spacers revealed that in some cases the solutions contain significant amounts of macrocyclic polymers. The formation of supramolecular rings from linear supramolecular polymers will be the subject of discussion of the next chapter.

Using hydrogen-bonding assemblies of melamine derivatives with complementary cyanurates, barbiturates, or mercyanine derivatives, Kitamura and co-workers have reported various supramolecular polymers.[140−144] Although much of their work is aimed at the formation of organogels, supramolecular copolymers based on the melamine−cyanuric acid system have also been reported in solution (**47**−**49**, Chart 10).[145,146]

The marginal structural difference between **47** and **48** in length of the alkyl linker was found to have a distinct influence on the resulting supramolecular structures. Whereas for **47**:**49** only discrete dimeric structures were observed, for **48**:**49** supramolecular polymers were formed in methylcyclohexane. Evidence for the formation of the supramolecular structures was obtained from variable-temperature UV−vis spectroscopy, suggesting that also $\pi-\pi$ interactions are involved during the supramolecular polymerization. The degree of aggregation was determined as a function of temperature, which showed a sigmoidal transition, indicative of an isodesmic growth mechanism (Figure 13).[147] Addition of **49** to **47** resulted in an increased thermal stability, as visible from the higher transition temperature. This was explained by the formation of a discrete, stable dimeric structure held together with 12 hydrogen bonds. Upon addition of **49** to **48**, only a small decrease in thermal stability was observed, which was explained by the generation of different types of supramolecular species through triple hydrogen bonding. Further support for the formation of discrete versus polymeric species for **47**:**49** and **48**:**49**, respectively, was obtained from dynamic light scattering and atomic force microscopy (AFM).

Using 2-fold hydrogen bonding, the group of Wärnmark reported the formation of a helical, tubular supramolecular polymer. They prepared a homoditopic monomer based on an enantiomerically pure bicycle[3.3.1]nonane skeleton functionalized with two self-complementary 2-pyridone groups (**50**, Chart 11).[148]

The formation of supramolecular polymers of **50** was monitored using concentration-dependent ^{1}H NMR spectroscopy in chloroform and dichloromethane (DCM). The NH proton resonance of the 2-pyridone moiety showed a clear concentration dependence, which could be modeled with the isodesmic binding isotherm, yielding a K value of 1.1×10^3 M^{-1} in deuterated dichloromethane and a value of 0.11×10^3 M^{-1} in deuterated chloroform at 299 K. This shows that the more acidic chloroform is a stronger competitor for hydrogen bonding than dichloromethane. Performing the ^{1}H NMR experiments at different temperatures allowed the determination of the ΔH_p and ΔS_p of association, which were both negative in value, indicating an enthalpy-driven supramolecular polymerization.

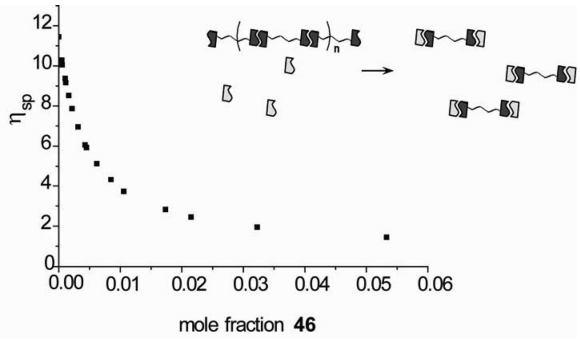

Figure 12. Effect of the addition of supramolecular chain stopper **46** on the specific viscosity of a 40 mM solution of **45** in chloroform. (Reprinted with permission from ref 22. Copyright 1997 American Association for the Advancement of Science.)

Chart 10

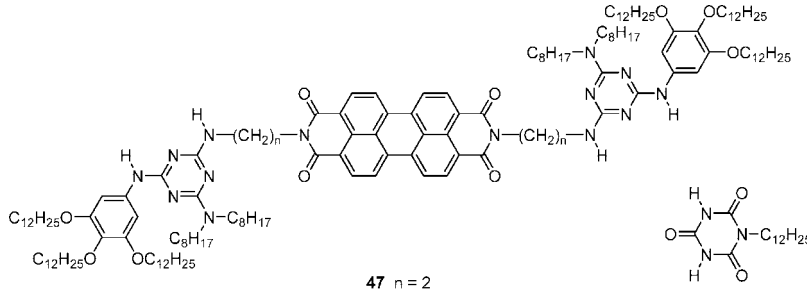

47 n = 2

48 n = 3

49

VPO was performed to exclude that only a monomer−dimer equilibrium is operative and also resulted in a value for the equilibrium constant comparable to the value obtained from the NMR measurements. However, for **50** in chloroform at 313 K, from VPO a degree of polymerization was found of only 4, which shows the detrimental effect of a low association constant on the DP_N in an isodesmic mechanism. Furthermore, UV−vis spectroscopy ruled out that $\pi-\pi$ stacking contributes to aggregation, whereas the formation of helical assemblies was detected with circular dichroism.

2.3.2.2. Supramolecular Polymers Based on Inclusion Complexes. A second type of noncovalent interaction by which supramolecular polymers can form is based on the formation of an encapsulation complex by reversible host−guest interactions. The research group of Rebek Jr. elegantly showed the formation of supramolecular polymers based on two calix[4]arene tetraureas covalently connected at their lower rims (**51**, Chart 12).[149] Encapsulation of ditopic guest molecules yielded supramolecular polymers.[150]

^{1}H NMR studies in deuterated chloroform performed on solutions of **51** revealed that polymeric species were formed by encapsulation of solvent molecules, as was deduced from the chemical shifts and the broadening of the signals. Fluorescence resonance energy transfer studies on dye-labeled calixarenes provided association constants for the aryl urea derived calixarene **51** of 2.4×10^6 M^{-1} in chloroform and 4×10^7 M^{-1} in benzene.[151]

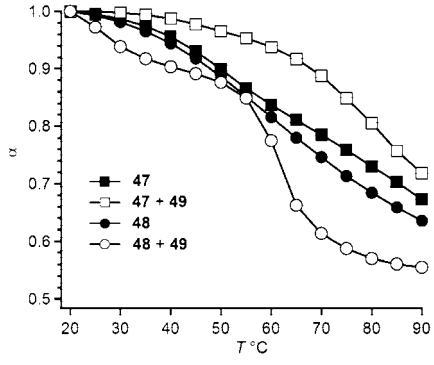

Figure 13. Fraction of aggregated molecules versus temperature for **47**, **48**, **47**:**49**, and **48**:**49**. (Reprinted from ref 145. Copyright 2008 American Chemical Society.)

Chart 11

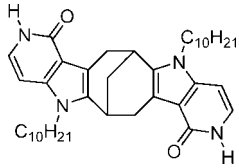

50

Upon addition of *p*-difluorobenzene to a chloroform solution of **51**, the encapsulated solvent was replaced by the guest molecule due to a higher association constant of this guest while keeping the polymeric structure intact. Addition of a monotopic end-capper restored the sharpness of the NMR signals, showing depolymerization of the supramolecular polymer in favor of the formation of discrete, oligomeric complexes.

Further characterization of the supramolecular polymers formed by **52** was performed by solution viscometry studies in *o*-dichlorobenzene.[152] A clear transition from the dilute to semidilute concentration regime at a concentration of 0.6% by weight was observed (Figure 14A). Addition of methanol to a viscous solution of **52** decreased the viscosity 2 orders of magnitude due to the disruption of the hydrogen-bonded assembly (Figure 14B). Removal of the methanol by simply heating the solution to 50 °C restored the polymeric structure as evidenced by the restoration of the solution viscosity to its initial value, showing the reversibility of the system. Rheology studies on a solution of **52** in *o*-dichlorobenzene revealed that the polymer maintained its physical integrity under flow field deformation. Furthermore, in concentrated chloroform solutions, liquid crystalline phases were formed,[153] from which highly ordered fibers were drawn with a tensile strength on the order of 10^8 Pa.

Rebek and co-workers also exploited the fact that calix[4]arenes with aryl urea and sulfonyl urea derivatives will exclusively form heterodimers.[154] By preparing the homoditopic derivatives (**53** and **54**), as well as a heteroditopic derivative (**55**), polymeric assemblies were obtained in which informational content was preserved.

Rudkevich et al. reported on amine-functionalized monotopic and ditopic calix[4]arene monomers that form su-

Chart 12

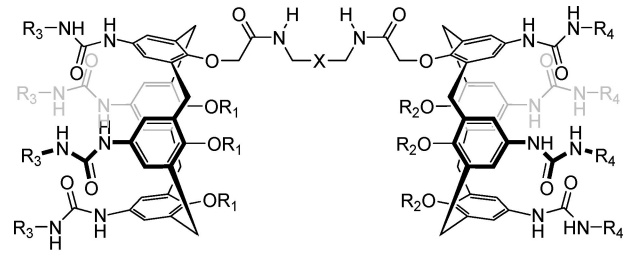

51	$R_1 = R_2 = C_3H_7$	$R_3 = R_4 = C_6H_4$-*p*-CH_3	X = *p*-C_6H_4
52	$R_1 = R_2 = C_{10}H_{21}$	$R_3 = R_4 = C_6H_4$-*p*-CH_3	X = *p*-C_6H_4
53	$R_1 = R_2 = C_3H_7$	$R_3 = R_4 = C_6H_4$-*p*-C_7H_{15}	X = *p*-C_6H_4
54	$R_1 = R_2 = C_{10}H_{21}$	$R_3 = R_4 = SO_2C_6H_4$-*p*-CH_3	X = $(CH_2)_6$
55	$R_1 = R_2 = C_3H_7$	$R_3 = C_6H_4$-*p*-C_7H_{15}, $R_4 = SO_2C_6H_4$-*p*-CH_3	X = *p*-C_6H_4

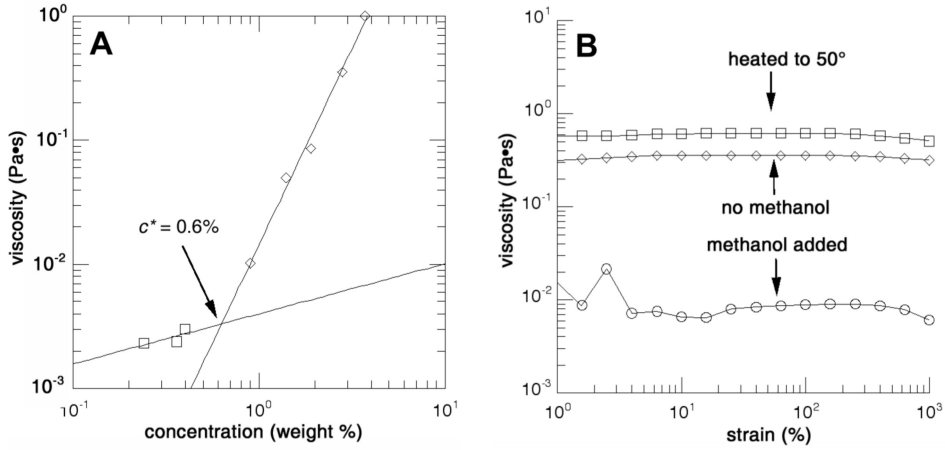

Figure 14. (A) Viscosity of **52** in *o*-dichlorobenzene as a function of concentration; (B) viscosity of a 2.8% solution of **52** in *o*-dichlorobenzene before and after addition of methanol and after heating to 50 °C. (Reprinted with permission from ref 152. Copyright 2000 National Academy of Sciences, U.S.A.)

pramolecular polymers, as was evidenced by ^{1}H NMR, viscometry, and chain-stopper experiments. Introduction of CO_2 resulted in the formation of the supramolecular polymer in the case of the monotopic monomer and in cross-linking for the ditopic monomer, because the amino group reacts with CO_2 to form carbamate salt bridges.[155−157] Haino et al. used ditopic calix[5]arenes with ditopic fullerene-functionalized monomers to prepare supramolecular polymers.[158]

Dalcanale and co-workers reported on a new class of supramolecular polymers based upon the complexation of methylpyridinium guests by tetraphosphonate cavitands.[159] These cavitands are resorcinarene-based molecular receptors presenting four phosphonate moieties as bridging units, which can complex positively charged species with very high association constants, $K = 10^7-10^9$ M^{-1}.[160] In their paper a tetraphosphonate cavitand was functionalized with a single methylpyridinium unit at the lower rim, yielding a heteroditopic monomer. Isothermal titration calorimetry (ITC) on a mixture of this heteroditopic monomer and a (monotopic) tetraphosphonate ligand yielded an association constant exceeding 10^7 M^{-1}. Moreover, on the basis of the ITC results, the complexation was found to be driven not only by enthalpy but also by entropy, showing the importance of solvation. With static light scattering (SLS) an increase in molecular weight of the polymer in solution with increasing concentration was observed. With SLS also the effect of introduction of a monotopic (end-capper) or tetratopic monomer (cross-linker) could be observed, which resulted in a decrease or increase in the averaged molecular weight, respectively. Finally, the disassembly of the polymer upon addition of a competing guest (*N*-butylmethylammonium iodide), acting as an end-capper, was monitored with ^{1}H NMR.

Besides calixarenes, cyclodextrins have also been used to prepare supramolecular polymers based on reversible host−guest interactions. Harada and co-workers have prepared various supramolecular polymers in water using cyclodextrins together with a suitable functional group as a guest, as recently reviewed by them.[25] A supramolecular polymer studied in detail is based on heteroditopic monomer **56** (Chart 13), which was prepared by coupling of a cinnamic acid derivative to an amino group at the 3-position of an α-cyclodextrin (α-CD). Earlier studies had already revealed that α-CD can accommodate a cinnamic acid derivative in its cavity with a high association constant.[161]

Chart 13

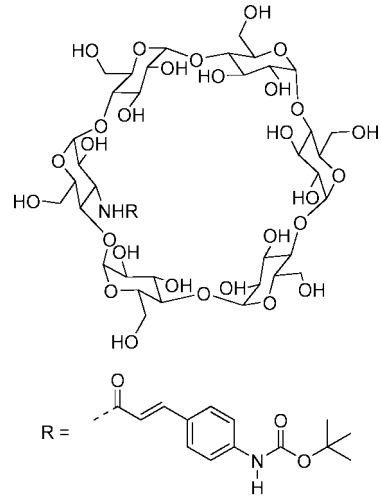

56

Concentration-dependent ^{1}H NMR studies on solutions of **56** in water revealed strong upfield shifts of the protons of the cinnamoyl moiety, which were related to the formation of intermolecular complexes.[162] 2-D ROESY NMR revealed a rotational nuclear Overhauser effect between the protons on the cinnamoyl moiety and the inner protons of the α-CD part, indicating that the ^{t}Boc group is deeply included in the α-CD cavity. The increase in size of the supramolecular polymers as a function of concentration was verified by VPO, revealing an increase in molecular weight with increasing concentration. Furthermore, pulsed field gradient NMR measurements as a function of concentration showed a decreasing diffusion coefficient, which is in agreement with an increasing size of the aggregates. This was further supported by solution viscometry. Finally, with turbo ion spray mass spectrometry, oligomers up to the 14-mer were detected.

Interestingly, for solutions of **56** a concentration-dependent circular dichroic effect was observed, which indicates the presence of a helical supramolecular polymer in water.[162] The CD effect was found to increase nonlinearly with concentration, which was interpreted as cooperative transfer of chirality from the molecular to the supramolecular level. Adding native α-CD resulted in a decrease in CD intensity, showing that the native α-CD acts an end-capping agent that breaks down the supramolecular polymer.

Chart 14

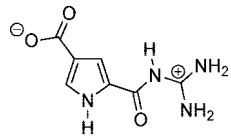

57

In subsequent work Harada and co-workers also combined α-cyclodextrins and β-cyclodextrins, to arrive at supramolecular copolymers with an alternating structure[163] or that form a supramolecular [2]rotaxane polymer.[164] The characterization of these supramolecular polymers was performed with the above-mentioned techniques (^{1}H NMR, 2D NMR, VPO, circular dichroism). Furthermore, β-cyclodextrins were covalently linked to obtain homoditopic monomers, which were shown to form supramolecular polymers upon addition of a homoditopic guest containing adamantyl groups.[165,166]

2.3.2.3. Supramolecular Polymers Based on Coulombic Interactions. Coulomb interactions occur between permanent charges and dipoles and may be of the ion−ion (ion pair), ion−dipole, or ion−quadrupole type. Attractive interaction occurs between fixed and complementary ionizable groups and is modulated by co- and counterions. Ion−ion type Coulombic interactions are nondirectional, but are among the strongest of all noncovalent interactions. Because of the high strength of Coulombic interactions in solvents of high polarity, it is possible to create supramolecular polymers in water.[167,168]

One example of a supramolecular polymer that is formed in polar medium due to Coulombic interactions was reported by Schmuck, who used a zwitterionic monomer (**57**, Chart 14).[169]

Concentration-dependent^{1}H NMR in deuterated dimethyl sulfoxide (DMSO) showed clear broadening of the resonance of the guanidinium NH proton. The change in chemical shift upon increasing concentration was fitted with a dimerization model, yielding a K_{dim} value of 22.2 M^{-1}. However, because oligomers longer than the dimer were formed, the data are better analyzed with the isodesmic model (which would yield a K value of 44.4 M^{-1}). Considering the low association constant, high concentrations (up to 0.1 M) were necessary to observe oligomerization of **57**. However, even for a concentration of 0.1 M in DMSO, still only short oligomers were formed, with a DP_N of only 2.5. As was also noted by the authors, to increase the DP_N concentrations even higher than 0.1 M are required.

Furthermore, by performing the NMR experiments at different temperatures, the enthalpic and entropic contributions to supramolecular polymerization were determined. This revealed that both the ΔH_p and ΔS_p values were positive, indicating that the polymerization is entropy-driven.

Huang and Gibson reported the formation of supramolecular polymers based on a homoditopic cylindrical bis(crown ether) host (**58**) in combination with a bisparaquat derivative (**59**, Chart 15).[170]

Due to the rigidity of the structures of both monomers, no cyclic species could be formed in solution, and only linear supramolecular poly[3]pseudorotaxanes were formed. This was supported by variable-concentration ^{1}H NMR, mass spectrometry, viscometry studies, and chain-stopper experiments.

Gattuso et al. and Pappalardo et al. reported on supramolecular polymers based on the complex formed by alkylammonium ions and calix[5]arenes, using either homoditopic[171] or heteroditopic monomers.[172] ^{1}H NMR dilution experiments, diffusion-ordered NMR spectroscopy, and electron spray ionization mass spectrometry confirmed the formation of supramolecular polymers, whereas further analysis of the NMR data allowed for the determination of association constants.

2.3.2.4. Supramolecular Polymers Based on Metal−Ligand Coordination. Also, metal coordination has been used to prepare one-dimensional supramolecular polymers,[173−180] although the kinetic inertness of many metal−ligand interactions puts these examples out of the scope of this review. Few examples of kinetically labile coordination polymers, which form one-dimensional structures in solution, have been reported in the literature. One of the earliest examples of this class of supramolecular polymers was reported by the group of Rehahn on labile Ag(I) and Cu(I) complexes.[181,182] Furthermore, Craig and co-workers showed that the main-chain dynamics of a supramolecular polymer based on NCN−pincer−metal−ligand complexes was enhanced by tuning the bulkiness of the alkyl ligand.[183] Using ^{1}H NMR, viscometry, and quasi-elastic light scattering, they showed that supramolecular coordination polymers were formed in 1:1 mixtures of **60**:**62** or **61**:**62** (Chart 16) in DMSO.

For supramolecular polymers **60**:**62** and **61**:**62** similar results were obtained from viscometry and light scattering data, suggesting equilibrium structures that are nearly identical. ^{1}H NMR studies (coalescence and spin magnetization transfer studies), on monotopic model compounds, revealed a difference in dissociation rate of a factor of 50−100 between the complexes with an *N*-methyl (**60**) or an *N*-ethyl (**61**) substituent (70 and 1.0 s^{-1} at 25 °C, respectively). Yet under these conditions nearly identical association constants for the two model compounds were determined, again suggesting similar equilibrium structures. This study showed that steric effects in a ligand exchange process offer a mechanism to study and also control the dynamic properties in supramolecular polymers. Recently, the contribution of kinetics (and thermodynamics) in supramolecular polymers to their mechanical properties was reviewed by Serpe and Craig.[184]

Weck and co-workers recently reported on main-chain supramolecular alternating block copolymers based on A−A and B−B bifunctional macromonomers in which the reversible AB interaction is based on the complexation of Pd−pincer complexes with functionalized pyridines.[185] The obtained macromonomers were synthesized without the use of postpolymerization functionalization using ring-opening metathesis polymerization (ROMP). Concentration-dependent viscometry clearly shows the formation of supramolecular polymers of which the degree of polymerization could be influenced by the addition of $AgBF_4$. The use of polymeric spacers results in a negligible concentration of cycles as was evidenced by the absence of a critical concentration in the specific viscosity versus concentration plots (vide infra).

2.4. Concluding Remarks on Isodesmic Supramolecular Polymerization

A closer look at the common features in the molecular structure of the systems discussed above shows that the orientation of all the bonds in the molecule is independent of its position in the supramolecular polymer or in its monomeric state. This suggests that the monomers do not need to adopt a high-energy conformation to allow for incorporation into the supramolecular polymer, which would

Chart 15

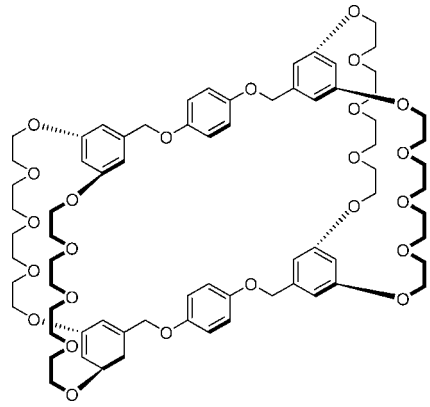

58

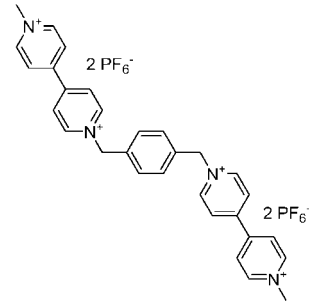

59

Chart 16

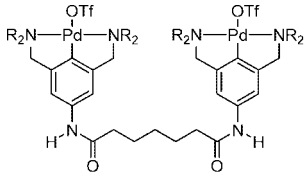

60 R = Me
61 R = Et

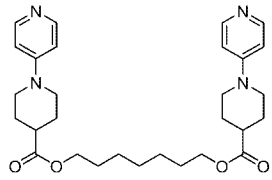

62

result in a cooperative supramolecular polymerization (vide infra). Apparently, this even holds for the slightly twisted C_3-symmetrical bipyridine discotics as well as for the twisted perylene compounds. As will be discussed later, the formation of chiral, helical structures is often associated with a cooperative growth mechanism due to the fact that the number of interactions formed upon subunit addition changes when the first loop of the helix is closed. Although in some of the discussed examples, chiral supramolecular polymers are being formed, the lack of cooperative growth in these structures is most probably the result of a large helical pitch, resulting in a weak average contact energy between nonadjacent units.

For electronically uncoupled monomers in which the binding groups are separated by a spacer, binding of one end group to another does not influence the reactivity of the other end group connected to the same spacer, which is a prerequisite for an isodesmic mechanism. Although the use of flexible spacers between two end groups can result in cycle formation (vide infra), the lack of cycles in the discussed examples is most likely the result of a low intermolecular binding constant, which hampers the observation of a true critical concentration at which the cycles ring open to form polymers or due to the fact that the spacers employed in these examples are either too long, too short, or too rigid.

In contrast, for the rigid discotic molecules in which the two end groups are electronically coupled, noncovalent association of one side of the monomer to another can result in a change of reactivity of the other side. It appears both from theory and from the discussed examples that nonnearest-neighbor interactions are negligible in most supramolecular polymerizations in which $\pi-\pi$ stacking is the dominant attractive force between the monomers, especially in apolar solvents.

3. Ring−Chain Supramolecular Polymerization

3.1. Definition and Covalent Counterpart

The second class of supramolecular polymerizations is represented by the reversible polymerization of a ditopic monomer in which each linear aggregate (including the monomer) in the assembly pathway is in equilibrium with its cyclic counterpart. In most examples of supramolecular polymers that will be encountered in this section, two reversibly associating end groups are connected via a flexible hydrocarbon tether.

As early as 1933, Carothers and co-workers[186,187] analyzed the formation of cyclic monomers and dimers using the depolymerization of covalent condensation polymers in the melt with the aid of a catalyst. In these insightful studies, Carothers convincingly showed that the yield of the cyclic products was highly dependent on both the number of atoms and the presence of oxygen substituents in the macrocyclic ring. Subsequent quantitative studies by Stoll and Rouvé[188] on the ring−chain polymerization of ω-hydroxy-n-alkyl carboxylic acids allowed for the first time the determination of the equilibrium constant for cyclization as a function of chain length.

It is now generally understood that the products of most step growth covalent polymerizations, whether under kinetic or under thermodynamic control, usually contain a few percent by weight of macrocyclic oligomers.[37,189,190] Moreover, detailed studies have shown that the yield of cyclic byproducts in covalent polymerizations is intimately linked to the conformational properties of the hydrocarbon chain separating the reactive end groups in the monomer.[191] An example of a covalent polymerization in which oligomeric rings are formed under kinetic control is the polycondensation of triethylene glycol (TEG)/hexamethylene-diisocyanate in the bulk at elevated temperatures.[192] If the linkages in the chain of a step growth polymer are reversibly broken and re-formed, an equilibrium is set up between oligomeric rings and linear chains. A well-studied example of a ring−chain equilibrium under thermodynamic control is the catalyzed equilibrium polymerization of disubstituted siloxanes as first reported by Scott[193] and analyzed in detail by Brown et al.,[194] Carmichael et al.,[195] and Semlyen and Flory.[196] Other examples of covalent ring−chain polymerizations under thermodynamic control are the entropically driven ring-opening metathesis polymerization of macrocyclic olefins[197] and the ring−chain polymerization of liquid sulfur.[198−200]

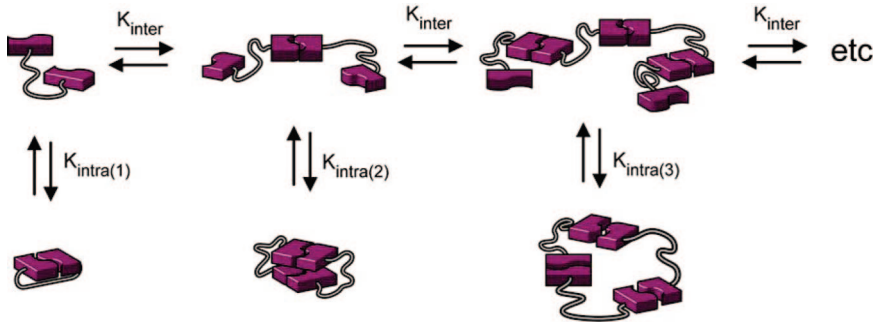

Figure 15. Schematic representation of a ring−chain supramolecular polymerization in which K_{inter} (M^{-1}) represents the intermolecular binding constant for bimolecular association and $K_{intra(i)}$ represents the dimensionless intramolecular equilibrium constant for *i*th ring closure.

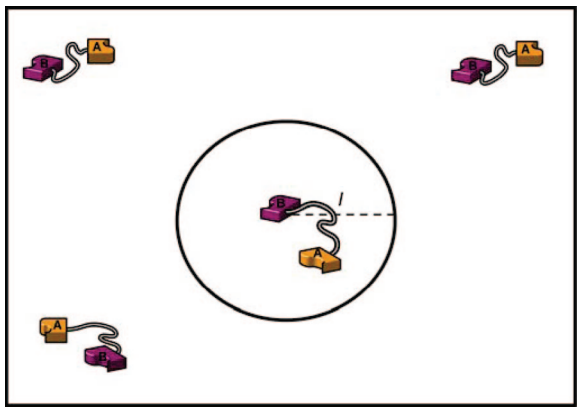

Figure 16. Schematic representation of the concept of effective concentration illustrated using a ditopic monomer substituted with two reversible associating end groups A and B. Because end group A cannot escape from the sphere of radius *l*, equal to the full length of the chain, end group B experiences an effective concentration of A. If this effective concentration is higher than the actual concentration of A end groups in solution, intramolecular association between A and B is favored.

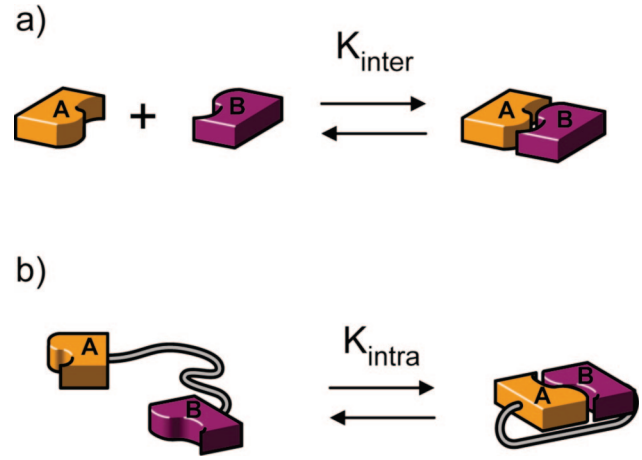

Figure 17. (a) Reversible association between two end groups (A and B) of a supramolecular monomer is characterized by an intermolecular equilibrium constant K_{inter} (M^{-1}); (b) when the two end groups are tethered to each other, the equilibrium constant, K_{intra}, is dimensionless and is related to K_{inter} by the effective molarity, *EM*.

In contrast to covalent polymerizations, macrocyclization reactions in supramolecular polymerizations always occur under thermodynamic control due to the fast association and dissociation of the reversible interaction.

3.2. Thermodynamic Aspects of Ring−Chain Supramolecular Polymerization

Supramolecular ring−chain polymerizations are characterized by the fact that linear oligomers and polymers are in equilibrium with their cyclic counterpart (Figure 15). As is the case in covalent polymerizations, the tendency for reversible intramolecular cyclization is largely determined by the conformational properties of the linker separating the two reversibly associating end groups (vide infra).

In the early 1930s Kuhn[201] introduced the concept of effective concentration (C_{eff}) to provide a relationship between the mean squared end-to-end length of a polymer chain obeying Gaussian statistics and the cyclization probability of the end groups. Furthermore, he predicted that the cyclization probability would decrease as $N^{-3/2}$, where N is the number of bonds in the chain. The effective concentration can be thought of as the local concentration of one chain end in the vicinity of the other chain end of the same molecule (Figure 16). Hence, the C_{eff} theoretically quantifies the advantage for an intra- versus an intermolecular interaction.

Theoretical methods from polymer physics can calculate the effective concentration as a function of chain length using random-flight statistics.[202] For long, flexible random-coil polymers under theta conditions, the distribution function of chain ends is Gaussian to a reasonable approximation.[191] However, as has been pointed out by Morawetz and Goodman,[203] the Gaussian chain model is only applicable for long, flexible chains. More recently, Zhou developed a more realistic worm-like chain model to calculate the C_{eff} for short, semiflexible polypeptide chains.[204,205] Crothers and Metzger[206] have estimated C_{eff} using a particle-in-a-sphere approximation.

The theoretical concept of effective concentration is often replaced by the identical, but empirical, concept of effective molarity.[207−212]

Whereas effective concentration is based on concentrations calculated from the physical properties of the chain connecting two end groups, effective molarity denotes the ratio of the intra- and intermolecular equilibrium constant

$$EM = \frac{K_{intra}}{K_{inter}} \quad (1)$$

in which K_{inter} (M^{-1}) is the association constant for an intermolecular model reaction and K_{intra} is the dimensionless equilibrium constant for the intramolecular reaction (Figure 17). Furthermore, when the chain separating the two end groups is considered to be strainless, the *EM* represents a pure entropic correction,[213] which applies when an intermolecular process is replaced by its intramolecular counterpart.

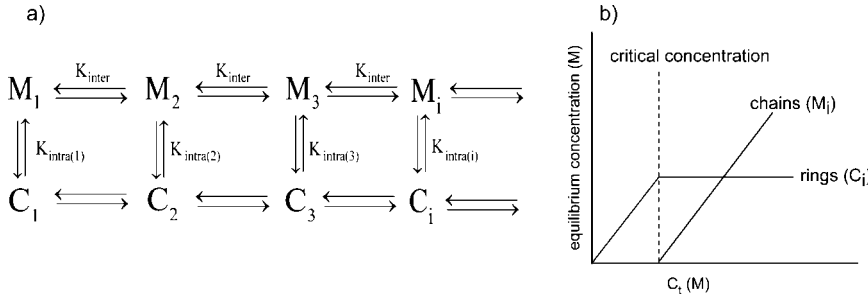

Figure 18. (a) Schematic display of a general ring−chain supramolecular polymerization defined by the intermolecular equilibrium constant K_{inter} (M^{-1}) and the intramolecular, dimensionless equilibrium constant for *i*th ring closure, $K_{intra(i)}$: (b) relationship between the total concentration of a ditopic monomer in dilute solution (C_t) and the equilibrium concentration of chains (M_i) and rings (C_i) in a ring−chain supramolecular polymerization displaying a critical concentration.

In the supramolecular polymerization of a bifunctional AB type monomer, the *EM* represents the limit concentration of the monomer below which cyclization is more favored than linear oligomerization. The effective molarity sets a common empirical scale for different cyclization reactions, and as such provides an absolute measure of the ease of cyclization of bifunctional substituted monomers that reversibly polymerize via noncovalent interactions.

Theoretical distributions of cyclic and linear products in thermodynamically controlled step-growth polymerizations were first described[214] by Jacobson and Stockmayer (JS), who pointed out the existence of a critical concentration, below which the system is composed of cyclic products only and above which the concentration of cyclic species remains constant and excess monomer only produces linear species. They also related the equilibrium constant for cyclization to the cyclization probability of the chain, thereby providing a direct link between the effective molarity and the effective concentration. Furthermore, they showed that the equilibrium constant for cyclization would decrease as $N^{-5/2}$ due to the fact that the cyclized polymer could reopen in *N* different ways. Ercolani[210] extended the treatment of JS to describe the distribution of cyclic oligomers under dilute conditions and a wide range of association constants. He pointed out that the phenomenon of a critical concentration is manifested only when the intermolecular association constant is sufficiently high ($>10^5$ M^{-1}). Recently, Ercolani et al. summarized[215] the assumptions of the JS theory: (1) the thermodynamic reactivity of the end groups is independent of the chain length; (2) all of the rings are strainless; (3) the end-to-end distribution function of a chain in solution is Gaussian; (4) the mean squared end-to-end distance is proportional to the number of skeletal bonds (i.e., theta conditions are assumed); and (5) the cyclization probability depends on the fraction of configurations for which the ends coincide without taking into account the torsional states of the polymer chain (i.e., no angle corrections are considered). This last point was addressed specifically by Flory and co-workers[196,216] in terms of the rotational isomeric state model. It is recognized that all of these assumptions must fail for short chains.

As most supramolecular polymerizations occur in relatively dilute solutions, the model proposed by Ercolani[210] is eminently suited to describe the equilibrium between cyclic and linear species in these equilibrium polymerizations. In contrast to an isodesmic polymerization, which is characterized by a single thermodynamic constant, the ring−chain model developed by Ercolani et al. is characterized by two distinct thermodynamic constants (Figure 18), that is, the intermolecular binding constant (K_{inter}) and the intramolecular binding constant for *i*th ring closure ($K_{intra(i)}$).

When all cycles are considered to be strainless and obey Gaussian statistics, the EM_i values for $i > 1$ can be conveniently written as a function of EM_1 (the effective molarity of the bifunctional substituted supramolecular monomer)

$$EM_i = \frac{K_{intra(i)}}{K_{inter}} = EM_1 i^{-5/2} \qquad (2)$$

in which *i* represents the degree of polymerization.

The presence of a critical concentration in supramolecular ring−chain polymerizations leads to characteristic features not present in isodesmic supramolecular polymerizations. To illustrate this, the fraction of monomer present in linear species together with the weight- and number-averaged degrees of polymerization (DP_W and DP_N) for a general ring−chain equilibrium assuming strainless cycles was calculated for various values of $K_{intra(1)}$ and a value of K_{inter} of 10^6 M^{-1} using the model as proposed by Ercolani.[210,217] As the value of $K_{intra(1)}$ increases, the transition between cyclic and linear materials at the critical concentration becomes much sharper as is evident from Figure 19a. Furthermore, both number- and weight-averaged degrees of polymerization abruptly increase once the total concentration (C_t) exceeds EM_1, whereas the sharpness of the transition depends on the value of $K_{intra(1)}$. This situation is in contrast with an isodesmic polymerization in which the degree of polymerization rises gradually as the concentration is increased. At high total concentration, isodesmic and ring−chain equilibria become indistinguishable and both the number- and weight-averaged degrees of polymerization are equal at a given concentration far above EM_1 (Figure 19b,c).

In a good solvent, for which excluded volume effects need to be taken into account, the exponent of 5/2 in eq 2 is expected to become somewhat larger.[191,218−220]

Recently, Dormidontova and co-workers investigated[221] the influence of spacer rigidity on the ring−chain equilibrium of supramolecular polymers. Monte Carlo simulations on ring−chain supramolecular polymerizations, in which hydrogen bonds were used as the reversible interaction, have shown that the critical concentration is strongly influenced by the rigidity of the spacer. From these studies it was found that the critical concentration decreases in the order rigid, semiflexible, flexible when all other factors such as spacer length and interaction energy between the end groups are considered to be constant. For semiflexible and rigid polymers, the probability of finding spacer ends within a

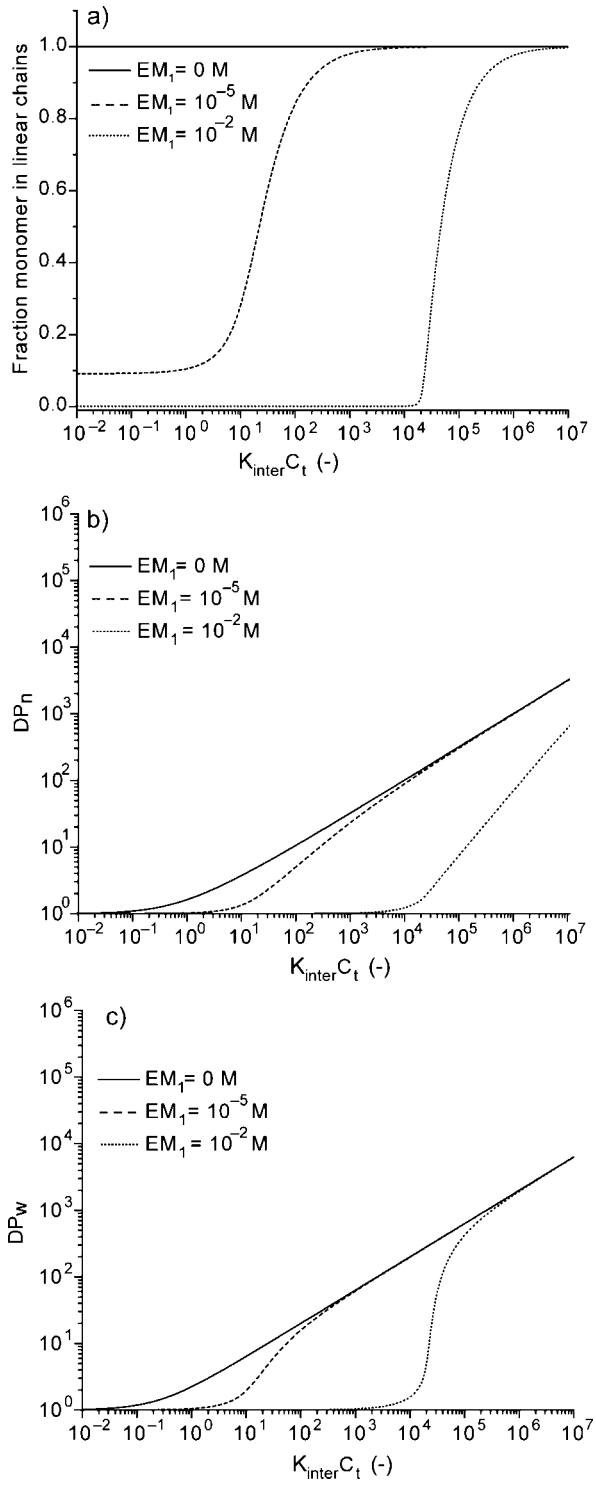

Figure 19. (a) Fraction of monomer present in linear chains as a function of the dimensionless concentration $K_{inter}C_t$ for various values of EM_1 and a fixed value of K_{inter} (10^6 M^{-1}); (b) number-averaged degree of polymerization (DP_N) as a function of the dimensionless concentration $K_{inter}C_t$ for various values of EM_1; (c) weight-averaged degree of polymerization (DP_W) as a function of the dimensionless concentration $K_{inter}C_t$ for various values of EM_1.[216]

bonding distance is smaller than for flexible polymers, which results in a decrease in the total fraction of rings.

It is important to realize that ring−chain equilibria also exhibit a critical temperature (T_c) as was first shown by Gee[198] and later by Tobolsky and Eisenberg[199] and Harris[222] for the equilibrium polymerization of sulfur. At this critical temperature there is a transition in the equilibrium between cyclic species and high molecular weight linear chains. As has been discussed in the section of isodesmic supramolecular polymerizations, two limiting cases can be distinguished. In the first case, there exists a ceiling temperature *above* which high molecular weight polymer is thermodynamically unstable with respect to cyclic monomer; in the other case there exists a floor temperature *below* which high molecular weight polymer is thermodynamically unstable with respect to cyclic monomer. The concept of floor and ceiling temperatures was developed by Dainton and Ivin[74] to describe the propagation step of a general equilibrium polymerization. Polymerization reactions that have negative enthalpy and entropy changes associated with their propagation steps are characterized by a ceiling temperature, whereas polymerizations in which the changes in enthalpy and entropy of propagation are positive exhibit a floor temperature below which polymerization is not possible.

Although the theory of Dainton and Ivin provides an accurate thermodynamic description of the *cause* of a ceiling or floor temperature (i.e., change in enthalpy versus change in entropy), it does not yield any indication of the *sharpness* of this transition. Tobolsky and Eisenberg[223] first showed that the transition between cyclic and linear polymers can be extremely sharp at the critical temperature. In their theoretical investigations on the ring−chain equilibrium polymerization of cyclic sulfur (S_8) they elegantly showed that the sharpness of this transition is dependent on the ratio of inter- and intramolecular equilibrium constants. Interestingly, Wheeler[224−226] and co-workers have shown that the ring−chain theory of Tobolsky and Eisenberg can be considered as a mean-field approximation for a second-order phase transition in the Ehrenfest sense.

Most examples of covalent ring-opening polymerizations involve the opening of strained rings. Such polymerizations are mainly enthalpy driven and hence display a ceiling temperature above which virtually all species are cyclic (examples are the cationic polymerization of tetrahydrofuran and dioxolane). However, in some cases, ring-opening polymerizations can be driven by a gain in entropy and display a floor temperature. Examples of entropy-driven[227] ring-opening polymerizations are the ring-opening polymerization of cyclic S_8 in liquid sulfur[222] and the ring-opening metathesis polymerization of strainless, macrocyclic olefins.[197]

3.3. Examples of Supramolecular Polymerization Processes Involving Ring−Chain Equilibria

Our research group reported the isodesmic polymerization in dilute solutions of bifunctional ureido-pyrimidinone (UPy) derivatives equipped with an unsubstituted hexane spacer to form high molecular weight linear chains.[22] Detailed analysis of the supramolecular polymerization process by ^{1}H NMR spectroscopy and viscometry revealed that solutions of bifunctional UPy molecules in $CHCl_3$ always contain a certain amount of cyclic species in equilibrium with high molecular weight chains.[228] It was anticipated that selective preorganization toward cyclic species could be achieved by conformational effects in the spacer unit. To this end, a series of bifunctional UPy derivatives **63**−**70** with several substituted linear spacers was synthesized (Chart 17). Because the resonances corresponding to cyclic UPy dimers are in slow exchange on the NMR time scale with the signals of the linear UPy chains, ^{1}H NMR spectroscopy proved to be a

Chart 17

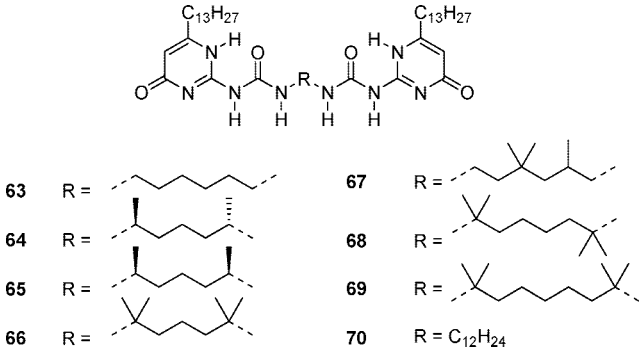

convenient technique to quantify the critical concentration for all UPy derivatives (Figure 20). Ubbelohde viscometry studies were used to confirm the presence and magnitude of the critical concentration. Indeed, the high binding constant of the UPy quadruple hydrogen bond array results in a true critical concentration as predicted by theory.[229]

At low concentrations all compounds formed cyclic dimers in solution, whereas at higher concentration linear polymers were obtained. However, the concentration-dependent specific viscosity of solutions of **63**−**67** in $CHCl_3$ (Figure 20a, inset) showed that for **63** extremely high viscosity at a concentration of 75 mM can be obtained, whereas solutions of **64** and **66** at this concentration are much less viscous due to a higher fraction of small cycles.

Substitution of the alkyl linker with methyl groups at the α-position relative to the urea of the UPy moieties strongly increases the concentration of cyclic dimers in solution. This change in critical concentration has been attributed to a shift in the equilibrium between the different *anti* and *gauche* conformations of the linker, resulting in a preferred conformation in which the methyl groups are positioned in an *anti* conformation with respect to the rest of the linker. In this way the UPy end groups become preorganized for cyclic dimer formation, which in turn results in a significant rise in the critical concentration.

An extreme case of structural rigidity is displayed by **71** (Chart 18), which forms cyclic dimers at all concentrations.[231] Hailes and co-workers showed that secondary interactions can also be employed to increase the tendency to cyclize.[232] Due to intermolecular hydrogen bonding between the carbamate amide and the carbonyl group of the pyrimidinone ring, a cyclic structure is enforced for compounds **73**−**75**. Especially in the case of **76**, the replacement of the hydrogen-bonding amide in the carbamate moiety significantly reduced the rigidity and enabled linear polymerization at high concentration. Besides the structural rigidity to induce ring formation, the conformation of the UPy moiety also plays a decisive role in this equilibrium.[233] When **63** and **72** were separately polymerized, the critical concentration was too low to be determined with viscometry as cyclization was strongly hampered by the flexibility of the alkyl linkers. However, the antiparallel arrangement of **72** enables the formation of heterodimeric cycles with **63** as evident from viscometry and diffusion-ordered spectroscopy (DOSY) of the mixture.

In contrast to UPy derivatives **63**, **65**, and **66**,[229] which are all examples of enthalpically driven supramolecular polymerizations, a remarkable example of an entropically driven supramolecular ring-opening polymerization from cycles to linear polymers is displayed by bifunctional UPy monomer **67**.[230] Heating solutions of **67** in $CHCl_3$ dramatically increased the viscosity of the solution, corresponding to a shift in the equilibrium toward linear chains at higher temperatures. More recently, the incorporation of π-conjugated elements between the UPy moieties also displayed ring formation for UPy containing oligofluorenes and oligo(*p*-phenylene vinylenes).[234] Ring formation was absent when a perylene bisimide derivative was used as a spacer between the two UPy end groups.

The supramolecular polymerization of an AB type heteroditopic monomer **77** (Chart 19) in dilute $CHCl_3$ solutions was also investigated.[235] In this system, the reversible AB interaction is based on the strong complementary quadruple hydrogen bond array between the hydrogen-bonding acceptor−donor−donor−acceptor (**ADDA**) array of 2-ureido-6[1*H*]-pyrimidinone with the complementary **DAAD** array of 2,7-diamido-1,8-naphthyridine[236,237] ($K_a = 6 \times 10^6$ M^{-1} in $CHCl_3$). Using concentration-dependent ^1H NMR and viscosity measurements, a sharp transition from cyclic species at low concentrations to linear species at high concentrations was observed. Due to the significantly lower association constant for heterocomplexation than homodimer formation, the naphthyridine derivatives act as chain stoppers, resulting in "self-stoppered" behavior and thereby limiting the degree of polymerization. The introduction of a dibutylamino group at the UPy moiety in **79** lowered the dimerization constant of the UPy dimer compared to that of the AB monomer **78** due to the stabilization of the enol form in **79**. However, the strength of the heterocomplexation was not affected.[84] This change resulted in a reduction of the "self-stoppered" effect at high concentration, whereas the ring−chain equilibrium was shifted toward an increase in cycle formation at lower concentration as a result of the higher fidelity for heterocomplexation.

The research groups of Stoddart and Williams have used pseudorotaxane formation as a key step in the supramolecular polymerization of crown ether derivatives with positively charged amines **80** and **81**. The charged amines are connected to a crown ether by a rigid aromatic linker (for examples, see Chart 20). Cyclic and linear structures were reported in solution as well as in the solid and gas phases.[238,239] Especially, cyclic dimeric structures of **80** showed remarkably high stability in solution, as evidenced by ^1H and ^{19}F NMR studies, as well as in the gas phase (using liquid secondary ion mass spectrometry) and in the solid state (by single-crystal X-ray diffraction).[240]

The [24]crown-8 ring in **80** was extended by one carbon atom to a [25]crown-8 ring in **81**. Again, the elegant combination of ^1H NMR and ^{19}F NMR allowed the determination of cyclic and linear oligomers, which now exceeded the dimeric state. In addition, the equilibrium constants for the formation of the different cycles and the linear species as schematically depicted in Figure 21 could be obtained. Van't Hoff analysis enabled the determination of the enthalpy and entropy of oligomerization and cyclization and showed that the formation of cycles larger than dimers was enthalpically favored. As an explanation it was suggested that the additional carbon atom in **81** disrupts the π−π interactions between the catechol moieties that are present in **80** that accounts for the high stability of the cyclic dimer in the case of the latter, whereas a multiplicity of cyclic structures can be observed for **81**.

Gibson and co-workers have reported cycle formation when a homoditopic crown ether-functionalized monomer

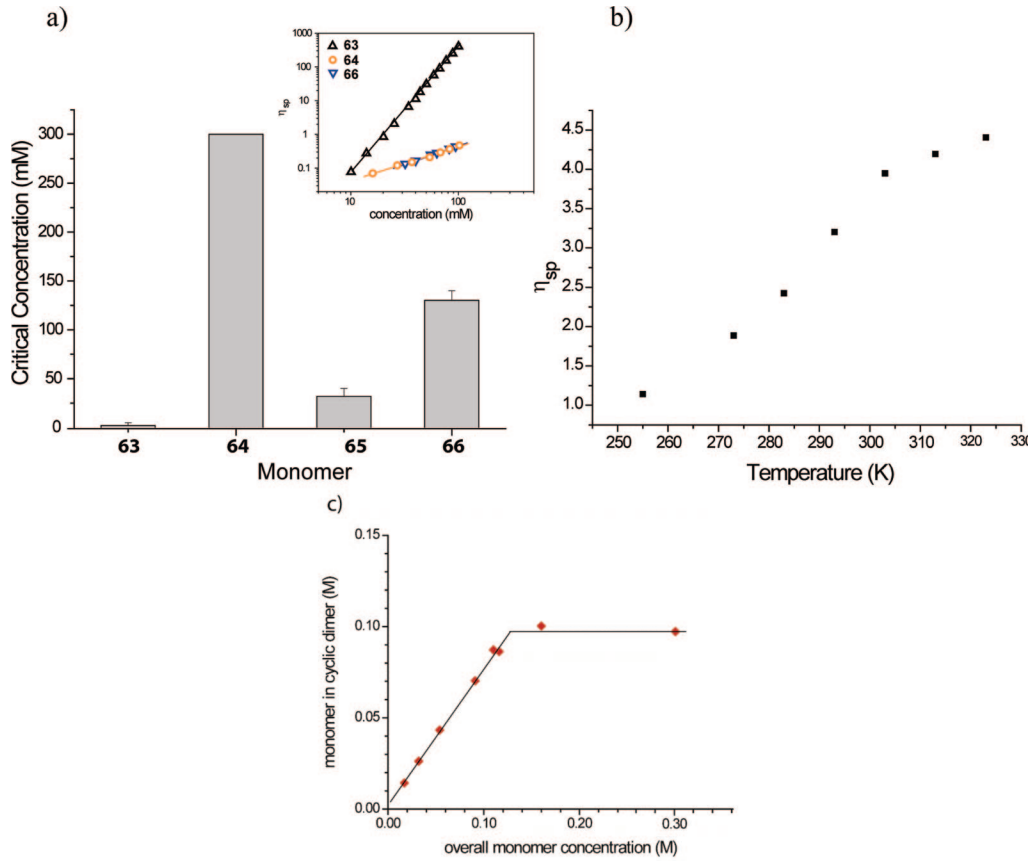

Figure 20. (a) Critical concentration of UPy derivatives **63**−**66** in $CDCl_3$ solution as determined by ^1H NMR analysis. (Inset) Concentration-dependent specific viscosity of chloroform solutions of **63**, **64**, and **66** versus the concentration (293 K). (b) Specific viscosity, η_{sp}, of a 0.145 M solution of **67** as a function of temperature. (c) Concentration of monomer in cyclic dimers determined by ^1H NMR for various concentrations of **66** in $CDCl_3$. (Reprinted from refs 228 and 230. Copyright 2004 American Chemical Society.)

Chart 18

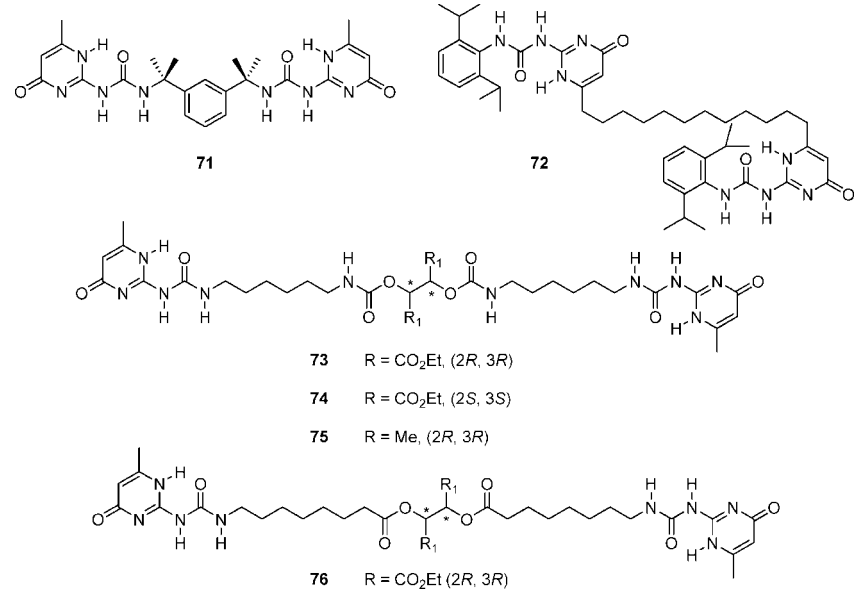

and a homoditopic dibenzylammonium derivative (Chart 21) are supramolecularly polymerized.[241,242]

It was observed that at low concentrations, equimolar mixtures of **82** and **85** in acetone/chloroform form a cyclic dimer as was evidenced by ^1H NMR spectroscopy.[241] Three sets of signals for the benzylic protons of **85** could be identified, of which one was assigned to uncomplexed **85**, whereas the other two could be ascribed to complexed **85** in either a cyclic dimer or a linear chain. From variable-concentration ^1H NMR spectroscopy the composition of the solution as a function of concentration was calculated. At low concentration ($<1.0 \times 10^{-2}$ M), the cyclic dimer was the most abundant species (66% at 1.0×10^{-2} M), whereas at high concentration (>1.0 M) most of the material was present in linear chains (90.2% at 1.0 M). The formation of long linear chains at higher concentrations was further

Chart 19

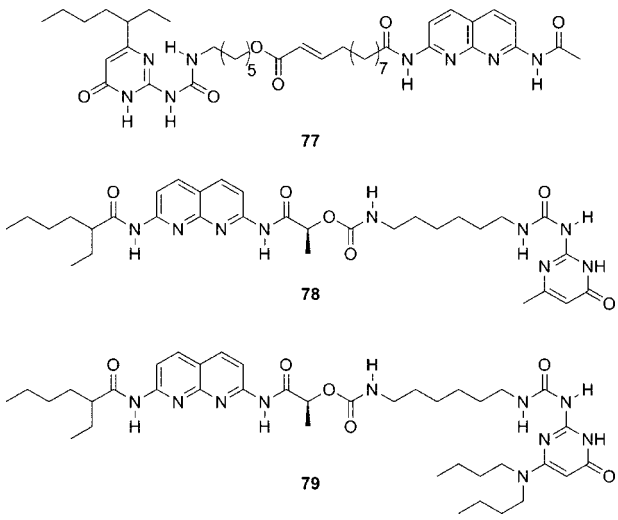

confirmed by a strong increase in the solution viscosity. As a continuation of their research, Gibson and co-workers prepared homoditopic monomers with linkers of variable length (Chart 21).[242] The length of the alkyl spacer between the two benzylammonium moieties, q, was varied by 4, 10, and 22 carbon atoms, whereas the alkyl spacer between the crown ether groups, p, was 2 or 8 carbon atoms in length. Using ^{1}H NMR spectroscopy at low concentration, it was possible to quantify the fraction of monomer, cyclic dimer, and linear dimer in solution (acetone/chloroform mixture) for equimolar mixtures of the crown ether-functionalized monomer and the homoditopic dibenzylammonium monomer. On the basis of these results, the association constant for the linear chain and the equilibrium constant for cyclic dimer formation were determined. It was found that increasing the linker length q resulted in a lower effective molarity, as the value decreased from 9.6×10^{-4} M ($q = 4$), via 2.3×10^{-4} M ($q = 10$), to 6.0×10^{-5} M ($q = 22$). These values clearly show that as the linker length is increased, the effective molarity is lowered and the formation of cyclic dimer is suppressed. Furthermore, performing the ^{1}H NMR experiments at different temperatures allowed the determination of the enthalpy change related to the formation of linear chains (ΔH_{linear}), as well as the enthalpy change related to the formation of cyclic dimers (ΔH_{cyclic}). It was found that when the spacer length q increased, ΔH_{linear} became more negative, whereas ΔH_{cyclic} became less negative.

Also, the concentration dependence of the formation of cyclic dimers was studied by ^{1}H NMR spectroscopy for the different mixtures of the homoditopic crown ether-functionalized monomer and the homoditopic dibenzylammonium monomer. For all mixtures, it was found that increasing the concentration resulted in a decrease in the fraction of cyclic dimer, whereas the fraction of material in linear chains increased. The fraction of cyclic dimer in solution was higher for the shorter linker length, in accordance with the results obtained at low concentration (vide supra). Using an isodesmic polymerization model and ignoring the formation of the cyclic dimer—a valid assumption at high concentrations—the average degree of polymerization, DP_N, of the linear chains could be calculated. This predicted DP_N could be related to the degree of polymerization found experimentally by determination of the fraction of free end groups with ^{1}H NMR spectroscopy. The experimentally determined DP_N was lower than predicted, which was ascribed to the deleterious effect of the high ionic strength and *exo* complexation (non-pseudorotaxane hydrogen bonding of the crown ether and the ammonium salt moieties) at high concentration. The formation of linear supramolecular polymers could be further characterized by viscometry, mass spectrometry, and electron microscopy.

More recently, Gibson et al. observed the formation of cyclic structures in solutions of homoditopic crown ether derivative **87** and homoditopic bis-paraquat derivative **88** (Chart 22).[243] For the **87**:**88** system, the formation of cyclic structures was deduced from concentration-dependent viscosity studies (Figure 22). The slope of 1.02 in the low-concentration regime, demonstrating a linear relationship between the specific viscosity and concentration, is characteristic for noninteracting species of constant size,[244] which was suggested to be the cyclic dimer.

Above a total concentration of 8.0×10^{-3} M a sharp increase in viscosity was observed as the slope increased to 2.08. This corresponds to a critical concentration of **87** and **88** of 4.0×10^{-3} M. This stronger concentration dependence is indicative of the formation of linear supramolecular polymers of increasing degree of polymerization. The formation of considerable amounts of cyclic dimers at low concentration in this system was ascribed to the relatively short linker length and its rigidity, which leads to a relatively high effective molarity.

Huang et al. combined the selective interactions between a bis(*p*-phenylene)-[34]crown-10 and a paraquat derivative, on the one hand, and a dibenzo-[24]crown-8 and a dibenzylammonium derivative, on the other hand, to obtain self-sorting supramolecular polymers.[245] To this end a bis(*p*-phenylene)-[34]crown-10 moiety was covalently connected to a dibenzylammonium derivative (**90**, Chart 23), whereas a dibenzo-[24]crown-8 group was linked to a paraquat derivative (**89**). The self-sorting assembly of **89** and **90** leads to an alternating arrangement of the two monomers, leading to the formation of supramolecular copolymers, as could be confirmed by ^{1}H NMR spectroscopy, CV, DLS, and SEM. The two linkers between the host and guest moieties were designed to have in total more than 20 atoms, which should result in a low critical concentration. Indeed, concentration-dependent viscometry showed a critical concentration of around 40 mM, indicative of a transition from cyclic species (at low concentration) to linear supramolecular polymers (at high concentration).

The formation of giant supramolecular porphyrin arrays was reported by Kobuke and co-workers (Figure 23).[247] The coordination between the imidazole unit and the zinc−porphyrin drives the supramolecular polymerization (Chart 24). The monomers **91**−**95** comprise linked zinc−porphyrin systems, either with or without a rigid linker. In the absence of a linker, as for example in monomer **91**, the polymerization yields only linear species of which the polymerization was influenced by the addition of a manganese porphyrin that was designed to act as a chain stopper.[248] A careful examination of the different association constants for homodimerization and heterodimerization allowed control over the length of the oligomers as a function of the amount of chain stopper added, as demonstrated using size exclusion chromatography.

As a consequence of preorganization due to the rigid linker present in monomers **92**−**95**, the formation of both linear as well as cyclic oligomers was observed.[246,249−251] A variety of techniques, including size exclusion chromatography,

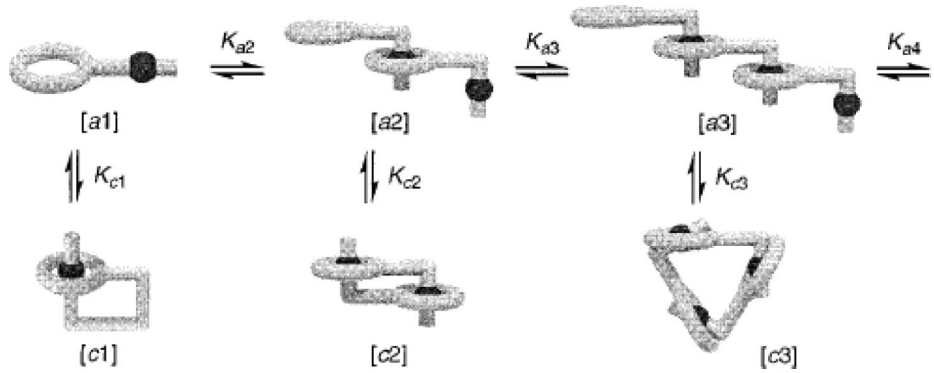

Figure 21. Schematic representation of the supramolecular polymerization of **81**. (Reprinted from ref 240. Copyright 2001 American Chemical Society.)

Chart 20

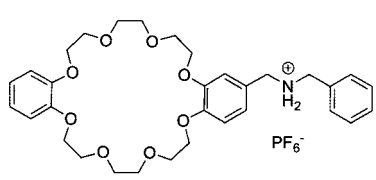

80

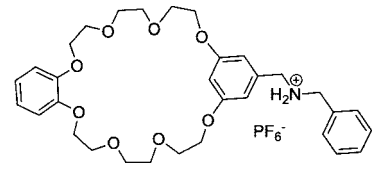

81

Chart 21

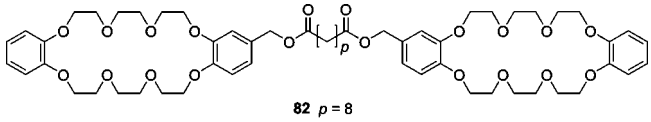

82 $p = 8$
83 $p = 2$

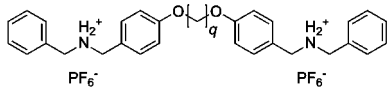

84 $q = 4$
85 $q = 10$
86 $q = 22$

Chart 22

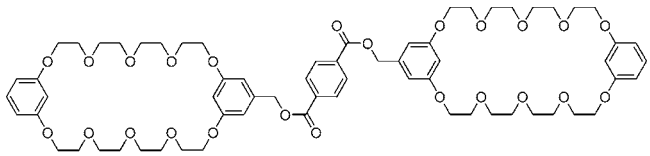

87

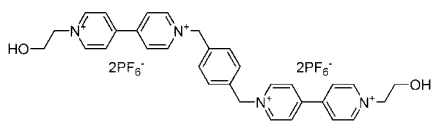

88

small-angle X-ray scattering, ^{1}H NMR and UV−vis absorption spectroscopy allowed the visualization of the cyclic and linear oligomers. To mimic the light harvesting system observed in Nature, an attempt was made to shift the ring−chain equilibrium toward the cyclic structure. By depolymerization of the linear polymer with a coordinating solvent and a reduction of the concentration to favor ring formation, slow evaporation of the coordinating solvent enabled the selective formation of cyclic structures. The size and distribution of the cycles depended on the flexibility of

Chart 23

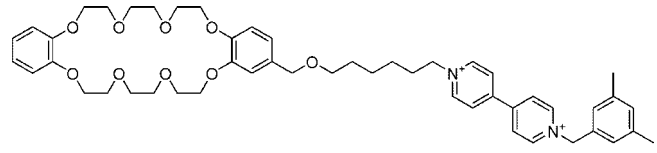

89

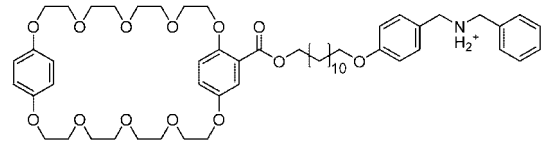

90

the linker between the zinc−porphyrins, where an increase in flexibility decreased the ring size.

Similar to the work of Kobuke, Hunter and co-workers reported on the supramolecular polymerization of cobalt−porphyrins **96** and **97** with pyridine as a ligand (Chart 25).[252,253] In this case the synthesis of a linked porphyrin was achieved by the addition of two pyridine ligands to the

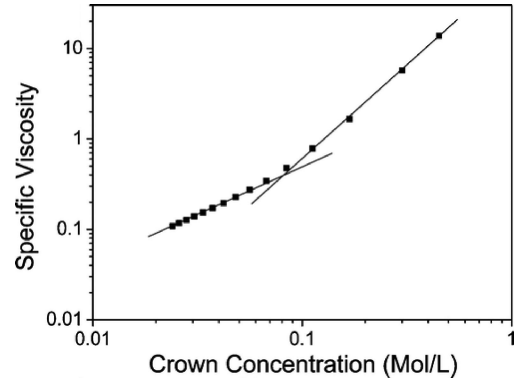

Figure 22. Specific viscosity of acetone solutions of equimolar mixtures of **87** and **88** as a function of the total concentration. (Reprinted from ref 243. Copyright 2007 American Chemical Society.)

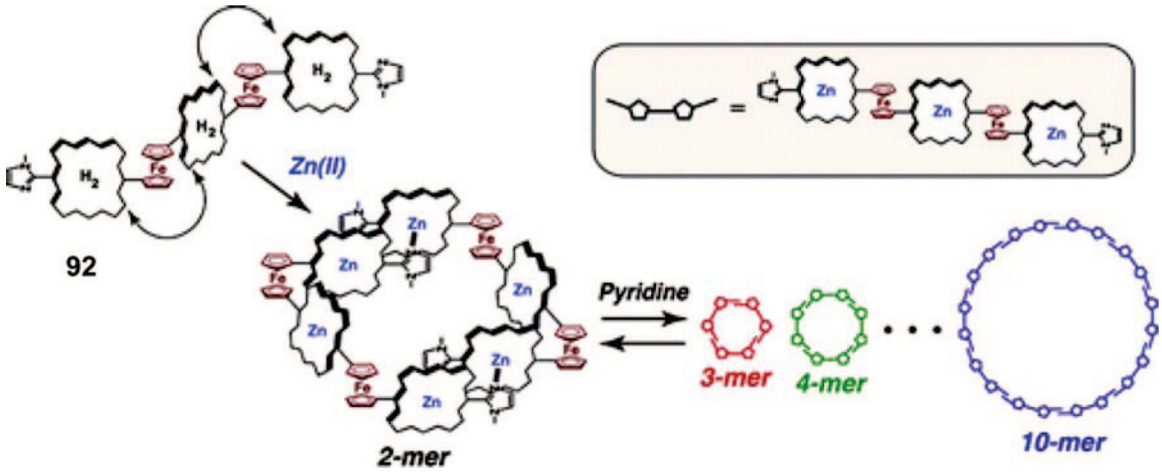

Figure 23. Schematic representation of the supramolecular polymerization of **92** (Chart 24). (Reprinted from ref 246. Copyright 2005 American Chemical Society.)

porphyrin. Because cobalt is able to form a six-coordinate metal complex, this molecular arrangement can give rise to cyclic or linear polymers. The steric demand of the linker in **96** enforces the formation of linear polymers, whereas **97** gives rise to a cyclic dodecamer that can be polymerized by ring-opening polymerization into polymeric structures at concentrations higher than the critical concentration of 0.5 mM as evident from size exclusion chromatography.[253]

Recently, we have also found evidence for ring−chain equilibria in supramolecular polymers based on reversible metal−ligand complexation.[178,254] The reversible coordination polymers were obtained by complexation of bifunctional phosphorus ligands and palladium dichloride. Because of the slow dynamics, the supramolecular polymerization process could be investigated by concentration-dependent size exclusion chromatography. This technique, together with diffusion-

Chart 24

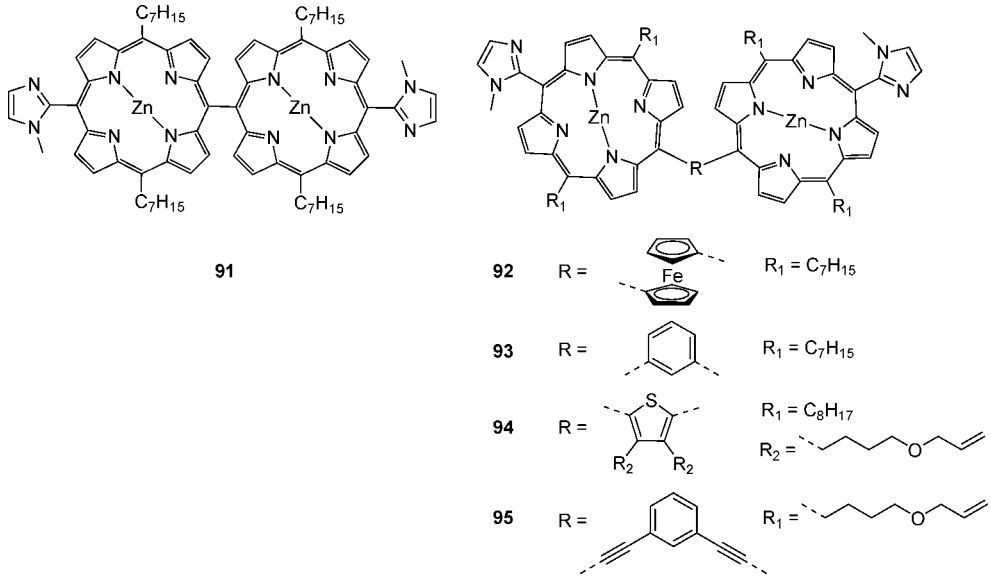

Chart 25

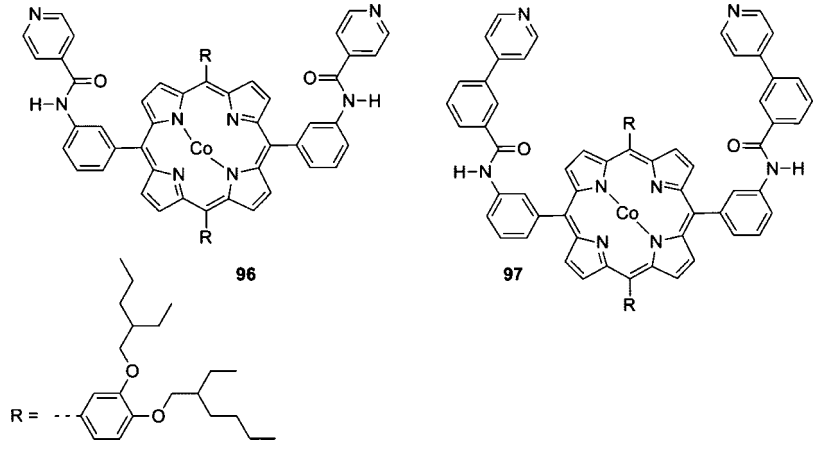

Chart 26

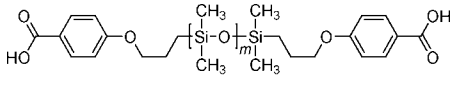

98 $m = 7$
99 $m = 13$
100 $m = 22$

ordered spectroscopy and concentration-dependent ^{1}H NMR, showed the formation of cyclic oligomers at low concentrations.[254] The critical concentration was shown to be dependent on the size of the aliphatic linker connecting the two phosphorus ligands and the nature of the substituent on the phosphorus ligand. The reversibility of the coordination polymers was also demonstrated by titration of a monofunctionalized stopper, which resulted in a decrease in the degree of polymerization as evidenced by size exclusion chromatography.[254]

Bouteiller et al. also reported on the formation of cyclic oligomers during the supramolecular polymerization of an carboxylic acid-terminated poly(dimethylsiloxane) (Chart 26).[255]

Three monomers differing in the length of the poly(dimethyl)siloxane linker were prepared, **98**−**100**, which were found to form supramolecular polymers, as was shown with FT-IR spectroscopy and viscometry. With the latter technique, a clear critical concentration could be observed when the reduced viscosity was plotted versus the concentration, which indicates a transition from cyclic species to linear supramolecular polymers. To describe the equilibrium between cyclic and linear (supramolecular) polymer chains, a quantitative model based on the theory of Jacobson and Stockmayer[214] in combination with mass balance equations was derived and is analogous to the model derived by Ercolani et al.[210] as was discussed previously. With this model the concentration-dependent FT-IR absorption was analyzed, yielding the dimerization constant for the acid functionalities, as well as the Jacobson−Stockmayer cyclization constants B_1 and B. The Jacobson−Stockmayer cyclization constant B_1 described the cyclization of the monomer, whereas the Jacobson−Stockmayer cyclization constant B describes cyclization of all linear oligomers larger than the monomer. Extending the poly(dimethylsiloxane) linker length resulted in an increase in the parameter B_1, showing that a larger fraction of cyclic monomers was present. No clear trend in the parameter B was found, which was ascribed to the fact that B depends on two parameters, the length of the linker and the (average) stiffness of the linker, which have opposite effects in this particular system. The ratio B/B_1 was found to decrease to a value close to unity for longer linker lengths, indicating the formation of strainless cyclic monomers. On the basis of the determined values for K, B_1, and B, the authors were able to describe the molecular weight distribution of cyclic and linear species in solution as a function of concentration.

Harada et al. showed that the length of the linker between two adamantyl groups can have a detrimental effect on the degree of cycle formation upon mixing the homoditopic adamantyl derivative **102**−**104** with a homoditopic β-cyclodextrin derivative, **101** (Chart 27), in aqueous solutions.[256]

For each of the three adamantyl derivatives, addition of **101** resulted in the formation of an inclusion complex between the adamantyl guest and the β-cyclodextrin cavity, as could be determined from ROESY ^{1}H NMR spectroscopy in deuterated water. However, only for **102** were supramolecular structures with a high molecular weight obtained, as evidenced by vapor pressure osmometry in water. With this technique only relatively low molecular weights could be measured for solutions consisting of molecules **103** and **104** only, independent of the concentration. The ^{1}H NMR spectra of **101**:**103** and **101**:**104** showed that all of the adamantane moieties are included and no free (nonincluded) adamantane groups were detected, suggesting that **103** and **104** form cyclic oligomers with **101** because of their flexibility. AFM indeed revealed cyclic structures for **101**:**103** and **101**:**104** when prepared from a concentrated solution in water. The discussed results show that increasing the linker length and flexibility leads to the formation of cyclic structures and to a strong decrease in the degree of polymerization of the linear chains.

Examples of supramolecular polymers in which two end groups are tethered by a flexible spacer and associate exclusively via $\pi-\pi$ interactions are scarce. Martín et al. describe the head-to-tail supramolecular polymerization of an AB monomer in which the AB interaction is based on the complexation of [60]fullerene and a π-extended analogue of tetrathiafulvalene (exTTF).[257] The two end groups are tethered by a small aliphatic spacer. Tapping mode AFM, concentration- and temperature-dependent ^{1}H NMR, pulse-field-gradient NMR, and DLS studies clearly showed the formation of supramolecular polymers. Furthermore, the variable-temperature ^{1}H NMR studies provided evidence for the competition between oligomeric rings and linear supramolecular polymers.

Craig and co-workers used an elegant approach to quantify the fraction of cyclic species present in a system consisting of oligonucleotide-based monomers, in which two oligonucleotide sequences were covalently linked, either directly or via a synthetic spacer.[258,259] Their approach is based on the selective digestion of linear polymers by an exonuclease enzyme, which will leave only the cyclic species intact. Viscometry, static and dynamic light scattering, UV−vis spectroscopy, and size exclusion chromatography were used to show the formation of supramolecular polymers with rising concentration of the oligonucleotide-based monomers. When the oligonucleotide segments were directly linked, only a small amount of cyclic structures was observed, as could be deduced from concentration-dependent multiangle light scattering (MALS).[258] The authors showed that it was possible to quantify the degree of cyclization.[259] To this end all supramolecular species were covalently linked using a DNA ligase enzyme, after which the covalent polymers could be characterized by gel electrophoresis. Addition of an exonuclease enzyme to the gel resulted in the selective digestion of all linear species, leaving only 10% of materials attributable to cyclic species. In contrast, for the monomers with a linker (either a hexa(ethylene glycol) or a propyl spacer) the MALS data showed that in solution a high number of cyclic structures was present. The increased fraction of cycles was a consequence of the higher flexibility of the linker. Although for these monomers no quantification of the degree of cyclization was reported, the authors acknowledge the increased probability of cyclization with longer, flexible linkers.

In an impressive study Reinhoudt and colleagues studied the parameters that can influence the equilibrium between linear (tape-like) and cyclic structures that can be formed

Chart 27

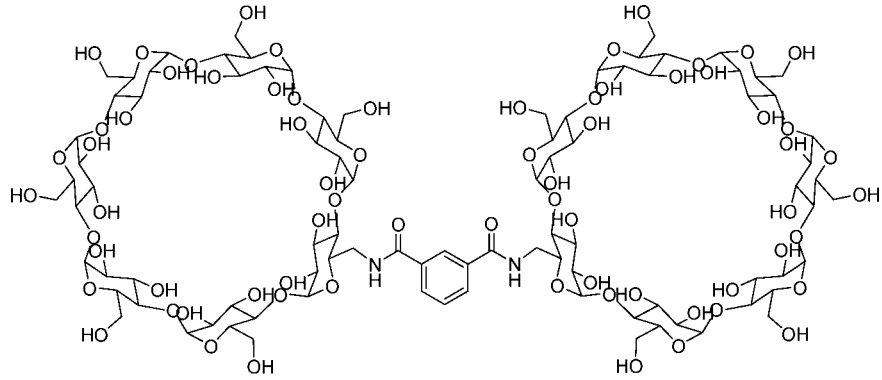

101

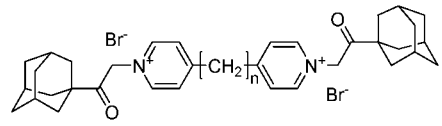

102 $n = 0$

103 $n = 2$

104 $n = 3$

Scheme 4. Schematic Representation of the Equilibrium between Infinite Linear Tapes (Top) and Hexameric Rosettes (Bottom) of Cyanurate and Melamine Derivatives

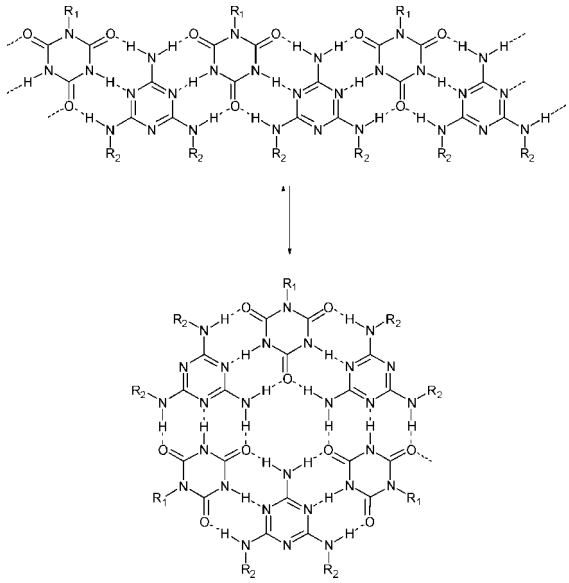

from a 1:1 mixture of cyanuric acid and melamine derivatives (Scheme 4).[260]

A model was developed to describe the equilibria between the various linear species and the hexameric rosette structure. It was assumed that under the experimental conditions linear structures consisting of no more than eight components were present. However, due to the possibility of stereoisomerism, in total 270 species could be formed with a length of at most eight components, which were all considered in the model. Furthermore, eight steric parameters were included to describe the different types of steric interactions within the assemblies. Next to these steric parameters, the model is characterized by a bimolecular association constant of a cyanurate and melamine group and the equilibrium constant for cyclization of a linear hexamer.

Indeed, a higher equilibrium constant for cyclization strongly increased the concentration of rosette over tape-like structures. More interesting, it was found that steric repulsions within the tape-like structure had only a minor effect on the fraction of rosette in the mixture, whereas the model predicted a strong sensitivity for the steric parameter that directly influences the stability of the cyclic rosette structure. In light of their predictions, the concept of peripheral crowding, as put forward by Whitesides,[261−263] was re-evaluated. The authors argued that the solubility differences for tape-like structures with bulky and nonbulky substituents, as a result of the nonplanarity of the former, provide a suitable explanation for the preferential crystallization of the rosette in the case of bulky substituents on the melamine. Gas-phase simulations indeed showed that the planarity of short tapes was lost as the size of the melamine substituents was increased.

The formation of discrete cyclic structures can be enhanced by careful design of the molecular structure of the monomer, as was already discussed above. Although beyond the scope of this review, we will discuss one additional example of this concept of molecular preorganization, as was reported by Ducharme and Wuest on dipyridones **105** and **106** (Chart 28).[264]

The authors showed with VPO and ^{1}H NMR spectroscopy that asymmetric **105** preferentially formed dimeric structures in solution, whereas symmetric **106** supramolecularly polymerized into planar, linear structures. X-ray studies also showed that in the solid state a supramolecular organization, similar to the organization found for each monomer in solution, was obtained.

Using the concept of conformational preorganization not only dimers but also higher oligomeric cycles have been prepared with high selectivity. For a more extensive discussion on this topic, the reader is referred to the reviews by Timmerman et al.[265] and by our own research group.[266] Finally, as shown by Hunter and Thomas, cyclization plays an important role in the construction of linear supramolecular objects of discrete size by the Vernier principle.[267]

Chart 28

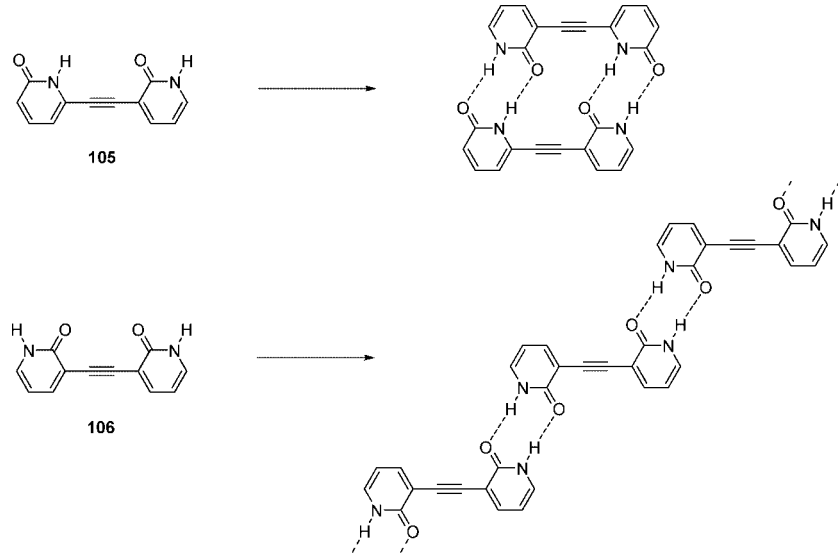

4. Cooperative Supramolecular Polymerization

4.1. Definition and Covalent Counterparts

In the third class of supramolecular polymerization mechanisms we discern, the growth of the supramolecular polymer occurs in at least two distinct stages, resulting in cooperative or anticooperative growth. In a cooperative supramolecular polymerization the first step in the formation of the supramolecular polymer consists of linear isodesmic polymerization with an association constant K_n for the addition of each monomer. The polymerization process continues until a nucleus of degree of polymerization s is formed. Due to various cooperative effects that will be discussed later, the addition of an additional monomer then occurs with an association constant K_e that is higher than K_n. The supramolecular polymerization then proceeds by linear isodesmic polymerization but the association constant is now K_e (elongation phase) rather than K_n.

For cooperative supramolecular polymerizations a distinction can be made between nucleated and downhill supramolecular polymerizations. In accordance with the definition as put forward by Ferrone,[268] a cooperative supramolecular polymerization is classified as a nucleated supramolecular polymerization when in the initial stages of the polymerization the Gibbs free energy of the oligomers increases with respect to the monomer (Figure 24). The polymerization process continues until a nucleus of degree of polymerization s is formed, corresponding to a maximum in the free energy diagram (Figure 24), after which polymerization becomes energetically favorable. In a nucleated supramolecular polymerization, the nucleus is the least stable and hence least prevalent species in the reaction and acts as a bottleneck against the formation of new supramolecular polymers.

In almost all examples of nucleated supramolecular polymerization the formation of the nucleus is assumed to occur via homogeneous nucleation of the monomer in solution. Typically, the term heterogeneous nucleation is used for nucleation on a foreign substrate[269] such as foreign molecules[270−272] (impurities), external surfaces,[273] dust particles, or secondary nucleation of monomers to form a polymer on an existing polymer. Secondary nucleation has been found to be a dominant mechanism for several biological supramolecular polymerizations such as the supramolecular polymerization of sickle cell hemoglobin,[274−277] islet amyloid polypeptide,[278] and β_2 microglobulin.[279]

In a recent review,[280] Frieden has defined three criteria on which nucleation−elongation can be differentiated from isodesmic supramolecular polymerizations: (1) There is a time-dependent lag in the formation of the supramolecular polymer. (2) The lag can be abolished by the addition of a preformed nucleus (seeding). (3) There is a critical concentration or critical temperature representing the monomer in equilibrium with the supramolecular polymer.

In contrast to a cooperative nucleated supramolecular polymerization, a cooperative downhill supramolecular polymerization is not characterized by an initial increase in the Gibbs free energy but only by the fact that initial growth occurs with a lower association constant than subsequent elongation (Figure 25). Hence, in a cooperative downhill[281] supramolecular polymerization the highest energy species in the assembly pathway is the monomer. In agreement with the definition by Powers and Powers,[282] the nucleus in a downhill supramolecular polymerization is the oligomer length at which the absolute value of $d\Delta G°/di$ suddenly

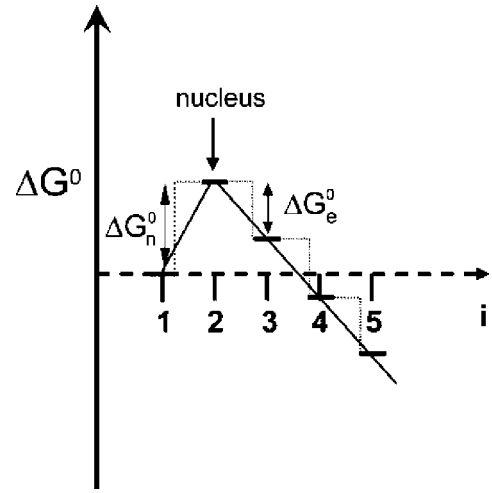

Figure 24. Schematic energy diagram of a cooperative nucleated supramolecular polymerization. The abscissa in this plot represents the size of the oligomer (i), whereas the ordinate measures the free energy $\Delta G°$ in arbitrary units. The nucleus size, s, was chosen to be 2 (dimeric nucleus).

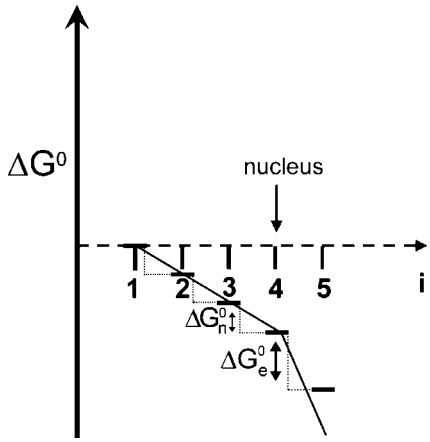

Figure 25. Schematic energy diagram of a cooperative downhill supramolecular polymerization. The nucleus was chosen to be a tetramer. The abscissa in this plot represents the size of the oligomer (*i*), whereas the ordinate measures the free energy $\Delta G°$ in arbitrary units.

increases. It must be understood that this distinction between a cooperative downhill and a cooperative nucleated polymerization is dependent on the concentration and a nucleated polymerization can become a downhill polymerization at high total monomer concentrations.[282,283] A recent kinetic analysis by Powers and Powers has shown that concentration-dependent kinetic experiments can readily differentiate between a downhill or a nucleated supramolecular polymerization.[282] The nucleus in a downhill supramolecular polymerization is different from the nucleus in a nucleated polymerization as in the first case the nucleus is a stable species, whereas in the latter case the nucleus is an unstable species, with respect to the monomer.

For anticooperative supramolecular polymerization the initial formation of oligomers occurs with a higher association constant than subsequent elongation. Although anticooperative growth in supramolecular polymerizations has received much less attention then cooperative growth, the anticooperative growth of supramolecular polymers can result in the formation of discrete objects with low polydispersities, in contrast to cooperative growth, which results in supramolecular polymers with a high polydispersity index. Pioneering work on the self-assembly of surfactants by Mukerjee[54,284−287] and Tanford[288,289] has shown how the initial stages of micellar growth are characterized by a high degree of cooperativity resulting in the formation of large aggregates instead of molecular clusters of dimers and trimers. More importantly, they showed the dominant role of anticooperative effects, originating from electrostatic and steric interactions between the polar head groups, in constraining the micelles to remain of finite size.

It is tempting to compare the cooperative supramolecular polymerization with the chain polymerization as the covalent counterpart. The initiation in the radical or ionic polymerization can be compared with the formation of the nucleus in cooperative supramolecular polymerizations. The propagation is also present in both systems; however, the termination is mostly absent in the supramolecular polymerization. A large number of characteristics of these living ionic or radical polymerizations are useful in the understanding of cooperative supramolecular polymerization. For instance, the fact that halfway through the polymerization the sample consists of polymer in the presence of monomers is characteristic for chain polymerization as well as for cooperative supramolecular polymerizations. However, next to living chain polymerization, there are also examples in covalent polymerizations where cooperative effects have influenced condensation polymerizations. Changes in electronic properties of the end group upon growth of the polymer have been observed for polycondensation reactions that do not obey Flory's "principle of equal reactivity",[37] but in which the reactivity of the polymer end groups becomes more reactive than the monomer and in which the reaction of monomers with each other is prevented. An example of such a polymerization is the polycondensation of phenyl 4-(alkylamino)benzoate in the presence of phenyl 4-nitrobenzoate as initiator and a base in THF (Scheme 5).[290] Due the abstraction of the proton from the amino group of the monomer (phenyl 4-(alkylamino)benzoate) by the base, the reactivity of the phenyl ester moiety is deactivated, which prevents monomers from reacting with each other. The anion produced by proton abstraction from the monomer will only react with initiator, leading to an activated monomer that possesses a more reactive phenyl ester moiety compared to the anionic monomer. As a result, only activated monomer will react, resulting in a chain-growth polycondensation[291,292] instead of a step-growth polycondensation.

In the case of structural cooperativity, initial polymerization is thermodynamically less favorable than elongation and polymerization becomes favorable only when the growing polymer has reached a critical length at which, due to a conformational or structural change in the growing polymer, growth becomes more favorable. The critical oligomer length at which polymer elongation becomes more favorable than dissociation is called the nucleus. In the case of cooperativity arising from structural changes, the nucleus is the smallest possible species at which an unstructured, disordered oligomer is converted into an ordered conformation.

In classical covalent polymerizations structural cooperativity has been observed for the acid-initiated polymerization of isocyanides to form a helical polymer. For this polymerization, a mechanism was proposed in which an initial helical oligomer needs to be formed, which then acts as a template for the incorporation of subsequent monomeric units.[293] Okamoto and co-workers reported the asymmetric, anionic polymerization of triphenyl methyl methacrylate initiated by 9-fluorenyllithium, in the presence of chiral ligands, to form a one-handed helical polymer.[294] They observed that the reactivity of each oligomer anion depended on the degree of polymerization, which was correlated to the specific conformation of the oligomer anions. Only when a stable helical conformation of the oligomer was formed, which occurred for a DP of 7−9 units, did further monomer addition occur more readily. Oya and co-workers proposed a similar cooperative growth mechanism for the heterogeneous polymerization of amino acid anhydrides into synthetic polypeptides.[295,296] In the early stages of the polymerization, only antiparallel β-sheet type oligopeptides were observed due to the fact that the chains are too short to give the α-helical structure. When the degree of polymerization reaches a value of approximately 8, a conformational change to an α-helical conformation occurs and chain growth proceeds more favoarbly via addition of monomers to the active chain end into the α-helical conformation.

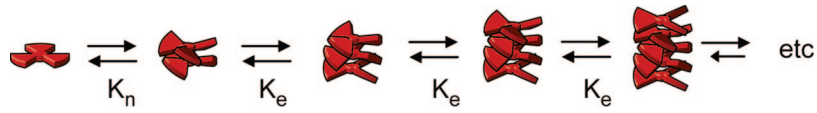

Figure 26. Schematic representation of a cooperative ($K_n < K_e$) supramolecular polymerization of a rigid discotic molecule. In this cartoon, the dimer is the nucleus.

Scheme 5. Chain-Growth Polycondensation of Phenyl 4-(Alkylamino)benzoate Ester 107 in the Presence of Initiator 109 To Yield Polyamide 110 (Reprinted with Permission from Reference 291. Copyright 2007 Elsevier)

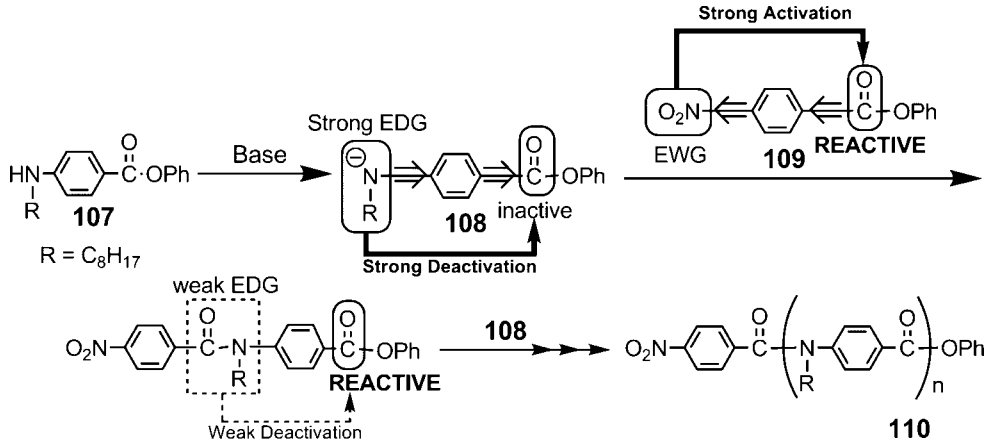

Scheme 6

$$M_1 + M_1 \overset{K_2}{\rightleftharpoons} M_2 \qquad [M_2]=K_2[M_1]^2$$

$$M_2 + M_1 \overset{K}{\rightleftharpoons} M_3 \qquad [M_3]=KK_2[M_1]^3$$

$$\cdots \qquad \cdots$$

$$M_{i-1} + M_1 \overset{K}{\rightleftharpoons} M_i \qquad [M_i]= K_2K^{i-2}[M_1]^i = \sigma K^{-1}(K[M_1])^i \quad i = 2, 3,\ldots,\infty$$

4.2. Thermodynamic Aspects of Cooperative Supramolecular Polymerizations

In contrast to isodesmic supramolecular polymerizations, cooperative supramolecular polymerizations are characterized by at least two different association constants in the assembly pathway (Figure 26). As a result, cooperative supramolecular polymerizations are characterized by a critical concentration or temperature at which the supramolecular polymer starts growing.

To illustrate the concentration-dependent properties of cooperative supramolecular polymerizations in ideal solutions, several characteristic properties have been calculated using the mean-field chemical equilibrium model, as discussed, for example, by Zhao and Moore.[48] This model is a modification of the isodesmic model in which the dimerization step has a different equilibrium constant from that of the elongation constant, which can be schematically represented by Scheme 6 in which K_2 represents the equilibrium constant of dimerization and K represents the equilibrium constant for all following steps. As a measure for the degree of cooperativity the parameter σ can be defined as the ratio of K_2/K, which is smaller than unity for a cooperative process and larger than unity for an anticooperative process. Although this model is limited to cooperative supramolecular polymerizations in which the nucleus is a dimer, it has the advantage that it can be solved analytically. Using this K_2-K model, characteristic features of cooperative supramolecular polymerizations can be understood. Figure 27a displays the mole fraction of self-assembled material, ϕ, as a function of the dimensionless concentration KC_t for three different values of σ (with C_t defined as the total concentration of monomer and ϕ defined as $(C_t - M_1)/C_t$). Increasing the cooperativity (i.e., smaller values of σ) has a clear influence on the growth profile of the polymeric species. Whereas for the isodesmic growth ($\sigma = 1$) a gradual increase in polymeric species is observed with increasing concentration, for the cooperative systems, below a critical dimensionless concentration of 1, hardly any polymeric species are formed. Only when the concentration is raised above the critical concentration does chain growth occur and all monomers are converted into high molecular weight polymers over a relatively small concentration range (Figure 27b). Furthermore, in sharp contrast to isodesmic supramolecular polymerizations, higher *DP* values can be obtained not only by increasing K but also by decreasing σ.

Figure 27c depicts the dimensionless equilibrium concentration of monomer (KM_1) and polymer (defined as the total concentration of all chains $M_2 + M_3 + M_4 + \ldots + M_\infty$ multiplied by K) as a function of the dimensionless concentration KC_t. As discussed in the section on isodesmic supramolecular polymerization, a characteristic feature of isodesmic supramolecular polymerizations is that equilibrium polymer and monomer concentrations rise simultaneously. In sharp contrast, for cooperative supramolecular polymerizations the equilibrium concentration of supramolecular polymer starts increasing only after reaching a critical concentration at which the equilibrium concentration of monomer does not increase anymore with increasing total concentration. Just as is the case for isodesmic supramolecular polymerization, the monomer concentration reaches a maximum value equal to K^{-1}.

Finally, a cooperative supramolecular polymerization is characterized by a bimodal mass distribution that is the result of the presence of (nonactivated) monomers and activated supramolecular polymers that have elongated after activation (Figure 27d). Similar to the case of an isodesmic supramolecular polymerization, the size distribution in the high molecular weight limit corresponds to a broad exponential distribution.[297]

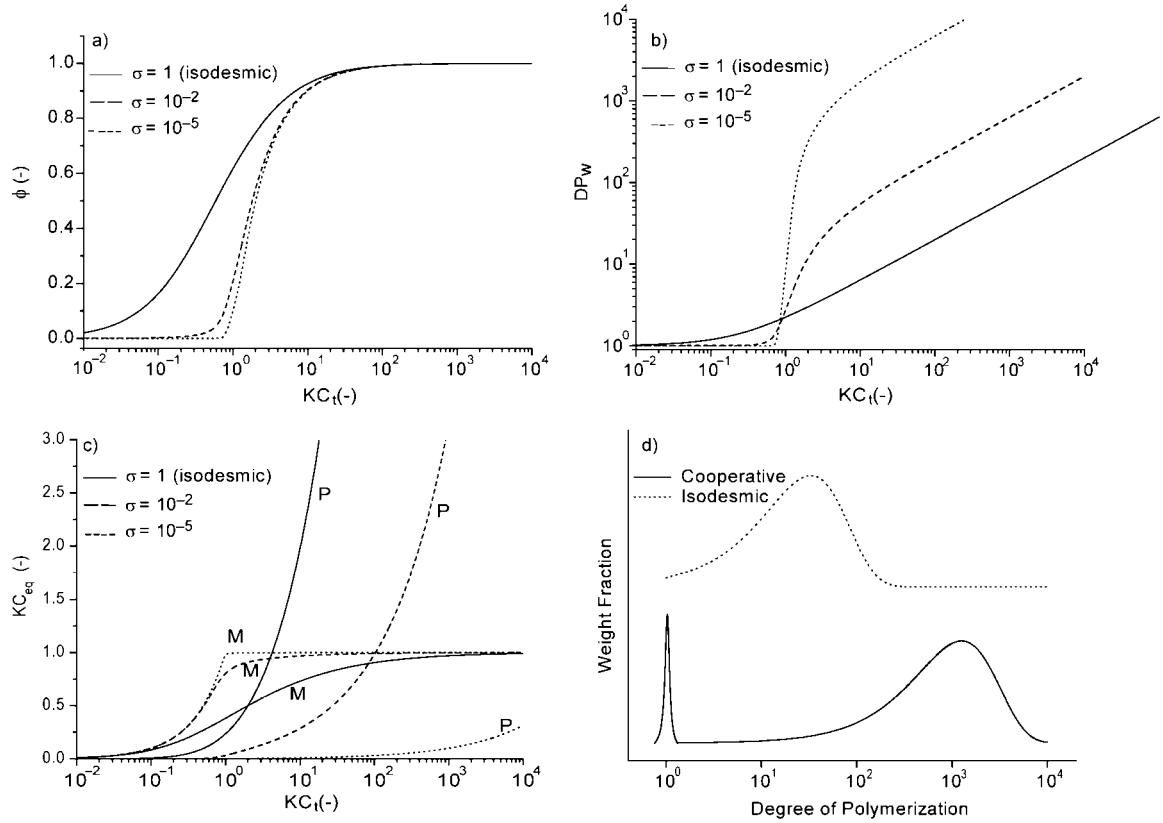

Figure 27. Characteristic concentration-dependent properties of nucleated supramolecular polymerizations illustrated using the K_2-K model: (a) fraction of polymerized material, ϕ, as a function of the dimensionless concentration KC_t for several values of σ (defined as K_2/K); (b) weight-averaged degree of polymerization (DP_W) as a function of the dimensionless concentration for three values of σ; (c) dimensionless concentration of monomer (KM_1) and polymer (defined as $K(M_2 + M_3 + ... + M_\infty)$) as a function of the dimensionless concentration KC_t for three values of σ; (d) schematic representation of the molecular weight distribution as a function of the degree of polymerization for an isodesmic supramolecular polymerization mechanism and a cooperative supramolecular polymerization mechanism.

Scheme 7

$$M_1 + M_i \underset{}{\overset{K_n}{\rightleftharpoons}} M_{i+1} \qquad i<s \qquad i=1, 2,...,s\text{-}1$$

$$M_1 + M_i \overset{K}{\rightleftharpoons} M_{i+1} \qquad i \geq s \qquad i=s, s+1,...,\infty$$

Interestingly, the curves shown in Figure 27 for the cooperative polymerization according to the K_2-K model show a strong resemblance to the curves obtained for the AB polymerization with cycle formation, as shown in Figure 19 in the previous chapter. This resemblance is a result of the fact that in both mechanisms the growth of the supramolecular polymer is governed by two different equilibrium constants. As a result, both mechanisms are characterized by a sharp transition in the fraction of polymerized material accompanied by a rapid increase in the degree of polymerization once critical conditions are reached.

The above K_2-K model can be used to obtain thermodynamic constants of supramolecular polymerization processes, provided it is known a priori that the size of the nucleus is 2. Goldstein and Stryer have generalized this model for cooperative polymerization processes using a variable nucleus size (Scheme 7).[298]

In the mean-field chemical equilibrium model developed by Goldstein and Stryer, isodesmic growth of the supramolecular polymer from the monomer occurs with an equilibrium constant K_n. When the growing polymer reaches the nucleus with length s, further growth occurs with a different equilibrium constant K. Again, it is possible to define σ as the ratio between K_n and K such that for a cooperative supramolecular polymerization $\sigma < 1$. However, as argued by Goldstein and Stryer, the growth of the supramolecular polymer is not determined by σ alone but also by the size of the nucleus s, which led them to define a cumulative cooperativity ω, defined as σ^{s-1}. Using the mass balance equation as provided by Goldstein and Stryer, the fraction of polymerized material (again defined as $(C_t - M_1)/C_t$) and the weight-averaged degree of polymerization[299] (DP_W) were calculated for various situations (Figure 28). Panels a and b of Figure 28 plot the fraction of polymerized material ϕ and the weight-averaged degree of polymerization as a function of the total dimensionless concentration for different nucleus sizes but equal values of the cumulative cooperativity parameter ω. As can be observed, the curves of equal ω quickly coalesce when $KC_t > 1$, that is, the total concentration of monomer exceeds the critical concentration. Furthermore, for large values of the nucleus size, a significant amount of material is already polymerized before the critical concentration is reached. However, as is shown in Figure 28b, the system in such a case mainly consists of monomers and dimers, and high molecular weight polymers are obtained only when the critical concentration is surpassed. Another important conclusion that can be drawn from the calculations in panels b and d of Figure 28 is that the degree of polymerization of the supramolecular polymers is completely determined by ω alone.

Panels c and d of Figure 28 plot the fraction of polymerized material and the DP_W for a nucleus size of 4 but for different values of ω as a function of the total dimensionless concentration. In contrast to the situation in Figure 28a, the

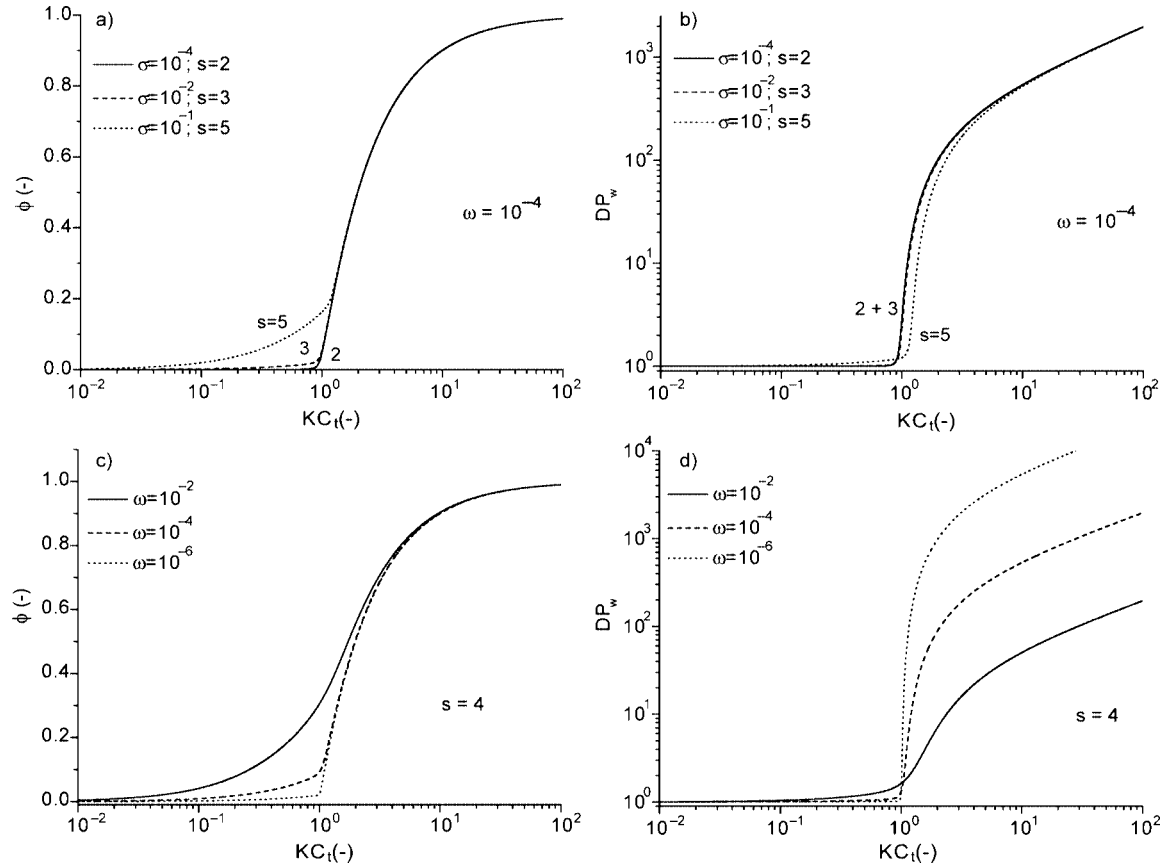

Figure 28. Concentration-dependent properties of cooperative supramolecular polymerizations in ideal solutions illustrated using the general nucleation−elongation model as proposed by Goldstein and Stryer: (a) fraction of polymerized material, ϕ (defined as $(C_t - M_1)/C_t$), as a function of the dimensionless concentration KC_t for nucleus sizes of 2, 3, and 5 and a cumulative cooperativity constant of $\omega = \sigma^{s-1} = 10^{-4}$; (b) weight-averaged degree of polymerization (DP_W) as a function of the dimensionless concentration KC_t for nucleus sizes of 2, 3, and 5 and a cumulative cooperativity constant of $\omega = 10^{-4}$; (c) fraction of polymerized material, ϕ (defined as $(C_t - M_1)/C_t$), as a function of the dimensionless concentration KC_t for a constant nucleus size of 4 and various values of the cumulative cooperativity constant ω (10^{-2}, 10^{-4}, and 10^{-6}); (d) weight-averaged degree of polymerization (DP_W) as a function of the dimensionless concentration KC_t for a constant nucleus size of 4 and various values of the cumulative cooperativity constant ω (10^{-2}, 10^{-4}, and 10^{-6}).

curves in Figure 28c coalesce less quickly when the total concentration is higher than the critical concentration. Finally, from Figure 28d it is clear that higher molecular weight polymer can be obtained by lowering the cumulative cooperativity constant ω.

Due to the mean-field nature of the K_2-K model and the general cooperative supramolecular polymerization model of Goldstein and Stryer, excluded volume interactions between the polymeric chains and between the polymeric chains and solvent are neglected. As was discussed in the section on isodesmic supramolecular polymerizations, non-mean-field effects such as excluded volume interactions can have a large impact on the growth of supramolecular polymers, in both the dilute and semidilute regimes.

For cooperative (i.e., both thermally and chemically activated) supramolecular polymerizations, the influence of excluded volume interactions has been recently taken into account using scaling theory.[300,301] An important conclusion from this work is that the presence of excluded volume interactions in thermally activated cooperative supramolecular polymerizations results in a more cooperative supramolecular polymerization as would have been the case for ideal, noninteracting chains in the dilute regime. In addition, the effect of excluded volume interactions between polymer and inert solvent has been recently analyzed by treating the solvent as a hard particle.[302]

As has already been mentioned, the determination of average chain lengths for supramolecular polymers is a nontrivial task due to the fact that most analytical techniques cannot be used to probe the degree of polymerization. This information needs to be obtained from mathematical models, which require thermodynamic parameters as an input. In contrast to isodesmic supramolecular polymerizations, obtaining thermodynamic parameters for cooperative supramolecular polymerizations is not a trivial task. The difficulty arises from the fact that the cooperativity constant σ and the nucleus size s cannot be obtained independently from concentration-dependent measurements due to the strong dependency between these two parameters, although it is still possible to obtain the cumulative cooperativity constant ω from concentration-dependent measurements.

In most of the synthetic examples of cooperative supramolecular polymerizations that have been analyzed, the nucleus size is assumed to be 2 (vide supra). Using this assumption, the dimerization constant K_2 and elongation constant K can be determined and used to calculate the concentration-dependent degree of polymerization and product composition. Hence, although an exact value of the nucleus size is not required to obtain information on the average chain lengths of the supramolecular polymers, a reliable estimate of the nucleus size results in important information regarding the underlying molecular mechanism responsible for the coop-

erative transition (i.e., electronic effects, structural effects, or the hydrophobic effect if the supramolecular polymerization occurs in water). In biological supramolecular polymerizations, obtaining reliable estimates of the nucleus size has been a subject of intense research for over 40 years, starting from the first kinetic experiments by Oosawa and Kasai on the quantification of the nucleus size in the reversible polymerization of actin.[303,304] The kinetics of polymerization reactions were developed initially for the field of polymer chemistry by Flory[37] and were applied to protein systems by Oosawa and Kasai. Because the basic equations governing the reversible polymerization form an infinite interrelated set of nonlinear differential equations that cannot be solved analytically, simplified assumptions had to be used because computers that were able to solve such systems via numerical methods were still scarce. By assuming that certain reverse rate constants and the concentration of prenucleus oligomers are negligible, Oosawa and Kasai obtained a single differential equation that could be integrated and which was used to estimate the size of the nucleus using the concentration dependence of the half-life of polymerization (i.e., the time to reach 50% conversion). However, Frieden[305,306] and co-workers have shown by numerical examples that the assumptions made in such an approach are rather restrictive and that the nucleus size is not simply related to the half-life of polymerization. Moreover, the simplified assumption that the concentration of prenucleus oligomers is negligible has recently been shown not to be valid at high total concentration of monomer.[282] Due to the advancements of modern computer power, fitting of large systems of coupled differential equations to kinetic data has become a trivial task. In an impressive study, Radford and co-workers recently estimated the nucleus size in the nucleated supramolecular polymerization of β_2-microglobulin using over 1000 coupled differential equations to globally fit the 235 experimentally determined kinetic curves.[279] An additional complication in the determination of the nucleus size is the fact that in some cases the nucleus size is concentration-dependent, and concentration-dependent nucleus size models have to be used to estimate this parameter. This situation is most likely to be encountered when secondary nucleation plays a dominant role in the supramolecular polymerization mechanism.[275,276]

After this reflection on concentration-dependent properties, the temperature-dependent properties of cooperative supramolecular polymerizations will now be discussed. Due to the highly cooperative nature of these polymerizations there is a sharply defined ceiling or floor temperature characterized by a sudden change in the fraction of polymerized material.[41] As has already been noted in the previous sections, entropy driven supramolecular polymerizations are characterized by a floor temperature above which the system polymerizes and below which the fraction of polymerized material is zero. In contrast, enthalpy driven supramolecular polymerizations are characterized by a ceiling temperature below which the system polymerizes and above which the fraction of polymerized material is zero. Interestingly, entropically driven cooperative polymerizations are most commonly encountered in biological systems, notable examples being the self-assembly of type I collagen fibrils,[307,308] the reversible polymerization of tau protein,[309] the self-assembly of bovine brain tubulin,[310] the self-assembly of β-amyloids[311,312] and the formation of tubular polymer of sickle cell deoxyhemoglobin.[313] In most cases, the entropic driving force for the formation of large polymers in biological systems has been attributed to hydrophobic interactions between the apolar surfaces of a protein in the highly polar solvent water. Although the hydrophobic effect remains a subject of intense discussion[314,315] it is now generally accepted that the aggregation of apolar solutes in water is entropically favored[316−318] due to subtle variations of the hydrogen-bonding network near an apolar solute molecule. More recently, however, it has been argued that depletion interactions also contribute significantly to the interaction energy of biological supramolecular polymers.[319] The depletion interaction, as first described by Asakura and Oosawa,[320] is an entropic attractive interaction between two large macromolecules (solute) caused by the inaccessibility of smaller molecules (solvent) to the volume between the two large macromolecules, resulting in an attractive osmotic force between the two large macromolecules. Interestingly, Kamien and Snir recently showed that depletion interactions can result in an entropically driven helix formation.[321]

Scheme 8

$$M_1 \xrightleftharpoons{K_a \text{ or } \Delta H_a, \Delta S_a} M_1^* \qquad \textit{Activation}$$

$$M_1^* + M_1 \xrightleftharpoons{T_e, \Delta H_e \text{ or } \Delta H_p, \Delta S_p} M_2 \qquad \textit{Elongation}$$

$$\cdots$$

$$M_i + M_1 \xrightleftharpoons{T_e, \Delta H_e \text{ or } \Delta H_p, \Delta S_p} M_{i+1} \qquad i = 2, 3, \ldots, \infty$$

In contrast to biological supramolecular polymerizations, most examples of synthetic cooperative supramolecular polymerizations are enthalpically driven and polymerize upon cooling. To illustrate the temperature-dependent properties of cooperative supramolecular polymers, two mean-field models will be illustrated, both treating cooperative supramolecular polymerizations as thermally activated equilibrium polymerizations.[199] In these types of polymerizations, only a small portion of the monomers are active and able to polymerize. The remaining monomers are in an inactive state and unable to grow into long polymeric species. The active and inactive states of the monomers are in thermal equilibrium, and the equilibrium strongly favors the inactive state, resulting in a cooperative supramolecular polymerization. Such a polymerization is described by the reaction shown in Scheme 8, where the activated species M_1* reacts only with nonactivated monomers M_1 to form dimers, but M_1* does not participate in the successive chain elongation steps. An alternative model in which dimers are formed by linking two activated monomers M_1* and in which chain growth exclusively occurs through the addition of M_1* is mathematically isomorphic to that given by the reactions depicted in Scheme 8.[41]

In the first model analyzed by van der Schoot,[43] the monomeric activation step is described by a dimensionless activation constant K_a, whereas subsequent elongation of the polymers is described by a temperature-independent elongation enthalpy (ΔH_e) and a concentration-dependent elongation temperature T_e. For supramolecular polymers that polymerize upon cooling, the elongation enthalpy is negative (i.e., $\Delta H_e < 0$).

In the model analyzed by van der Schoot, the critical elongation temperature, T_e, separates two polymerization regimes. Above the critical elongation temperature, most of the molecules in the system are in an inactive state (nucleation regime), which means that the activation step between inactive and active monomer lies almost completely to the left. At the critical elongation temperature activation

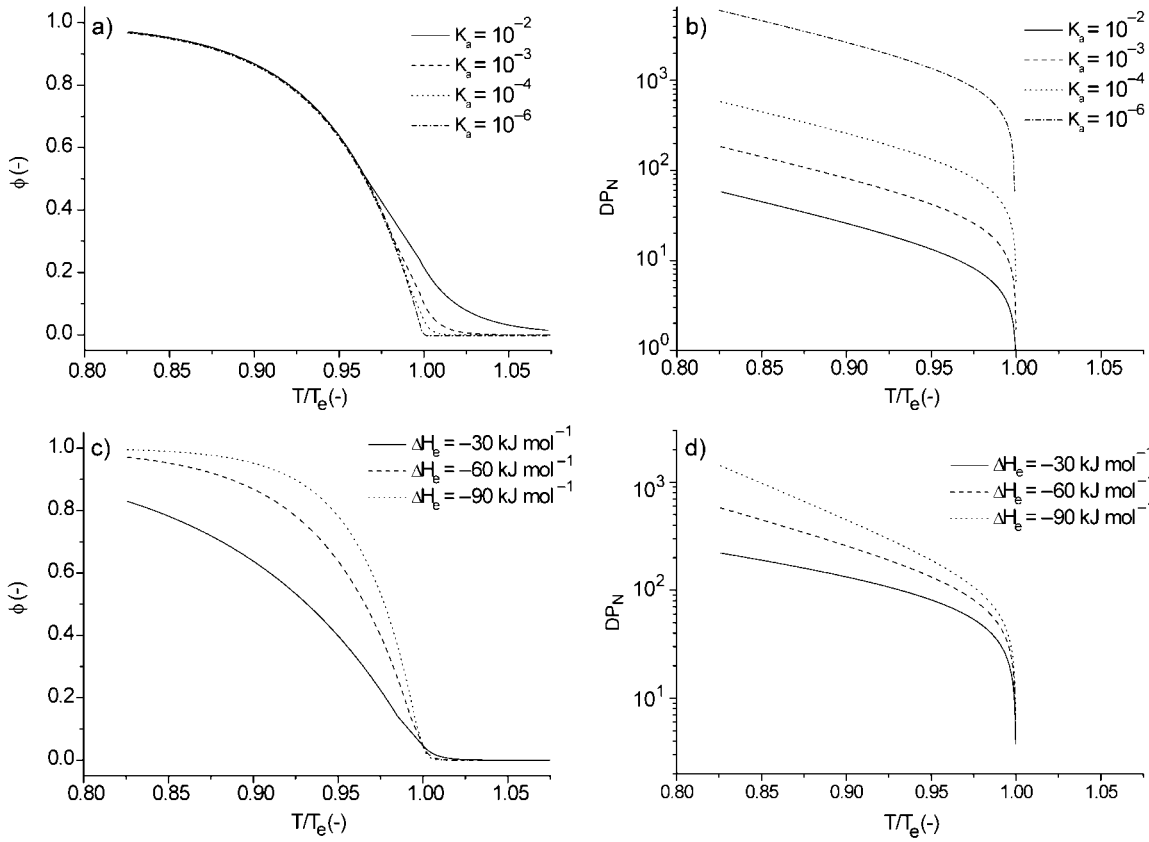

Figure 29. Temperature-dependent properties of cooperative supramolecular polymerizations illustrated using the mean-field thermally activated equilibrium model as analyzed by van der Schoot:[43] fraction of polymerized material, ϕ (a), and number-averaged degree of polymerization, DP_N (b), as a function of the dimensionless temperature T/T_e for four values of K_a, with $\Delta H_e = -60$ kJ mol^{-1}; mole fraction of polymerized material, ϕ (c), and number-averaged degree of polymerization, DP_N (d), as a function of the dimensionless temperature T/T_e for three values of ΔH_e, with $K_a = 10^{-4}$.

occurs, meaning that the equilibrium describing the elongation steps is shifted to the right. As a result, below the critical elongation temperature, the small fraction of activated monomer can readily elongate to form supramolecular polymers with a high *DP*. With this model similar polymerization characteristics can be observed as was shown for the K_2-K model, although now as a function of temperature. For low values of K_a, implying low and relatively high concentrations of activated and nonactivated monomers, respectively, hardly any polymeric species are present at temperatures above the critical temperature T_e. Below the critical temperature T_e the fraction of polymerized material increases abruptly (Figure 29a) and the transition becomes sharper as K_a becomes smaller. Hence, the dimensionless activation constant K_a in this model has a role identical to that of the cooperativity parameter σ in the K_2-K model. At the critical temperature T_e, the number-averaged degree of polymerization, counted over all polymerizing species, is proportional to $K_a^{-1/3}$. The number-averaged degree of polymerization in Figure 29b at temperatures below T_e starts to show an exponential growth, whereas the *DP* becomes proportional to $K_a^{-0.5}$. That is, higher *DP* values can be reached when the cooperativity is increased, as was also observed in the K_2-K model. Similarly, a higher enthalpy release ΔH_e in the elongation regime, corresponding to a higher equilibrium constant for elongation (K_e), will lead to more favorable chain growth (Figure 29c) and higher *DP* values (Figure 29d), as was also observed for the K_2-K model. In contrast to isodesmic supramolecular polymerizations, the shape of the curves that describe the fraction of aggregated material as a function of temperature is clearly nonsigmoidal, although the transition is still rounded. In the limit $K_a \rightarrow 0$ this behavior resembles a true second-order phase transition and nonrounded (i.e., stepwise) behavior is predicted.[43,45,226]

The second model used to illustrate the temperature-dependent properties of supramolecular polymerizations is the activated equilibrium polymerization model as first analyzed by Dudowicz, Douglas, and Freed (DDF) and is based on the reactions depicted in Scheme 8.[41] Similar to their "free association" (isodesmic) model (F), the DDF activated equilibrium polymerization model (A) is based on a mean-field Flory−Huggins incompressible lattice model and includes a polymer flexibility parameter and a monomer−solvent interaction parameter that describes weak van der Waals interactions between monomers. Although the monomer−solvent interaction parameter is important in the calculation of the osmotic compressibility, the second virial coefficient, and the spinodal curve, its influence on the mole fraction of polymerized species (ϕ), the number-averaged degree of polymerization (DP_N), and the constant volume specific heat (C_V) is negligible in the treatment of DDF.[45] The DDF activated equilibrium polymerization model is described by four free energy parameters: the enthalpy ΔH_a and entropy ΔS_a of activation and the enthalpy ΔH_p and entropy ΔS_p of polymerization (i.e., elongation). Figure 30 depicts the temperature-dependent properties (ϕ, C_V, and DP_N) of cooperative supramolecular polymerizations illustrated using the mean-field activated equilibrium polymerization model (A) of DDF. For comparison, the results of the "free association" (isodesmic) model have also been included. The values of the free energy parameters ΔH_a, ΔS_a,

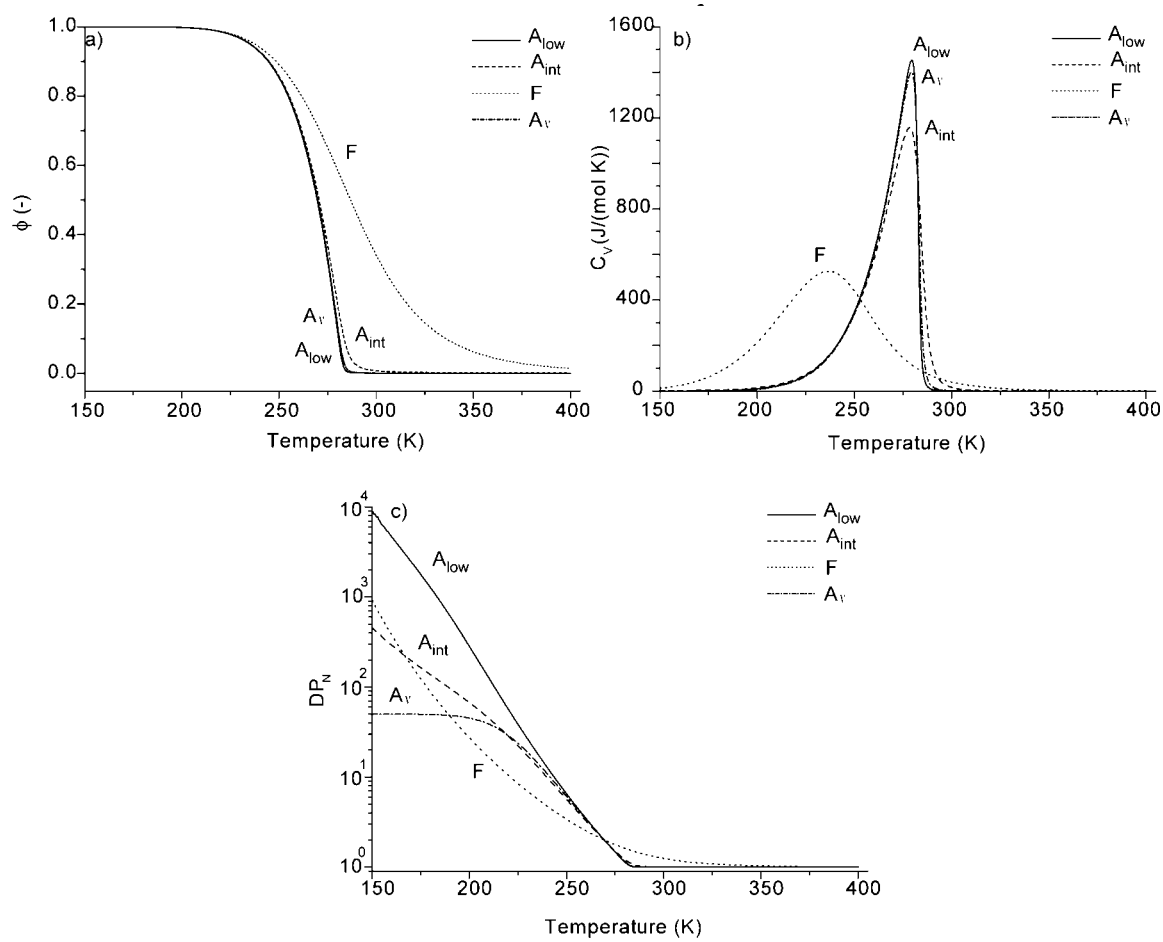

Figure 30. Temperature-dependent properties of cooperative supramolecular polymerizations and comparison to isodesmic supramolecular polymerizations illustrated using the mean-field "free association" model (F) and thermally activated equilibrium model (A) as analyzed by Douglas, Dudowicz, and Freed:[45] (a) Fraction of polymerized material, ϕ, for several values of ΔH_p, ΔH_a, ΔS_p, ΔS_a corresponding to the free association (F) and thermal activation models of equilibrium polymerization (A). The two activation models A_{low} and A_{int} correspond to low and intermediate values of the equilibrium constant K_a ($\Delta S_p = \Delta S_a$ in both cases), whereas the A_ν model corresponds to a polymerization in which $\Delta S_a/\Delta S_p > 1$ and $\Delta H_p = \Delta H_a$. The values of ΔH_p, ΔH_a, ΔS_p, and ΔS_a are given in Table 1. (b) Constant volume heat capacity C_V versus temperature corresponding to the free association (F) and thermal activation models of equilibrium polymerization (A). (c) Number-averaged degree of polymerization, DP_N, versus temperature corresponding to the free association (F) and thermal activation models of equilibrium polymerization (A). In all calculations a cubic lattice and fully flexible chains were assumed. The initial volume fraction of monomer in all calculations was set to 0.1.

Table 1. Values of Free Energy Parameters Used in the Calculations of the Curves in Figure 30 Using the Free Association (F) Model and Activated Equilibrium (A) Model As Analyzed by Douglas, Dudowicz, and Freed

	model			
parameter	F	A_{low}	A_{int}	A_ν
ΔH_p (kJ mol^{-1})	−35	−35	−35	−35
ΔS_p (J mol^{-1} K^{-1})	−105	−105	−105	−105
ΔH_a (kJ mol^{-1})	NA	−10	−17.5	−35
ΔS_a (J mol^{-1} K^{-1})	NA	−105	−105	−185

ΔH_p, and ΔS_p in the comparative analysis of the equilibrium models are summarized in Table 1 and are taken directly from ref 45.

The A_{low} case as depicted in Figure 30 corresponds to a situation in which the overall equilibrium constant for activation is low and the majority of monomers remains present as nonactivated species (M_1). As a result, chain growth is favorable due to the fact that chain propagation occurs via the inactive monomer resulting in a cooperative supramolecular polymerization. When this situation is compared to an isodesmic supramolecular polymerization (F), the activation process results in a much sharper (and nonsigmoidal) transition in the fraction of polymerized material (Figure 30a) and also results in a higher degree of polymerization at a given temperature (Figure 30c). Furthermore, the temperature-dependent heat capacity shows a sharp and asymmetric transition for the A_{low} case compared to the much broader and symmetric transition of the F case (Figure 30b). When the equilibrium constant for activation is increased, corresponding to the A_{int} case, the curve describing the fraction of polymerized material (Figure 30a) still has a clear nonsigmoidal shape. However, the number-averaged degree of polymerization is decreased considerably compared to the A_{low} case due to the much lower fraction of inactivated monomers as chain elongation can only occur due to the addition of inactivated monomers.[41] For the F, A_{low}, and A_{int} models the number-averaged degree of polymerization is unbounded as the temperature is lowered, resulting in an increase in the average chain length of the polymers. In contrast, the growth of the polymers is limited at low temperatures in the A_ν model for which $\Delta S_a/\Delta S_p > 1$ and $\Delta H_p = \Delta H_a$.. Although the growth of the polymers is limited in the A_ν model, the polymerization transition is still extremely sharp as judged by the sudden increase in the

fraction of polymerized material (Figure 30a) and the sharp and asymmetric transition observed in C_V as the temperature is lowered (Figure 30b). As has been argued by Dudowicz, Douglas, and Freed, the A_ν model shows all of the characteristic temperature-dependent properties of living polymerizations and cooperative micelle formation.[45,78]

In conclusion, the temperature-dependent properties of cooperative supramolecular polymerizations have been illustrated using mean-field thermally activated equilibrium models in which an inactive monomer is in thermal equilibrium with an active monomer. Both the helix−coil transition,[322,323] the ordering in magnetic spin systems with applied magnetic field, and the formation of cooperative supramolecular polymers[324,325] can be described in terms of the activated equilibrium model, showing the generality of the approach.

4.3. Hysteresis Effects in Supramolecular Polymers

In the previous section we have discussed the temperature-dependent thermodynamic properties of cooperative supramolecular polymerizations. When the heating and cooling rates are equal, identical temperature-dependent curves should in principle be obtained by heating a solution from the aggregated state to the molecular dissolved state or by cooling a solution of the monomer in its molecular dissolved state to the aggregated, polymeric state. However, often it is found that the heating and cooling curves of a cooperative self-assembly process are not identical, a phenomenon that is termed hysteresis. Examples include the cooperative supramolecular polymerization of C_3-symmetric trisurea discs,[108] the nucleated self-assembly of triple-stranded nucleic acid structures,[326] the cooperative self-assembly of ganglioside micelles,[327] the nucleated self-assembly of virus capsids,[328−330] and the nucleated formation of DNA ribbons[331] and tubes.[332] Furthermore, recent Monte Carlo simulations on a coarse-grained model of an isodesmic supramolecular polymer that was able to undergo a nucleated bundling transition also displayed thermal hysteresis.[333]

Hysteresis is a kinetic phenomenon and implies failure of opposing reactions to equilibrate. As such, hysteresis occurs when there is a large kinetic barrier in the assembly or disassembly pathway, for example, when self-assembly is dominated by homogeneous nucleation. In an insightful study on the self-assembly of long ribbons from DNA tiles, Schulman and Winfree convincingly showed the relationship between homogeneous nucleation rates and the width of the hysteric region deduced from the experimentally determined annealing and melting curves. Furthermore, they were able to show that the addition of a ribbon seed resulted in the disappearance of the hysteresis as heterogeneous nucleation now dominates the self-assembly pathway of these ribbons.

Although such detailed mechanistic studies on hysteresis effects in supramolecular polymers are lacking, we expect that there will be a similar relationship between nucleation rate and hysteresis in the formation of supramolecular polymers when the underlying dynamics is slow.

Because heterogeneous nucleation plays a major role in many different types of self-assemblies, including supramolecular polymerization, we will now discuss the differences between homogeneous and heterogeneous nucleation.

4.4. Heterogeneous versus Homogeneous Nucleation

Nucleation plays a dominant role in cooperative supramolecular polymerization processes, especially at low concentrations. Nucleation can either be homogeneous or heterogeneous in nature. Heterogeneous nucleation occurs much more often than homogeneous nucleation. For a homogeneous nucleation in which the monomer is in (unfavorable) thermodynamic equilibrium with the nucleus, the fraction of aggregated material grows parabolic as a function of time at the beginning of the reaction and only a weak lag phase is observed.[268] For linear supramolecular polymers, homogeneous nucleation is observed in only those cases where all secondary interactions responsible for the polymerization are complementary. When some of these interactions are in conflict with each other, the homogeneous nucleation is strongly hampered and is often taken over by heterogeneous nucleation. In a heterogeneous nucleation, the nucleus forms at a preferential site such as a phase boundary or on impurities such as dust. Typically, nucleation via a heterogeneous mechanism requires less energy than homogeneous nucleation. For example, Dawson and co-workers found that deliberate addition of nanoparticles (copolymer particles, cerium oxide particles, quantum dots, and carbon nanotubes) enhances the probability of appearance of a critical nucleus for nucleation of protein fibrils from human β_2-microglobulin.[272] Heterogeneous nucleation can also occur when nucleation is catalyzed by the surface of an existing supramolecular polymer (secondary nucleation). Initially, nuclei are formed from monomers, but after the creation of a certain amount of supramolecular polymer, the secondary pathway takes control of the growth. The classic example is the double-nucleation mechanism of sickle cell hemoglobin polymerization as proposed by Ferrone.[268] Homogeneous nucleation and heterogeneous nucleation due to secondary surface nucleation can be readily differentiated by studying the kinetics of the supramolecular polymerization. When nucleation occurs via secondary surface nucleation, the fraction of aggregated material grows exponentially as a function of time and a very pronounced lag phase is observed.[268] The reason for this autocatalytic growth is that once a few polymers are nucleated and elongate, they result in a large number of secondary nuclei. After this discussion on the concentration- and temperature-dependent properties of cooperative supramolecular polymerizations, some interesting properties of anticooperative supramolecular polymerizations will be discussed.

4.5. Thermodynamic Aspects of Anticooperative Supramolecular Polymerizations

Figure 31 schematically depicts the Gibbs free energy versus aggregate size i for an anticooperative supramolecular polymerization. As can be observed, the absolute value of $d\Delta G°/di$ decreases for larger aggregate sizes. To illustrate the characteristic properties of anticooperative supramolecular polymerizations, the open-association model of Goldstein and Stryer will be used.[298] In the model analyzed by Goldstein and Stryer, the growth of oligomers smaller than the critical nucleus length is governed by a single equilibrium constant, K_n, whereas the growth of the oligomers after reaching the critical nucleus length, s, is governed by a single equilibrium constant, K. As has been shown in the previous section, cooperative supramolecular polymerizations are

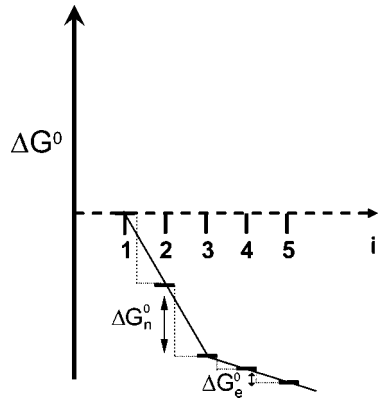

Figure 31. Schematic energy diagram of an anticooperative supramolecular polymerization. The abscissa in this plot represents the size of the oligomer (*i*), whereas the ordinate measures the free energy ΔG° in arbitrary units.

characterized by the fact that $K_n/K < 1$. In contrast, for anticooperative supramolecular polymerizations $K_n/K > 1$ and initial oligomerization is energetically more favorable than subsequent elongation.

It must be stressed that, in contrast to cooperative polymerizations, defining a critical nucleus length for an anticooperative supramolecular polymerization is ambiguous as repulsive interactions (such as steric and electrostatic interactions), which cause anticooperative growth, are more likely to build up gradually as the chain length increases. In that respect, binding models in which the equilibrium constants gradually tamper off, such as the attenuated *K* growth model[42] or the isoenthalpic[334] indefinite self-association model, are probably more realistic models to describe anticooperative growth of supramolecular polymers. However, by use of the conceptual simple model of Goldstein and Stryer and the additional properties calculated by us, an important consequence of anticooperative growth can be illustrated. Figure 32a shows the number-averaged degree of polymerization versus the dimensionless concentration for various values of ω (defined as $(K_n/K)^{s-1}$) and a nucleus size of 5. As can be observed from this graph, for increasing values of ω a finite concentration region develops for which the number-averaged degree of polymerization remains constant. Moreover, the polydispersity index, characteristic for the breadth of the molecular weight distribution at equilibrium, is close to unity within this concentration range, indicating the formation of monodisperse supramolecular polymers (Figure 32b). Only at high values of the dimensionless concentration does the number-averaged degree of polymerization start to increase again, accompanied by a concomitant increase in the polydispersity index to a value of 2. The most important conclusion from these calculations is that anticooperativity in the growth of supramolecular polymers can result in very narrow (almost monodisperse) size distributions within a finite concentration range.

The development of monodisperse supramolecular polymers remains an area of active investigation. Due to their highly reversible nature and absence of suitable supramolecular initiators, the polydispersity of supramolecular polymers is mainly controlled by thermodynamics and not by kinetics as is common in the development of covalent polymers of low polydispersity. Recent examples[335−339] of templated supramolecular polymerizations have shown that the addition of a template can provide another way to create monodisperse supramolecular polymers. In contrast, the self-

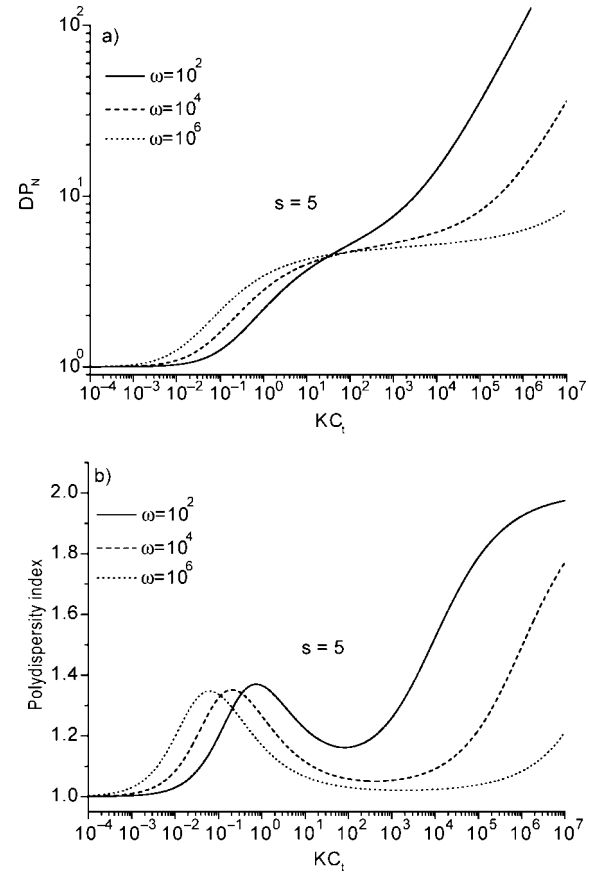

Figure 32. Concentration-dependent properties of anticooperative supramolecular polymerizations in ideal solutions illustrated using the general nucleation−elongation model as proposed by Goldstein and Stryer: (a) number-averaged degree of polymerization, DP_N, versus dimensionless concentration, KC_t, for various values of ω (defined as $(K_n/K)^{s-1}$) for a nucleus size of 5; (b) polydispersity index (defined as the ratio of the weight- and number-averaged degrees of polymerization) versus dimensionless concentration, KC_t, for various values of ω for a nucleus size of 5.

assembly of surfactants into micelles of low polydispersity does not require a template but is based on a delicate balance[340] between attractive hydrophobic forces and repulsive electrostatic and steric interactions, resulting in a nonuniform[341] distribution of the Gibbs free energy as a function of aggregate size. Whereas the hydrophobic effect is responsible for the initial cooperative growth of micelles[289] from monomeric surfactants, anticooperativity arising due to steric and Coulombic interactions between the surfactant head groups results in a gradual decrease in the monomer association constant for larger aggregate sizes. As has been shown by Tanford, this anticooperativity in the growth of micelles results in a decrease of the absolute value of $d\Delta G^\circ/di$ for large values of the aggregate size *i*, in a similar way as is shown in Figure 31.[342] Although micelles cannot be strictly viewed as linear supramolecular polymers, similar free energy diagrams as encountered for micelles can be encountered in the growth of true linear supramolecular polymers due to a combination of cooperative and anticooperative effects (vide infra). For example, Everett has analyzed micelle formation using an indefinite open association (i.e., supramolecular polymerization) model and shown how the presence of an inflection point in ΔG° versus *i* results in both a critical concentration and a nonmonotic size distribution.[343]

4.6. General Molecular Mechanisms of Cooperative Supramolecular Polymerizations

The molecular origin of cooperative growth of supramolecular polymers can be classified into three different groups, that is, cooperativity arising due to electronic effects (both short-range polarization and long-range electrostatic effects), structural effects (both helix formation and allosteric conformational changes), or the hydrophobic effect. In this section we will discuss these three different groups and give examples of each.

4.6.1. Electronic Effects

Cooperativity arising due to electronic effects is commonly encountered in linear supramolecular polymers that reversibly polymerize via hydrogen bonds. As early as 1956, Davies and Thomas reported[344,345] on the supramolecular polymerization of amides in benzene using vapor pressure studies and noted that a single equilibrium constant for the association constant was not sufficient to explain their experimental results. Subsequent thermodynamic studies on the self-assembly of *N*-mono-substituted amides in various apolar solvents performed by LaPlanche[346] and co-workers showed that in all cases two equilibrium constants were needed to describe their experimental data. In both studies it was found that initial dimerization was less favorable compared to subsequent elongation, indicating a cooperative supramolecular polymerization. Further thermodynamic studies on the self-association of *N*-methylacetamide in apolar solvents probed using dielectric spectroscopy,[347] FT-IR,[348] and PGSE NMR diffusion[349] measurements have shown the generality of the results obtained by Davies, Thomas, and LaPlanche. On the basis of the values of the dimerization and elongation equilibrium constant that were reported in these studies, σ values between 10^{-1} and 10^{-3} can be calculated for systems that polymerize via amide type hydrogen bonds. In contrast, FT-IR studies on the supramolecular polymerization of *N*,*N*′-dialkylureas in apolar solutions reported σ values on the order of 10^{-1}, much higher (i.e., less cooperative) than the systems that polymerize via amide type hydrogen bonds.[350]

As a justification for the lower equilibrium constant of dimerization with respect to elongation, LaPlanche and co-workers argued that the difference in the two equilibrium constants can be regarded as an entropic effect due to the fact that the loss of entropy when two monomers form a dimer is greater than when only one monomer and a higher polymer unite, in accordance with the statistical treatment of associated solutions by Saroléa-Mathot.[351] In the treatment of Saroléa-Mathot, the dimerization equilibrium constant is smaller than the elongation equilibrium constant by a factor of p, where p is the number of possible energetically equivalent orientations of the monomer. From this view, the origin of cooperativity in hydrogen-bonded systems is mainly due to entropic reasons. However, more recent ab initio and DFT calculations have shown that the high degrees of cooperativity that are often encountered in the supramolecular polymerization of hydrogen-bonded systems also have an enthalpic contribution arising due to electronic effects. In particular, Dannenberg and co-workers reported extensive HF, DFT, and MP2 calculations on linear hydrogen-bonded systems consisting of linear chains of urea[352,353] and formamide[354,355] molecules. On the basis of these calculations, it was shown that a cooperative effect of almost 200% of the dimer interaction energy operates in long hydrogen-bonding formamide[354] chains, whereas for the urea[353] chains this value was found to be much less (46%), in agreement with the above-mentioned experimental results. Furthermore, calculations on formamide chains of various lengths show that the hydrogen bond length becomes shorter as the number of monomers in the chain increases, whereas the total dipole moment of the chain increases in a nonlinear fashion to an asymptotic value.[354] As discussed by Dannenberg et al.,[354] the unusually large cooperative interactions between hydrogen bonds in formamide chains are the result of several electronic effects: (1) pairwise electrostatic interactions (mainly long-range dipole−dipole interactions), (2) nonpairwise short-range (mutual) polarization, and (3) resonance-assisted hydrogen bonding.[356,357] In the last two cases, the hydrogen bonds increase in strength due to redistribution of the electron density along the chain. Using a pairwise model for the long-range dipole−dipole interactions, Dannenberg estimated that the contribution from nonpairwise electronic interactions to the total hydrogen bond cooperativity was as high as 75%. More recent calculations[358] on the cooperativity of hydrogen bond interactions in a model system for α-helix formation have shown that nonpairwise electronic effects account for half of the total cooperativity that is observed in this system, whereas DFT and MP2 calculations[359] on hydrogen-bonded chains of 1,2-ethanediols and 1,3-propanediones have shown that the natural bond orbital (NBO) atomic charges of oxygen become increasingly more negative with increasing number of monomers in the chain, a clear sign of electron redistribution along the chain. Taking all of these theoretical results into account, it can be concluded that electronic effects can contribute significantly to the total cooperativity in supramolecular polymers that reversibly polymerize via hydrogen bonds and in which the hydrogen-bonding end groups are not separated by a flexible spacer.

4.6.2. Structural Effects

Cooperativity in the growth of supramolecular polymers due to structural effects can arise via two fundamentally different phenomena, that is, the formation of an ordered helical or tubular structure or allosteric effects in which conformational changes alter the affinity between the subunits in the growing chain. These two different causes of cooperativity will now be discussed in more detail.

Cooperativity due to formation of ordered helical and tubular supramolecular polymers arises from the unique disposition of repeating units in the helical and tubular structures as each monomer is simultaneously in contact with multiple repeating units after a certain critical oligomer length is reached (Figure 33). At this point it is important to make the distinction between single-stranded and multiple-stranded supramolecular polymers. For quasi one-dimensional helical single-stranded supramolecular polymers (Figure 33a), the first step consists of isodesmic association with equilibrium constant K_n. The supramolecular polymerization then continues until a nucleus of degree of polymerization s is formed. The addition of one additional monomer then completes the first turn of the helix, after which elongation of the polymer continues with an equilibrium constant for monomer addition K_e. Due to additional favorable interactions between non-adjacent monomer units, K_e is higher than K_n and the overall process of helix formation is cooperative (vide infra). An additional energetic advantage of this intramolecular contact results from the fact that the free energy of formation does

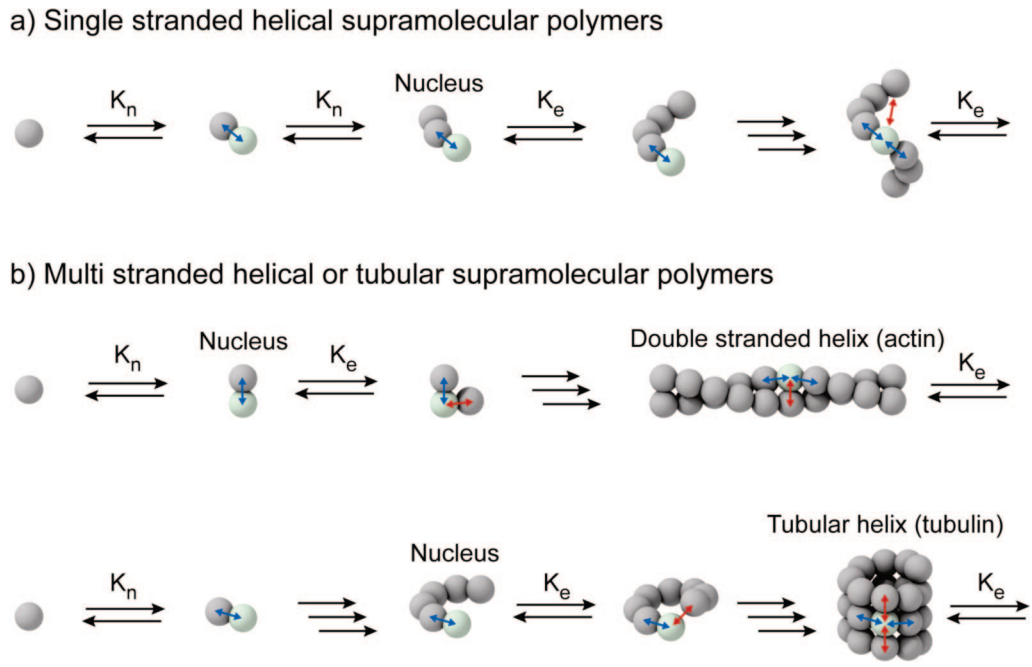

Figure 33. Schematic representation of supramolecular polymerizations in which cooperativity in the growth of the supramolecular polymer arises due to formation of an ordered (helical or tubular) structure: (a) quasi one-dimensional single-stranded helical supramolecular polymers and (b) quasi two-dimensional multistranded helical or tubular structures. The red arrows indicate the secondary interactions responsible for the cooperative growth.

not contain a contribution from the loss of cratic entropy in contrast to the intermolecular interactions.[360]

Cooperative growth of multistranded supramolecular polymers (Figure 33b) is observed in numerous biological polymers, notable examples being the nucleated formation of actin[303,304,306,361,362] (double-stranded helix, nucleus size $\sim$ 3−6), tubulin[363] (tubular helix, nucleus size $\sim$ 15), and sickle cell hemoglobin[274−277] (helical bundles of 14 strands, homogeneous nucleus size $\sim$ 7), although the analysis of the latter polymerization is complicated due to the presence of a double-nucleation pathway. It is generally understood[304,364,365] that the cooperativity in these quasi two-dimensional structures arises due to the presence of multiple interactions per monomeric unit with more than two nearest neighbors (Figure 33b). As a result, molecules at a boundary with some bond sites unoccupied are in a higher energy state than those whose bonding potential is saturated within the aggregate. As is often observed for multistranded biological polymers as well as for crystallizations, the initial stage of growth under these conditions is highly unstable and thus follows a nucleated pathway. Only when such an aggregate exceeds the critical nucleus size is further growth favorable.

Oosawa and Kasai were the first to formulate a thermodynamic treatment[303,304] of multistranded helical polymerizations, which took into account the fact that the equilibrium constant for adding monomers to form the initiating nucleus will generally be lower than the equilibrium constant for continued addition to the helical structure. The simple geometrical explanation of this behavior is that more stabilizing bonds can be formed by adding a unit to the growing helix than to the incomplete first turn, as is schematically depicted in Figure 33b. Their thermodynamic analysis showed that helical polymerizations can exhibit a critical concentration below which the monomers will not assemble into polymers and above which virtually all additional monomer polymerizes rapidly into helical polymers. Furthermore, they also showed that, for extremely cooperative helical polymerizations, near the critical concentration only a small amount of helical polymer is formed but that the average degree of polymerization of these helical polymers is extremely high. Somewhat later, Erickson[364] formulated a more general cooperative model for multistranded reversible polymerizations taking into account the loss of translational/rotational entropy upon association of free monomers into the polymer. This entropic factor was shown to be an important factor in determining the overall cooperativity in the growth of multistranded supramolecular polymers.

Caspar[365] was the first to suggest the role of conformational changes (allosteric effects) as a dominant mechanism to achieve high degrees of cooperativity in biological polymerizations. In the assembly mechanism proposed by Caspar, which he termed "autostery", polymerization induces the subunit to change conformation to a state favoring further association, resulting in a cooperative growth. As noted by Caspar, autostery in protein associations can give the appearance of highly cooperative polymerizations even for the formation of linear, one-dimensional polymers. Allosteric effects as a cause of cooperative growth of linear supramolecular polymers have recently gained significant interest. Several groups[366,367] recently proposed such a mechanism to explain the high degrees of cooperativity found in the nucleated polymerization of FtsZ, the bacterial homologue of tubulin. In contrast to many biological polymers, FtsZ is a linear single-stranded polymer, and hence the cooperativity in the growth of the one-dimensional structure cannot arise in a similar way as for multistranded polymers.

Thomas and Romberg[366] recently formulated an insightful and extensive mathematical model to investigate the influence of conformational changes on the growth of one-dimensional reversible polymerizing systems (Figure 34). In the generic allosteric model for linear polymerizations formulated by Thomas and Romberg, subunits convert between two different conformations, H and L, governed by an equilibrium

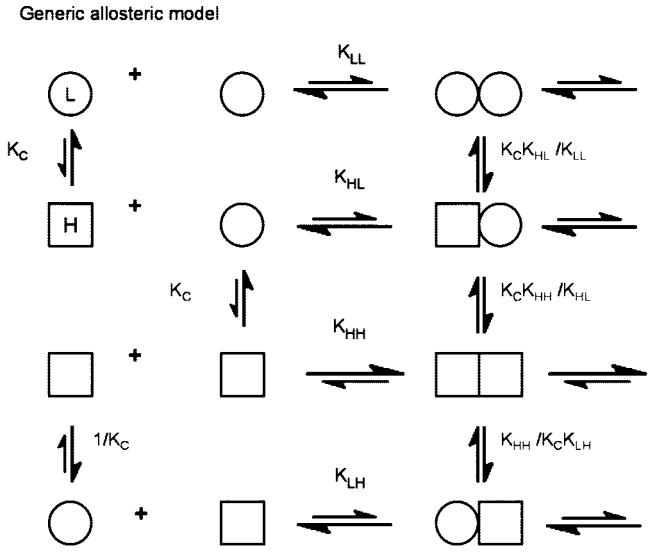

Figure 34. Generic allosteric model for linear polymerizations as proposed by Thomas and Romberg.[366] In this model K_C represents the equilibrium constant governing the conformational equilibrium between the low-affinity L subunit and the high-affinity H subunit. The two types of monomers can associate to form four types of dimers with four independent equilibrium constants (K_{LL}, K_{HH}, K_{HL}, and K_{LH}). (Reprinted with permission from ref 366. Copyright 2008 Elsevier.)

constant K_c. Subunits in both conformations can polymerize but do so with different affinities. Whereas subunits in the L conformation polymerize with low affinity, subunits in the H conformation polymerize with high affinity such that K_{HH} is larger than K_{LH}, K_{LH}, and K_{LL} (see Figure 34).

Various versions of the allosteric polymerization model were investigated for their ability to exhibit sharp critical concentrations, a hallmark of cooperative growth. For the general allosteric model, it was shown that the largest cooperativity resulted when K_{HH} was as large as possible and K_C, K_{LL}, K_{LH}, and K_{HL} were as small as possible. This is because for the polymerization to proceed in a cooperative manner, monomers should not associate easily and hence should be primarily in the low-affinity conformation ($K_C \ll 1$), whereas subunits in the polymer should be in the high-affinity conformation to associate strongly ($K_{HH} \gg K_{LL}$). Furthermore, Thomas and Romberg investigated other models for allosteric linear polymerization such as monomer activation followed by isodesmic polymerization ($K_{LL} = K_{HL} = K_{LH} = 0$) and a model in which only one end changes conformation ($K_{HL} = K_{HH}$, and $K_{LH} = K_{LL}$). It was shown that the first model indeed exhibits a sharp critical concentration, indicative of a cooperative growth mechanism, whereas in the latter case no cooperativity in the growth of the one-dimensional polymer was found. On the basis of the above-discussed examples, structural effects are likely to play an important role in the cooperative growth of synthetic supramolecular polymers.

4.6.3. Cooperativity Arising Due to the Hydrophobic Effect

The hydrophobic effect, the tendency for nonpolar solutes to aggregate in aqueous solutions, is a major driving force for self-assembly both in biological[289,368] and in synthetic[167,369] systems, including supramolecular polymers.

As has been argued by Chandler,[370] the tendency for hydrophobic particles to associate in water can be readily understood in terms of the dependence of hydrophobic solvation on solute size. Following the arguments of Chandler, imagine n identical small hydrophobic particles solvated in water, all well separated and thus solvated separately. When these n solutes assemble together to form a hydrophobic unit with a large surface area (>1 nm), the overall free energy changes from growing linearly with solvated volume to growing linearly with solvated surface area. As the volume to surface area ratio becomes larger as the assembly grows, the aggregate will reach a critical volume characterized by a critical number of solute molecules, at which the solvation free energy of the assembly becomes lower than the individually solvated solute molecules, thereby providing a favorable driving force for aggregate formation. As the individual solute molecules combine to form a large aggregate, it is no longer possible to describe hydrophobic forces using pairwise interactions and a breakdown of additivity takes place.[370,371] The breakdown of additivity of hydrophobic forces is a manifestation of the cooperative nature of hydrophobic interactions and has been a subject of recent investigations. Levitt and co-workers performed extensive molecular dynamic simulations of methane assemblies in water using an explicit solvent model.[372] Their simulations show that the formation of a methane aggregate is a cooperative process; that is, the change in free energy of adding a methane molecule to a assembly of given size becomes more negative as the assembly size increases. Moreover, it was shown that the formation of small methane aggregates is thermodynamically unfavorable ($\Delta G° > 0$). More recent simulations on the self-assembly of three methane molecules using an explicit water model have shown that three body hydrophobic interactions can be either cooperative or anticooperative depending on temperature.[373] Furthermore, Scheraga[374] and co-workers performed extensive simulations on aggregates of four methane molecules and found that the cooperativity in hydrophobic interactions is much more pronounced compared to the three-particle case. It has been suggested[374] that the origin of the breakdown of additivity in hydrophobic interactions is due to dewetting of large apolar interfaces as dewetting is a collective, many-particle phenomenon.[375]

Although no systematic studies on the role of hydrophobic cooperativity on the polymerization mechanism of supramolecular polymers in water have been reported, it is interesting to note that hydrophobic cooperativity has been suggested as a dominant mechanism for amyloid nucleation.[376]

4.7. Examples of Cooperative Supramolecular Polymerization

In this section examples will be discussed that are shown or suggested to polymerize via a cooperative supramolecular polymerization mechanism. The examples are classified according to the origin of the cooperativity, which can be categorized as being due to three main effects: electronic, structural, or hydrophobic. Because multiple effects can contribute to the origin of cooperative growth, it is not always clear which effect is the major contributor. Furthermore, given the resemblance between a nucleated and a downhill supramolecular polymerization mechanism, it is not always straightforward, on the basis of thermodynamic data, to distinguish between these two mechanisms. In that case, kinetic experiments will help to ascertain which of the two mechanisms is operative. In the final part of this section examples of anticooperative supramolecular polymerizations will be discussed.

Chart 29

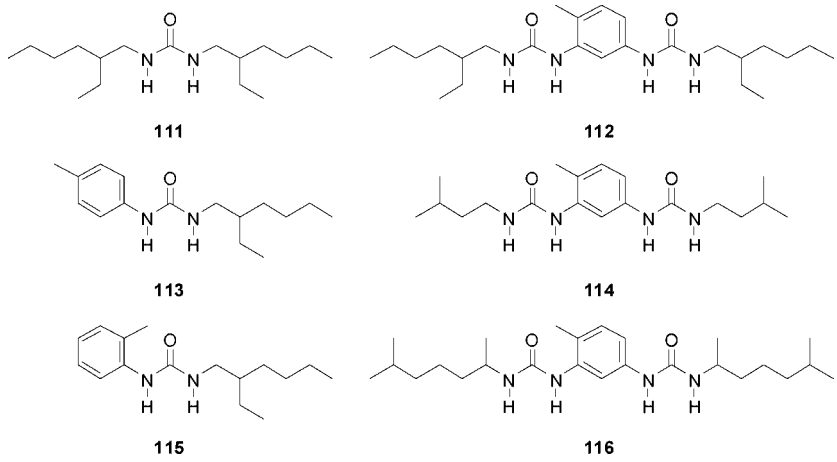

4.7.1. Cooperativity Due to Electronic Effects

Bouteiller and co-workers have studied in great detail the cooperative supramolecular polymerization of urea derivatives into linear, one-dimensional aggregates. The first urea compounds that were reported by this group were monourea derivative **111** and bis-urea derivative **112** (Chart 29). Both **111** and **112** were found to aggregate in apolar solvents via intermolecular hydrogen bonds, as was determined by IR spectroscopy in solution, whereas solution viscometry confirmed the formation of supramolecular polymers.[377] At a concentration of 4×10^{-4} M in carbon tetrachloride, at 25 °C, **111** was fully dissociated into monomers, whereas **112** was completely polymerized. Furthermore, **112** remained fully aggregated when the concentration was decreased an additional order of magnitude, which indicates that the association constant for **112** is orders of magnitude larger than that for **111**. The very strong association for bis-urea derivative **112** also allowed the study of the structural and rheological properties of this supramolecular polymer in apolar solvent using SANS and rheology.[378] These studies indicated that **112** organizes into long, rigid fibrillar structures due to reversible intermolecular hydrogen bonding.

To get a better understanding on the supramolecular polymerization mechanisms of bis-urea-based supramolecular polymers in chloroform, Bouteiller and co-workers studied a series of bis-urea derivatives, as well as some monourea model derivatives (Chart 29).[379] Using the IR absorption band of the free, nonassociated monomer, it was possible to determine the fraction of free N−H groups at each concentration and, hence, also the fraction of polymerized material. No satisfactory fit of the data could be obtained with an isodesmic supramolecular polymerization model. However, the cooperative K_2-K model yielded an excellent fit of the concentration-dependent data, resulting in a K value of 1400 M^{-1} and a σ value of 1.5×10^{-2} in chloroform at room temperature. The two monourea model compounds (**113** and **115**) yielded K values >2 orders in magnitude lower compared to the bis-urea compounds (17 and 8.0 M^{-1}, respectively), showing the cooperative effect when going from one to two urea functionalities per molecule. On the basis of the equilibrium constants, the degree of polymerization and the polydispersity were determined as a function of concentration for **112** and compared to an isodesmic polymerization having the same association constant. For the two other bis-urea derivatives, **114** and **116**, higher K values (2300 and 1700 M^{-1}, respectively) were determined, as well as a higher degree of cooperativity, as expressed by lower σ values (3.0×10^{-3} and 8.2×10^{-3}, respectively). These differences were explained by the reduced steric hindrance of the 3-methylbutyl substituent compared to the 1,5-dimethylhexyl and 2-ethylhexyl groups. The origin of the cooperativity for these bis-urea derivatives was attributed to polarization of the urea function after the formation of dimers, as was discussed in the previous section. This polarization effect was also used to account for the observed cooperativity in the supramolecular polymerization of monourea derivatives.[380] Although Bouteiller and co-workers used the K_2-K model for their analysis, they acknowledge the fact that this model is an approximation because the association constants for the formation of trimers and higher oligomers are probably not equal to each other.[380]

Chart 30

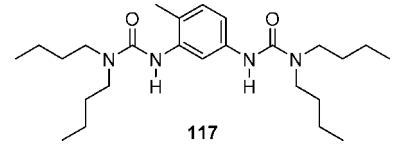

To obtain more evidence for the cooperative formation of supramolecular polymers of **112** in chloroform, ITC was employed.[381] The obtained enthalpograms at different concentrations could be satisfactorily analyzed only by using the K_2-K model, yielding a K value of 1700 M^{-1} and a σ value of 3.4×10^{-3} at 20 °C. These values were in good agreement with the previously determined values from solution IR studies. Furthermore, repeating the experiment at different temperatures revealed that the K value, as expected, decreased with increasing temperature, whereas the σ value increased. This indicates that the degree of cooperativity is reduced when the temperature is raised.

Compound **117** (Chart 30), which is a very poor hydrogen bond donor and hence will mainly act as a hydrogen bond acceptor, was found to act as a chain stopper when it was introduced to a solution of **112** in carbon tetrachloride.[382] Using IR spectroscopy, viscometry, light scattering, and ITC experiments, it was shown that the chain stopper can strongly reduce the concentration dependence of the degree of polymerization over a realistic concentration range.[382] Furthermore, rheology experiments on mixtures of **117**:**112** confirmed the dynamic nature of the supramolecular polymer and revealed that the polymer is semiflexible.[55]

Bouteiller and co-workers serendipitously found that the viscosity of **112** in toluene suddenly dropped above 40

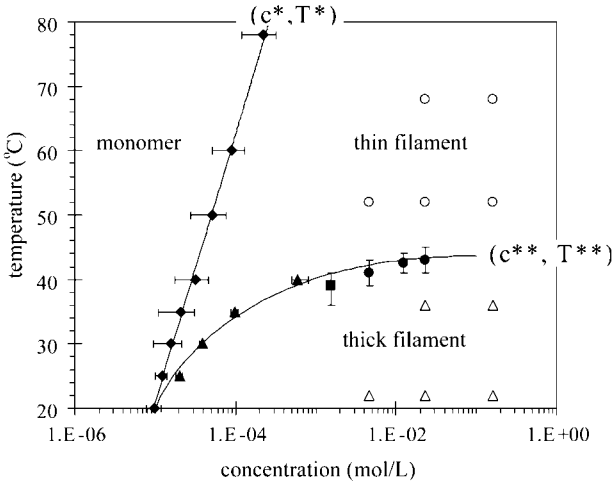

Figure 35. Pseudophase diagram of **112** solutions in toluene. (Reprinted from ref 383. Copyright 2005 American Chemical Society.)

°C.[383,384] This drop in viscosity could not be ascribed to the disassembly of the supramolecular polymer into monomers, because IR spectroscopy did not reveal any free N−H vibrations at these temperatures.[383] SANS showed that at 40 °C a transition occurred from a thin threadlike structure (with a single molecule per cross section) at high temperature to a thick threadlike structure at low temperature (with three molecules in the cross section). ITC in combination with the SANS results allowed for the construction of a pseudophase diagram for **112** in toluene (Figure 35).

Very recently, Bellot and Bouteiller showed that the supramolecular polymerization of **112** in toluene could be described by a model (Scheme 9) that describes a competition between the thin filamentous structure (F_n supramolecular polymer) and the thick, rigid tube-like structures (T_n supramolecular polymer).[385] On the basis of this model, a thermodynamic study was undertaken to validate the proposed pseudophase diagram (Figure 35).

Similar to the results described in chloroform,[379] also in toluene a cooperative K_2-K model could be used to describe the supramolecular polymerization of **112**. Because there are two types of supramolecular polymers, four equilibrium constants are needed to describe the system. Furthermore, by introducing the temperature dependence of each equilibrium constant, eight parameters are required to describe the whole system (as each equilibrium constant is a function of an enthalpy of association ΔH_p and a reference temperature T_0). Using high-sensitivity DSC and ITC, Bellot and Bouteiller could elegantly determine all eight parameters. At 25 °C the supramolecular polymerization from monomer to polymer F_n was characterized by a K of 77×10^3 M^{-1} and σ of 1.1×10^{-2}, whereas for polymer T_n these values were 87×10^3 M^{-1} and 2.8×10^{-6}, respectively. With these parameters the experimental pseudophase diagram (Figure 35) could be verified and was subsequently confirmed with viscometry measurements.

Chart 31

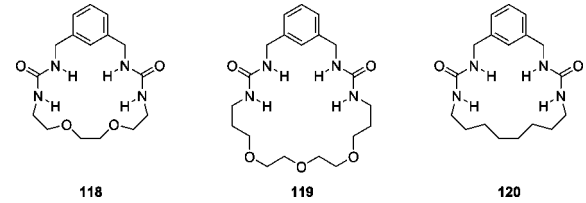

Additional $\pi-\pi$ interactions introduced by the incorporation of oligo(*p*-phenylene vinylene) moieties to a bis-urea group did not alter the cooperative nature of the supramolecular polymerization, as was shown by Kitamura and coworkers.[386]

Shimizu et al. prepared cyclic monomers containing the bis-urea moiety connected via an *m*-xylene linker and either an oligo(ethylene glycol) or an alkyl linker (Chart 31).[387] In 1,1,2,2-tetrachloroethane these monomers polymerized via intermolecular hydrogen bonding as could be deduced from concentration-dependent ^{1}H NMR and solution FT-IR studies. Due to the presence of heteroatoms in **118** and **119**, at low concentration (typically 0.5−1.0 mM) also intramolecular hydrogen bonding was present in the monomer, which was more pronounced for **119** because of its more flexible ring.

The concentration-dependent FT-IR absorption data could be analyzed by the K_2-K model to determine the association constants, yielding for **118** and **119** very similar K_2 and K values ($K_2 = 39$ M^{-1} and $K = 36$ M^{-1} for **118**; $K_2 = 13$ M^{-1} and $K = 5$ M^{-1} for **119**). This shows that for these heteroatom-containing cyclic structures no cooperativity could be found in the supramolecular polymerization and that even a small degree of anticooperativity is present, which might be related to competitive intramolecular hydrogen bonding between the oxygens and the urea moiety. In contrast, for **120** a cooperative polymerization process was found with a K_2 of 30 M^{-1} and K value of 600 M^{-1} (i.e., $\sigma = 5.0 \times 10^{-2}$). The lower elongation constant of **120** in 1,1,2,2-tetrachloroethane, as compared with the linear bis-urea derivatives (**112** and **114**, vide supra) studied in chloroform, was explained by the difference in solvent polarity.

Feringa and van Esch have reported the cooperative self-assembly of 1,2-bis-ureido cyclohexane derivatives (Chart 32).[388]

^{1}H NMR measurements on solutions of **121** in chloroform showed a strong downfield shift of the N−H proton with increasing concentration, indicative for the formation of supramolecular polymers through intermolecular hydrogen bonding. The concentration dependence of the chemical shift

Scheme 9. Association Equilibria Describing the Polymerization of Monomers (M) into Two Supramolecular Polymers (F_n and T_n) (Reprinted from Reference 385; Copyright 2008 American Chemical Society)

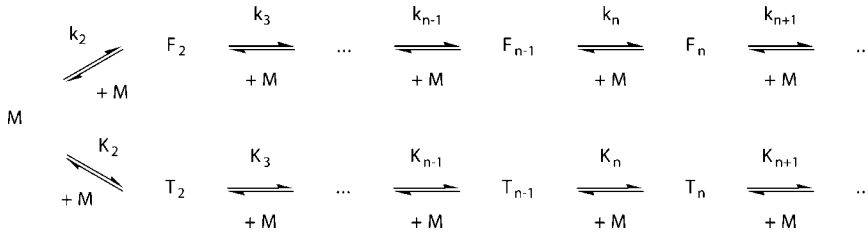

Chart 32

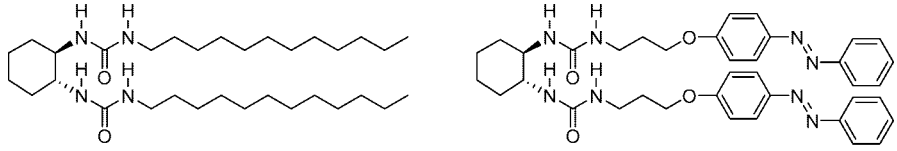

121 122

Chart 33

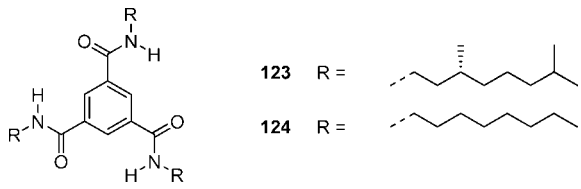

of the N−H proton could not be analyzed by an isodesmic binding isotherm. However, the K_2-K model could describe the experimental data, yielding a K_2 value of 25 M^{-1} and a K value of 179 M^{-1} (i.e., $\sigma = 1.4 \times 10^{-1}$) at 50 °C. Introduction of a 1,2-bis-ureido cyclohexane derivative functionalized with two azobenzene chromophores, **122**, was found to influence the dimerization constant K_2 of **121**, which was reduced to 4 M^{-1}, without altering the elongation constant K (i.e., $\sigma = 2.3 \times 10^{-2}$). Although the authors do not comment on the origin of cooperativity, it can be anticipated that similar electronic effects as reported by Bouteiller (vide supra) are operative in these 1,2-bis-ureido cyclohexane derivatives.[379,380]

Next to supramolecular polymers that self-assemble in a cooperative fashion as a result of electronic effects due to hydrogen-bonding urea groups, also monomers containing amide moieties have been reported to polymerize via a cooperative growth mechanism.

Our group has reported the cooperative supramolecular polymerization of C_3-symmetrical trialkylbenzene-1,3,5-tricarboxamides (Chart 33).[325] Previously it was shown that these discotic molecules self-assemble into helical columnar stacks both in the liquid crystalline state and in dilute alkane solutions.[108,389,390] The helicity in the stacks is caused by amide bonds that are rotated out of the plane of the central aromatic ring to allow for intermolecular hydrogen bonds, as X-ray studies on a related benzene-1,3,5-tricarboxamide in the solid state demonstrated.[391]

Using temperature-dependent spectroscopic measurements, insights into the cooperative supramolecular polymerization of discotics **123** and **124** could be obtained. Upon cooling of a heptane solution of **123** from 90 to 20 °C the appearance of a bisignated Cotton effect was observed, which is indicative for the formation of chiral helical columnar aggregates (Figure 36A). A hypsochromic shift in UV−vis absorption of 15 nm was observed when the temperature of the solution was lowered (Figure 36B). This indicates the formation of H-type aggregates, which is in agreement with the helical, columnar structure. By monitoring the CD and UV−vis absorption of **123** at a wavelength characteristic for aggregation, the fraction of polymerized material as a function of temperature could be determined (Figure 36C).

Both spectroscopic techniques revealed an identical, non-sigmoidal transition, whereas analysis by the model developed by van der Schoot,[43] as discussed previously, allowed the determination of the thermodynamic parameters. This resulted in an enthalpy release, ΔH_e, of −60 kJ mol^{-1} and a K_a value of 10^{-6} at $T = T_e$. Performing experiments at different concentrations allowed for the construction of a modified van 't Hoff plot in which the logarithm of the concentration was plotted versus the reciprocal T_e. The slope found in this van 't Hoff plot of −66 kJ mol^{-1} corresponded nicely to the value of −60 kJ mol^{-1} found for the enthalpy release by analysis of the absorption data using the model by van der Schoot. Remarkably, replacing the chiral alkyl side chains with achiral octyl tails was found to significantly influence the supramolecular polymerization as is evident from the higher enthalpy release (−70 kJ mol^{-1}) and lower K_a value (10^{-4}) determined for **124**. As a result of the decreased degree of cooperativity, the degree of polymerization at room temperature was calculated to be lower than for **123** under otherwise equal conditions.

Similar to the bis-urea derivatives, the origin of this cooperativity is likely to be an electronic effect and could be related to polarization effects and the orientation of the dipoles, which changes during aggregation and thereby influences the intermolecular hydrogen bonding strength.[392,393] This suggestion is strengthened by the results obtained for the bipyridinyl-based C_3-symmetrical discs **22** and **23** (Chart 4) discussed above. These discotics, in which only intramolecular hydrogen bonds are present, self-assemble via an isodesmic growth mechanism in apolar solvents, whereas C_3-symmetrical discs **123**−**124**, capable of forming intermo-

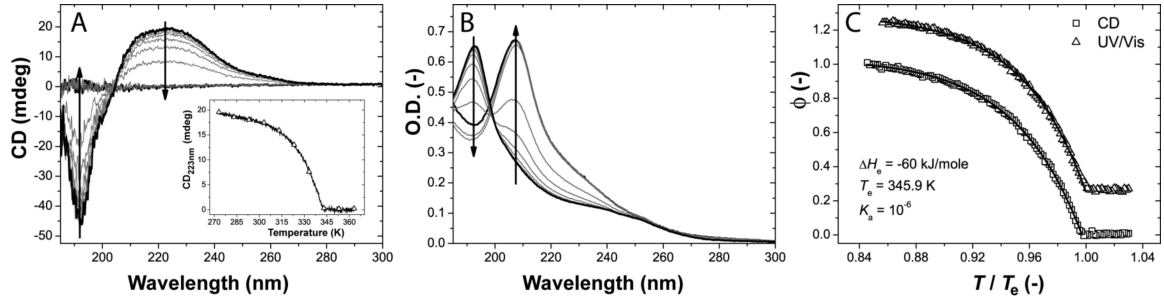

Figure 36. CD (A) and UV−vis (B) spectra of **123** in heptane (1.4×10^{-5} M) at temperatures between 20 and 90 °C with 10 °C intervals. Arrow indicates increase in temperature. The inset in (A) shows the CD effect at 223 nm as a function of temperature. (C) Mole fraction of polymerized material, ϕ, as a function of the dimensionless temperature, T/T_e, based on CD and UV−vis absorption data recorded at $\lambda = 223$ nm. For clarity, the data based on the UV−vis absorption are depicted with a 0.25 offset in the y-direction. (Reprinted from ref 325. Copyright 2008 American Chemical Society.)

Chart 34

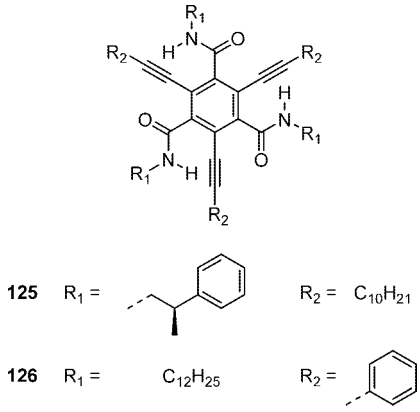

lecular hydrogen bonds, display a highly cooperative supramolecular polymerization mechanism.

The group of Nuckolls has prepared supramolecular polymers based on C_3-symmetrical hexasubstituted aromatic molecules, in the solid state, in the liquid crystalline state, in solution, and on surfaces.[394−400] Similar to the discotics reported by our group (Chart 33), discotics **125** and **126** (Chart 34) are equipped with three 1,3,5-*meta*-positioned amide groups, but are also equipped with three 2,4,6-*meta*-positioned alkynyl substituents. Molecular modeling showed that the amide groups were forced out of the plane of the central amide core by these substituents (Figure 37).

To study the self-assembly of the crowded aromatics **125** and **126** in solution, fluorescence spectroscopy was employed.[395] In dichloromethane, at a concentration of 10^{-5} M, both **125** and **126** show a fluorescence emission spectrum in which two peaks are discernible, which were interpreted as a sharp monomer peak and a broad aggregate peak. Comparing the ratio of monomer/aggregate peak for **125** and **126** showed that the concentration of monomers in solution is higher for **126**. The broad emission spectrum of the aggregates suggests a wide distribution of aggregate sizes. As the concentration of **126** was increased, the monomer emission was reduced in favor of the aggregate emission, confirming the growth of the supramolecular polymer. To estimate the aggregate size, AFM and SEM were employed, which revealed self-assembled objects with high aspect ratios for both **125** and **126**, suggesting that a considerable degree of polymerization is reached.

The equilibrium between monomers and polymers with high DP_N implies a bimodal distribution, which is indicative of a cooperative supramolecular polymerization process. This is in accordance with the cooperative polymerization of the

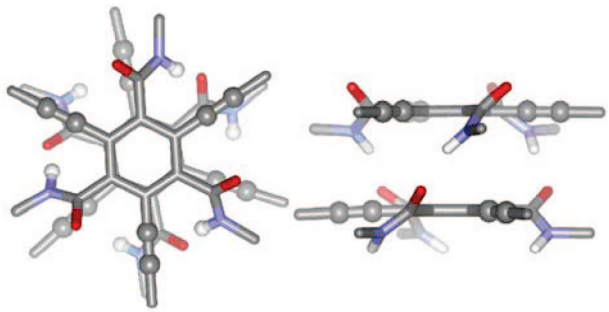

Figure 37. Energy-minimized molecular model of the crowded aromatics. (Reproduced with permission from ref 394 by permission of the PCCP Owner Societies. Copyright 2007 The Royal Society of Chemistry.)

Chart 35. Molecular Structure (Left) and Self-Assembled, Nanotubular Structure (Right) of the Cyclic Eight-Residue Peptide (For Clarity, Only the Backbone Structure Is Represented)

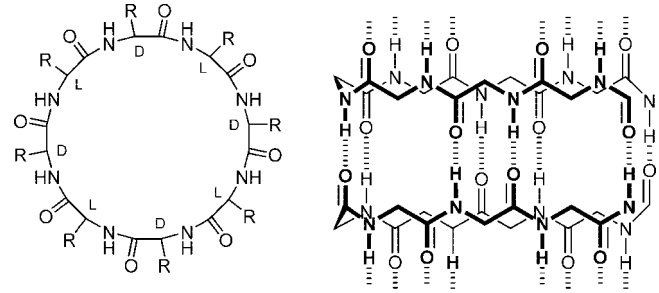

127

discotics reported by our group (Chart 33); that is, in both systems a dipole is present in each molecule and for both the self-assembly is driven by intermolecular hydrogen bonding and to a lesser extent by $\pi-\pi$ interactions.

Ghadiri et al. have reported the use of hydrogen-bonding interactions between cyclic peptides to arrive at supramolecular polymers that can form nanotubes in aqueous media.[401−410] Their initial research was based on a cyclic eight-residue peptide with alternating L- and D-configuration, **127** (Chart 35).[401,402,404,406]

FT-IR spectroscopy confirmed that intermolecular hydrogen bond formation drives the supramolecular polymerization of the cyclic peptides.[401,406] FT-IR data, in combination with electron diffraction on crystals, revealed that the peptide units are stacked in an antiparallel β-sheet-like arrangement.[406] The low solubility and the high stability of the nanotubes in solution were attributed to a highly cooperative supramolecular polymerization. The origin of this cooperativity was ascribed to a significant preorganization of the monomers (suggesting also an allosteric cooperative effect) and the simultaneous formation of multiple noncovalent interactions.[406,410] In line with this, it has been shown by computational studies that the formation of antiparallel β-sheets occurs via a cooperative mechanism.[411−413] Selective backbone *N*-alkylation was used as a suitable approach to limit the supramolecular polymerization to only the formation of peptide dimers, for which the corresponding dimerization constant in chloroform was determined from concentration-dependent ^{1}H NMR spectroscopy.[408,410] Modification of the cyclic peptide structure by incorporation of a 1,4-disubstituted-1,2,3-triazole ε-amino acid in a four-residue cycle was found to result in an anticooperative supramolecular polymerization (vide infra).[414]

Smith et al. studied the gel formation of a family of four gelators with lysine units attached to both ends of an aliphatic diamine with different peripheral groups.[415] They observed that prior to the sol−gel transition a cooperative one-dimensional supramolecular polymerization, mediated by intermolecular amide hydrogen bonds, was operative. Analysis of the concentration-dependent chemical shift of the NH protons using the K_2-K model showed that the degree of cooperativity was modulated by the nature, number, and location of the peripheral groups. This study shows for the first time how the minimum gelation concentration and macroscopic thermal stability of low molecular weight gelators can be rationalized in terms of the solubility and cooperative self-assembly of molecular scale building blocks.

The supramolecular polymerization of merocyanine dyes (Chart 36) has been studied in detail by Würthner and co-

Chart 36

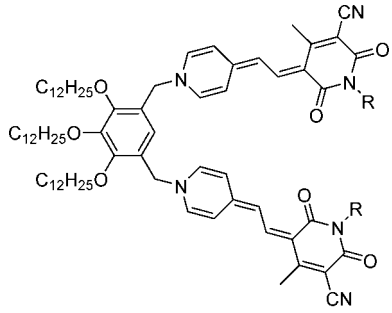

128 R = *n*-$C_{12}H_{25}$

129 R = 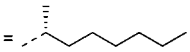

130 R = 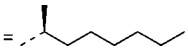

workers. The polymerization is achieved by the antiparallel association of the dipole moments in the monomers (schematically depicted in Figure 38), because the extremely high dipole moment of 17 D allows for a high dimerization constant of $K_{dim} > 10^6$ M^{-1} in tetrachloromethane, as determined using concentration-dependent UV−vis spectroscopy.[416]

In solvents of lower polarity, such as methylcyclohexane (MCH), the dimerization constant was increased to values exceeding 10^8 M^{-1}. Dimerization of bifunctional merocyanine dye **128** results in the formation of small oligomeric structures at low concentration in apolar solvents as well as in solvents with higher polarity, such as tetrachloroethane, as evidenced by viscosity measurements. These oligomeric structures further assemble into fiber-like aggregates, for which force field calculations suggested that these aggregates consist of six linear intertwined oligomers.[417] X-ray diffraction on the supramolecular fiber-like polymers showed an additional $\pi-\pi$ interaction with an additional neighboring molecule, besides the one already present in the original oligomer. This second interaction indicates that the polymerization is not purely one-dimensional in nature and should be categorized as quasi two-dimensional (Figure 33). As a result of the increased $\pi-\pi$ interactions the absorption maximum was hypsochromically shifted, and hence this

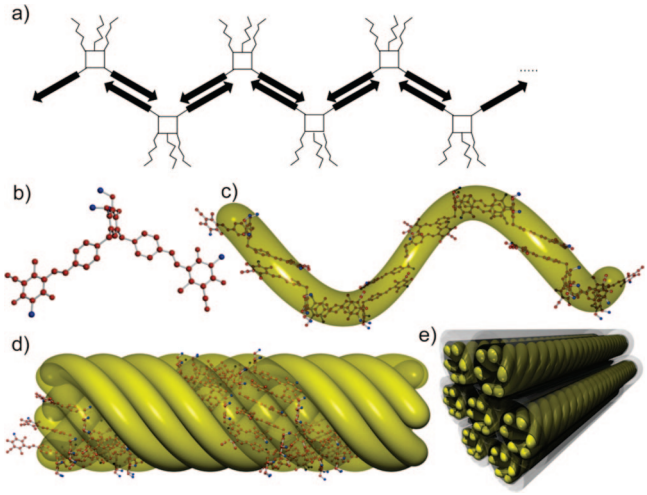

Figure 38. Mode of polymerization and hierarchical supramolecular organization of the merocyanine dyes. (Reprinted with permission from ref 416 Copyright 2003 John Wiley & Sons, Inc.)

polymer is referred to as the H-type aggregate. The formation of this polymer was studied by temperature-dependent and solvent polarity-dependent UV−vis spectroscopy. By increasing the amount of MCH in the THF/MCH mixture, a sharp increase in intensity at the absorption maximum of the H-type aggregate and a sharp decrease at both the monomer and oligomer bands could be observed. This sharp increase is indicative for a cooperative supramolecular polymerization process. However, direct evidence was obtained by temperature-dependent measurements, where also a sharp nonsigmoidal transition was observed. An increase in concentration allowed the bundling of the supramolecular polymer that grew to such an extent that solvent gelation could be achieved. By the addition of a monofunctional dye that can act as a chain stopper, the reversible nature of the polymerization was revealed by a drop in the viscosity at increasing amounts of chain stopper.[416] Intriguingly, the introduction of chirality in **129** allowed the visualization of two H-type supramolecular polymers showing opposite helicity and a difference in thermodynamic stability.[418] Thus, for the supramolecular polymerization of **129** three different types of supramolecular arrangements can be obtained. The synthesis of the enantiomer **130** and the use of the already available achiral derivative allowed "Sergeant and Soldiers" and "Majority Rules" experiments to be performed. Instead of performing a thermodynamic analysis, the chiral amplification was followed as a function of time by CD and UV−vis spectroscopy. The Sergeant and Soldiers experiments revealed an increasing amplification rate when the amount of chiral Sergeant present in the system was increased.[419] Because three types of assemblies could be formed, the kinetic data of the Majority Rules experiments could be analyzed in great detail.[420] Prior to chiral amplification, the transition from the oligomers to the first H-type aggregate, the kinetic data showed a lag phase in the UV−vis traces indicative of a nucleated supramolecular polymerization. After formation of the H-type aggregate, an autocatalytic amplification of chirality was revealed, which was attributed by the authors to the autocatalytic generation of secondary nuclei with preferred helicity that grew into larger domains. In total, both the thermodynamic analysis and the kinetic analysis strongly suggest a nucleated supramolecular polymerization mechanism for the merocyanine dyes. Because the supramolecular polymerization is mainly driven by a dipole−dipole interaction, the cooperativity is most likely the result of the creation of a large net dipole over the whole supramolecular polymer, which should strengthen the interaction of the merocyanine dyes. However, from the data it is difficult to distinguish if the cooperativity is related to the pure one-dimensional polymerization or if it is associated with the intertwining of the six oligomeric strands or a combination thereof.

Lehn and co-workers have prepared supramolecular polymers based on rigid bent-shaped molecules bearing a self-complementary quadruple hydrogen-bonding array, **131** (Chart 37), and shown to follow a cooperative polymerization process.[421]

The supramolecular polymerization of **131** in chloroform was studied with concentration-dependent ^{1}H NMR spectroscopy. When the concentration of **131** in chloroform was increased, self-assembly through hydrogen bonding was observed, as evidenced from the chemical shifts of the amide N−H and pyrimidine NH_2 group. However, only a monomer−

Chart 37

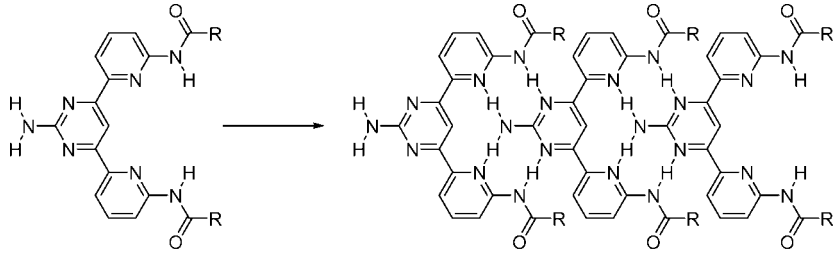

131

dimer equilibrium was found to be operative in this solvent with a dimerization constant of 20 M^{-1}.

The supramolecular polymerization of **131** was also studied in decaline using UV−vis and fluorescence spectroscopy. The UV−vis absorption spectrum of **131** at 1.0×10^{-4} M in decaline showed a clear red shift compared to a **131** solution of equal concentration in chloroform (where **131** is molecularly dissolved). The absorption data are consistent with enhanced π-conjugation, resulting from an increased planarity due to polymerization through intermolecular hydrogen bonding. The fluorescence emission spectrum in decaline showed a red-shifted maximum relative to that in chloroform. In addition, variable-temperature ^{1}H NMR at 1.0×10^{-2} M in decaline confirmed the presence of supramolecular polymers at room temperature, which were dissociated upon heating of the solution (i.e., enthalpy-driven supramolecular polymerization).

To gain more insight into the self-assembly of **131** in decaline, temperature-dependent UV−vis absorption spectroscopy was employed. When the temperature of a 1.0×10^{-4} M solution in decaline was increased, from 25 to 65 °C, a blue shift was observed, indicative of a transition from the polymerized to the monomeric state (Figure 39).

The transition from monomer to supramolecular polymer could be followed by plotting the UV−vis absorption at 349 nm. Although the authors have interpreted this transition to be sigmoidal, in our view the transition is more reminiscent of a nonsigmoidal shape and hence indicative of a cooperative supramolecular polymerization process. We hypothesize that the origin of this cooperativity could be related to

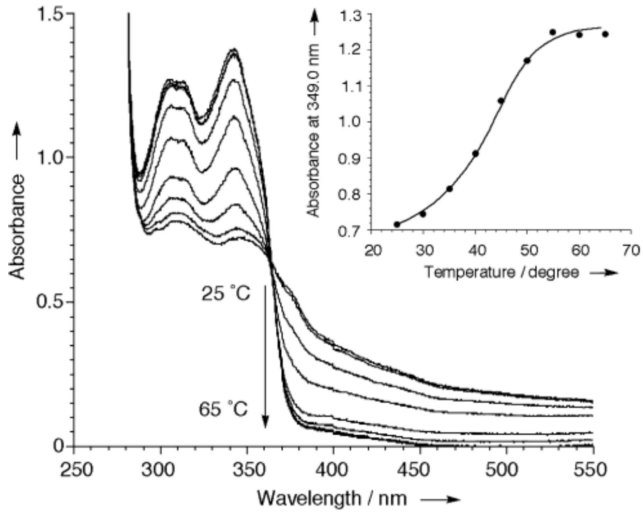

Figure 39. Temperature-dependent UV−vis spectra of **131** in decaline (1.0×10^{-4} M). (Inset) UV−vis absorption at 349 nm at different temperatures. (Reprinted with permission from ref 421 Copyright 2005 John Wiley & Sons, Inc.)

electronic effects, such as long-range dipole−dipole interactions and polarization effects, as discussed in the previous section. However, also an allosteric effect due to planarization of the π-system during polymerization might contribute to the cooperativity.

4.7.2. Structural/Allosteric Cooperativity

The supramolecular polymerization of oligo(*p*-phenylene vinylenes) **132**−**134** (abbreviated OPV, Chart 38) equipped with an ureidotriazine self-complementary quadruple hydrogen-bonding unit in alkane solvents was investigated by our group using temperature-dependent optical and chiroptical techniques in solution.[324]

The enantiomeric purity of the chiral side tails was expressed at the supramolecular level leading to one-handed quasi one-dimensional helical structures, as evidenced from the bisignated circular dichroism spectrum at room temperature. At high temperature these molecules were shown to exist in their monomeric form or as hydrogen-bonded dimers,[422,423] which have been studied in detail with scanning tunneling microscopy (STM)[423,424] and ^{1}H NMR spectroscopy.[422] At low temperatures AFM and SANS showed the presence of supramolecular polymers.[423] To probe the supramolecular polymerization, temperature-dependent CD and UV−vis spectroscopy were employed, which resulted in a sharp nonsigmoidal transition (Figure 40). The nonsigmoidal growth process strongly indicates the presence of a cooperative supramolecular polymerization mechanism, which was analyzed by the model developed by van der Schoot (vide supra). For **133** an enthalpy release, ΔH_e, of -56 kJ mol^{-1} and a K_a value of $10^{-4}-10^{-5}$ at $T = T_e$, depending on the concentration, were determined. The presence of a cooperative transition was further confirmed by a sharp nonsymmetric peak in the temperature-dependent heat capacity measurements performed at constant pressure.

By combining the chiroptical data with the optical data, it was suggested that disordered preaggregates precede the formation of the chiral supramolecular polymer (Figure 40). The gradual increase in the UV−vis measurement in that temperature domain indicated an isodesmic supramolecular polymerization for the formation of the preaggregates, whereas after the introduction of order by a helical twist, the supramolecular polymerization seems to become more favorable for the formation of long polymers. This behavior is typical for a cooperative supramolecular polymerization. By using the model developed by van der Schoot (vide supra) a degree of polymerization at the T_e could be determined, which, interestingly, seems to coincide with the number of molecules necessary to complete one helical turn.[425] A closer look at the molecular structure in the polymerized material indicates that the molecule should be flat to be incorporated

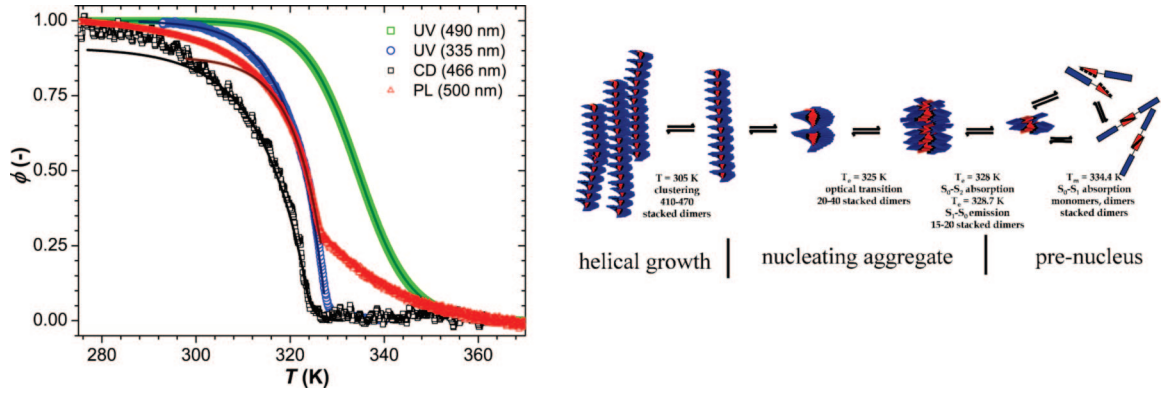

Figure 40. Degree of aggregation, ϕ, based on UV−vis, CD, and PL spectroscopy for **133** and the schematic representation of the supramolecular polymerization of **132**−**134**. (Reprinted with permission from ref 324. Copyright 2006 American Association for the Advancement of Science.)

Chart 38

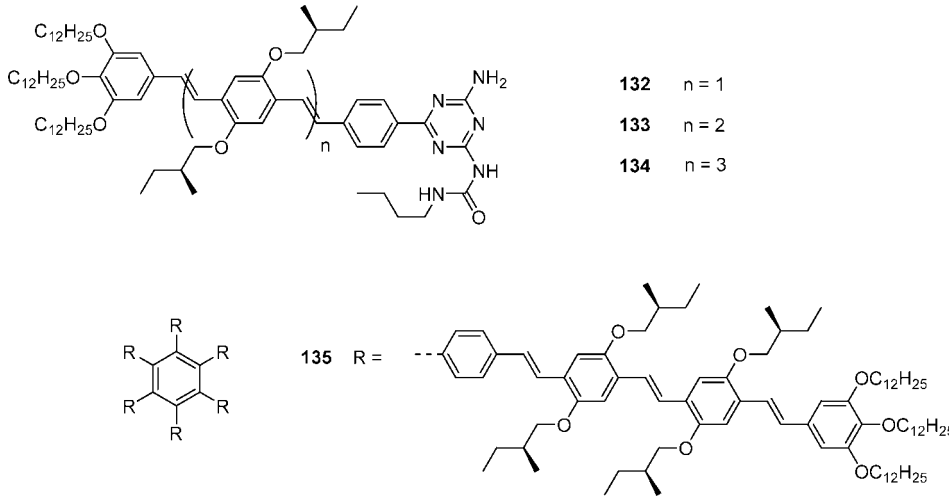

in the stack. However, in their monomeric or hydrogen-bonded dimeric form the OPV segment most likely has a nonzero dihedral angle with the ureidotriazine unit. To obtain the monomeric structure that is able to polymerize, the dihedral angle needs to be reduced to zero and hence a thermodynamically less favorable conformation should be reached. It is likely that this allosteric property contributes to the cooperative nature of the supramolecular polymerization of **132**−**134**. Additionally, interactions between non-neighboring monomers upon formation of the helix could also contribute to the cooperativity.

Covalently linking two ureidotriazine groups, each equipped with a gallic moiety instead of an OPV segment, also showed a cooperative supramolecular polymerization as was established with optical and chiroptical techniques.[426,427]

Hexa-OPV-substituted benzenes **135** displayed a similar behavior in dilute solution, having a sharp change in the temperature-dependent CD and UV−vis absorption in alkane solvent.[428] In contrast to the OPV derivatives **132**−**134**, the T_e of **135** is in both techniques observed at the same temperature, which excludes the formation of achiral pre-aggregates. Much higher degrees of cooperativity and enthalpy release were determined for these systems when compared to the OPV ureidotriazine derivatives, which was related to the increased number of OPV units in the molecule. Furthermore, these molecules could not be disassembled at 90 °C at a concentration of 2×10^{-7} M in heptane, showing a remarkable increase in stability when compared to their hydrogen-bonded hexameric counterparts.[429] It is likely that the OPVs are arranged perpendicular with respect to the central benzene in the molecularly dissolved state of **135**. A rotation around this bond to reduce the dihedral angle is necessary to achieve the preferred structure that can supramolecularly polymerize. This means that a thermodynamic barrier needs to be overcome, thus resulting in a cooperative supramolecular polymerization mechanism.

Also, in the case of oligothiophenes a planarization is necessary to achieve supramolecular polymerization as was determined by temperature-dependent UV−vis spectroscopy.[430] In line with this observation, a nucleated mechanism was recently established for the supramolecular polymerization of oligothiophenes having enantiomerically pure oligo(ethylene glycol) side chains.[270]

Very recently, Würthner and co-workers have reported on the cooperative supramolecular polymerization of perylene bisimide chromophores.[431] Instead of using only the $\pi-\pi$ interactions as the driving force for the supramolecular polymerization (section 2.3.1), they elegantly designed the system in such a way that hydrogen bonding was incorporated. The concentration-dependent UV-vis and CD studies revealed a critical concentration for the supramolecular polymerization, and the UV−vis absorption data could be analyzed with the K_2-K model, giving $K_2 = 13$ L mol^{-1} and $K = 2.3 \times 10^6$ L mol^{-1} ($\sigma = 10^{-6} - 10^{-5}$). By careful analysis of the AFM, STM, and optical data they showed that helical fibers could be formed, suggesting an allosteric

Chart 39

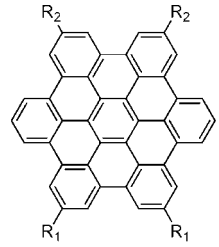

136	$R_1 = C_{12}H_{25}$	$R_2 = ArO(CH_2CH_2O)_3CH_3$	**141**	$R_1 = C_{16}H_{33}$	$R_2 = ArO(CH_2CH_2O)_3CH_3$
137	$R_1 = C_{12}H_{25}$	$R_2 = ArO(CH_2CH_2O)_2CH_3$	**142**	$R_1 = C_{13}H_{27}$	$R_2 = ArO(CH_2CH_2O)_3CH_3$
138	$R_1 = C_{12}H_{25}$	$R_2 = ArOCH_2CH_2OCH_3$	**143**	$R_1 = C_8H_{17}$	$R_2 = ArO(CH_2CH_2O)_3CH_3$
139	$R_1 = C_{12}H_{25}$	$R_2 = ArOCH_3$	**144**	$R_1 = H$	$R_2 = ArO(CH_2CH_2O)_3CH_3$
140	$R_1 = C_{12}H_{25}$	$R_2 = Ph$	**145**	$R_1 = C_{12}H_{25}$	$R_2 = C{\equiv}CO(CH_2CH_2O)_3CH_3$

effect for the cooperativity. However, the dipole moment of the dimer was around 20% higher for the dimers (8.8 D) than for the monomers (6.1 D), which can indicate an electronic contribution to the cooperativity.

Aida and co-workers reported on the supramolecular polymerization of amphiphilic hexa-*peri*-hexabenzocoronenes **136**−**145** (Chart 39) in THF and THF/water mixtures, where the HBC core was used to produce conductive graphene-like nanotubes.[432] The formation of tubular structures already indicates that this polymerization should be considered as quasi two-dimensional (Figure 33) and not as a pure one-dimensional supramolecular polymer.

The HBCs formed a stacked bilayer structure (Figure 41) in which the alkyl tails are interdigitated in the center of the bilayer and the ethylene glycol tails are located at the periphery, allowing the aggregate to be soluble in polar solvents such as THF and water. The authors were able to covalently fix the supramolecular assemblies by redox-mediated polymerization,[433] photodimerization of coumarine,[434] and ring-opening metathesis polymerization.[435] By aid of the latter they were able to trap the intermediate nanocoil structure before the more stable nanotube was formed, showing that HBCs can form different types of structures.[436] More recently, an elaborate study revealed the effect of the side groups on the supramolecular polymerization of the HBCs by the synthesis of **137**−**145**.[437] A decrease in length of the ethylene glycol chains as performed for **137**−**140** did not hinder the self-assembly, but made the supramolecular polymer increasingly less soluble in THF. This showed that the function of the ethylene glycol is merely for solubilizing the supramolecular polymer and is not essential for guiding the supramolecular polymerization into nanotubes. In contrast, the length of the alkyl tail did show a significant influence, where the dodecyl **136**, tridecyl **142**, and hexadecyl **141** yielded nanotubular assemblies and the octyl **143** and branched 3,7-dimethyloctyl derivatives resulted in ill-defined aggregates. It was concluded that a certain alkyl length was needed to allow for the crystallization of the aliphatic tails by interdigitation and hence enable nanotube formation. The most striking result from this study was the drastic influence of the phenyl group that is used to attach the ethylene glycol tails to the HBC core. Removal of this phenyl group as done for **145** did not yield nanotubes and hence proved to be crucial to drive the supramolecular polymerization. No report has been made about the specific mechanism of supramolecular polymerization, but given the long length of the polymer and the dependence of the polymerization on the phenyl group, a cooperative mechanism is highly plausible. Again, a rotation around the phenyl is most likely the reason for the cooperativity, and therefore this system is different from the isodesmic supramolecular polymerization of the HBC as reported by Müllen and co-workers (vide supra). In addition, these supramolecular polymers are purely one-dimensional, whereas the nanotubes of Aida and co-workers are considered to be quasi two-dimensional. Besides the suspected presence of the allosteric effect, this difference in dimensionality of the polymeric structure could also account for the different supramolecular polymerization mechanisms. In line with this postulation it would be interesting to compare these results to the structures that bear additional phenyl groups as reported by the group of Müllen.[104]

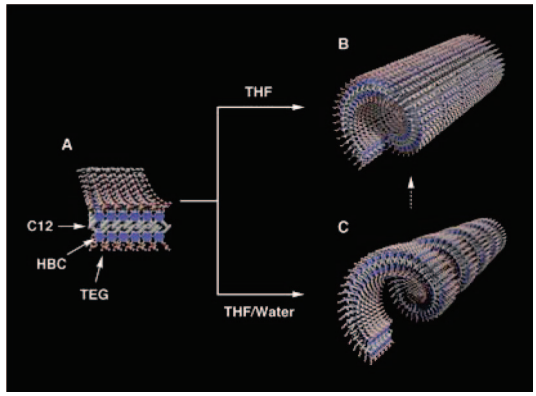

Figure 41. Schematic picture of the supramolecular polymer based on the HBC motif. (Reprinted with permission from ref 432. Copyright 2004 American Association for the Advancement of Science.)

The research group of Rowan and Nolte reported on the surface patterning of porphyrin trimers **146** (Chart 40) via supramolecular polymerization and dewetting,[438] where the polymerization occurred by a combination of hydrogen bonding and $\pi-\pi$ interactions. They showed an impressive control over the formation of highly ordered line patterns on a surface as evidenced by AFM. In a later stage they also investigated in detail the supramolecular polymerization in solution by temperature- and concentration-dependent ^{1}H NMR, CD, and UV−vis spectroscopy.[439] Concentration-dependent ^{1}H NMR in chloroform enabled the determination of a critical concentration of ~0.2 mM for the supramolecular

Chart 40

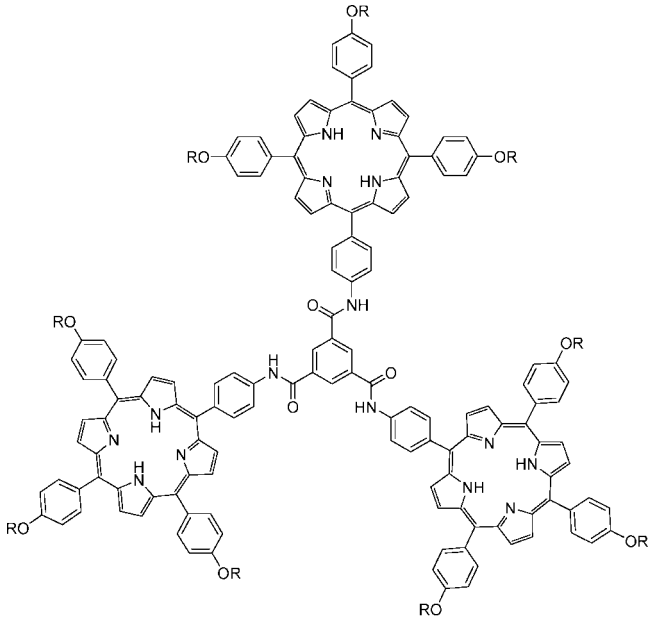

polymerization of **146**, whereas, in hexane, the disassembly could not be visualized by this technique. The appearance of a critical concentration strongly indicates the presence of a cooperative mechanism for the supramolecular polymerization. Concentration-dependent UV−vis spectroscopy in hexane and cyclohexane on **147** showed clear isosbestic points, indicating a two-state equillibrium. However, with CD spectroscopy different organizations were observed. Remarkably, in hexane a face-to-face type packing was obtained, whereas in cyclohexane solutions the UV−vis absorption indicated that the porphyrins were arranged in a head-to-tail and a face-to-face type organization. These results stress the importance of the solvent for the structure of the polymer. Because hydrogen bonding is present in these structures, it would seem likely that the electronic effects account for the cooperativity in the system. However, the position of the porphyrin with respect to the amides is most stable when the porphyrin plane is coplanar with the amide. Therefore, an allosteric effect, expressed as a rotation of the porphyrin around the phenyl−porphyrin bond, can also add to the cooperativity. However, at this point it is unclear to what extent the allosteric and electronic effects contribute to the high degree cooperativity observed in this system.

Ajayaghosh et al. studied gel formation as well as supramolecular polymerization in dilute solution of linear π-systems and have recently extensively reviewed this work.[440,441] Using the hydrophobicity of cholesterol derivatives, OPV trimers equipped with one or two cholesteric groups, **148**−**153** (Chart 41), showed supramolecular polymerization in decane solutions.[442] The packing arrangement depends on the number of cholesteric units that are attached; **148**−**150** showed H-type assembly, whereas **151**−**153** revealed J-type aggregation by UV−vis spectroscopy. In addition, an opposite chirality was observed for the two structures.[442] These interesting features could make it worthwhile to study the supramolecular polymerization mechanism in more detail. For now this system is thought to be a cooperative supramolecular polymerization mainly by the fact that the π-conjugated system and the cholesterol unit have to be combined to drive the supramolecular polymerization. In addition, a nucleation step could be involed in the self-assembly.

Another system concerns oligo(*p*-phenylene ethynylene) derivatives bearing a benzylic alcohol group at the telechelic position, **154**.[443] The combination of $\pi-\pi$ interactions and hydrogen bonding allows the supramolecular polymerization into ribbon-like structures that eventually form vesicles. The necessity of hydrogen bond formation was confirmed by the fact that no polymeric structures could be obtained for **155**. Initially, a kinetically stable assembly was formed that underwent slow transformation into a thermodynamically more stable supramolecular polymer. Temperature-dependent UV−vis spectroscopy showed a sharp change in intensity at a specific temperature that was followed by a second transition at higher temperature (Figure 42). The sharp change indicates a cooperative supramolecular polymerization; however, it is difficult to assign the cooperativity to the formation of the linear polymer or to the process of vesicle formation from this linear polymer.

In the beginning of this decade, Woolfson and co-workers reported on the supramolecular polymerization of peptide sequences.[446] Their design is based on the leucine zipper motif and its ability to form dimeric α-helical coiled coils.[446−448] The 28-peptide residue was specifically designed to have a leucine zipper motif connected to peptide sequences having either a net positive or a net negative charge. This ensured that the formation of the α-helical coiled coil

Chart 41

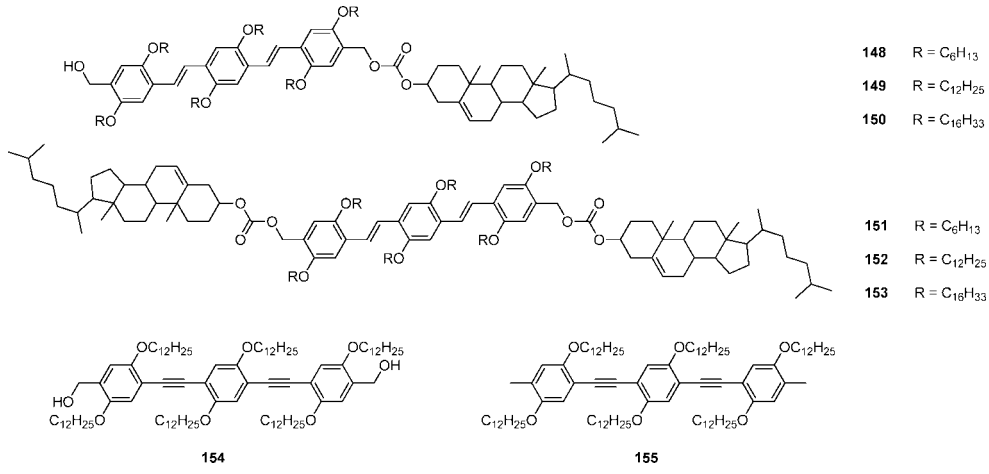

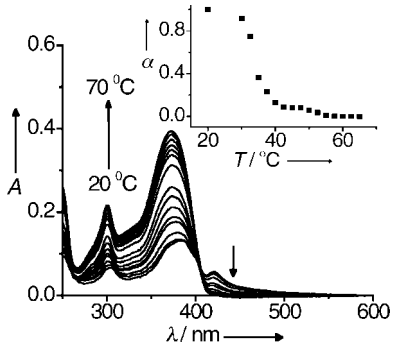

Figure 42. Temperature-dependent UV−vis absorption for **154** in decane (1.1×10^{-5} M). (Inset) Fraction of polymerized material, α, versus temperature, as derived from the absorption at 380 nm. (Reprinted with permission from ref 443. Copyright 2006 John Wiley & Sons, Inc.)

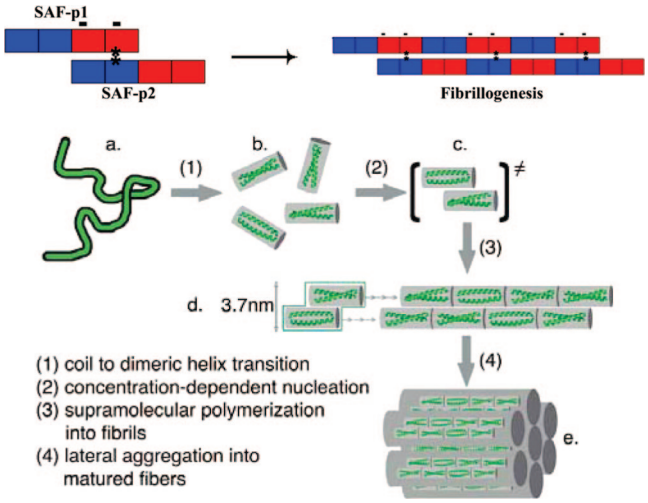

Figure 43. Schematic representation of the sticky end assembly of the peptide sequences (top) by Woolfson and the mechanism proposed by Hartgerink (bottom). (Reprinted with permission from refs 444 and 445. Copyright 2006 John Wiley & Sons, Inc., and copyright 2008 American Chemical Society.)

heterodimer facilitated two overhanging ends with opposite charge that was suggested to further nucleate the polymerization by Coulombic interactions (Figure 43). Therefore, the coiled coil formation by the leucine zipper complex is crucial for the supramolecular polymerization of the peptide sequences. Heterodimer formation of the leucine zipper motif was confirmed by a combination of CD spectroscopy and X-ray diffraction techniques. It is the coiled coil formation that makes this polymerization quasi two-dimensional in nature. TEM showed that polymerization yielded fiber-like structures that further coagulated into bundles. The research was expanded by inducing a change in the morphology of the fibers by coassembling, for example, branched or T-shaped peptide sequences that were complementary to the sticky ends of the heterodimer.[449−451] The supramolecular polymerization could only be achieved at low pH and low salt concentration and for eventual biomedical applications, the peptides should be able to polymerize in physiological conditions. An improved design resulted in a lowering of the critical concentration for supramolecular polymerization from 60 to 4 μM as determined by concentration-dependent TEM and allowed supramolecular polymerization under physiological conditions.[444] The temperature-dependent CD spectroscopy showed an increase in thermal stability from 22 to 65 °C for the improved peptide sequences. With

Chart 42

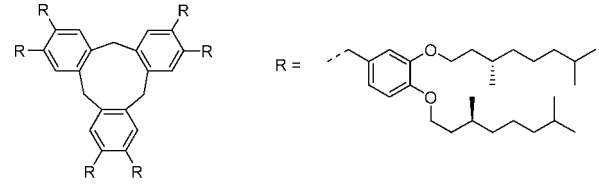

156

increasing temperature, the CD signal showed a sharp transition related to the disappearance of the α-helical coiled coil, which the authors assigned to being sigmoidal. However, a nonsigmoidal transition is highly indicative of a cooperative supramolecular polymerization mechanism, and thus it is likely that the supramolecular polymerization proceeds via a cooperative mechanism. By careful analysis of the melting curves obtained with CD spectroscopy, different supramolecular polymers were observed when the improved oligopeptide was allowed to polymerize at either 5 or 22 °C. For the latter temperature an increase in internal order of the polymer was observed with TEM, and thus a higher melting temperature was obtained. A recent study by the group of Hartgerink proposed an additional mechanism for the polymerization of oligopeptides without charged end groups.[452] Similar to Woolfson et al. the formation of an α-helical coiled coil prior to further polymerization is crucial. In this case the aggregation is not driven by Coulombic interactions, but by van der Waals interactions (Figure 43). Because the supramolecular polymerization of the peptides described by the groups of Woolfson and Hartgerink is achieved in an aqueous environment, it is expected that the cooperativity observed in both systems is a result of the hydrophobic effect. However, both groups emphasize the necessity of the α-helical coiled coil formation for the supramolecular polymerization, and hence an allosteric effect is most likely a stronger contributor to the cooperativity.

Percec and co-workers have prepared supramolecular polymers based on cyclotriveratrylene derivatives equipped with dendrons.[453,454] The self-assembly of a library of 14 dendronized cyclotriveratrylene derivatives was studied in great detail in the bulk (liquid crystalline) state by X-ray studies and in solution by CD spectroscopy, which rendered insights in the mechanisms for the transfer and amplification of structural information from the molecular to the supramolecular level.[454]

In an earlier report, cyclotriveratrylene derivative **156** (Chart 42) was studied with CD and UV−vis spectroscopy in dodecane solutions as a function of temperature (Figure 44).[453] The appearance of a CD effect upon cooling is indicative of the formation of a helical supramolecular polymer, which could be related to the long-range helical correlation demonstrated by X-ray diffraction on oriented fibers.

Although the authors do not comment explicitly on the nonsigmoidal transition observed for the temperature-dependent CD and UV−vis absorption, it strongly points toward a cooperative supramolecular polymerization. The origin of this cooperativity could be related to the requirement of the dendron moieties to change their conformation prior to supramolecular polymerization, suggesting an allosteric effect.

The group of Percec also reported on dendronized dipeptides that were found to polymerize into helical pores, in

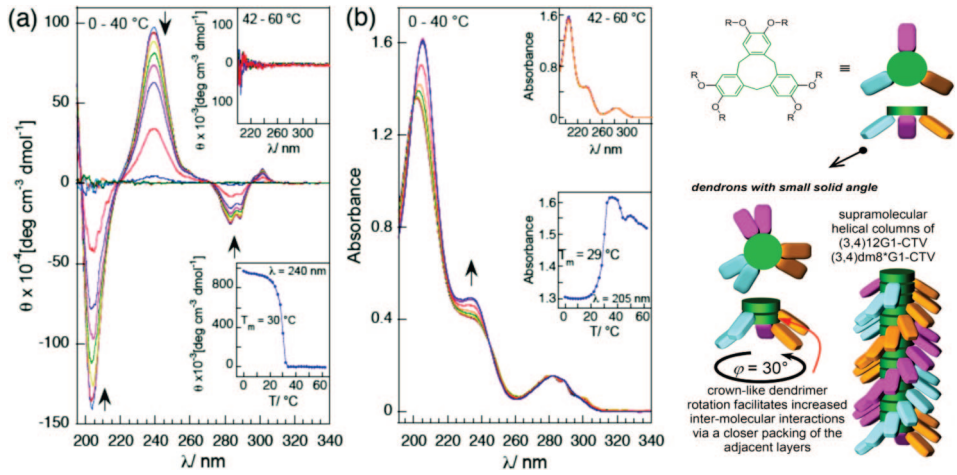

Figure 44. Temperature-dependent CD (a) and UV−vis (b) of **156** in dodecane (6.0×10^{-5} M). Arrows indicate trends upon increasing temperature; the lower insets depict changes in molecular ellipticity and absorbance as a function of temperature. (c) Schematic representation of the helical self-assembly of **156**. (Reprinted from ref 453. Copyright 2008 American Chemical Society.)

Chart 43

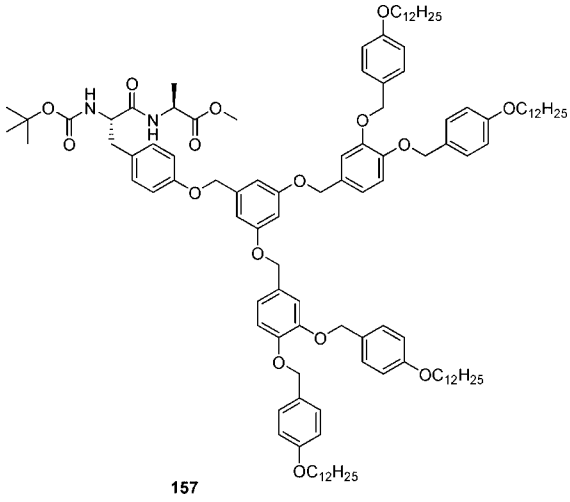

157

bulk and in solution.[16,455−459] Their initial work was based on a protected Boc-Tyr-Ala-OMe dipeptide equipped with a second-generation 3,4-disubstituted benzyl ether-based Fréchet-type dendronic wedge **157** (Chart 43).[16] Although Percec et al. prepared all of the possible stereoisomers for the Tyr-Ala dipeptide, in this review only the supramolecular polymerization of the L,L-enantiomer **157** is discussed.

In apolar solvents **157** was found to supramolecularly polymerize due to intermolecular hydrogen bonds, as determined from ^{1}H NMR, CD, and UV−vis spectroscopy. Temperature-dependent UV−vis spectroscopy revealed two transitions upon cooling (Figure 45A). From 60 to 42 °C a transition from a globular dendron structure, containing a mixture of *trans* and *gauche* benzyl ether conformers, to an *all-trans* tapered dendron was observed. Below 30 °C this *trans*-tapered dendron was found to polymerize, forming a helical supramolecular polymer, as was confirmed by the appearance of a CD effect (Figure 45B). At about 12 °C, the equilibrium between the tapered dendron and the polymer was completely shifted to the polymer. X-ray diffraction, TEM, and molecular modeling showed that the helical polymer forms a porous column, with 12 molecules completing a single helical turn and which is stabilized by hydrogen bonds between neighboring layers (Figure 45C).

Following the UV−vis and CD absorption as a function of temperature revealed a sharp, nonsigmoidal transition upon the formation of the supramolecular polymer below 30 °C (insets in Figure 45A,B). This strongly suggests a cooperative supramolecular polymerization for **157**. The origin of this cooperativity was in a later paper ascribed by the authors to an allosteric effect, involving a conformational change in the alanine residue to allow for intermolecular hydrogen bonding prior to polymerization.[456] Furthermore, the cooperativity could be related to the additional stabilization of the column that is obtained once the first helical turn is completed. Continuing their studies on pore-forming dendritic dipeptides, Percec et al. have studied the role of the protective group[455] and the length of the alkoxy tail at the periphery of the dendron,[457] as well as the choice of amino acids on the supramolecular organization.[459] These comprehensive studies showed that a cooperative supramolecular polymerization is generally observed for these dendritic dipeptide derivatives.

4.7.3. Cooperativity through the Hydrophobic Effect

The supramolecular polymerization of hydrogen-bonded six-membered rosettes was studied by the group of Fenniri.[460] They synthesized molecules such as **158** (Chart 44) featuring a hydrophobic base unit having the Watson−Crick hydrogen-bonding array of the guanosine on one side of the molecule and the complementary array of the cytosine on the other.

The spatial arrangement of these arrays results in the formation of a six-membered ring possessing 18 hydrogen bonds as was evidenced by NOE studies in water. The hydrophobicity of the central core was increased by methylation of the amine, whereas the solubility was increased by using an optically pure amino acid as solubilizing tail. CD spectroscopy showed that the optical purity of the side chain was expressed at the supramolecular level, yielding a preferred helicity for the supramolecular polymer. The application of temperature-dependent CD and UV−vis spectroscopy in water was used to determine the nature of the supramolecular polymerization. Both optical techniques showed a nonsigmoidal transition when the temperature was increased, indicative of a cooperative supramolecular polymerization process. The hyperchromic shift in the absorption measurement in combination with the disappearance of the CD effect indicated the disassembly of the nucleic acid aggregate. Because the degree of polymerization is lowered by an increase in temperature, the supramolecular polym-

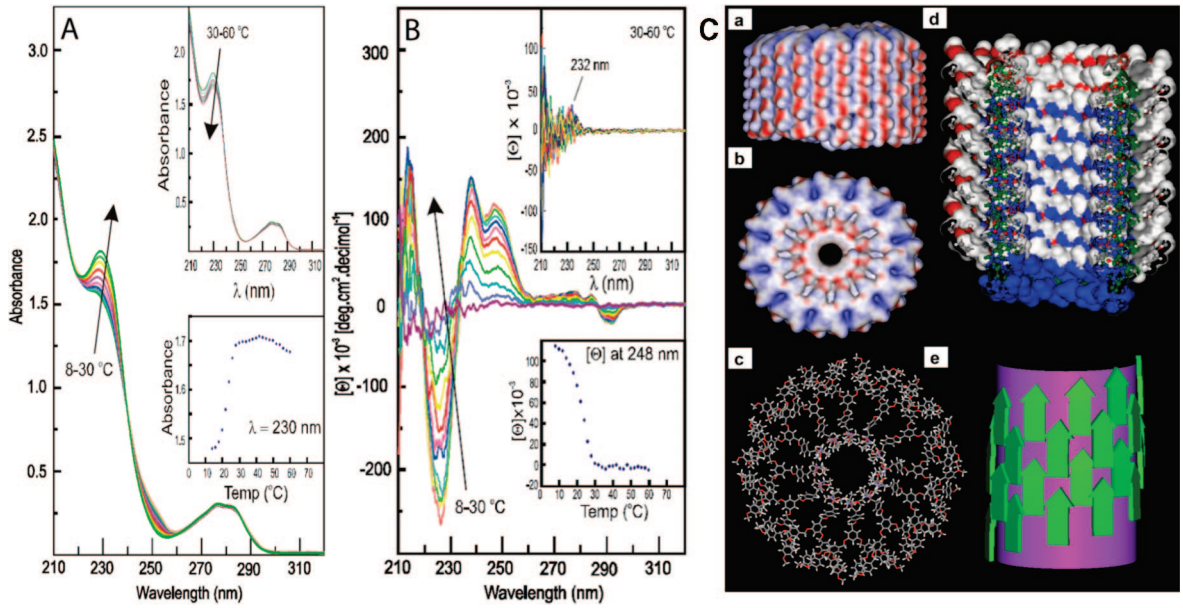

Figure 45. Temperature-dependent UV−vis (A) and CD (B) of **157** in cyclohexane (1.6×10^{-4} M). Arrows indicate trends upon increasing temperature; the lower insets depict changes in absorbance and molecular ellipticity at 230 nm as a function of temperature. (C) Molecular models of the helical porous columns formed by **157**. (Reprinted with permission from ref.[16] Copyright 2004 Nature Publishing Group.)

Chart 44

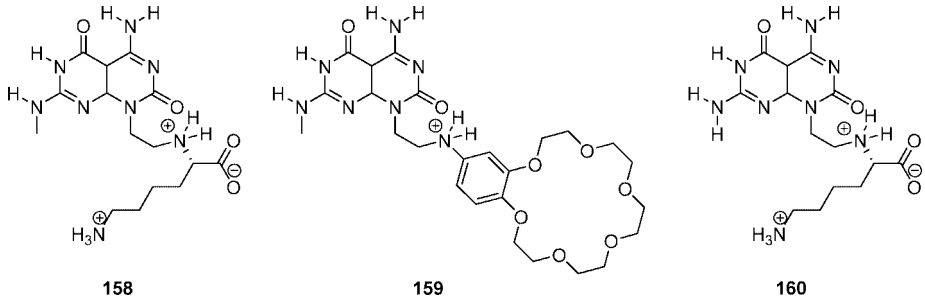

158 **159** **160**

erization is an enthalpically driven process. This suggests that besides the hydrophobic effect also hydrogen bonding and $\pi-\pi$ interactions drive the supramolecular polymerization.

Remarkably, the introduction of a crown ether at the periphery of the molecule, **159** (Chart 44), altered this feature considerably. Light scattering experiments showed that for these molecules an increase in temperature resulted in longer polymers, which is highly indicative of an entropically driven supramolecular polymerization consistent with the hydrophobic effect being the main driving force.[461] Addition of chiral amino acids that are able to bind to the crown ether moiety showed dramatic influences on the polymerization of the rosettes.[462] The chemical structure of the amino acid proved to be crucial for its ability to induce the chirality and to increase the stability of the helical rosette nanotubes in a methanol solution. An all-or-nothing relationship was determined for the amino acids, meaning that all of the crown ethers need to be occupied to bias the chirality. The kinetic data revealed the ability of the rosette nanotubes to induce their own formation in an autocatalytic fashion strongly, suggesting a nucleated supramolecular polymerization.[462]

In a further study, the exocyclic methyl group, **160** (Chart 44), was removed and the influence on the supramolecular polymerization in both aqueous and methanolic media was investigated.[463] CD and UV−vis spectroscopy showed the formation of a W-chiromer (in water) and an M-chiromer (methanol), having a similar packing arrangement but an opposite chirality. It was shown that the W-chiromer is more stable and thus the thermodynamic product, whereas the M-chiromer proved to be the kinetic product of the supramolecular polymerization. Transformation of the M-chiromer to the W-chiromer proceeded through an autocatalytic process, and hence additional evidence for a nucleated supramolecular polymerization was given. Although the cooperativity is in large part the result of the hydrophobic effect, a computational study showed a linear increase of the free energy of stacking (206 kcal mol^{-1}) for each monomer addition, suggesting the formation of a macrodipole.[464] Therefore, both the hydrophobic effect and an electronic effect can account for the cooperativity. Recently, the synthesis of hydrophobic bases was reported, and they were shown to reversibly polymerize in apolar media.[465] It would be interesting to study the mechanism of supramolecular polymerization of these compounds and to compare it with the compounds discussed above, to gain additional insight into the effect of hydrophobicity as a driving force for supramolecular polymerization.

Already in the early 1970s several independent studies were reported about the aggregation properties of cationic and anionic porphyrins[466,467] The group of Pasternack has reported a kinetic study concerning the supramolecular polymerizations of the water-soluble porphyrin **161** (Chart 45).[468] The porphyrin was shown to polymerize in acidic aqueous media (pH ~1) into J-type aggregates by UV−vis spectroscopy. The strong cohesive interaction of water promotes the supramolecular polymerization by the hydro-

Chart 45

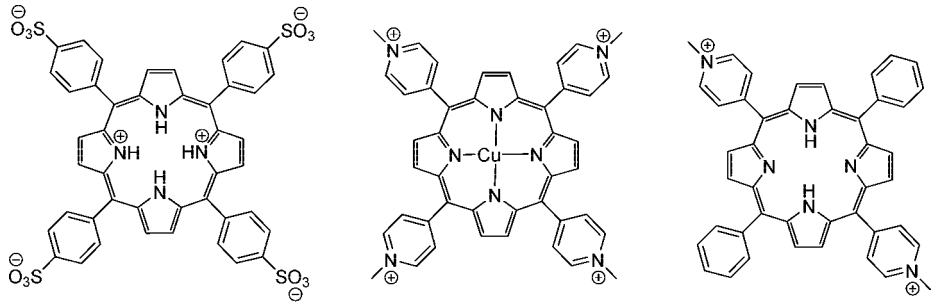

161 **162** **163**

phobic effect.[469] Injection of a concentrated solution of molecularly dissolved **161** into acidic water facilitated the polymerization; however, in this case the rates were too fast to be recorded.[468] By lowering the injection concentration the rates were significantly slowed to such a level that it could easily be studied. Stirring of the solution after injection increased the kinetics and the smoothness of the curve. In the last two examples there is a clear concentration-dependent lag phase before the supramolecular polymerization is initiated, and therefore it can be concluded that a nucleated mechanism is operative in the polymerization of **161**. By analyzing the kinetic traces using an autocatalytic nucleation model, a nucleus size of ~5−6 molecules could be determined, whereas the size of the nucleus seemed to be independent of the initial porphyrin concentration (Figure 46). In contrast, the rate of polymerization highly depends on this concentration. Because nucleus formation is the rate-determining step, it was suggested that prenuclear species are rapidly produced at higher porphyrin concentration, and hence the rate is enhanced.

In addition, an elaborate light scattering study showed a decreased polymerization length at higher concentration, which was explained by the formation of an increased number of nuclei at this higher concentration.[470] To demonstrate the importance of the nucleation on the supramolecular polymerization, a small amount of seeds was added to a solution of **161**, and the kinetics were probed.[468] A significantly faster polymerization rate was obtained for the solution containing the small amount of seeds, suggesting that the supramolecular polymerization is indeed nucleated.

Although not explicitly stated, Purello and co-workers found a similar supramolecular polymerization mechanism,

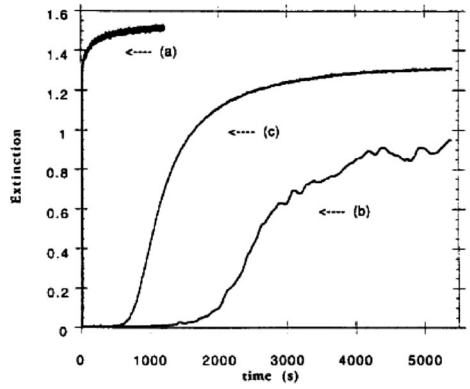

Figure 46. Supramolecular polymerization kinetics of **161** using different mixing methods, at the same final porphyrin concentration (4.5×10^{-6} M in 0.3 M HCl aqueous solution): (a) addition of highly concentrated porphyrin solution to the acidic water, (b) same as (a) but a lower concentration of initial porphyrin concentration; (c) similar to (b), but now the solution was stirred. (Reprinted with permission from ref 468. Copyright 2000 Elsevier.)

Chart 46

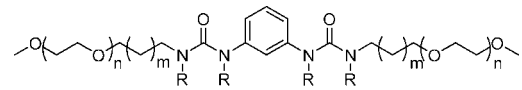

164 n = 7.2 m = 9 R = H
165 n = 7.2 m = 9 R = CH_3
166 n = 6 m = 0 R = H

because they used a stretched exponential for the description of the supramolecular polymerization kinetics of **161** and **162** with phenyl aniline.[471,472] Further evidence came from the experiments showing the ability of the porphyrin system to memorize the chirality of the polymer after its depolymerization. This was explained by the presence of small undetectable chiral seeds that are able to nucleate the polymerization into helical structures with a single handedness.[473,474]

The research group of Ribó is well-known for its work on the chiroptical response of supramolecular polymers based on water-soluble porphyrins.[475−477] A very recent contribution from this group showed the effect of an unidentified chiral contaminant in the solvent that proved to be able to induce the chirality in the supramolecular polymer of the disodium salt of **161** by acting as a nucleation site.[478] This example indicates the importance of heterogeneous nucleation in the supramolecular polymerization of **161**.

Monsù Scolaro and co-workers have also reported on nucleation effects in the supramolecular polymerization of **163** in water containing NaCl.[479,480] Furthermore, similar to the description of Pasternack et al., a decrease in polymer length upon increasing concentration of **161** was observed with light scattering.[481] More recently, the supramolecular polymerization was attempted in chlorinated organic solvents, such as dichloromethane, by the addition of acids.[482,483]

Although water is able to compete with hydrogen bonding, Bouteiller and co-workers reported on the supramolecular polymerization based on hydrogen bonding in this solvent.[484] By a careful design (Chart 46), balancing hydrophilic and hydrophobic parts in **164**, one-dimensional polymers were observed by viscometry and neutron scattering measurements in solvents with a polarity range from water to toluene. In contrast to this **165**, which is not able to form hydrogen bonds, and **166**, having only a short hydrophobic spacer between the urea hydrogen bonds and the ethylene oxide chain, did not yield any polymeric structures in solution. Isothermal titration calorimetry showed the dynamic nature of the polymers in all solvents, and a qualitative thermodynamic analysis for the supramolecular polymerization was reported. In acetonitrile and toluene, the enthalpy of association was negative, indicating that the polymerization is enthalpically driven. In contrast, the enthalpy of association in water was positive, implying an entropically driven

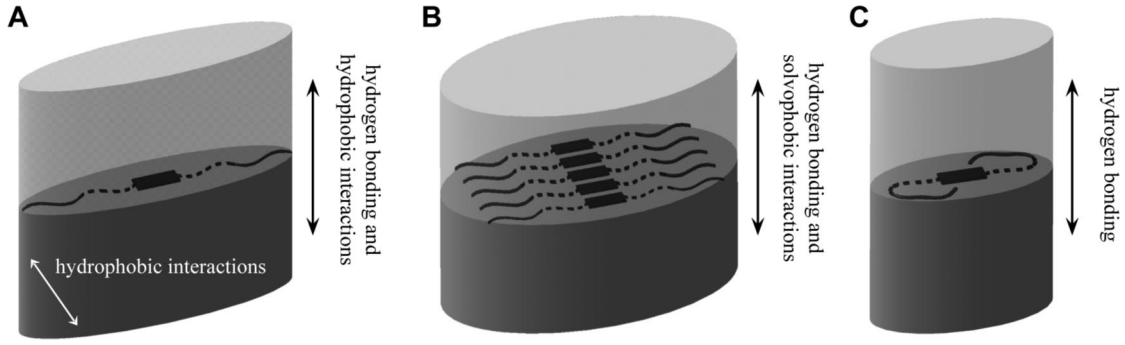

Figure 47. Schematic picture of the organization of **164** in the supramolecular polymer, depending on the driving forces present for the polymerization in (A) water, (B) acetonitrile, and (C) toluene. (Reprinted from ref 484 Copyright 2007 American Chemical Society.)

Chart 47

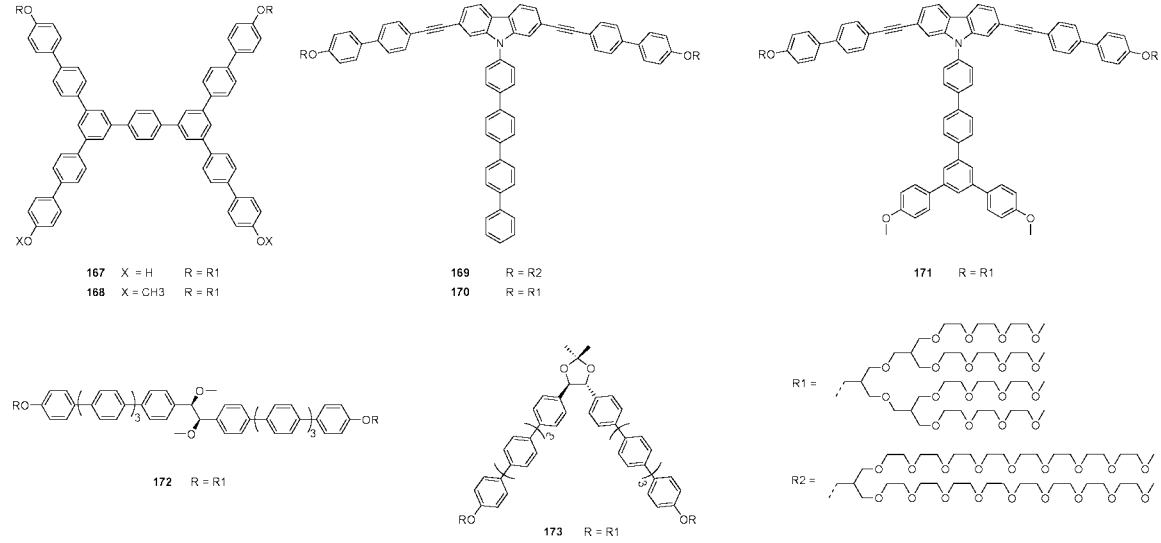

supramolecular polymerization, which is likely to be caused by the hydrophobic effect. From this study it was clear that different driving forces in the solvents yielded different arrangements of the molecules within the supramolecular polymer, as schematically depicted in Figure 47, and hence significant changes in the thermodynamic parameters could be obtained. Considering the structural similarity of **164** to the bis-urea derivatives discussed previously (**111**−**116**), it can be anticipated that in toluene a cooperative mechanism is operative for **164**. This research opens up the possibility to investigate the influence of the hydrophobic effect on the degree of cooperativity.

By equipping π-conjugated segments with ethylene glycol dendrons, supramolecular polymerization can be achieved in water.[485] M. Lee and co-workers synthesized a large variety of oligo(*p*-phenylene) derivatives (Chart 47) that were shown to polymerize into cylindrical micelles[485,486] (**167**−**170**), coiled coils,[471] (**172** and **173**) and, more recently, supramolecular capsules with gated pores.[487] The latter falls outside the scope of this review and hence will not be discussed further.

Light scattering experiments in combination with UV−vis spectroscopy showed the supramolecular polymerization of **169** and **170** in water, whereas TEM allowed the visualization of the cylindrical micelles. Similar to the nanotubes of Aida, these micelles can be characterized as quasi two-dimensional structure. By introducing a twist in the aromatic part, as was done for **171**, supramolecular polymerization could not be achieved, showing the importance of $\pi-\pi$ interactions for the polymerization and indicating an allosteric effect. For **172** and **173**, the enantiomeric purity is expressed at a supramolecular level as visualized by CD spectroscopy. In addition, for **172** helical fibers were observed with TEM; however, in this case the helicity of the fibers was different from the handedness determined with CD spectroscopy. This was explained by the formation of a superhelix, again hinting toward a polymerization driven by a structural change. The presence of the hydrophobic effect and the notion of the presence of an allosteric effect in the supramolecular polymerization of these molecules indicate that the formation of the polymers most likely proceeds via a cooperative or nucleated mechanism.

The research group of Stupp has reported on the supramolecular polymerization of peptide amphiphiles that yield long one-dimensional nanotubes in an aqueous environment.[488] The general design of the molecule is such that a long aliphatic tail is connected to a peptide segment that contains hydrophilic end groups to ensure solubility in water. CD measurements have shown a β-sheet formation of the peptides. Introduction of bioactive epitopes at the hydrophilic side of the molecule allowed the nanotubes to be used as scaffolds in tissue engineering.[489,490] By attaching a peptide sequence known to bind to heparin (Chart 48 and Figure 48), the nucleation of the nanofibers was achieved on the heparin fiber, indicating that heterogeneous nucleation can significantly influence the supramolecular polymerization of **174**.[491]

Chart 48

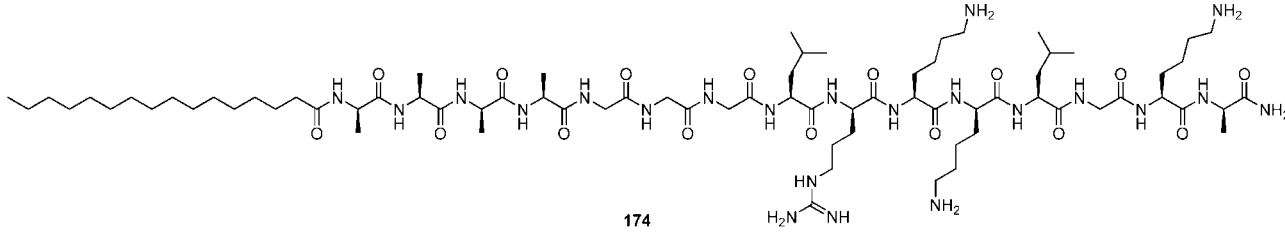

174

A detailed study of the internal structure of the peptide amphiphile by the combination of TEM and polarization modulation−infrared reflection−absorption spectroscopy was reported.[492] The β-sheet was shown to be parallel to the long axis of the nanotube, and the internal order depends highly on the molecular architecture and peptide sequence. Recent molecular simulation studies on peptide amphiphile self-assembly by De la Cruz and co-workers have elegantly shown that the interplay between hydrophobic forces and hydrogen bonding results in the formation of assemblies of different morphology, in particular single β-sheets, stacks of parallel β-sheets, spherical micelles, and long cylindrical fibers. Furthermore, this study showed that the equilibrium between the different morphological aggregates is governed by nucleation seeds.[493] Although no mechanistic study on the cooperativity in the growth of these nanotubular structures is reported due to its complicated nature, we hypothesize that the supramolecular polymerization of peptide amphiphiles into nanotubular structures follows a highly cooperative growth mechanism. This hypothesis is based on examples and calculations found in the literature on the self-assembly of peptides into β-sheets, which suggest that this proces occurs via a cooperative growth mechanism.[411,413,494,495]

In addition M. Lee and co-workers also reported on the presence of a critical concentration for peptide amphiphiles having the Tat cell penetrating peptide sequence, which is normally present in the human immunodeficiency virus type-1,[496] suggesting a cooperative mechanism. The exact reason for the cooperativity is difficult to assign at the moment, because several different contributions can be identified.

4.7.4. Solvent Effects

As has been discussed in the section on isodesmic supramolecular polymerization, macrocyclic structures **6** and **9** reported by Tobe and co-workers reversibly polymerize according to an isodesmic growth mechanism in THF.[96] However, when the solvent is changed to acetone and toluene for **9** and to acetone for **6**, the isodesmic growth model was not able to describe the data. Analysis of the concentration-dependent spectroscopic data in these solvents using several cooperative growth models showed that the supramolecular polymerization process is cooperative. It was reasoned that the formation of higher order oligomers was more favorable due to solvophobic effects, and a nucleation mechanism was suggested.

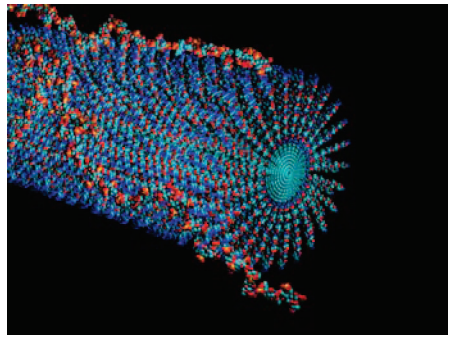

Figure 48. Schematic picture of the nanotubular structure built up of **174** with heparin attached to its outer layer. (Reprinted from ref 491 Copyright 2006 American Chemical Society.)

A similar solvent-dependent effect was found for the C_3-symmetrical bipyridine-based molecules reported by our group. Aliphatic tails were replaced by ethylene oxide chains (**24**), both chiral and achiral, to allow the supramolecular polymerization in more polar solvents, such as *n*-butanol and water.[497] A sharp transition was observed in the temperature-dependent CD and UV−vis spectroscopy, indicative of a cooperative supramolecular polymerization mechanism in *n*-butanol.[498] Ultrasensitive differential scanning calorimetry measurements supported this conclusion, because a sharp, nonsymmetrical peak in the heat capacity at constant pressure was observed. Remarkably, SANS revealed the formation of small structures at higher temperatures than the transition temperature found using CD spectroscopy. In addition, temperature-dependent UV−vis spectroscopy and fluorescence lifetime traces showed an isodesmic transition that preceded the cooperative transition. The combined results suggest that the formation of a helical structure triggers a highly favorable growth of the polymer and hence accounts for the cooperativity in the polymerization mechanism.

4.8. Anticooperative Supramolecular Polymerization

The examples of supramolecular polymerizations considered hitherto in this chapter were all shown or suggested to grow via a cooperative mechanism; that is, initial oligomerization is unfavorable as compared to further polymerization. However, also some examples of supramolecular polymers have been reported in the literature that are characterized by a more favorable oligomerization step compared to the consecutive polymerization steps. For these anticooperative supramolecular polymerizations, addition of the monomer to the growing polymer up to a certain length *n* is characterized by an equilibrium constant that is larger than the equilibrium constant governing the equilibria beyond this length *n*.

One example of an anticooperative supramolecular polymer was reported by Bouteiller et al., who studied the supramolecular polymerization of amphiphilic perylene derivative **175** (Chart 49) in water.[499]

Chart 49

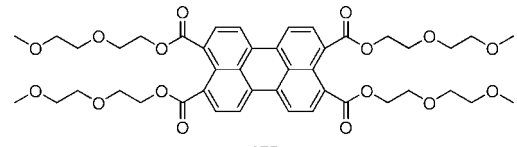

175

Scheme 10

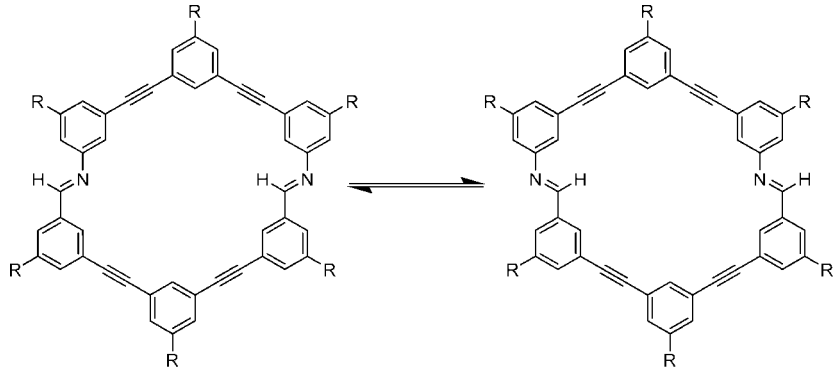

176 R = $CO_2(CH_2CH_2O)_3CH_3$

Chart 50

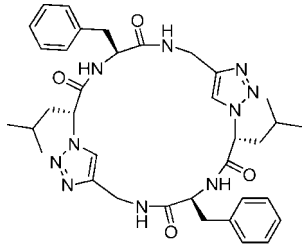

177

The supramolecular polymerization of **175** in water was studied by concentration-dependent ^{1}H NMR and fluorescence spectroscopy, which yielded the fraction of free monomer versus concentration. These data could be analyzed with the K_2-K model, yielding a K_2 value of 6×10^6 M^{-1} and a K value of 8×10^5 M^{-1}, which means σ (K_2/K) is larger than unity; hence, the growth of the supramolecular polymer is anticooperative. The origin of this anticooperativity was ascribed by the authors to an electronic effect and the bulkiness of the hydrophilic side chains, which hinders further polymerization beyond the dimer.

A remarkable example of anticooperativity was reported by the research group of Moore for the supramolecular polymerization of **176** (Scheme 10). In sharp contrast with the phenyl acetylene based macrocycles (vide supra, section on isodesmic model) and the results obtained by Tobe et al., **176** displays anticooperative behavior in acetone as determined with concentration-dependent ^{1}H NMR and VPO measurements. As suggested by the authors the imine functionality creates a dipole moment in the molecules. Dimerization of the macrocycles most likely is favored in an antiparallel orientation with respect to the imine bond, as viewed along the C═N bond. The symmetry of the dimeric structure is such that it would diminish or even eliminate the net dipole moment of the dimer, and hence subsequent additions of monomers are less favored.[95]

Ghadiri et al. have reported the anticooperative supramolecular polymerization of a cyclic peptide derivative **177**, which comprises alternating α- and ε-amino acids (Chart 50).[414] The formation of a supramolecular nanotubular structure was evidenced by a combination of ^{1}H NMR spectroscopy, mass spectrometry, and X-ray crystallography.

The supramolecular polymerization process of **177** was studied in deuterated chloroform with concentration-dependent ^{1}H NMR experiments. The ^{1}H NMR data could be analyzed with a K_2-K model, which yielded a dimerization constant K_2 of 8.6×10^4 M^{-1} and an elongation equilibrium constant K of 3.8×10^4 M^{-1} (i.e., $\sigma = 2.3$). The authors do not comment on the observed (small degree of) anticooperativity, which is clearly the opposite of the observed cooperativity in the previously studied cyclic eight-residue peptide **127**.[406,410] Solution FT-IR spectroscopy could perhaps yield insight in the role of hydrogen bonding during the supramolecular polymerization to account for the observed anticooperativity.

Stupp and co-workers have reported the formation of supramolecular structures with a regular and finite size, based on a miniaturized triblock copolymer (**178**−**179**, Chart 51).[500,501] Although not strictly a one-dimensional supramolecular polymer, the polymerization of **178**−**179** serves as an illustrative example of how a delicate balance between attractive and repulsive interactions (this latter interaction results in an anticooperative supramolecular polymerization at high oligomer length) can yield nanosized structures with finite size and low polydispersity.

Compound **178** was found to self-assemble in chloroform into nearly identical nanosized structures, as was evidenced from TEM on drop-cast films of **178**.[500] The explanation for the limited size of the structures was ascribed to the balance between the attractive $\pi-\pi$ interactions between biphenyl ester segments and the repulsive steric interactions between the fairly large oligostyrene segments. From molecular

Chart 51

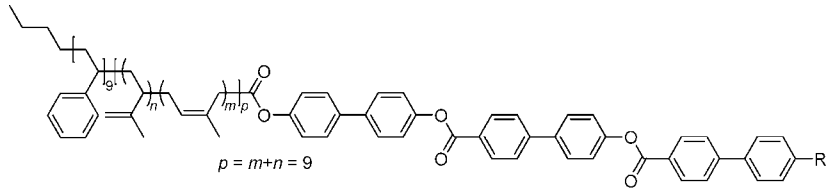

178 R = OH

179 R = CF_3

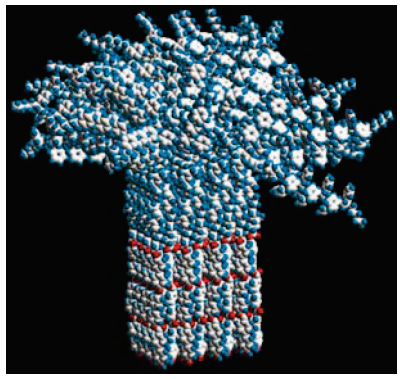

Figure 49. Molecular model of the supramolecular unit composed of 100 triblock molecules of **178**. (Reprinted with permission from ref 500. Copyright 1997 American Association for the Advancement of Science.)

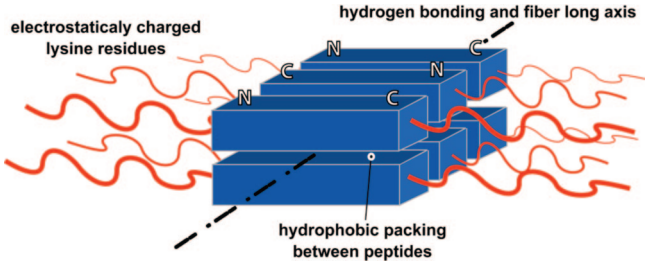

Figure 50. Proposed model of nanofiber formation of ABA peptide block copolymer **180**. (Reprinted from ref 502. Copyright 2007 American Chemical Society.)

modeling, it was found that the final structure contains about 100 molecules (Figure 49).

The bulkiness of the oligostyrene segment of the molecules prevents further growth of the supramolecular structure beyond these 100 molecules. More evidence for the formation of discrete nanosized objects was found by gel permeation chromatography on the cross-linked polymer of **179**, obtained after **179** had been annealeed in the liquid crystalline phase at 250 °C.[501] For the obtained polymeric structure, dissolved in tetrahydrofuran, a polydispersity index as low as 1.11 was determined.

The interplay between attractive and repulsive intermolecular interactions was employed by Hartgerink et al. to arrive at supramolecular structures of finite size.[502] A series of nine peptides, organized in an ABA block motif, was prepared. The central B part consisted of alternating hydrophilic (glutamine) and hydrophobic (leucine) amino acids, whereas the outer A parts comprised charged lysine residues (Chart 52).

Intermolecular hydrogen bonding, leading to β-sheet formation, and hydrophobic interactions between the leucine side chains in the central B block, lead to the formation of supramolecular structures in aqueous environment. These favorable interactions are counterbalanced by the repulsive interactions between the charged lysine residues in the outer A blocks, leading to molecular frustration (Figure 50). It was found that for **180** the length of both blocks is such that there is a balance between assembly and disassembly, leading to the formation of supramolecular structures of finite size, as evidenced from cryo-TEM. Increasing the pH or the ion concentration was found to dramatically increase the length and the length distribution, which was attributed to the disrupted balance between the attractive and repulsive interactions.

5. Functional Supramolecular Polymers

Unprecedented functions have become available by the unique properties of supramolecular polymers. Although this review primarily focuses on the way supramolecular polymers are formed and how the mechanism of supramolecular polymerization influences the properties of the polymers obtained, at the end of this review we address the reason why these supramolecular polymers have attracted so much attention recently. Often the question is raised as to what these dynamic systems offer that traditional macromolecular polymers cannot. Obviously, supramolecular polymers are not competing with engineering plastics that need to function at elevated temperatures or with bulk polyolefins that possess a unique price−performance relationship. However, the properties that bring new functions compared to those known for macromolecules are all related to the dynamic and reversible nature of the supramolecular systems. The control over mechanism of formation, the huge variety of self-assembling units, and the control of the stability of structures formed offer an enormous range of frequencies in the dynamic properties of these supramolecular polymers. This control yields unique processing capabilities of responsive materials but also creates a modular approach to construct functional materials.

Three major classes of functional materials can be discriminated, where in recent years progress has been enormous. Some of the supramolecular polymer materials are close to commercial application and in a few cases are already successful commercially. The three distinctive different areas are (1) functions based on excellent mechanical properties with a unique ease in processing, (2) electronic functions based on π-conjugated repeating units leading to supramolecular electronics, and (3) biomedical functions in regenerative medicine of biologically active supramolecular polymers.

5.1. Mechanical Properties

Probably the most unexpected property that has been achieved with supramolecular polymers is the mechanical strength that can be obtained by the proper choice of the building blocks. When the association constant of the interacting units, responsible for the formation of the supramolecular system, is high enough, the supramolecular polymer possesses material properties similar to those of macromolecules. Because additional interactions between the chains determine the macroscopic properties in both (covalent and noncovalent) polymeric systems, a large range of materials can be made, including thermoplastic supramolecular elastomers, high T_g supramolecular polymers, and even semicrystalline supramolecular polymers.

Supramolecular polymer **67**, presented as a plastic material in Figure 2, is used here as an illustration.[22] In Figure 51 are shown the master curves of the storage and loss moduli of **67**. A sharp viscoelastic transition is observed, indicating that at a single relaxation time the polymer chains start to flow. Closer examination of the master curve of the moduli of **67** indicates that the apparent lifetime of the hydrogen-bonded units has to be comparable to or somewhat shorter than the reptation time of the polymer chains.

At higher temperatures, the lifetime of the hydrogen bond becomes shorter, and hence the viscosity decreases drastically. The apparent activation energy can be determined according to the Andrade−Eyring equation and is found to

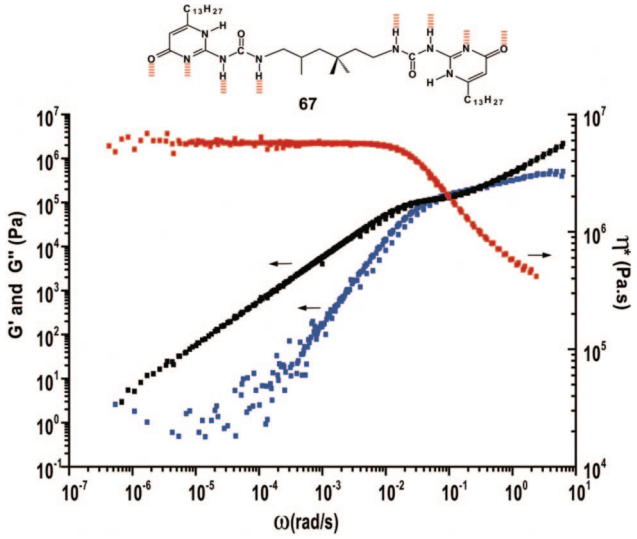

Figure 51. Master curves of storage and loss moduli (left axis) and dynamic melt viscosity (right axis) of compound **67**.

Chart 52

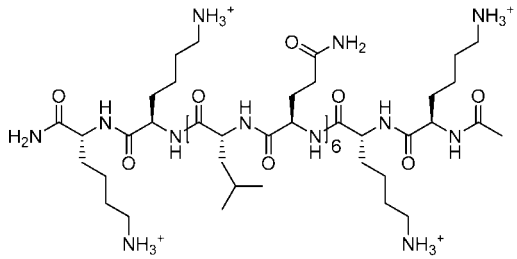

180

be 105 kJ mol^{-1}, which is significantly higher than that of traditional macromolecules. This explains the ease of processing of supramolecular polymers. Hence, applications as hot-melt are very attractive.

The dynamic nature of supramolecular polymers also creates a unique possibility to fabricate self-healing materials. Leibler and co-workers recently disclosed[503] their hydrogen-bonded network that upon fracture can restore the hydrogen-bonded patterns when the broken pieces are pushed to each other at the fracture site, leading to a self-healed interface. The system of Leibler consists of di- and tri-functionalized urea and amide-functionalized molecules derived from fatty acids (Figure 52). In this mixture, a supramolecular network is formed between a large number of these di- and tri-functional building blocks with various strongly hydrogen bonding urea and amide molecules. The self-healing properties of this material were shown to lie in the dynamics and density of associating hydrogen-bonding groups. Upon rupture of the elastomer, the hydrogen bonds of the supramolecular network rather than the covalent bonds are broken, resulting in a high density of nonassociated hydrogen bonds at the interface. When the broken pieces are brought into contact, these nonassociated hydrogen bonds located at the two interfaces can engange in the formation of new hydrogen bonds, thereby restoring the original supramolecular network of the rubber.

The quadruple hydrogen-bonded unit has been further employed in the chain extension of telechelic polysiloxanes, poly(ethylene/butylenes), polyethers, polyesters, and polycarbonates.[504] In these compounds, the material properties were shown to improve dramatically upon functionalization, resulting in materials that combine many of the mechanical properties of conventional macromolecules with the low melt viscosity of low molecular weight organic compounds. The reversibility of supramolecular polymers adds new aspects to many of the principles that are known from condensation polymerizations. For example, a mixture of different supramolecular monomers will yield copolymers, but it is extremely simple to adjust the copolymer composition instantaneously by adding an additional monomer. Moreover, the use of monomers with a functionality of three or more will give rise to network formation. However, in contrast to condensation networks, the "self-healing" supramolecular network can reassemble to form the thermodynamically most favorable state, thus forming denser networks. What started as a scientific curiosity grew in less than 10 years into a system with technological relevance.

5.2. Electronic Properties

Self-assembling molecules can form structures with useful electronic properties.[505] These supramolecular materials combine the benefits of polymers with those of organic

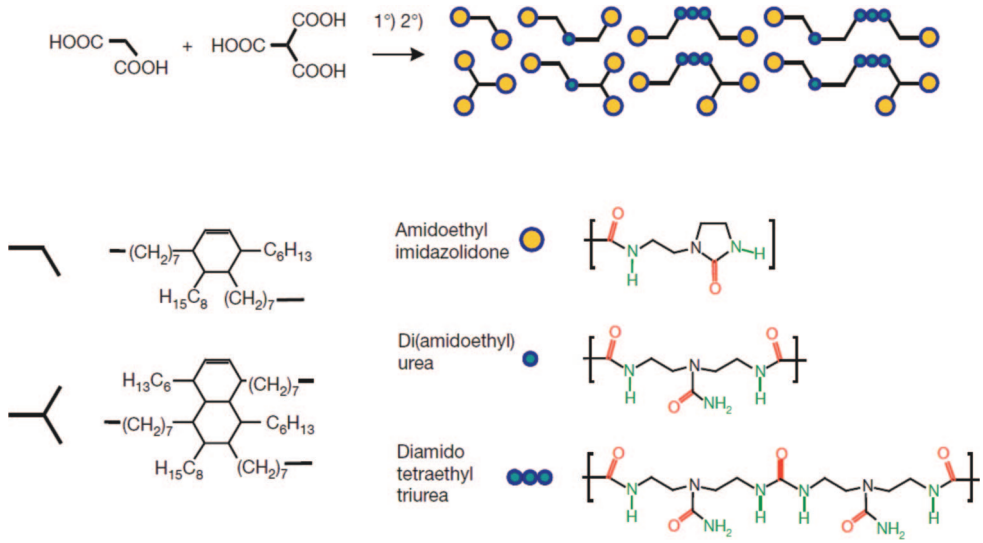

Figure 52. Schematic representation and molecular structures of the materials used in the self-healing rubber reported by Leibler and co-workers. (Reprinted with permission from ref 503. Copyright 2008 Nature Publishing Group.)

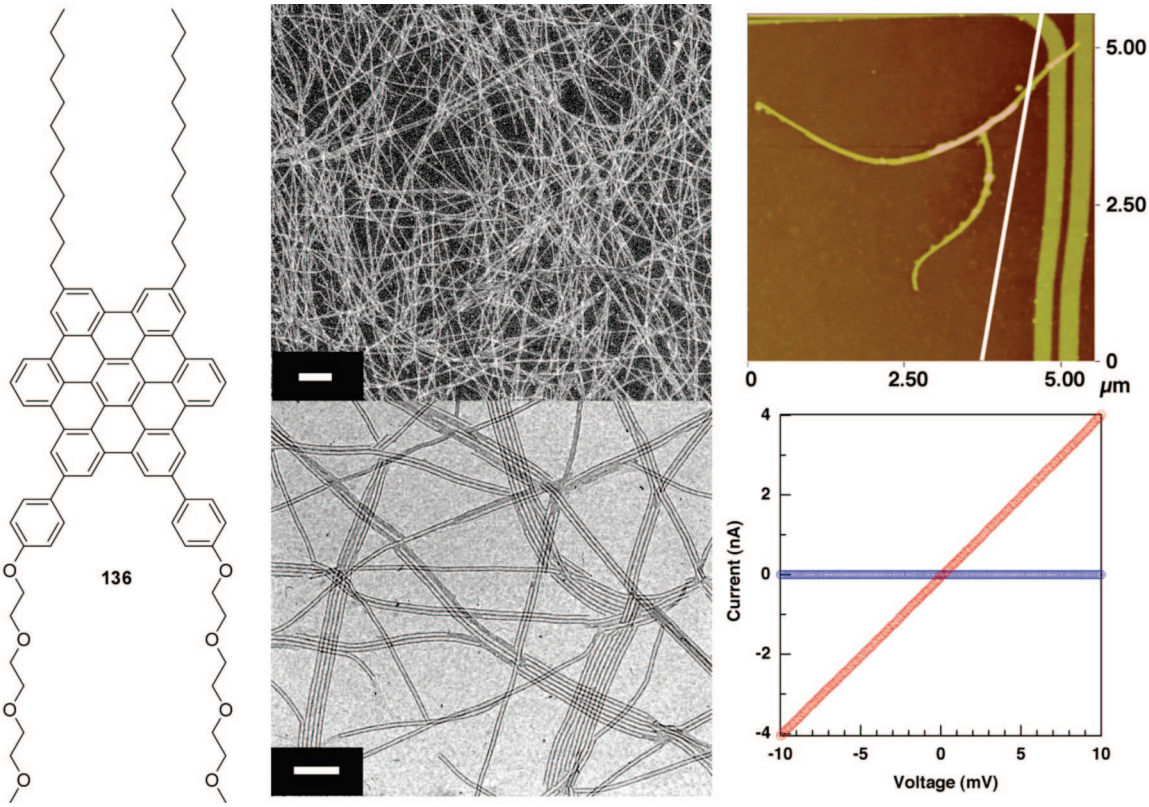

Figure 53. Amphiphilic hexa-*peri*-hexabenzocoronene **136**, which forms tubes that can be placed between two electrodes. (Reprinted with permission from ref 432. Copyright 2004 American Association for the Advancement of Science.)

crystalline systems. To create new electronic devices, physicists and engineers have had to rely increasingly on the originality of chemists in designing, synthesizing, and characterizing molecular systems possessing useful properties. Exciting results have been obtained with both polymer-based light-emitting diodes and organic transistors, in which molecular scale layers are deposited from the vapor phase, but these two semiconducting classes of material have different virtues. The particular advantage of the polymer systems is that they are cheap and highly processable, that is, easy to synthesize, manipulate, and incorporate into devices. The advantage of the organic materials is the precise ordering of their thin crystalline layers, which supports the high charge-carrier (electron and hole) mobility essential to electronic performance. The dream for many scientists is to bring these two features together in one class of materials and to produce easy-to-process yet highly ordered molecular systems.

Supramolecular polymers based on π-conjugated monomers have been shown to possess exactly the required balance. As an illustration, the modified discotic hexa-*peri*-hexabenzocoronene are selected as being one of the most appealing systems presented so far. As initiated by the group of Müllen, the long one-dimensional stacks of hexa-*peri*-hexabenzocoronene possess properties that are very close to those obtained by π-conjugated polymers. In a next step, the group of Aida[432] was able to fabricate amphiphilic hexa-*peri*-hexabenzocoronenes that self-assemble in THF into nanotubes that have an aspect ratio of >1000 and are 14 nm wide (**136** in Figure 53). The walls of the tubes consist of helical arrays of π-stacked coronenes covered by hydrophilic glycol chains. Interestingly, an individual nanotube could be positioned across Pt nanogap electrodes (180 nm) on a SiO_2 substrate. The tube was essentially insulating, however, after oxidation with $NOBF_4$ revealed an I−V profile with an ohmic behavior having a resistance of 2.5 MΩ at 285 K. This value is comparable to that of inorganic semiconductor nanotubes.

More recently, Aida and co-workers reported on trinitrofluorenone appended gemini-shaped amphiphilic hexabenzocoronenes, which form nanotubes with different photochemical properties.[506] In these nanotubes, a molecular layer of electron-accepting trinitrofluorenone laminates an electron-donating graphitic layer of π-stacked hexabenzocoronene. It was shown that the coaxial nanotubular structure allows photochemical generation of separated charge carriers and a quick photoconductive response with a large on/off ratio. These examples illustrate that supramolecular polymers offer great potential for optoelectronic applications, such as nanoscale photovoltaics and photodetectors.

5.3. Biological Properties

High control over both stability and dynamics of bioactive materials might be accomplished by using supramolecular polymers. The adaptability of the biomaterial to the host tissue is of major importance for good interaction between cells (with their cell membrane receptors) and the bioactive molecules on the biomaterial. Therefore, it is important to mimic the natural environment, the cell in its natural environment, its niche. Tissues are not static; signals are being turned on and off, receptors are moving over the cell membrane, cells are moving on the extracellular matrix (ECM), cell membrane receptors adjust to the ECM and vice versa, pathways will be activated, and so on. These are very dynamic events, in which (almost) all interactions are based on recognition and on specific noncovalent, supramolecular interactions.

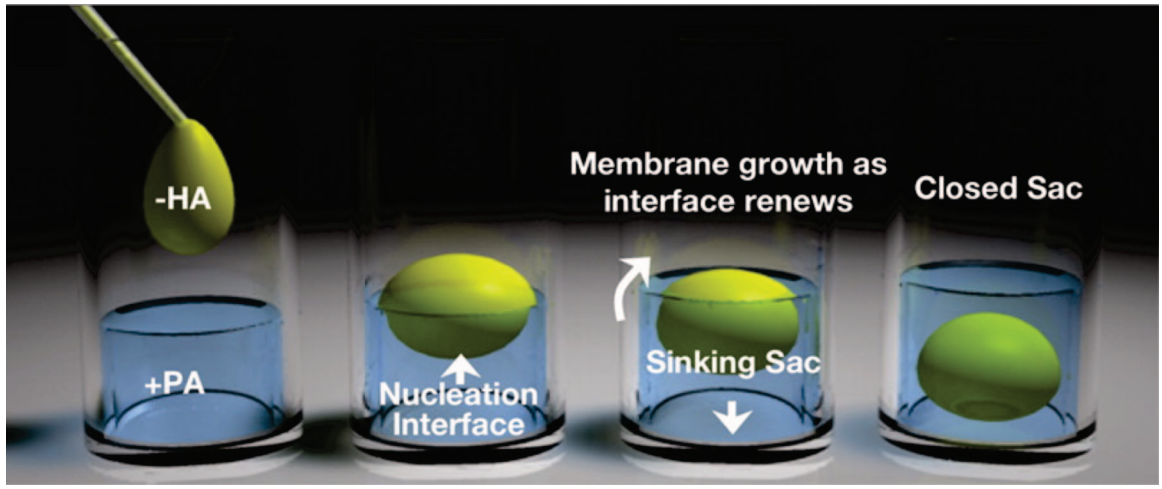

Figure 54. Schematic representation of the hierarchical formation of ordered sacs. Upon addition of a dense negatively charged hyaluronic acid (HA) solution onto a positively charged peptide amphiphile (PA) solution, the immediate formation of a solid membrane localized at the interface between the two liquids is observed. As the heavier hyaluronic acid sinks, the peptide amphiphile molecules engulf the negatively charged polymer, thereby creating a closed sac with the HA solution trapped inside the membrane. (Reprinted with permission from ref 510. Copyright 2008 American Association for the Advancement of Science.)

Therefore, there is a need for a new materials design, and supramolecular materials that can adapt to their environment are ideally equipped for that purpose.[490,507]

Seminal work from the research group of Stupp beautifully illustrates the unique character of supramolecular biomaterials based on peptide amphiphiles.[488,489,492,508,509] The peptide amphiphiles as discussed in more detail in section 4.7.3 self-assemble at the correct pH into stiff nanotubes that can subsequently form hydrogels. Once injected in tissue, the molecules form a gel that brings the bioactive component to direct cell growth in the preferred direction, yielding profound biological response.[489,509] More recently, the group reported on a supramolecular system of hyaluronic acid with this small oligopeptide amphiphile that, upon mixing, instantly forms a flexible but strong sac (Figure 54).[510] Stupp and co-workers subsequently showed that human stem cells engulfed by the self-assembly process remained viable for several weeks and that the stem cells were able to differentiate. It is hoped that this sac, if used for cell therapy, could cloak the stem cells from the human body's immune system and biodegrade upon arriving at its destination, releasing the stem cells to do their work.

Following the ideas of Stupp, our research group has combined the quadruple hydrogen-bonding supramolecular polymers with peptide-modified structures to arrive at bioactive materials with tunable mechanical properties.[511] In less than 10 years, the bottom-up approach in which novel biomaterials are assembled molecule by molecule has become an integral part of nanomaterials manufacture.

6. Conclusions and Prospects

In recent years, supramolecular polymers have positioned themselves as a new paradigm in the field of polymer science. The progress in supramolecular chemistry has paved the way to assemble small molecules by specific directional secondary interactions into polymer arrays, yielding supramolecular polymers that possess many of the well-known properties of "traditional" macromolecules. Due to the reversibility in the bonding, these supramolecular polymers are often in thermodynamic equilibrium and their properties can be adjusted by external stimuli. Recently, functional supramolecular polymers have been prepared with a wealth of new applications, where in all cases control over the dynamic nature of the reversible bonding is used to arrive at responsive properties.

The current review has introduced a classification of supramolecular polymers that follows the outstanding ideas of Wallace H. Carothers published more than 75 years ago.[1] By using the different mechanisms of formation of supramolecular polymers as the key discriminator, we are able to analyze many systems reported in the literature, in some cases requiring reinterpretation of experimental data. Although the multidimensional nature of the supramolecular polymer in some cases and the possibility of hysteresis effects in other cases make interpretation of literature data rather difficult and challenging, we hope that this review can aid and stimulate researchers in the area of supramolecular polymers to actively investigate the supramolecular polymerization mechanism of the wealth of novel supramolecular polymers they so ingeniously produce. Although isodesmic and ring−chain-mediated supramolecular polymerizations are well understood, cooperative supramolecular polymerizations are much less understood due to the presence of hysteresis effects and heterogeneous nucleation. To get a better understanding of cooperative supramolecular polymerizations, it is therefore vital that kinetic studies on various cooperative supramolecular polymerizations are performed. As demonstrated in this review, in many cases kinetic and thermodynamic models are already available from the large body of biophysical literature on protein aggregations.

It is tempting to make a direct comparison between the three mechanisms for supramolecular polymers and the well-known classes—chain, step, and ring-opening—for covalent macromolecules. In analogy with these covalent polymers, it could be envisioned that for each area of application for supramolecular polymers an explicit supramolecular polymerization mechanism for the monomers is necessary to meet the imposed requirements. However, the reversible nature of the bonding between the noncovalently connected monomer units makes this new class of materials distinctively different from their covalent counterparts. It is the dynamic nature that allows adaptation of the supramolecular polymers to continuously changing surroundings, for example, a biological environment. In addition, as was addressed in the

previous section, the processability of these polymers becomes more practical than for covalent polymers. Although the reversibility of the supramolecular bond is often a major advantage, it may also complicate the formation of more structurally diverse architectures. The covalent synthesis of block copolymers and alternating copolymers has become straightforward by using living polymerization techniques. In this case the kinetic inertness of the covalent bond allows the formation of such well-defined architectures. However, one can imagine that the reversibility of the noncovalent bond hampers the formation of supramolecular block and alternating copolymers. Furthermore, the living polymerization techniques applied in covalent chemistry can yield polydispersity indices that approach unity. In contrast, the current level for the polydispersity index obtained for supramolecular polymerizations is closer to 2.0, whereas only in special cases can it be decreased to a lower value.[84,501,512] Both control over the monomer sequence in supramolecular copolymers and control over the polydispersity of supramolecular polymers are future challenges that have yet to be addressed by supramolecular chemists.

Natural supramolecular polymers are very well-known, and the level of sophistication for these supramolecular systems is unprecedented. However, the observed complexity is not the result of a thermodynamically controlled polymerization process, but caused by the natural supramolecular polymerization occurring far from thermodynamic equilibrium. This process is often referred to as self-organization.[513] Whereas self-assembly is reserved for spontaneous processes tending toward equilibrium, self-organization implies a nonequilibrium process in which energy dissipation maintains a nonequilibrium steady state. The critical requirement for self-organizing polymers is the presence of autocatalytic reactions in the supramolecular polymerization process together with a supply of chemical energy and competing diffusion of molecules. The supramolecular polymerization of microtubules serves as an illustrative example of a self-organization process in nature.[514] Due to strong kinetic nonlinearities in the growth process and the continuous supply of chemical energy via GTP hydrolysis, these structures exhibit higher level emergent phenomena such as dynamic instabilities in their growth,[515] oscillatory kinetics,[516] and macroscopic states of different morphology.[517,518]

To approach the level of sophistication of natural systems in artificial supramolecular polymers, supramolecular polymerizations far from equilibrium resulting in self-organization must be developed. It is anticipated that the current understanding of thermodynamically controlled supramolecular polymerization, the subject of this review, could act as a starting point for the development of supramolecular polymerizations operating either under kinetic control or under dissipative conditions. This should open the possibility for supramolecular chemists to design systems that can approach the level of complexity observed in nature's self-organized supramolecular polymers.

7. Acknowledgments

We acknowledge P. Korevaar, M. Nieuwenhuizen, Prof. Dr. G. Ercolani, Dr. P. van der Schoot, and Dr. J. Dudowicz for insightful discussions. We also acknowledge Dr. K. Pieterse for providing some of the artwork. This work is supported by the Council for Chemical Sciences of The Netherlands Organization for Scientific Research (CW-NWO).

8. References

(1) Carothers, W. H. *Chem. Rev.* **1931**, *8*, 353.
(2) Staudinger, H. *Ber. Dtsch. Chem. Ges.* **1920**, *53*, 1073.
(3) Wang, X.; Guerin, G.; Wang, H.; Wang, Y.; Manners, I.; Winnik, M. A. *Science* **2007**, *317*, 644.
(4) Schappacher, M.; Deffieux, A. *Science* **2008**, *319*, 1512.
(5) Tang, C.; Lennon, E. M.; Fredrickson, G. H.; Kramer, E. J.; Hawker, C. J. *Science* **2008**, *322*, 429.
(6) Ruokolainen, J.; Makinen, R.; Torkkeli, M.; Makela, T.; Serimaa, R.; Ten Brinke, G.; Ikkala, O. *Science* **1998**, *280*, 557.
(7) Pochan, D. J.; Chen, Z.; Cui, H.; Hales, K.; Qi, K.; Wooley, K. L. *Science* **2004**, *306*, 94.
(8) Cui, H.; Chen, Z.; Zhong, S.; Wooley, K. L.; Pochan, D. J. *Science* **2007**, *317*, 647.
(9) Cornelissen, J. J. L. M.; Fischer, M.; Sommerdijk, N. A. J. M.; Nolte, R. J. M. *Science* **1998**, *280*, 1427.
(10) Fréchet, J. M. J. *Proc. Natl. Acad. Sci. U.S.A.* **2002**, *99*, 4782.
(11) Kato, T.; Mizoshita, N.; Kishimoto, K. *Angew. Chem., Int. Ed.* **2006**, *45*, 38.
(12) Kato, T.; Hirai, Y.; Nakaso, S.; Moriyama, M. *Chem. Soc. Rev.* **2007**, *36*, 1857.
(13) Sivakova, S.; Rowan, S. J. *Chem. Soc. Rev.* **2005**, *34*, 9.
(14) Pollino, J. M.; Weck, M. *Chem. Soc. Rev.* **2005**, *34*, 193.
(15) Weck, M. *Polym. Int.* **2007**, *56*, 453.
(16) Percec, V.; Dulcey, A. E.; Balagurusamy, V. S. K.; Miura, Y.; Smidrkal, J.; Peterca, M.; Nummelin, S.; Edlund, U.; Hudson, S. D.; Heiney, P. A.; Duan, H.; Magonov, S. N.; Vinogradov, S. A. *Nature* **2004**, *430*, 764.
(17) Feldman, K. E.; Kade, M. J.; de Greef, T. F. A.; Meijer, E. W.; Kramer, E. J.; Hawker, C. J. *Macromolecules* **2008**, *41*, 4694.
(18) Worsfold, D. J.; Bywater, S. *J. Polym. Sci.* **1957**, *26*, 299.
(19) Leonard, J.; Maheux, D. *J. Macromol. Sci., Part A: Pure Appl. Chem.* **1973**, 7.
(20) Jochim, S.; Bartenstein, M.; Altmeyer, A.; Hendl, G.; Riedl, S.; Chin, C.; Hecker Denschlag, J.; Grimm, R. *Science* **2003**, *302*, 2101.
(21) Brodsky, F. M.; Chen, C. Y.; Knuehl, C.; Towler, M. C.; Wakeham, D. E. *Annu. Rev. Cell Dev. Biol.* **2001**, *17*, 517.
(22) Sijbesma, R. P.; Beijer, F. H.; Brunsveld, L.; Folmer, B. J. B.; Hirschberg, J. H. K. K.; Lange, R. F. M.; Lowe, J. K. L.; Meijer, E. W. *Science* **1997**, *278*, 1601.
(23) de Greef, T. F. A.; Meijer, E. W. *Nature* **2008**, *453*, 171.
(24) Bouteiller, L. *Adv. Polym. Sci.* **2007**, *207*, 79.
(25) Harada, A.; Takashima, Y.; Yamaguchi, H. *Chem. Soc. Rev.* **2009**, *38*, 875.
(26) Lehn, J. M. *Makromol. Chem., Macromol. Symp.* **1993**, *69*, 1.
(27) Zimmerman, N.; Moore, J. S.; Zimmerman, S. C. *Chem. Ind.* **1998**, 604.
(28) Ciferri, A. *J. Macromol. Sci., Polym. Rev.* **2003**, *C43*, 271.
(29) Wilson, A. J. *Soft Matter* **2007**, *3*, 409.
(30) Rieth, S.; Baddeley, C.; Badjic, J. D. *Soft Matter* **2007**, *3*, 137.
(31) *Supramolecular Polymers*, 2nd ed.; Taylor & Francis: London, U.K., 2005.
(32) Shimizu, L. S. *Polym. Int.* **2007**, *56*, 444.
(33) Lehn, J.-M. *Polym. Int.* **2002**, *51*, 825.
(34) ten Brinke, G.; Ruokolainen, J.; Ikkala, O. *Adv. Polym. Sci.* **2007**, *207*, 113.
(35) Binder, W. H.; Zirbs, R. *Adv. Polym. Sci.* **2007**, *207*, 1.
(36) Brunsveld, L.; Folmer, B. J. B.; Meijer, E. W.; Sijbesma, R. P. *Chem. Rev.* **2001**, *101*, 4071.
(37) Flory, P. J. *Principles of Polymer Chemistry*; Cornell University Press: Ithaca, NY, 1953.
(38) Ueberreiter, K.; Engel, M. *Makromol. Chem.* **1977**, *178*, 2257.
(39) This is further supported by a patent of Flory, which describes the polycondensation of 1,10-decamethylene glycol with sebacoyl chloride. After reaction of the bifunctional monomers in the bulk, a highly viscous material is obtained, which corresponds to linear polyesters of high molecular weight: Flory, P. J.; Leunter, F. S. U.S. Patent 2589687, 1952.
(40) Ciferri, A. *Macromol. Rapid Commun.* **2002**, *23*, 511.
(41) Dudowicz, J.; Freed, K. F.; Douglas, J. F. *J. Chem. Phys.* **2003**, *119*, 12645.
(42) Martin, R. B. *Chem. Rev.* **1996**, *96*, 3043.
(43) van der Schoot, P. Theory of Supramolecular Polymerization. In *Supramolecular Polymers*, 2nd ed.; Ciferri, A., Ed.; Taylor & Francis: London, U.K., 2005.
(44) Henderson, J. R. *Phys. Rev. E* **1997**, *55*, 5731.
(45) Douglas, J. F.; Dudowicz, J.; Freed, K. F. *J. Chem. Phys.* **2008**, *128*, 224901.
(46) Mukerjee, P.; Ghosh, A. K. *J. Am. Chem. Soc.* **1970**, *92*, 6408.
(47) Connors, K. A. *Binding Constants: The Measurement of Molecular Complex Stability*; Wiley: New York, 1987.
(48) Zhao, D.; Moore, J. S. *Org. Biomol. Chem.* **2003**, *1*, 3471.

(49) Flory, P. J. *J. Am. Chem. Soc.* **1936**, *58*, 1877.
(50) Cates, M. E. *J. Phys. (Paris)* **1988**, *49*, 1593.
(51) Schäfer, L. *Phys. Rev. B* **1992**, *46*, 6061.
(52) van der Schoot, P. *Europhys. Lett.* **1997**, 25.
(53) Wittmer, J. P.; Milchev, A.; Cates, M. E. *J. Chem. Phys.* **1998**, *109*, 834.
(54) Mukerjee, P. *J. Phys. Chem.* **1972**, *76*, 565.
(55) Knoben, W.; Besseling, N. A. M.; Bouteiller, L.; Cohen Stuart, M. A. *Phys. Chem. Chem. Phys.* **2005**, *7*, 2390.
(56) Cates, M. E.; Candau, S. J. *J. Phys.: Condens. Matter* **1990**, 6869.
(57) Lou, X.; Zhu, Q.; Lei, Z.; van Dongen, J. L. J.; Meijer, E. W. *J. Chromatogr., A* **2004**, *1029*, 67.
(58) Braswell, E. H. *J. Phys. Chem.* **1984**, *88*, 3653.
(59) Coggeshall, N. D.; Saier, E. L. *J. Am. Chem. Soc.* **1951**, *73*, 5414.
(60) Bierzynski, A.; Kozlowska, H.; Wierzchowski, K. L. *Biophys. Chem.* **1977**, *6*, 213.
(61) Gajewska, J.; Bierzynski, A.; Bolewska, K.; Wierzchowski, K. L.; Petrov, A. I.; Sukhorukov, B. I. *Biophys. Chem.* **1982**, *15*, 191.
(62) Broom, A. D.; Schweizer, M. P.; Ts'o, P. O. P. *J. Am. Chem. Soc.* **1967**, *89*, 3612.
(63) Gilligan, T. J.; Schwarz, G. *Biophys. Chem.* **1976**, *4*, 55.
(64) Stoesser, P. R.; Gill, S. J. *J. Phys. Chem.* **1967**, *71*, 564.
(65) Price, W. S.; Tsuchiya, F.; Arata, Y. *J. Am. Chem. Soc.* **1999**, *121*, 11503.
(66) van Holde, K. E.; Rossetti, G. P. *Biochemistry* **1967**, *6*, 2189.
(67) Bretz, R.; Lustig, A.; Schwarz, G. *Biophys. Chem.* **1974**, *1*, 237.
(68) Tojo, H.; Horiike, K.; Shiga, K.; Nishina, Y.; Watari, H.; Yamano, T. *J. Biol. Chem.* **1985**, *260*, 12607.
(69) Buurma, N. J.; Haq, I. *J. Mol. Biol.* **2008**, *381*, 607.
(70) Greer, S. C. *Annu. Rev. Phys. Chem.* **2002**, *53*, 173.
(71) Greer, S. C. *J. Phys. Chem. B* **1998**, *102*, 5413.
(72) Greer, S. C. *Adv. Chem. Phys.* **1996**, *94*, 261.
(73) Dainton, F. S.; Ivin, K. J. *Nature* **1948**, *162*, 705.
(74) Dainton, F. S.; Ivin, K. J. *Q. Rev.* **1958**, *12*, 61.
(75) Dudowicz, J.; Freed, K. F.; Douglas, J. F. *J. Chem. Phys.* **1999**, *111*, 7116.
(76) Dudowicz, J.; Freed, K. F.; Douglas, J. F. *J. Chem. Phys.* **2000**, *112*, 1002.
(77) Dudowicz, J.; Freed, K. F.; Douglas, J. F. *J. Chem. Phys.* **2000**, *113*, 434.
(78) Rah, K.; Freed, K. F.; Dudowicz, J.; Douglas, J. F. *J. Chem. Phys.* **2006**, *124*, 144906.
(79) Douglas, J. F.; Dudowicz, J.; Freed, K. F. *J. Chem. Phys.* **2007**, *127*, 224901.
(80) Flory, P. J. *J. Chem. Phys.* **1942**, *10*, 51.
(81) Huggins, M. L. *Ann. N.Y. Acad. Sci.* **1942**, *4*, 1.
(82) The insensitivity of these parameters to the presence of weak van der Waals interactions no longer applies when the polymer has an interaction parameter with the solvent different from that of the monomer (see ref 41).
(83) Odille, F. G. J.; Jónsson, S.; Stjernqvist, S.; Rydén, T.; Wärnmark, K. *Chem.—Eur. J.* **2007**, *13*, 9617.
(84) de Greef, T. F. A.; Ercolani, G.; Ligthart, G. B. W. L.; Meijer, E. W.; Sijbesma, R. P. *J. Am. Chem. Soc.* **2008**, *130*, 13755.
(85) Schaefgen, J. R.; Flory, P. J. *J. Am. Chem. Soc.* **1948**, *70*, 2709.
(86) Grimme, S. *Angew. Chem., Int. Ed.* **2008**, *47*, 3430.
(87) Ye, X.; Li, Z.-H.; Wang, W.; Fan, K.; Xu, W.; Hua, Z. *Chem. Phys. Lett.* **2004**, *397*, 56.
(88) Tauer, T. P.; Sherrill, C. D. *J. Phys. Chem. A* **2005**, *109*, 10475.
(89) Rogel, E. *Langmuir* **2002**, *18*, 1928.
(90) Beshnova, D. A.; Lantushenko, A. O.; Davies, D. B.; Evstigneev, M. P. *J. Chem. Phys.* **2009**, *130*, 165105.
(91) Zhao, D.; Moore, J. S. *Chem. Commun.* **2003**, 807.
(92) Shetty, A. S.; Zhang, J.; Moore, J. S. *J. Am. Chem. Soc.* **1996**, *118*, 1019.
(93) Hunter, C. A.; Sanders, J. K. M. *J. Am. Chem. Soc.* **1990**, *112*, 5525.
(94) Lahiri, S.; Thompson, J. L.; Moore, J. S. *J. Am. Chem. Soc.* **2000**, *122*, 11315.
(95) Zhao, D.; Moore, J. S. *J. Org. Chem.* **2002**, *67*, 3548.
(96) Tobe, Y.; Utsumi, N.; Kawabata, K.; Nagano, A.; Adachi, K.; Araki, S.; Sonoda, M.; Hirose, K.; Naemura, K. *J. Am. Chem. Soc.* **2002**, *124*, 5350.
(97) Lin, C. H.; Tour, J. *J. Org. Chem.* **2002**, *67*, 7761.
(98) Enozawa, H.; Hasegawa, M.; Takamatsu, D.; Fukui, K.-I.; Iyoda, M. *Org. Lett.* **2006**, *8*, 1917.
(99) García-Frutos, E. M.; Gómez-Lor, B. *J. Am. Chem. Soc.* **2008**, *130*, 9173.
(100) Wu, J.; Pisula, W.; Müllen, K. *Chem. Rev.* **2007**, *107*, 718.
(101) Kastler, M.; Pisula, W.; Wasserfallen, D.; Pakula, T.; Müllen, K. *J. Am. Chem. Soc.* **2005**, *127*, 4286.
(102) Feng, X.; Pisula, W.; Takase, M.; Dou, X.; Enkelmann, V.; Wagner, M.; Ding, N.; Müllen, K. *Chem. Mater.* **2008**, *20*, 2872.
(103) Dou, X.; Pisula, W.; Wu, J.; Bodwell, G. J.; Müllen, K. *Chem.—Eur. J.* **2008**, *14*, 240.
(104) Pisula, W.; Tomović, Ž.; Watson, M. D.; Müllen, K.; Kussmann, J.; Ochsenfeld, C.; Metzroth, T.; Gauss, J. *J. Phys. Chem. B* **2007**, *111*, 7481.
(105) Haino, T.; Tanaka, M.; Fukazawa, Y. *Chem. Commun.* **2008**, 468.
(106) Kraft, A.; Osterod, F.; Frohlich, R. *J. Org. Chem.* **1999**, *64*, 6425.
(107) Palmans, A. R. A.; Vekemans, J. A. J. M.; Havinga, E. E.; Meijer, E. W. *Angew. Chem., Int. Ed. Engl.* **1997**, *36*, 2648.
(108) van Gorp, J. J.; Vekemans, J. A. J. M.; Meijer, E. W. *J. Am. Chem. Soc.* **2002**, *124*, 14759.
(109) Palmans, A. R. A.; Vekemans, J. A. J. M.; Fischer, H.; Hikmet, R. A.; Meijer, E. W. *Chem.—Eur. J.* **1997**, *3*, 300.
(110) Palmans, A. R. A.; Vekemans, J. A. J. M.; Hikmet, R. A.; Fischer, H.; Meijer, E. W. *Adv. Mater.* **1998**, *10*, 873.
(111) Metzroth, T.; Hoffmann, A.; Martín-Rapún, R.; Smulders, M. M. J.; Pieterse, K.; Palmans, A. R. A.; Vekemans, J. A. J. M.; Meijer, E. W.; Spiess, H. W.; Gauss, J. 2009, manuscript in preparation.
(112) Chen, Z.; Lohr, A.; Saha-Möller, C. R.; Würthner, F. *Chem. Soc. Rev.* **2009**, *38*, 564.
(113) Würthner, F.; Thalacker, C.; Diele, S.; Tschierske, C. *Chem.—Eur. J.* **2001**, *7*, 2245.
(114) Jelley, E. E. *Nature* **1936**, *138*, 1009.
(115) Würthner, F.; Chen, Z.; Dehm, V.; Stepanenko, V. *Chem. Commun.* **2006**, 1188.
(116) Chen, Z.; Stepanenko, V.; Dehm, V.; Prins, P.; Siebbeles, L. D. A.; Seibt, J.; Marquetand, P.; Engel, V.; Würthner, F. *Chem.—Eur. J.* **2007**, *13*, 436.
(117) Chen, Z.; Baumeister, U.; Tschierske, C.; Würthner, F. *Chem.—Eur. J.* **2007**, *13*, 450.
(118) Dehm, V.; Chen, Z.; Baumeister, U.; Prins, P.; Siebbeles, L. D. A.; Würthner, F. *Org. Lett.* **2007**, *9*, 1085.
(119) Huber, V.; Sengupta, S.; Würthner, F. *Chem.—Eur. J.* **2008**, *14*, 7791.
(120) van Herrikhuyzen, J.; Syamakumari, A.; Schenning, A. P. H. J.; Meijer, E. W. *J. Am. Chem. Soc.* **2004**, *126*, 10021.
(121) Feng, J.; Liang, B.; Wang, D.; Wu, H.; Xue, L.; Li, X. *Langmuir* **2008**, *24*, 11209.
(122) Wang, W.; Han, J. J.; Wang, L. Q.; Li, L. S.; Shaw, W. J.; Li, A. D. Q. *Nano Lett.* **2003**, *3*, 455.
(123) Fouquey, C.; Lehn, J.-M.; Levelut, A.-M. *Adv. Mater.* **1990**, *2*, 254.
(124) Kotera, M.; Lehn, J.-M.; Vigneron, J.-P. *J. Chem. Soc., Chem. Commun.* **1994**, *2*, 197.
(125) Kotera, M.; Lehn, J.-M.; Vigneron, J.-P. *Tetrahedron* **1995**, *51*, 1953.
(126) St. Pourcain, C. B.; Griffin, A. C. *Macromolecules* **1995**, *28*, 4116.
(127) Bladon, P.; Griffin, A. C. *Macromolecules* **1993**, *26*, 6604.
(128) Berl, V.; Schmutz, M.; Krische, M. J.; Khoury, R. G.; Lehn, J.-M. *Chem.—Eur. J.* **2002**, *8*, 1227.
(129) Kolomiets, E.; Buhler, E.; Candau, S. J.; Lehn, J.-M. *Macromolecules* **2006**, *39*, 1173.
(130) Buhler, E.; Candau, S. J.; Schmidt, J.; Talmon, Y.; Kolomiets, E.; Lehn, J.-M. *J. Polym. Sci., Part B: Polym. Phys.* **2007**, *45*, 103.
(131) Kolomiets, E.; Lehn, J.-M. *Chem. Commun.* **2005**, 1519.
(132) Park, T.; Zimmerman, S. C. *J. Am. Chem. Soc.* **2006**, *128*, 13986.
(133) Park, T.; Todd, E. M.; Nakashima, S.; Zimmerman, S. C. *J. Am. Chem. Soc.* **2005**, *127*, 18133.
(134) Park, T.; Zimmerman, S. C.; Nakashima, S. *J. Am. Chem. Soc.* **2005**, *127*, 6520.
(135) Park, T.; Zimmerman, S. C. *J. Am. Chem. Soc.* **2006**, *128*, 11582.
(136) Park, T.; Zimmerman, S. C. *J. Am. Chem. Soc.* **2006**, *128*, 14236.
(137) de Greef, T. F. A.; Ligthart, G. B. W. L.; Lutz, M.; Spek, A. L.; Meijer, E. W.; Sijbesma, R. P. *J. Am. Chem. Soc.* **2008**, *130*, 5479.
(138) Beijer, F. H.; Sijbesma, R. P.; Kooijman, H.; Spek, A. L.; Meijer, E. W. *J. Am. Chem. Soc.* **1998**, *120*, 6761.
(139) Söntjens, S. H. M.; Sijbesma, R. P.; van Genderen, M. H. P.; Meijer, E. W. *J. Am. Chem. Soc.* **2000**, *122*, 7487.
(140) Yagai, S.; Higashi, M.; Karatsu, T.; Kitamura, A. *Chem. Commun.* **2006**, 1500.
(141) Yagai, S.; Kinoshita, T.; Higashi, M.; Kishikawa, K.; Nakanishi, T.; Karatsu, T.; Kitamura, A. *J. Am. Chem. Soc.* **2007**, *129*, 13277.
(142) Yagai, S.; Karatsu, T.; Kitamura, A. *Langmuir* **2005**, *21*, 11048.
(143) Yagai, S.; Higashi, M.; Karatsu, T.; Kitamura, A. *Chem. Mater.* **2005**, *17*, 4392.
(144) Yagai, S.; Higashi, M.; Karatsu, T.; Kitamura, A. *Chem. Mater.* **2004**, *16*, 3582.
(145) Seki, T.; Yagai, S.; Karatsu, T.; Kitamura, A. *J. Org. Chem.* **2008**, *73*, 3328.
(146) Yagai, S.; Monma, Y.; Kawauchi, N.; Karatsu, T.; Kitamura, A. *Org. Lett.* **2007**, *9*, 1137.
(147) Little care has to be taken due to the limited number of data points, which cannot completely rule out a cooperative growth mechanism.
(148) Stonius, S.; Orentas, E.; Butkus, E.; Öhrström, L.; Wendt, O. F.; Wärnmark, K. *J. Am. Chem. Soc.* **2006**, *128*, 8272.
(149) Rebek, J., Jr. *Chem. Commun.* **2000**, 637.

(150) Castellano, R. K.; Rudkevich, D. M.; Rebek, J., Jr. *Proc. Natl. Acad. Sci. U.S.A.* **1997**, *94*, 7132.
(151) Castellano, R. K.; Craig, S. L.; Nuckolls, C.; Rebek, J., Jr. *J. Am. Chem. Soc.* **2000**, *122*, 7876.
(152) Castellano, R. K.; Clark, R.; Craig, S. L.; Nuckolls, C.; Rebek, J., Jr. *Proc. Natl. Acad. Sci. U.S.A.* **2000**, *97*, 12418.
(153) Castellano, R. K.; Nuckolls, C.; Eichhorn, S. H.; Wood, M. R.; Lovinger, A. J.; Rebek, J., Jr. *Angew. Chem., Int. Ed.* **1999**, *38*, 2603.
(154) Castellano, R. K.; Kim, B. H.; Rebek, J., Jr. *J. Am. Chem. Soc.* **1997**, *119*, 12671.
(155) Xu, H.; Rudkevich, D. M. *Chem.—Eur. J.* **2004**, *10*, 5432.
(156) Xu, H.; Rudkevich, D. M. *J. Org. Chem.* **2004**, *69*, 8609.
(157) Xu, H.; Rudkevich, D. M. *Org. Lett.* **2005**, *7*, 3223.
(158) Haino, T.; Matsumoto, Y.; Fukazawa, Y. *J. Am. Chem. Soc.* **2005**, *127*, 8936.
(159) Yebeutchou, R. M.; Tancini, F.; Demitri, N.; Geremia, S.; Mendichi, R.; Dalcanale, E. *Angew. Chem., Int. Ed.* **2008**, *47*, 4504.
(160) Delangle, P.; Mulatier, J.-C.; Tinant, B.; Declercq, J.-P.; Dutasta, J.-P. *Eur. J. Org. Chem.* **2001**, *2001*, 3695.
(161) Miyauchi, M.; Kawaguchi, Y.; Harada, A. *J. Inclusion Phenom. Macrocyclic Chem.* **2004**, *50*, 57.
(162) Miyauchi, M.; Takashima, Y.; Yamaguchi, H.; Harada, A. *J. Am. Chem. Soc.* **2005**, *127*, 2984.
(163) Miyauchi, M.; Harada, A. *J. Am. Chem. Soc.* **2004**, *126*, 11418.
(164) Miyauchi, M.; Hoshino, T.; Yamaguchi, H.; Kamitori, S.; Harada, A. *J. Am. Chem. Soc.* **2005**, *127*, 2034.
(165) Hasegawa, Y.; Miyauchi, M.; Takashima, Y.; Yamaguchi, H.; Harada, A. *Macromolecules* **2005**, *38*, 3724.
(166) Kuad, P.; Miyawaki, A.; Takashima, Y.; Yamaguchi, H.; Harada, A. *J. Am. Chem. Soc.* **2007**, *129*, 12630.
(167) Oshovsky, G. V.; Reinhoudt, D. N.; Verboom, W. *Angew. Chem., Int. Ed.* **2007**, *46*, 2366.
(168) Rehm, T.; Schmuck, C. *Chem. Commun.* **2008**, 801.
(169) Schmuck, C. *Tetrahedron* **2001**, *57*, 3063.
(170) Huang, F.; Gibson, H. W. *Chem. Commun.* **2005**, 1696.
(171) Gattuso, G.; Notti, A.; Pappalardo, A.; Parisi, M. F.; Pisagatti, I.; Pappalardo, S.; Garozzo, D.; Messina, A.; Cohen, Y.; Slovak, S. *J. Org. Chem.* **2008**, *73*, 7280.
(172) Pappalardo, S.; Villari, V.; Slovak, S.; Cohen, Y.; Gattuso, G.; Notti, A.; Pappalardo, A.; Pisagatti, I.; Parisi, M. F. *Chem.—Eur. J.* **2007**, *13*, 8164.
(173) Knapp, R.; Schott, A.; Rehahn, M. *Macromolecules* **1996**, *29*, 478.
(174) Schubert, U. S.; Eschbaumer, C. *Macromol. Symp.* **2001**, *163*, 177.
(175) Schubert, U. S.; Eschbaumer, C. *Angew. Chem., Int. Ed.* **2002**, *41*, 2892.
(176) Chen, H.; Cronin, J. A.; Archer, R. D. *Macromolecules* **1994**, *27*, 2174.
(177) Sauvage, J. P.; Collin, J. P.; Chambron, J. C.; Guillerez, S.; Coudret, C.; Balzani, V.; Barigelletti, F.; De Cola, L.; Flamigni, L. *Chem. Rev.* **1994**, *94*, 993.
(178) Paulusse, J. M. J.; Sijbesma, R. P. *Chem. Commun.* **2003**, 1494.
(179) Burnworth, M.; Knapton, D.; Rowan, S.; Weder, C. *J. Inorg. Organomet. Polym. Mater.* **2007**, *17*, 91.
(180) Dobrawa, R.; Würthner, F. *J. Polym. Sci., Part A: Polym. Chem.* **2005**, *43*, 4981.
(181) Velten, U.; Rehahn, M. *Chem. Commun.* **1996**, 2639.
(182) Velten, U.; Lahn, B.; Rehahn, M. *Macromol. Chem. Phys.* **1997**, *198*, 2789.
(183) Yount, W. C.; Juwarker, H.; Craig, S. L. *J. Am. Chem. Soc.* **2003**, *125*, 15302.
(184) Serpe, M. J.; Craig, S. L. *Langmuir* **2007**, *23*, 1626.
(185) Yang, S. K.; Ambade, A. V.; Weck, M. *Chem.—Eur. J.* **2009**, *15*, 6605.
(186) Hill, J. W.; Carothers, W. H. *J. Am. Chem. Soc.* **1933**, *55*, 5031.
(187) Spanagel, E. W.; Carothers, W. H. *J. Am. Chem. Soc.* **1935**, *57*, 935.
(188) Stoll, M.; Rouvé, A.; Stoll-Comte, G. *Helv. Chim. Acta* **1934**, *17*, 1289.
(189) Semlyen, J. A. *Cyclic Polymers*; Kluwer Academic: Dordrecht, The Netherlands, 2000.
(190) Kuchanov, S.; Slot, H.; Stroeks, A. *Prog. Polym. Sci.* **2004**, *29*, 563.
(191) Winnik, M. A. *Chem. Rev.* **1981**, *81*, 491.
(192) Kricheldorf, H. R.; Schwarz, G. *Macromol. Rapid Commun.* **2003**, *24*, 359.
(193) Scott, D. W. *J. Am. Chem. Soc.* **1946**, *68*, 2294.
(194) Brown, J. F.; Slusarczuk, G. M. J. *J. Am. Chem. Soc.* **1965**, *87*, 931.
(195) Carmichael, J. B.; Winger, R. *J. Polym. Sci. Part A: Gen. Pap.* **1965**, *3*, 971.
(196) Flory, P. J.; Semlyen, J. A. *J. Am. Chem. Soc.* **1966**, *88*, 3209.
(197) Hodge, P.; Kamau, S. D. *Angew. Chem., Int. Ed.* **2003**, *42*, 2412.
(198) Gee, G. *Trans. Faraday Soc.* **1952**, *48*, 515.
(199) Tobolsky, A. V.; Eisenberg, A. *J. Am. Chem. Soc.* **1959**, *81*, 780.
(200) Steudel, R.; Mäusle, H.-J.; Rosenbauer, D.; Möckel, H.; Freyholdt, T. *Angew. Chem., Int. Ed. Engl.* **1981**, *20*, 394.
(201) Kuhn, W. *Kolloidn. Zh.* **1934**, *68*, 2.
(202) Flory, P. J. *Statistical Mechanics of Chain Molecules*; Wiley-Interscience: New York, 1969.
(203) Morawetz, H.; Goodman, N. *Macromolecules* **1970**, *3*, 699.
(204) Zhou, H.-X. *J. Phys. Chem. B* **2001**, *105*, 6763.
(205) Zhou, H.-X. *J. Mol. Biol.* **2003**, *329*, 1.
(206) Crothers, D. M.; Metzger, H. *Immunochemistry* **1972**, *9*, 341.
(207) Mandolini, L. *Adv. Phys. Org. Chem.* **1986**, *22*, 1.
(208) Page, M. I.; Jencks, W. P. *Proc. Natl. Acad. Sci. U.S.A.* **1971**, *68*, 1678.
(209) Page, M. I. *Chem. Soc. Rev.* **1972**, *2*, 295.
(210) Ercolani, G.; Mandolini, L.; Mencarelli, P.; Roelens, S. *J. Am. Chem. Soc.* **1993**, *115*, 3901.
(211) Galli, C.; Mandolini, L. *Eur. J. Org. Chem.* **2000**, *2000*, 3117.
(212) Kirby, A. J. *Adv. Phys. Org. Chem.* **1980**, *17*, 183.
(213) Hamacek, J.; Borkovec, M.; Piguet, C. *Dalton Trans.* **2006**, 1473.
(214) Jacobson, H.; Stockmayer, W. H. *J. Chem. Phys.* **1950**, *18*, 1600.
(215) Ercolani, G.; Di Stefano, S. *J. Phys. Chem. B* **2008**, *112*, 4662.
(216) Flory, P. J.; Suter, U. W.; Mutter, M. *J. Am. Chem. Soc.* **1976**, *98*, 5733.
(217) For the case that all cycles are considered to be strainless, the mass-balance equation takes the form

$$C_t = \frac{1}{K_{\text{inter}}}\frac{x}{(1-x)^2} + EM_1\sum_{i=1}^{\infty} i^{-3/2}x^i \qquad (3)$$

in which C_t is the total concentration of monomer, K_{inter} is the intermolecular equilibrium constant, EM_1 is the effective molarity of the monomer, i is the degree of polymerization, and x is the fraction of associated end groups in the chain fraction. Furthermore, the number-averaged degree of polymerization (DP_N) is calculated using eq 4

$$DP_N = \frac{C_t}{\frac{1}{K_{\text{inter}}}\frac{x}{(1-x)} + EM_1\sum_{i=1}^{\infty} i^{-5/2}x^i} \qquad (4)$$

and the weight-averaged degree of polymerization (DP_W) is calculated as

$$DP_W = \frac{\frac{1}{K_{\text{inter}}}\frac{x(1+x)}{(1-x)^3} + EM_1\sum_{i=1}^{\infty} i^{-1/2}x^i}{C_t} \qquad (5)$$

Using a combination of bisection, secant, and inverse quadratic interpolation methods, eq 3 was solved for x at each initial monomer concentration C_t. Instead of evaluating the sum in eq 3 from 1 to infinity, it was evaluated to ring sizes up to 100. For each resulting value of x both the weight-averaged degree of polymerization (DP_W) and the number-averaged degree of polymerization (DP_N) were calculated.
(218) Chan, H. S.; Dill, K. A. *J. Chem. Phys.* **1989**, *90*, 492.
(219) Hiley, B. J.; Sykes, M. F. *J. Chem. Phys.* **1961**, *34*, 1531.
(220) Martin, J. L.; Sykes, M. F.; Hioe, F. T. *J. Chem. Phys.* **1967**, *46*, 3478.
(221) Chen, C.-C.; Dormidontova, E. E. *Macromolecules* **2004**, *37*, 3905.
(222) Harris, R. E. *J. Phys. Chem.* **1970**, *74*, 3102.
(223) Tobolsky, A. V.; Eisenberg, A. *J. Colloid Sci.* **1962**, *17*, 49.
(224) Petschek, R. G.; Pfeuty, P.; Wheeler, J. C. *Phys. Rev. A* **1986**, *34*, 2391.
(225) Wheeler, J. C.; Petschek, R. G.; Pfeuty, P. *Phys. Rev. Lett.* **1983**, *50*, 1633.
(226) Wheeler, J. C.; Kennedy, S. J.; Pfeuty, P. *Phys. Rev. Lett.* **1980**, *45*, 1748.
(227) Hodge, P.; Colquhoun, H. M. *Polym. Adv. Technol.* **2005**, *16*, 84.
(228) ten Cate, A. T.; Kooijman, H.; Spek, A. L.; Sijbesma, R. P.; Meijer, E. W. *J. Am. Chem. Soc.* **2004**, *126*, 3801.
(229) ten Cate, A. T.; Sijbesma, R. P. *Macromol. Rapid Commun.* **2002**, *23*, 1094.
(230) Folmer, B. J. B.; Sijbesma, R. P.; Meijer, E. W. *J. Am. Chem. Soc.* **2001**, *123*, 2093.
(231) Folmer, B. J. B.; Sijbesma, R. P.; Kooijman, H.; Spek, A. L.; Meijer, E. W. *J. Am. Chem. Soc.* **1999**, *121*, 9001.
(232) Lafitte, V. G. H.; Aliev, A. E.; Horton, P. N.; Hursthouse, M. B.; Hailes, H. C. *Chem. Commun.* **2006**, 2173.
(233) Söntjens, S. H. M.; Sijbesma, R. P.; van Genderen, M. H. P.; Meijer, E. W. *Macromolecules* **2001**, *34*, 3815.

(234) Abbel, R.; Grenier, C.; Pouderoijen, M. J.; Stouwdam, J. W.; Leclère, P. E. L. G.; Sijbesma, R. P.; Meijer, E. W.; Schenning, A. P. H. J. *J. Am. Chem. Soc.* **2009**, *131*, 833.
(235) Scherman, O. A.; Ligthart, G. B. W. L.; Sijbesma, R. P.; Meijer, E. W. *Angew. Chem., Int. Ed.* **2006**, *45*, 2072.
(236) Corbin, P. S.; Zimmerman, S. C. *J. Am. Chem. Soc.* **1998**, *120*, 9710.
(237) Wang, X.-Z.; Li, X.-Q.; Shao, X.-B.; Zhao, X.; Deng, P.; Jiang, X.-K.; Li, Z.-T.; Chen, Y.-Q. *Chem.—Eur. J.* **2003**, *9*, 2904.
(238) Ashton, P. R.; Baxter, I.; Cantrill, S. J.; Fyfe, M. C. T.; Glink, P. T.; Stoddart, J. F.; White, A. J. P.; Williams, D. J. *Angew. Chem., Int. Ed.* **1998**, *37*, 1294.
(239) Ashton, P. R.; Parsons, I. W.; Raymo, F. M.; Stoddart, J. F.; White, A. J. P.; Williams, D. J.; Wolf, R. *Angew. Chem., Int. Ed.* **1998**, *37*, 1913.
(240) Cantrill, S. J.; Youn, G. J.; Stoddart, J. F.; Williams, D. J. *J. Org. Chem.* **2001**, *66*, 6857.
(241) Yamaguchi, N.; Gibson, H. W. *Angew. Chem., Int. Ed.* **1999**, *38*, 143.
(242) Gibson, H. W.; Yamaguchi, N.; Jones, J. W. *J. Am. Chem. Soc.* **2003**, *125*, 3522.
(243) Huang, F.; Nagvekar, D. S.; Zhou, X.; Gibson, H. W. *Macromolecules* **2007**, *40*, 3561.
(244) Einstein, A. *Ann. Phys.* **1906**, *324*, 289.
(245) Wang, F.; Han, C.; He, C.; Zhou, Q.; Zhang, J.; Wang, C.; Li, N.; Huang, F. *J. Am. Chem. Soc.* **2008**, *130*, 11254.
(246) Shoji, O.; Okada, S.; Satake, A.; Kobuke, Y. *J. Am. Chem. Soc.* **2005**, *127*, 2201.
(247) Ogawa, K.; Kobuke, Y. *Angew. Chem.* **2000**, *39*, 4070.
(248) Furutsu, D.; Satake, A.; Kobuke, Y. *Inorg. Chem.* **2005**, *44*, 4460.
(249) Takahashi, R.; Kobuke, Y. *J. Am. Chem. Soc.* **2003**, *125*, 2372.
(250) Takahashi, R.; Kobuke, Y. *J. Org. Chem.* **2005**, *70*, 2745.
(251) Fujisawa, K.; Satake, A.; Hirota, S.; Kobuke, Y. *Chem.—Eur. J.* **2008**, *14*, 10735.
(252) Michelsen, U.; Hunter, C. A. *Angew. Chem., Int. Ed.* **2000**, *39*, 764.
(253) Haycock, R. A.; Hunter, C. A.; James, D. A.; Michelsen, U.; Sutton, L. R. *Org. Lett.* **2000**, *2*, 2435.
(254) Paulusse, J. M. J.; Huijbers, J. P. J.; Sijbesma, R. P. *Macromolecules* **2005**, *38*, 6290.
(255) Abed, S.; Boileau, S.; Bouteiller, L. *Macromolecules* **2000**, *33*, 8479.
(256) Ohga, K.; Takashima, Y.; Takahashi, H.; Kawaguchi, Y.; Yamaguchi, H.; Harada, A. *Macromolecules* **2005**, *38*, 5897.
(257) Fernández, G.; Pérez, E. M.; Sánchez, L.; Martín, N. *Angew. Chem., Int. Ed.* **2008**, *47*, 1094.
(258) Xu, J.; Fogleman, E. A.; Craig, S. L. *Macromolecules* **2004**, *37*, 1863.
(259) Fogleman, E. A.; Yount, W. C.; Xu, J.; Craig, S. L. *Angew. Chem., Int. Ed.* **2002**, *41*, 4026.
(260) Bielejewska, A. G.; Marjo, C. E.; Prins, L. J.; Timmerman, P.; de Jong, F.; Reinhoudt, D. N. *J. Am. Chem. Soc.* **2001**, *123*, 7518.
(261) Zerkowski, J. A.; Seto, C. T.; Whitesides, G. M. *J. Am. Chem. Soc.* **1992**, *114*, 5473.
(262) Mathias, J. P.; Simanek, E. E.; Zerkowski, J. A.; Seto, C. T.; Whitesides, G. M. *J. Am. Chem. Soc.* **1994**, *116*, 4316.
(263) Seto, C. T.; Whitesides, G. M. *J. Am. Chem. Soc.* **1993**, *115*, 1330.
(264) Ducharme, Y.; Wuest, J. D. *J. Org. Chem.* **1988**, *53*, 5787.
(265) Prins, L. J.; Reinhoudt, D. N.; Timmerman, P. *Angew. Chem., Int. Ed.* **2001**, *40*, 2382.
(266) Sijbesma, R. P.; Meijer, E. W. *Curr. Opin. Colloid Interface Sci.* **1999**, *4*, 24.
(267) Hunter, C. A.; Tomas, S. *J. Am. Chem. Soc.* **2006**, *128*, 8975.
(268) Ferrone, F.; Ronald, W. Analysis of protein aggregation kinetics. In *Methods of Enzymology*; Academic Press: New York, 1999; Vol. 309, pp 256.
(269) Kashchiev, D. *Nucleation: Basic Theory with Applications*; Butterworth-Heinemann: Oxford, U.K., 2000.
(270) Wolffs, M.; Korevaar, P. A.; Jonkheijm, P.; Henze, O.; Feast, W. J.; Schenning, A. P. H. J.; Meijer, E. W. *Chem. Commun.* **2008**, 4613.
(271) Cabaleiro-Lago, C.; Quinlan-Pluck, F.; Lynch, I.; Lindman, S.; Minogue, A. M.; Thulin, E.; Walsh, D. M.; Dawson, K. A.; Linse, S. *J. Am. Chem. Soc.* **2008**, *130*, 15437.
(272) Linse, S.; Cabaleiro-Lago, C.; Xue, W.-F.; Lynch, I.; Lindman, S.; Thulin, E.; Radford, S. E.; Dawson, K. A. *Proc. Natl. Acad. Sci. U.S.A.* **2007**, *104*, 8691.
(273) Rogers, S. S.; Krebs, M. R. H.; Bromley, E. H. C.; van der Linden, E.; Donald, A. M. *Biophys. J.* **2006**, *90*, 1043.
(274) Ferrone, F. A.; Hofrichter, J.; Sunshine, H. R.; Eaton, W. A. *Biophys. J.* **1980**, *32*, 361.
(275) Ferrone, F. A.; Hofrichter, J.; Eaton, W. A. *J. Mol. Biol.* **1985**, *183*, 591.
(276) Ferrone, F. A.; Hofrichter, J.; Eaton, W. A. *J. Mol. Biol.* **1985**, *183*, 611.
(277) Cao, Z.; Ferrone, F. A. *J. Mol. Biol.* **1996**, *256*, 219.
(278) Padrick, S. B.; Miranker, A. D. *Biochemistry* **2002**, *41*, 4694.
(279) Xue, W.-F.; Homans, S. W.; Radford, S. E. *Proc. Natl. Acad. Sci. U.S.A.* **2008**, *105*, 8926.
(280) Frieden, C. *Protein Sci.* **2007**, *16*, 2334.
(281) This mechanism is equal to the exponential growth mechanism as proposed by Dill: De Young, L. R.; Fink, A. L.; Dill, K. A. *Acc. Chem. Res.* **1993**, *26*, 614.
(282) Powers, E. T.; Powers, D. L. *Biophys. J.* **2006**, *91*, 122.
(283) Firestone, M. P.; De Levie, R.; Rangarajan, S. K. *J. Theor. Biol.* **1983**, *104*, 535.
(284) Mukerjee, P. *Adv. Colloid Interface Sci.* **1967**, *1*, 242.
(285) Mukerjee, P.; Mysels, K.; Kapauan, P. *J. Phys. Chem.* **1967**, *71*, 4166.
(286) Mukerjee, P. *J. Phys. Chem.* **1969**, *73*, 2054.
(287) Mukerjee, P. *J. Pharm. Sci.* **1974**, *63*, 972.
(288) Tanford, C. *J. Phys. Chem.* **1974**, *78*, 2469.
(289) Tanford, C. *The Hydrophobic Effect: Formation of Micelles and Biological Membranes*, 2nd ed.; Wiley-Interscience: London, U.K., 2000.
(290) Yokozawa, T.; Asai, T.; Sugi, R.; Ishigooka, S.; Hiraoka, S. *J. Am. Chem. Soc.* **2000**, *122*, 8313.
(291) Yokozawa, T.; Yokoyama, A. *Prog. Polym. Sci.* **2007**, *32*, 147.
(292) Yokoyama, A.; Yokozawa, T. *Macromolecules* **2007**, *40*, 4093.
(293) Metselaar, G. A.; Cornelissen, J. J. L. M.; Rowan, A. E.; Nolte, R. J. M. *Angew. Chem., Int. Ed.* **2005**, *44*, 1990.
(294) Nakano, T.; Okamoto, Y.; Hatada, K. *J. Am. Chem. Soc.* **1992**, *114*, 1318.
(295) Iwakura, Y.; Uno, K.; Oya, M. *J. Polym. Sci., Part A: Polym. Chem.* **1967**, *5*, 2867.
(296) Komoto, T.; Akaishi, T.; Oya, M.; Kawai, T. *Makromol. Chem.* **1972**, *154*, 151.
(297) Edelstein-Keshet, L.; Ermentrout, G. B. *Bull. Math. Biol.* **1998**, *60*, 449.
(298) Goldstein, R. F.; Stryer, L. *Biophys. J.* **1986**, *50*, 583.

(299) As shown by Goldstein and Stryer,[298] the mass balance equation for a nucleation−elongation supramolecular polymerization according to Scheme 7 is

$$\alpha_t = \sum_{i=1}^{s} i\sigma^{i-1}\alpha_1^i + \sum_{i=s+1}^{\infty} i\sigma^{s-1}\alpha_1^i = \frac{s\alpha_1^s\sigma^{s-1}}{1-\alpha_1} + \frac{\alpha_1^{s+1}\sigma^{s-1}}{(1-\alpha_1)^2} + \frac{\alpha_1(s(\sigma\alpha_1)^{s-1}-1)}{\sigma\alpha_1 - 1} - \frac{\sigma\alpha_1^2((\sigma\alpha_1)^{s-1}-1)}{(\sigma\alpha_1-1)^2} \quad (6)$$

in which α_t represents the dimensionless total concentration KC_t, α_1 represents the dimensionless equilibrium monomer concentration KM_1, σ represents cooperativity parameter (defined as K_n/K), and s is the size of the nucleus. The weight-averaged degree of polymerization is defined as

$$DP_W = \frac{\sum_{i=1}^{\infty} i^2\alpha_i}{\alpha_t} = \frac{\sum_{i=1}^{s} i^2\sigma^{i-1}\alpha_1^i + \sum_{i=s+1}^{\infty} i^2\sigma^{s-1}\alpha_1^i}{\alpha_t} \quad (7)$$

The two sums in the nominator of this expression can be evaluated using standard expressions for infinite converging series, which results in the following expressions:

$$\sum_{i=1}^{s} i^2\sigma^{i-1}\alpha_1^i = [(\sigma\alpha_1)^{s+1}(-2(s+1)\sigma^2\alpha_1^2 + 2(s+1)\sigma\alpha_1 + \sigma^2\alpha_1^2 + \sigma\alpha_1 + (s+1)^2\sigma^2\alpha_1^2 - 2(s+1)^2\sigma\alpha_1 + (s+1)^2)]/[\sigma(\sigma\alpha_1-1)^3] - \frac{\alpha_1(\sigma\alpha_1+1)}{(\sigma\alpha_1-1)^3} \quad (8)$$

$$\sum_{i=s+1}^{\infty} i^2\sigma^{s-1}\alpha_1^i = -\frac{\sigma^{s-1}\alpha^{s+1}((\alpha-1)^2s^2 + (2-2\alpha)s + 1 + \alpha)}{(\alpha-1)^3} \quad (9)$$

In a similar fashion, the number-averaged degree of polymerization is defined as

$$DP_N = \frac{\alpha_t}{\sum_{i=1}^{\infty} \alpha_i} = \frac{\alpha_t}{\sum_{i=1}^{s} \sigma^{i-1}\alpha_1^i + \sum_{i=s+1}^{\infty} \sigma^{s-1}\alpha_1^i} \quad (10)$$

The two sums in the denominator of this expression can be evaluated using standard expressions for infinite converging series, which results in the following expressions:

$$\sum_{i=1}^{s} \sigma^{i-1}\alpha_1^i = \frac{(\sigma\alpha)^{s+1}}{\sigma(\sigma\alpha - 1)} - \frac{\alpha}{\sigma\alpha - 1} \quad (11)$$

$$\sum_{i=s+1}^{\infty} \sigma^{s-1}\alpha_1^i = -\frac{\sigma^{s-1}\alpha^{s+1}}{\alpha - 1} \quad (12)$$

Finally, the polydispersity index at equilibrium (PDI) is defined as the ratio of eq 7 (DP_W) and eq 10 (DP_N).

(300) van der Schoot, P. *Macromolecules* **2002**, *35*, 2845.
(301) van Jaarsveld, J.; van der Schoot, P. *Macromolecules* **2007**, *40*, 2177.
(302) Hall, D.; Minton, A. P. *Biophys. Chem.* **2002**, *98*, 93.
(303) Oosawa, F.; Kasai, M. *J. Mol. Biol.* **1962**, *4*, 10.
(304) Oosawa, F.; Asakura, S. *Thermodynamics of the Polymerization of Protein*; Academic Press: London, U.K., 1975.
(305) Frieden, C.; Goddette, D. W. *Biochemistry* **1983**, *22*, 5836.
(306) Frieden, C. *Annu. Rev. Biophys. Biophys. Chem.* **1985**, *14*, 189.
(307) Kadler, K. E.; Hojima, Y.; Prockop, D. J. *J. Biol. Chem.* **1987**, *262*, 15696.
(308) Kadler, K. E.; Hojima, Y.; Prockop, D. J. *J. Biol. Chem.* **1988**, *263*, 10517.
(309) Friedhoff, P.; Schneider, A.; Mandelkow, E.-M.; Mandelkow, E. *Biochemistry* **1998**, *37*, 10223.
(310) Karr, T. L.; Purich, D. L. *Biochem. Biophys. Res. Commun.* **1980**, *95*, 1885.
(311) Shalaby, R. A.; Lauffer, M. A. *Arch. Biochem. Biophys.* **1985**, *236*, 390.
(312) Kardos, J.; Yamamoto, K.; Hasegawa, K.; Naiki, H.; Goto, Y. *J. Biol. Chem.* **2004**, *279*, 55308.
(313) Murayama, M. *Adv. Exp. Med. Biol.* **1972**, *28*, 243.
(314) Blokzijl, W.; Engberts, J. B. F. N. *Angew. Chem., Int. Ed. Engl.* **1993**, *32*, 1545.
(315) Southall, N. T.; Dill, K. A.; Haymet, A. D. J. *J. Phys. Chem. B* **2002**, *106*, 521.
(316) Anslyn, E. V.; Dougherty, D. A. *Modern Physical Organic Chemistry*; University Science: 2006.
(317) Smith, D. E.; Haymet, A. D. J. *J. Chem. Phys.* **1993**, *98*, 6445.
(318) Wu, J.; Prausnitz, J. M. *Proc. Natl. Acad. Sci. U.S.A.* **2008**, *105*, 9512.
(319) Marenduzzo, D.; Finan, K.; Cook, P. R. *J. Cell Biol.* **2006**, *175*, 681.
(320) Asakura, S.; Oosawa, F. *J. Polym. Sci.* **1958**, *33*, 183.
(321) Snir, Y.; Kamien, R. D. *Science* **2005**, *307*, 1067.
(322) ten Brinke, G.; Frank, E. K. *J. Chem. Phys.* **1983**, *79*, 2065.
(323) Pfeuty, P. M.; Wheeler, J. C. *Phys. Rev. A* **1983**, *27*, 2178.
(324) Jonkheijm, P.; van der Schoot, P.; Schenning, A. P. H. J.; Meijer, E. W. *Science* **2006**, *313*, 80.
(325) Smulders, M. M. J.; Schenning, A. P. H. J.; Meijer, E. W. *J. Am. Chem. Soc.* **2008**, *130*, 606.
(326) Rougee, M.; Faucon, B.; Mergny, J. L.; Barcelo, F.; Giovannangeli, C.; Garestier, T.; Helene, C. *Biochemistry* **1992**, *31*, 9269.
(327) Cantú, L.; Corti, M.; Del Favero, E.; Muller, E.; Raudino, A.; Sonnino, S. *Langmuir* **1999**, *15*, 4975.
(328) Singh, S.; Zlotnick, A. *J. Biol. Chem.* **2003**, *278*, 18249.
(329) Hagan, M. F.; Chandler, D. *Biophys. J.* **2006**, *91*, 42.
(330) van der Schoot, P.; Zandi, R. *Phys. Biol.* **2007**, *4*, 296.
(331) Schulman, R.; Winfree, E. *Proc. Natl. Acad. Sci. U.S.A.* **2007**, *104*, 15236.
(332) Yin, P.; Hariadi, R. F.; Sahu, S.; Choi, H. M. T.; Park, S. H.; LaBean, T. H.; Reif, J. H. *Science* **2008**, *321*, 824.
(333) Huisman, B. A. H.; Bolhuis, P. G.; Fasolino, A. *Phys. Rev. Lett.* **2008**, *100*, 188301.
(334) Chatelier, R. C. *Biophys. Chem.* **1987**, *28*, 121.
(335) Hannah, K. C.; Armitage, B. A. *Acc. Chem. Res.* **2004**, *37*, 845.
(336) Seifert, J. L.; Connor, R. E.; Kushon, S. A.; Wang, M.; Armitage, B. A. *J. Am. Chem. Soc.* **1999**, *121*, 2987.
(337) Miyagawa, T.; Yamamoto, M.; Muraki, R.; Onouchi, H.; Yashima, E. *J. Am. Chem. Soc.* **2007**, *129*, 3676.
(338) Janssen, P. G. A.; Jabbari-Farouji, S.; Surin, M.; Vila, X.; Gielen, J. C.; de Greef, T. F. A.; Vos, M. R. J.; Bomans, P. H. H.; Sommerdijk, N. A. J. M.; Christianen, P. C. M.; Leclère, P.; Lazzaroni, R.; van der Schoot, P.; Meijer, E. W.; Schenning, A. P. H. J. *J. Am. Chem. Soc.* **2009**, *131*, 1222.
(339) Janssen, P. G. A.; Vandenbergh, J.; vanDongen, J. L. J.; Meijer, E. W.; Schenning, A. P. H. J. *J. Am. Chem. Soc.* **2007**, *129*, 6078.
(340) Nagarajan, R.; Ruckenstein, E. *Langmuir* **1991**, *7*, 2934.
(341) Ben-Naim, A.; Stillinger, F. H. *J. Phys. Chem.* **1980**, *84*, 2872.
(342) Tanford, C. *Proc. Natl. Acad. Sci. U.S.A.* **1974**, *71*, 1811.
(343) Everett, D. H. *Colloids Surf.* **1986**, *21*, 41.
(344) Davies, M.; Thomas, D. K. *J. Phys. Chem.* **1956**, *60*, 763.
(345) Davies, M.; Thomas, D. K. *J. Phys. Chem.* **1956**, *60*, 767.
(346) LaPlanche, L. A.; Thompson, H. B.; Rogers, M. T. *J. Phys. Chem.* **1965**, *69*, 1482.
(347) Pralat, K.; Jadzyn, J.; Balanicka, S. *J. Phys. Chem.* **1983**, *87*, 1385.
(348) Akiyama, M.; Ohtani, T. *Spectrochim. Acta, Part A* **1994**, *50*, 317.
(349) Regan, D. G.; Chapman, B. E.; Kuchel, P. W. *Magn. Reson. Chem.* **2002**, *40*, S115.
(350) Jadzyn, J.; Stockhausen, M.; Zywucki, B. *J. Phys. Chem.* **1987**, *91*, 754.
(351) Saroléa-Mathot, L. *Trans. Faraday Soc.* **1953**, *49*, 8.
(352) Dannenberg, J. J.; Haskamp, L.; Masunov, A. *J. Phys. Chem. A* **1999**, *103*, 7083.
(353) Masunov, A.; Dannenberg, J. J. *J. Phys. Chem. B* **2000**, *104*, 806.
(354) Kobko, N.; Paraskevas, L.; del Rio, E.; Dannenberg, J. J. *J. Am. Chem. Soc.* **2001**, *123*, 4348.
(355) Kobko, N.; Dannenberg, J. J. *J. Phys. Chem. A* **2003**, *107*, 10389.
(356) Gilli, G.; Bellucci, F.; Ferretti, V.; Bertolasi, V. *J. Am. Chem. Soc.* **1989**, *111*, 1023.
(357) Bertolasi, V.; Gilli, P.; Ferretti, V.; Gilli, G. *J. Am. Chem. Soc.* **1991**, *113*, 4917.
(358) Morozov, A. V.; Tsemekhman, K.; Baker, D. *J. Phys. Chem. B* **2006**, *110*, 4503.
(359) Suh, S. B.; Kim, J. C.; Choi, Y. C.; Yun, S.; Kim, K. S. *J. Am. Chem. Soc.* **2004**, *126*, 2186.
(360) Timasheff, S. N.; Frigon, R. P.; Lee, J. C. *Fed. Proc.* **1976**, *35*, 1886.
(361) Sept, D.; McCammon, J. A. *Biophys. J.* **2001**, *81*, 667.
(362) Wegner, A.; Engel, J. *Biophys. Chem.* **1975**, *3*, 215.
(363) Flyvbjerg, H.; Jobs, E.; Leibler, S. *Proc. Natl. Acad. Sci. U.S.A.* **1996**, *93*, 5975.
(364) Erickson, H. P.; Pantaloni, D. *Biophys. J.* **1981**, *34*, 293.
(365) Caspar, D. L. *Biophys. J.* **1980**, *32*, 103.
(366) Miraldi, E. R.; Thomas, P. J.; Romberg, L. *Biophys. J.* **2008**, *95*, 2470.
(367) Huecas, S.; Llorca, O.; Boskovic, J.; Martín-Benito, J.; Valpuesta, J. M.; Andreu, J. M. *Biophys. J.* **2008**, *94*, 1796.
(368) Levy, Y.; Onuchic, J. N. *Annu. Rev. Biophys. Biomol. Struct.* **2006**, *35*, 389.
(369) Ryu, J.-H.; Hong, D.-J.; Lee, M. *Chem. Commun.* **2008**, 1043.
(370) Chandler, D. *Nature* **2005**, *437*, 640.
(371) Wood, R. H.; Thompson, P. T. *Proc. Natl. Acad. Sci. U. S. A.* **1990**, *87*, 946.
(372) Raschke, T. M.; Tsai, J.; Levitt, M. *Proc. Natl. Acad. Sci. U.S.A.* **2001**, *98*, 5965.
(373) Moghaddam, M. S.; Shimizu, S.; Chan, H. S. *J. Am. Chem. Soc.* **2005**, *127*, 303.
(374) Czaplewski, C.; Rodziewicz-Motowidlo, S.; Dabal, M.; Liwo, A.; Ripoll, D. R.; Scheraga, H. A. *Biophys. Chem.* **2003**, *105*, 339.
(375) Lum, K.; Chandler, D.; Weeks, J. D. *J. Phys. Chem. B* **1999**, *103*, 4570.
(376) Hills, R. D., Jr.; Brooks, C. L., III *J. Mol. Biol.* **2007**, *368*, 894.
(377) Boileau, S.; Bouteiller, L.; Lauprêtre, F.; Lortie, F. *New J. Chem.* **2000**, *24*, 845.
(378) Lortie, F.; Boileau, S.; Bouteiller, L.; Chassenieux, C.; Deme, B.; Ducouret, G.; Jalabert, M.; Lauprêtre, F.; Terech, P. *Langmuir* **2002**, *18*, 7218.
(379) Simic, V.; Bouteiller, L.; Jalabert, M. *J. Am. Chem. Soc.* **2003**, *125*, 13148.
(380) Lortie, F.; Boileau, S.; Bouteiller, L. *Chem.—Eur. J.* **2003**, *9*, 3008.
(381) Arnaud, A.; Bouteiller, L. *Langmuir* **2004**, *20*, 6858.
(382) Lortie, F.; Boileau, S.; Bouteiller, L.; Chassenieux, C.; Lauprêtre, F. *Macromolecules* **2005**, *38*, 5283.
(383) Bouteiller, L.; Colombani, O.; Lortie, F.; Terech, P. *J. Am. Chem. Soc.* **2005**, *127*, 8893.
(384) Pinault, T.; Isare, B.; Bouteiller, L. *ChemPhysChem* **2006**, *7*, 816.
(385) Bellot, M.; Bouteiller, L. *Langmuir* **2008**, *24*, 14176.
(386) Yagai, S.; Kubota, S.; Iwashima, T.; Kishikawa, K.; Nakanishi, T.; Karatsu, T.; Kitamura, A. *Chem.—Eur. J.* **2008**, *14*, 5246.
(387) Yang, J.; Dewal, M. B.; Sobransingh, D.; Smith, M. D.; Xu, Y.; Shimizu, L. S. *J. Org. Chem.* **2009**, *74*, 102.
(388) de Loos, M.; van Esch, J.; Kellogg, R. M.; Feringa, B. L. *Angew. Chem., Int. Ed. Engl.* **2001**, *40*, 613.
(389) Brunsveld, L.; Schenning, A. P. H. J.; Broeren, M. A. C.; Janssen, H. M.; Vekemans, J. A. J. M.; Meijer, E. W. *Chem. Lett.* **2000**, 292.

(390) Wilson, A. J.; Masuda, M.; Sijbesma, R. P.; Meijer, E. W. *Angew. Chem., Int. Ed.* **2005**, *44*, 2275.
(391) Lightfoot, M. P.; Mair, F. S.; Pritchard, R. G.; Warren, J. E. *Chem. Commun.* **1999**, 1945.
(392) Sakamoto, A.; Ogata, D.; Shikata, T.; Urakawa, O.; Hanabusa, K. *Polymer* **2006**, *47*, 956.
(393) Rochefort, A.; Bayard, É.; Hadj-Messaoud, S. *Adv. Mater.* **2007**, *19*, 1992.
(394) Nguyen, T.-Q.; Martel, R.; Bushey, M.; Avouris, P.; Carlsen, A.; Nuckolls, C.; Brus, L. *Phys. Chem. Chem. Phys.* **2007**, *9*, 1515.
(395) Nguyen, T.-Q.; Martel, R.; Avouris, P.; Bushey, M. L.; Brus, L.; Nuckolls, C. *J. Am. Chem. Soc.* **2004**, *126*, 5234.
(396) Bushey, M. L.; Nguyen, T.-Q.; Zhang, W.; Horoszewski, D.; Nuckolls, C. *Angew. Chem., Int. Ed. Engl.* **2004**, *43*, 5446.
(397) Bushey, M. L.; Nguyen, T.-Q.; Nuckolls, C. *J. Am. Chem. Soc.* **2003**, *125*, 8264.
(398) Nguyen, T.-Q.; Bushey, M. L.; Brus, L. E.; Nuckolls, C. *J. Am. Chem. Soc.* **2002**, *124*, 15051.
(399) Bushey, M. L.; Hwang, A.; Stephens, P. W.; Nuckolls, C. *Angew. Chem., Int. Ed.* **2002**, *41*, 2828.
(400) Bushey, M. L.; Hwang, A.; Stephens, P. W.; Nuckolls, C. *J. Am. Chem. Soc.* **2001**, *123*, 8157.
(401) Ghadiri, M. R.; Granja, J. R.; Milligan, R. A.; McRee, D. E.; Khazanovich, N. *Nature* **1993**, *366*, 324.
(402) Ghadiri, M. R.; Granja, J. R.; Buehler, L. K. *Nature* **1994**, *369*, 301.
(403) Khazanovich, N.; Granja, J. R.; McRee, D. E.; Milligan, R. A.; Ghadiri, M. R. *J. Am. Chem. Soc.* **1994**, *116*, 6011.
(404) Engels, M.; Bashford, D.; Ghadiri, M. R. *J. Am. Chem. Soc.* **1995**, *117*, 9151.
(405) Ghadiri, M. R.; Kobayashi, K.; Granja, J. R.; Chadha, R. K.; McRee, D. E. *Angew. Chem., Int. Ed. Engl.* **1995**, *34*, 93.
(406) Hartgerink, J. D.; Granja, J. R.; Milligan, R. A.; Ghadiri, M. R. *J. Am. Chem. Soc.* **1996**, *118*, 43.
(407) Clark, T. D.; Buehler, L. K.; Ghadiri, M. R. *J. Am. Chem. Soc.* **1998**, *120*, 651.
(408) Clark, T. D.; Buriak, J. M.; Kobayashi, K.; Isler, M. P.; McRee, D. E.; Ghadiri, M. R. *J. Am. Chem. Soc.* **1998**, *120*, 8949.
(409) Hartgerink, J. D.; Clark, T. D.; Ghadiri, M. R. *Chem.—Eur. J.* **1998**, *4*, 1367.
(410) Bong, D. T.; Clark, T. D.; Granja, J. R.; Ghadiri, M. R. *Angew. Chem., Int. Ed.* **2001**, *40*, 988.
(411) Kortemme, T.; Ramírez-Alvarado, M.; Serrano, L. *Science* **1998**, *281*, 253.
(412) Schenck, H. L.; Gellman, S. H. *J. Am. Chem. Soc.* **1998**, *120*, 4869.
(413) Rossmeisl, J.; Norskov, J. K.; Jacobsen, K. W. *J. Am. Chem. Soc.* **2004**, *126*, 13140.
(414) Horne, W. S.; Stout, C. D.; Ghadiri, M. R. *J. Am. Chem. Soc.* **2003**, *125*, 9372.
(415) Hirst, A. R.; Coates, I. A.; Boucheteau, T. R.; Miravet, J. F.; Escuder, B.; Castelletto, V.; Hamley, I. W.; Smith, D. K. *J. Am. Chem. Soc.* **2008**, *130*, 9113.
(416) Würthner, F.; Yao, S.; Beginn, U. *Angew. Chem., Int. Ed.* **2003**, *42*, 3247.
(417) Yao, S.; Beginn, U.; Gress, T.; Lysetska, M.; Würthner, F. *J. Am. Chem. Soc.* **2004**, *126*, 8336.
(418) Lohr, A.; Lysetska, M.; Würthner, F. *Angew. Chem., Int. Ed.* **2005**, *44*, 5071.
(419) Lohr, A.; Würthner, F. *Chem. Commun.* **2008**, 2227.
(420) Lohr, A.; Würthner, F. *Angew. Chem., Int. Ed.* **2008**, *47*, 1232.
(421) Ikeda, M.; Nobori, T.; Schmutz, M.; Lehn, J.-M. *Chem.—Eur. J.* **2005**, *11*, 662.
(422) Schenning, A. P. H. J.; Jonkheijm, P.; Peeters, E.; Meijer, E. W. *J. Am. Chem. Soc.* **2001**, *123*, 409.
(423) Jonkheijm, P.; Hoeben, F. J. M.; Kleppinger, R.; van Herrikhuyzen, J.; Schenning, A. P. H. J.; Meijer, E. W. *J. Am. Chem. Soc.* **2003**, *125*, 15941.
(424) Gesquiere, A.; Jonkheijm, P.; Hoeben, F. J. M.; Schenning, A. P. H. J.; De Feyter, S.; De Schryver, F. C.; Meijer, E. W. *Nano Lett.* **2004**, *4*, 1175.
(425) Beljonne, D.; Hennebicq, E.; Daniel, C.; Herz, L. M.; Silva, C.; Scholes, G. D.; Hoeben, F. J. M.; Jonkheijm, P.; Schenning, A. P. H. J.; Meskers, S. C. J.; Phillips, R. T.; Friend, R. H.; Meijer, E. W. *J. Phys. Chem. B* **2005**, *109*, 10594.
(426) Hirschberg, J. H. K. K.; Brunsveld, L.; Ramzi, A.; Vekemans, J. A. J. M.; Sijbesma, R. P.; Meijer, E. W. *Nature* **2000**, *407*, 167.
(427) Brunsveld, L.; Vekemans, J. A. J. M.; Hirschberg, J. H. K. K.; Sijbesma, R. P.; Meijer, E. W. *Proc. Natl. Acad. Sci. U.S.A.* **2002**, *99*, 4977.
(428) Tomović, Ž.; van Dongen, J.; George, S. J.; Xu, H.; Pisula, W.; Leclère, P.; Smulders, M. M. J.; DeFeyter, S.; Meijer, E. W.; Schenning, A. P. H. J. *J. Am. Chem. Soc.* **2007**, *129*, 16190.
(429) Jonkheijm, P.; Miura, A.; Zdanowska, M.; Hoeben, F. J. M.; De Feyter, S.; Schenning, A. P. H. J.; De Schryver, F. C.; Meijer, E. W. *Angew. Chem., Int. Ed.* **2004**, *43*, 74.
(430) Apperloo, J. J.; Janssen, R. A. J.; Malenfant, P. R. L.; Fréchet, J. M. J. *Macromolecules* **2000**, *33*, 7038.
(431) Kaiser, T. E.; Stepanenko, V.; Würthner, F. *J. Am. Chem. Soc.* **2009**, *131*, 6719.
(432) Hill, J. P.; Jin, W.; Kosaka, A.; Fukushima, T.; Ichihara, H.; Shimomura, T.; Ito, K.; Hashizume, T.; Ishii, N.; Aida, T. *Science* **2004**, *304*, 1481.
(433) Motoyanagi, J.; Fukushima, T.; Kosaka, A.; Ishii, N.; Aida, T. *J. Polym. Sci., Part A: Polym. Chem.* **2006**, *44*, 5120.
(434) Motoyanagi, J.; Fukushima, T.; Ishii, N.; Aida, T. *J. Am. Chem. Soc.* **2006**, *128*, 4220.
(435) Jin, W.; Fukushima, T.; Kosaka, A.; Niki, M.; Ishii, N.; Aida, T. *J. Am. Chem. Soc.* **2005**, *127*, 8284.
(436) Yamamoto, T.; Fukushima, T.; Yamamoto, Y.; Kosaka, A.; Jin, W.; Ishii, N.; Aida, T. *J. Am. Chem. Soc.* **2006**, *128*, 14337.
(437) Jin, W.; Yamamoto, Y.; Fukushima, T.; Ishii, N.; Kim, J.; Kato, K.; Takata, M.; Aida, T. *J. Am. Chem. Soc.* **2008**, *130*, 9434.
(438) van Hameren, R.; Schön, P.; van Buul, A. M.; Hoogboom, J.; Lazarenko, S. V.; Gerritsen, J. W.; Engelkamp, H.; Christianen, P. C. M.; Heus, H. A.; Maan, J. C.; Rasing, T.; Speller, S.; Rowan, A. E.; Elemans, J. A. A. W.; Nolte, R. J. M. *Science* **2006**, *314*, 1433.
(439) van Hameren, R.; van Buul, A. M.; Castriciano, M. A.; Villari, V.; Micali, N.; Schon, P.; Speller, S.; Monsù Scolaro, L.; Rowan, A. E.; Elemans, J. A. A. W.; Nolte, R. J. M. *Nano Lett.* **2008**, *8*, 253.
(440) Ajayaghosh, A.; Praveen, V. K. *Acc. Chem. Res.* **2007**, *40*, 644.
(441) Praveen, V. K.; Babu, S. S.; Vijayakumar, C.; Varghese, R.; Ajayaghosh, A. *Bull. Chem. Soc. Jpn.* **2008**, *81*, 1196.
(442) Ajayaghosh, A.; Vijayakumar, C.; Varghese, R.; George, S. J. *Angew. Chem., Int. Ed. Engl.* **2006**, *45*, 456.
(443) Ajayaghosh, A.; Varghese, R.; Praveen, V. K.; Mahesh, S. *Angew. Chem., Int. Ed.* **2006**, *45*, 3261.
(444) Smith, A. M.; Banwell, E. F.; Edwards, W. R.; Pandya, M. J.; Woolfson, D. N. *Adv. Funct. Mater.* **2006**, *16*, 1022.
(445) Dong, H.; Paramonov, S. E.; Hartgerink, J. D. *J. Am. Chem. Soc.* **2008**, *130*, 13691.
(446) Pandya, M. J.; Spooner, G. M.; Sunde, M.; Thorpe, J. R.; Rodger, A.; Woolfson, D. N. *Biochemistry* **2000**, *39*, 8728.
(447) Alber, T. *Curr. Opin. Genet. Dev.* **1992**, *2*, 205.
(448) Cohen, C.; Parry, D. A. D. *Proteins: Struct., Funct., Genet.* **1990**, *7*, 1.
(449) Ryadnov, M. G.; Woolfson, D. N. *Nat. Mater.* **2003**, *2*, 329.
(450) Ryadnov, M. G.; Woolfson, D. N. *Angew. Chem., Int. Ed.* **2003**, *42*, 3021.
(451) Ryadnov, M. G.; Woolfson, D. N. *J. Am. Chem. Soc.* **2005**, *127*, 12407.
(452) Dong, H.; Paramonov, S. E.; Hartgerink, J. D. *J. Am. Chem. Soc.* **2008**, *130*, 13691.
(453) Peterca, M.; Percec, V.; Imam, M. R.; Leowanawat, P.; Morimitsu, K.; Heiney, P. A. *J. Am. Chem. Soc.* **2008**, *130*, 14840.
(454) Percec, V.; Imam, M. R.; Peterca, M.; Wilson, D. A.; Heiney, P. A. *J. Am. Chem. Soc.* **2009**, *131*, 1294.
(455) Percec, V.; Dulcey, A. E.; Peterca, M.; Ilies, M.; Sienkowska, M. J.; Heiney, P. A. *J. Am. Chem. Soc.* **2005**, *127*, 17902.
(456) Percec, V.; Dulcey, A. E.; Peterca, M.; Ilies, M.; Ladislaw, J.; Rosen, B. M.; Edlund, U.; Heiney, P. A. *Angew. Chem., Int. Ed.* **2005**, *44*, 6516.
(457) Percec, V.; Dulcey, A. E.; Peterca, M.; Ilies, M.; Nummelin, S.; Sienkowska, M. J.; Heiney, P. A. *Proc. Natl. Acad. Sci. U.S.A.* **2006**, *103*, 2518.
(458) Kaucher, M. S.; Peterca, M.; Dulcey, A. E.; Kim, A. J.; Vinogradov, S. A.; Hammer, D. A.; Heiney, P. A.; Percec, V. *J. Am. Chem. Soc.* **2007**, *129*, 11698.
(459) Percec, V.; Dulcey, A. E.; Peterca, M.; Adelman, P.; Samant, R.; Balagurusamy, V. S. K.; Heiney, P. A. *J. Am. Chem. Soc.* **2007**, *129*, 5992.
(460) Fenniri, H.; Mathivanan, P.; Vidale, K. L.; Sherman, D. M.; Hallenga, K.; Wood, K. V.; Stowell, J. G. *J. Am. Chem. Soc.* **2001**, *123*, 3854.
(461) Fenniri, H.; Deng, B.-L.; Ribbe, A. E.; Hallenga, K.; Jacob, J.; Thiyagarajan, P. *Proc. Natl. Acad. Sci. U.S.A.* **2002**, *99*, 6487.
(462) Fenniri, H.; Deng, B.-L.; Ribbe, A. E. *J. Am. Chem. Soc.* **2002**, *124*, 11064.
(463) Johnson, R. S.; Yamazaki, T.; Kovalenko, A.; Fenniri, H. *J. Am. Chem. Soc.* **2007**, *129*, 5735.
(464) Moralez, J. G.; Raez, J.; Yamazaki, T.; Motkuri, R. K.; Kovalenko, A.; Fenniri, H. *J. Am. Chem. Soc.* **2005**, *127*, 8307.
(465) Tikhomirov, G.; Oderinde, M.; Makeiff, D.; Mansouri, A.; Lu, W.; Heirtzler, F.; Kwok, D. Y.; Fenniri, H. *J. Org. Chem.* **2008**, *73*, 4248.
(466) Fleischer, E. B.; Palmer, J. M.; Srivastava, T. S.; Chatterjee, A. *J. Am. Chem. Soc.* **1971**, *93*, 3162.

(467) Pasternack, R. F.; Huber, P. R.; Boyd, P.; Engasser, G.; Francesconi, L.; Gibbs, E.; Fasella, P.; Cerio Venturo, G.; Hinds, L. deC. *J. Am. Chem. Soc.* **1972**, *94*, 4511.
(468) Pasternack, R. F.; Fleming, C.; Herring, S.; Collings, P. J.; dePaula, J.; DeCastro, G.; Gibbs, E. J. *Biophys. J.* **2000**, *79*, 550.
(469) Kano, K.; Fukuda, K.; Wakami, H.; Nishiyabu, R.; Pasternack, R. F. *J. Am. Chem. Soc.* **2000**, *122*, 7494.
(470) Collings, P. J.; Gibbs, E. J.; Starr, T. E.; Vafek, O.; Yee, C.; Pomerance, L. A.; Pasternack, R. F. *J. Phys. Chem. B* **1999**, *103*, 8474.
(471) Lauceri, R.; Fasciglione, G. F.; D'Urso, A.; Marini, S.; Purrello, R.; Coletta, M. *J. Am. Chem. Soc.* **2008**, *130*, 10476.
(472) Kodaka, M. *Biophys. Chem.* **2004**, *107*, 243.
(473) Lauceri, R.; Raudino, A.; Monsù Scolaro, L.; Micali, N.; Purrello, R. *J. Am. Chem. Soc.* **2002**, *124*, 894.
(474) Mammana, A.; D'Urso, A.; Lauceri, R.; Purrello, R. *J. Am. Chem. Soc.* **2007**, *129*, 8062.
(475) Ribó, J. M.; Crusats, J.; Sagues, F.; Claret, J.; Rubires, R. *Science* **2001**, *292*, 2063.
(476) Escudero, C.; Crusats, J.; Díez-Pérez, I.; El-Hachemi, Z.; Ribó, J. M. *Angew. Chem., Int. Ed.* **2006**, *45*, 8032.
(477) El-Hachemi, Z.; Arteaga, O.; Canillas, A.; Crusats, J.; Escudero, C.; Kuroda, R.; Harada, T.; Rosa, M.; Ribó, J. M. *Chem.—Eur. J.* **2008**, *14*, 6438.
(478) El-Hachemi, Z.; Escudero, C.; Arteaga, O.; Canillas, A.; Crusats, J.; Mancini, G.; Purrello, R.; Sorrenti, A.; D'Urso, A.; Ribó, J. M. *Chirality* **2008**, *9999*, NA.
(479) Monsù Scolaro, L.; Castriciano, M.; Romeo, A.; Mazzaglia, A.; Mallamace, F.; Micali, N. *Physica A* **2002**, *304*, 158.
(480) Micali, N.; Monsù Scolaro, L.; Romeo, A.; Mallamace, F. *Physica A* **1998**, *249*, 501.
(481) Micali, N.; Villari, V.; Castriciano, M. A.; Romeo, A.; Monsù Scolaro, L. *J. Phys. Chem. B* **2006**, *110*, 8289.
(482) De Luca, G.; Romeo, A.; Monsù Scolaro, L. *J. Phys. Chem. B* **2006**, *110*, 14135.
(483) De Luca, G.; Romeo, A.; Monsù Scolaro, L. *J. Phys. Chem. B* **2006**, *110*, 7309.
(484) Obert, E.; Bellot, M.; Bouteiller, L.; Andrioletti, F.; Lehen-Ferrenbach, C.; Boue, F. *J. Am. Chem. Soc.* **2007**, *129*, 15601.
(485) Hong, D.-J.; Lee, E.; Lee, M. *Chem. Commun.* **2007**, 1801.
(486) Moon, K.-S.; Kim, H.-J.; Lee, E.; Lee, M. *Angew. Chem., Int. Ed.* **2007**, *46*, 6807.
(487) Kim, J.-K.; Lee, E.; Lim, Y.-b.; Lee, M. *Angew. Chem., Int. Ed.* **2008**, *47*, 4662.
(488) Hartgerink, J. D.; Beniash, E.; Stupp, S. I. *Science* **2001**, *294*, 1684.
(489) Silva, G. A.; Czeisler, C.; Niece, K. L.; Beniash, E.; Harrington, D. A.; Kessler, J. A.; Stupp, S. I. *Science* **2004**, *303*, 1352.
(490) Dankers, P. Y. W.; Meijer, E. W. *Bull. Chem. Soc. Jpn.* **2007**, *80*, 2047.
(491) Rajangam, K.; Behanna, H. A.; Hui, M. J.; Han, X.; Hulvat, J. F.; Lomasney, J. W.; Stupp, S. I. *Nano Lett.* **2006**, *6*, 2086.
(492) Jiang, H.; Guler, M. O.; Stupp, S. I. *Soft Matter* **2007**, *3*, 454.
(493) Velichko, Y. S.; Stupp, S. I.; de la Cruz, M. O. *J. Phys. Chem. B* **2008**, *112*, 2326.
(494) Zhao, Y.-L.; Wu, Y.-D. *J. Am. Chem. Soc.* **2002**, *124*, 1570.
(495) Sharman, G. J.; Searle, M. S. *J. Am. Chem. Soc.* **1998**, *120*, 5291.
(496) Lim, Y.-B.; Lee, E.; Lee, M. *Angew. Chem., Int. Ed.* **2007**, *46*, 9011.
(497) Brunsveld, L.; Zhang, H.; Glasbeek, M.; Vekemans, J. A. J. M.; Meijer, E. W. *J. Am. Chem. Soc.* **2000**, *122*, 6175.
(498) van der Schoot, P.; Michels, M. A. J.; Brunsveld, L.; Sijbesma, R. P.; Ramzi, A. *Langmuir* **2000**, *16*, 10076.
(499) Arnaud, A.; Belleney, J.; Boué, F.; Bouteiller, L.; Carrot, G.; Wintgens, V. *Angew. Chem., Int. Ed. Engl.* **2004**, *43*, 1718.
(500) Stupp, S. I.; LeBonheur, V.; Walker, K.; Li, L. S.; Huggins, K. E.; Keser, M.; Amstutz, A. *Science* **1997**, *276*, 384.
(501) Zubarev, E. R.; Pralle, M. U.; Li, L.; Stupp, S. I. *Science* **1999**, *283*, 523.
(502) Dong, H.; Paramonov, S. E.; Aulisa, L.; Bakota, E. L.; Hartgerink, J. D. *J. Am. Chem. Soc.* **2007**, *129*, 12468.
(503) Cordier, P.; Tournilhac, F.; Soulié-Ziakovic, C.; Leibler, L. *Nature* **2008**, *451*, 977.
(504) Folmer, B. J. B.; Sijbesma, R. P.; Versteegen, R. M.; van der Rijt, J. A. J.; Meijer, E. W. *Adv. Mater.* **2000**, *12*, 874.
(505) Hoeben, F. J. M.; Jonkheijm, P.; Meijer, E. W.; Schenning, A. P. H. J. *Chem. Rev.* **2005**, *105*, 1491.
(506) Yamamoto, Y.; Fukushima, T.; Suna, Y.; Ishii, N.; Saeki, A.; Seki, S.; Tagawa, S.; Taniguchi, M.; Kawai, T.; Aida, T. *Science* **2006**, *314*, 1761.
(507) Zhang, S. *Nat. Biotechnol.* **2003**, *21*, 1171.
(508) Hartgerink, J. D.; Beniash, E.; Stupp, S. I. *Proc. Natl. Acad. Sci. U.S.A.* **2002**, *99*, 5133.
(509) Tysseling-Mattiace, V. M.; Sahni, V.; Niece, K. L.; Birch, D.; Czeisler, C.; Fehlings, M. G.; Stupp, S. I.; Kessler, J. A. *J. Neurosci.* **2008**, *28*, 3814.
(510) Capito, R. M.; Azevedo, H. S.; Velichko, Y. S.; Mata, A.; Stupp, S. I. *Science* **2008**, *319*, 1812.
(511) Dankers, P. Y. W.; Harmsen, M. C.; Brouwer, L. A.; van Luyn, M. J. A.; Meijer, E. W. *Nat. Mater.* **2005**, *4*, 568.
(512) Todd, E. M.; Zimmerman, S. C. *J. Am. Chem. Soc.* **2007**, *129*, 14534.
(513) Halley, J. D.; Winkler, D. A. *Complexity* **2008**, *14*, 10.
(514) Tabony, J. *Biol. Cell* **2006**, *98*, 603.
(515) Mitchison, T.; Kirschner, M. *Nature* **1984**, *312*, 237.
(516) Carlier, M. F.; Melki, R.; Pantaloni, D.; Hill, T. L.; Chen, Y. *Proc. Natl. Acad. Sci. U.S.A.* **1987**, *84*, 5257.
(517) Tabony, J. *Science* **1994**, *264*, 245.
(518) Mandelkow, E.; Mandelkow, E. M.; Hotani, H.; Hess, B.; Muller, S. C. *Science* **1989**, *246*, 1291.

CR900181U